

ANALYSIS OF COMPOSITE PLATES WITH RANDOM MATERIAL PROPERTIES

by
SALIM S.



DEPARTMENT OF AEROSPACE ENGINEERING

INDIAN INSTITUTE OF TECHNOLOGY KANPUR

APRIL, 1995

AE
1995
D
SAH
ANA

ANALYSIS OF COMPOSITE PLATES WITH RANDOM MATERIAL PROPERTIES

A Thesis Submitted
in Partial Fulfillment of the Requirements
for the Degree of
Doctor of Philosophy

by
Salim S

to the
DEPARTMENT OF AEROSPACE ENGINEERING
INDIAN INSTITUTE OF TECHNOLOGY KANPUR
KANPUR 208 016, INDIA

April 1995

28 JUN 1956

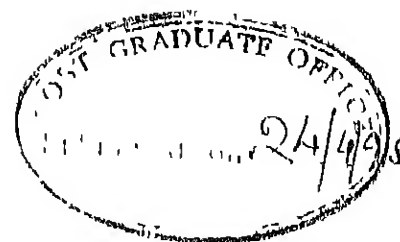
CENTRAL LIBRARY
111 T KANPUR
102 No. A 121745

AE-1995-D-SAL-ANA



A121746

CERTIFICATE



It is certified that work contained in the thesis entitled ANALYSIS OF COMPOSITE PLATES WITH RANDOM MATERIAL PROPERTIES, by Salim S , has been carried out under our supervision and that this work has not been submitted elsewhere for a degree

Y Y

N G R Iyengar

N G.R. Iyengar

Professor

Dept. of Aerospace Engineering

I.I.T. Kanpur

D Yadav

D Yadav

Professor

Dept of Aerospace Engineering

I.I.T Kanpur

24 April 1995

ACKNOWLEDGEMENTS

Fortunate I consider myself for having a number of good friends, all along during my stay at IIT Kanpur. I wish to remember all of them at this stage.

I thank my thesis supervisors Dr. N.G.R. Iyengar and Dr. D. Yadav for their encouragement and the freedom which they gave.

Muraly and Ligy have been really great friends. They have been of constant support for me at every stage.

I must remember my II-mid friends Prakash, Bala, Shankaran, Ravindha, Ramesh, Jimmy, Koshy and Siby.

A special thanks to Shaji for drawing most of the diagrams included in this thesis.

Giastus sir, Reeni chechi, Deepu and Jeetu have been a good company.

I will always remember the company of my friends Mansoor, Manoj, Santosh, Harish, Manoj V, Sunil.

I thank Aeronautical Research and Development Board (AR & DB) (Structures Panel) for the financial assistance given.

SALIM

dedicated to

B.M. NOOHOO

(1892 — 1955)

Teacher ALL RIGHT, CLASS, WHO WOULD LIKE TO GIVE HIS REPORT FIRST ?

Calvin : I WOULD I I WOULD I

Teacher • WHY CALVIN, WHAT A SURPRISE TO SEE YOU VOLUNTEER I

YOU MUST HAVE DONE A GOOD JOB

GO TO THE FRONT OF THE CLASS.

Calvin . OH BOY I

Teacher • NOW LET'S ALL PAY ATTENTION GO AHEAD, CALVIN

Calvin . THANK YOU. BEFORE I BEGIN, I'D LIKE EVERYONE TO NOTICE THAT
MY REPORT IS IN A PROFESSIONAL, CLEAR PLASTIC BINDER

Teacher • THAT'S VERY NICE GO AHEAD

Calvin : WHEN A REPORT LOOKS THIS GOOD, YOU KNOW IT'LL GET AN "A".
THAT'S A TIP, KIDS. WRITE IT DOWN

Calvin : MY REPORT IS ON BATS AHM

..

Reproduced without permission from .

SCIENTIFIC PROGRESS GOES "BOINK"

A Calvin and Hobbes Collection by Bill Watterson

SYNOPSIS

Composite materials with their well known advantages have found widespread use in various engineering structures. These have high strength to weight ratio, stiffness to weight ratio, excellent fatigue resistance and much better thermal expansion characteristics than metals. They outperform the conventional structural materials in many areas. Multi-ply laminates employing continuous fiber composites are the most important class among composites for structural applications.

Exercise of complete control on all aspects of any manufacturing / fabrication process is very difficult. This leads to uncertainties in the material properties and geometric dimensions of the components. This is especially true for laminated composites because of the large number of parameters that are associated with its fabrication. Uncertainties in several factors like the fiber volume fraction, fiber orientation, volume fraction, fibre-matrix interface parameters etc. are inherent in fiber reinforced composites. The difference between minimum and maximum values of some of the elastic properties can sometimes be as high as 100 percent. The uncertainties in the factors mentioned above are in turn reflected on the characteristics of the lamina stiffness parameters like the longitudinal modulus, transverse modulus, Poisson's ratio, shear modulus etc. These are treated as the primary variables, as these are the basic parameters that are considered for formulating a structural analysis.

problem. When parameters like modulus, density, Poisson's ratio etc are random, the derived response characteristics like deflections, natural frequencies, buckling loads, stresses, strains etc are also random, being functions of these basic random material parameters.

Conventional methods of analysis of structures assume the various parameters involved in the analysis — like system characteristics, boundary conditions etc — to be deterministic. In actual practice, however, these involve inherent uncertainties and are seldom deterministic. In most cases these parameters can at best be expressed in a probabilistic sense only. Use of the deterministic techniques yield the solution for the mean response only, which may lead to unconservative results. For aerospace and other sensitive applications it may be necessary to adopt the more accurate probabilistic approach of structural analysis.

The volume of literature that exist for problems related to isotropic metallic structures with uncertainties in parameters is considerable. Limited literature is available on response for structures made of composite materials, involving randomness in system properties. The present work was motivated by the fact that the literature available on the study of composites, considering the system properties as random variables is limited and there is a need for systematic investigation of the effects of this randomness.

The general formulation / solution techniques employed in this thesis are:

1 Perturbation

2 Monte Carlo simulation

In perturbation formulation the random parameters involved are expressed as a truncated asymptotic expansion, by introducing a *small parameter*. This kind of approximation can be used when the dispersion is smaller than the mean value of the random variable. This is true for many materials and the approach can be applied to most of the practical engineering problems. The system equations are analyzed to obtain relations in the deterministic mean and the superimposed zero-mean random part. These relations are solved to find the mean and the variance of the response.

In general, the governing equations of any structural analysis problem, with the system parameters modelled as random variables, can be expressed as,

$$[L_{ij}^R] \{A_i^R\} = \{q_i\}$$

where $[L_{ij}^R]$ is the random system matrix, $\{A_i^R\}$ is the random response vector and $\{q_i\}$ is the forcing vector. Here L_{ij}^R are known functions of a set of primary RVs b_i^R . A_i^R are unknown and also functions of b_i^R . The character of the primary random variables is assumed to be completely known. The forcing vector $\{q_i\}$ can be random or deterministic in nature. The problem, therefore, is to find the statistics of A_i^R when the statistics of the primary RVs, b_i^R are known.

Here the randomness in system properties is taken into account using a perturbation technique. Any random variable can be expressed as a zero mean random variable superimposed over a mean. This can be represented as

$$\text{random variable} = \text{mean} + \text{zero mean random variable}$$

For many practical engineering situations the random component is small compared to the mean. By introducing a small perturbation parameter ϵ , the above equation can again be expressed as

$$RV^R = RV^d + \epsilon RV^i$$

Based on these, equations to solve for the mean and standard deviation (SD) of the unknowns like plate deflection, natural frequencies, initial buckling load etc. are developed. From these the required unknown parameters are computed. The above technique is general in nature. This can be used to solve a variety of problems related to analysis of structures, involving random system parameters.

In Monte Carlo simulation, a random sample of the system parameters is generated first. This is used to get a sample of the desired results, by repeated numerical experiments. With the results from many such samples, statistics of the unknowns can be found. In the present work this technique is used for validation of results obtained with the perturbation technique.

The analysis technique is applied to composite laminates, based on the Classical Laminate Theory (CLT). Here the basic elastic properties of a composite lamina — like elastic moduli, Poisson's ratio etc — are assumed to be independent random variables. Starting from these, expressions for the expectation of various intermediate terms — like the reduced stiffness matrix Q_{ij} , bending stiffness matrix D_{ij} etc — are obtained. The above equations, are then utilized to solve for the characteristics of the random response using the perturbation technique outlined. Several application problems, employing the proposed method are discussed. The basic formulation of these problems is done by energy methods or other suitable conventional techniques available. A brief examination of the effect of coupling of the primary random variables is also done.

The first problem studied using the technique developed is deflection of composite plates with random system properties subjected to transverse static loads. The basic formulation of the problem is developed based on the CLT. The solution of the equations resulting from the formulation using energy methods is attempted by Rayleigh–Ritz technique. Rectangular plates with specially orthotropic and midplane symmetric stacking sequences are considered. Parametric study with variation in stacking sequence, fiber orientation, boundary conditions, aspect ratio, material properties etc. are presented. The approach and some assumptions used are validated by Monte Carlo simulation.

Some studies related to free vibration of rectangular composite plates with randomness in system parameters are attempted. The effect of randomness in system parameters is introduced using the perturbation technique. The governing equations obtained using energy formulation are solved by the Rayleigh–Ritz technique. The validation of the results obtained is done by Monte Carlo simulation. The statistics of random natural frequencies are obtained for various types of plates. A parametric study changing boundary conditions, aspect ratio, stacking sequence etc is also presented.

Discussions on problems in the area of initial buckling analysis of rectangular composite plates with randomness in system parameters are also presented. Here again the basic formulation is based on the CLT. The randomness in system parameters are analyzed using the perturbation technique. The governing equations are obtained using energy formulation. The solution is attempted by Rayleigh–Ritz technique. A parametric study for investigating the effect of SD of aspect ratio, stacking sequence etc on the initial buckling load is also conducted.

Lastly some of the general observations and conclusions are presented. Most of the results indicate a linear trend for the response SD in relation to variation of SD of input RVs. This indicates the negligible effect of higher order terms in the approximating functions used. For the problems considered the mean of the derived parameters coincide

with the values obtained using the usual deterministic analysis. Comparison of the present approximation with the results obtained from Monte Carlo simulation shows that for the range of SDs of input RVs considered, accuracy of results from the present formulation is excellent. At low levels of SD of input RVs, change in fiber orientation, aspect ratio etc. do not have much influence on the output SDs. The nature and magnitude of influence of each one of the primary RVs is different. If we consider unidirectional laminae, variation in E_{11} has maximum influence on the SD of results. The SD of buckling loads and natural frequencies are strongly dependent on the mode shape under consideration.

The analysis brings out clearly the importance of considering the randomness in material properties. The classical deterministic analysis may at times lead to nonconservative estimates. The amount of error, however, depends on the dispersion of the material parameters. The sensitivity of the SD of the response is a complex function of many factors like the basic random variable under consideration, aspect ratio, stacking sequence etc.

LIST OF PUBLICATIONS

The following publications have come out of this thesis work

- 1 Salim S.,Yadav D. and Iyengar N G R. (1992), Deflection of Composite Plates With Random Material Characteristics, *Proceedings of the International Symposium on Recent Advances in Aerospace Sciences and Engineering, Vol 1, Indian Institute of Science, Bangalore*, pp 236-239, Interline Publishers, Bangalore, India
- 2 Salim S.,Yadav D and Iyengar N G R (1993), Analysis of Composite Plates With Random Material Characteristics, *Mechanics Research Communications* 20(5), pp.405-414
3. Salim S., Iyengar N G.R and Yadav D (1994), Free Vibration of Composite Plates With Random Material Characteristics, *Structural Dynamics Recent Advances Vol 2, Proc of the Fifth International Conference on Structural Dynamics, Institute of Sound and Vibration Research, Univ of Southampton, England, July 1994*, pp.814-823
4. Salim S., Iyengar N G.R. and Yadav D. (1994), Buckling of Composite Plates With Random Material Characteristics, Communicated to *Composites Engineering*.

LIST OF SYMBOLS

A_{ij}	extensional stiffness coefficients
a	X – dimension of the plate
a_{ij}	coefficients of Fourier expansion of a function
a_{qij}	constants relating $E[U_q]$ with $E[Q_{ij}]$
AR	aspect ratio
B_{ij}	coupling stiffness coefficients
b	Y – dimension of the plate
b_i	basic random variables
C_{ijq}	functions of θ relating $E[\overline{Q}_{ij}]$ with $E[U_q]$
D_{ij}	bending stiffness coefficients
d	a deterministic term
$E[]$	expectation of
E_{ij}	elastic modulus
e_{ijl}	functions relating $E[Q_{ij}]$ with $E[b_l]$
f_{ij}	constants relating $E[Q_{ij}]$ with $E[b_l]$
$J()$	function of
G_{ij}	shear modulus
h	thickness of a laminate
N_{crit}	normalized critical buckling load
Q_{ij}	reduced stiffness coefficients
\overline{Q}_{ij}	transformed reduced stiffness coefficients
R	aspect ratio
R	random variable
r	zero-mean random variable
T	kinetic energy
t_i	Z – co-ordinates of lamina boundaries
RV	random variable
SD	standard deviation
U	strain energy
U_i	rotation invariant functions
u	deflection along X-axis
$\text{Var}(.)$	variance of
v	deflection along Y-axis
w	deflection along Z-axis
ϵ	small parameter
θ_i	lamina orientation
μ_{ij}, ν_{ij}	Poisson's ratio
ρ	effective mass density
ω_{ij}	natural frequencies

Contents

1	INTRODUCTION	1
1.1	FIBER REINFORCED COMPOSITES .	1
1.2	MANUFACTURING OF COMPOSITES .	4
1.3	SYSTEM MODELLING FOR DESIGN AND ANALYSIS	8
1.4	ANALYSIS OF COMPOSITES . .	14
1.5	MOTIVATION	16
1.6	LAYOUT OF THE THESIS	16
1.7	SUMMARY	17
2	LITERATURE SURVEY	18
2.1	INTRODUCTION	18
2.2	ISOTROPIC MATERIALS	19
2.3	COMPOSITE MATERIALS	26
2.4	OBSERVATIONS	28
2.5	OBJECTIVES	28
3	GENERAL FORMULATION	29
3.1	INTRODUCTION	29

3 2	GENERAL NATURE OF THE PROBLEM .	29
3 3	SYSTEM PROPERTY RANDOMNESS .	31
3 4	ANALYSIS OF LAMINATED COMPOSITE PLATES	34
3 5	SUMMARY	40
4	COMPOSITE PLATES — STATIC ANALYSIS	42
4 1	INTRODUCTION	42
4 2	FORMULATION	42
4 3	SPECIALLY ORTHOTROPIC LAMINATED PLATE	43
4.3 1	Simply Supported Plate .	44
4 3.2	Clamped Plate .	46
4.4	MIDPLANE SYMMETRIC LAMINATED PLATE	48
4.4 1	Simply Supported Plate .	49
4.4 2	Clamped Plate .	51
4.5	NUMERICAL RESULTS .	51
4.5 1	Validation of the Technique . .	51
4.5 2	Simply Supported Rectangular Plate . .	53
4.5.3	Clamped Rectangular Plate	57
4.6	SUMMARY	59
5	COMPOSITE PLATES — FREE VIBRATION ANAL- YSIS	81
5.1	INTRODUCTION	81
5.2	FORMULATION	81

5.3	SPECIALLY ORTHOTROPIC LAMINATED PLATE	82
5.3.1	Simply Supported Plate	83
5.3.2	Clamped Plate	86
5.4	MIDPLANE SYMMETRIC LAMINATED PLATE	87
5.4.1	Simply Supported Plate	87
5.4.2	Clamped Plate	89
5.5	NUMERICAL RESULTS	89
5.5.1	Validation of the Technique	90
5.5.2	Simply Supported Rectangular Plate	91
5.5.3	Clamped Rectangular Plate	95
5.6	SUMMARY	96
6	COMPOSITE PLATES — BUCKLING ANALYSIS	118
6.1	INTRODUCTION	118
6.2	FORMULATION	118
6.3	SPECIALLY ORTHOTROPIC LAMINATED PLATE	119
6.3.1	Simply Supported Plate	120
6.3.2	Clamped Plate	122
6.4	MIDPLANE SYMMETRIC LAMINATED PLATE	124
6.4.1	Simply Supported Plate	125
6.4.2	Clamped Plate	126
6.5	NUMERICAL RESULTS	127
6.5.1	Validation of the Technique	128

6 5 2	Simply Supported Rectangular Plate .	128
6 5 3	Clamped Rectangular Plate .	132
6 6	SUMMARY . .	133
7	COUPLING OF BASIC MATERIAL PROPERTIES	150
7 1	INTRODUCTION . .	150
7 2	ANALYSIS .	150
7 3	SUMMARY	154
8	GENERAL OBSERVATIONS AND CONCLUSIONS	156
8 1	INTRODUCTION	156
8.2	CONCLUSIONS	156
8 3	LIMITATIONS	158
8 4	SUGGESTIONS	158

List of Figures

1.1	Influence of molding lot series on four mechanical characteristics of a CFRP laminate . . .	6
1.2	Tensile strength and tensile modulus of E-glass woven roving/polyester hand-layup laminates	8
1.3	Correlation between tensile strength and four mechanical characteristics . . .	9
1.4	Different types of problems, with randomness in parameters — isotropic plate	10
1.5	Various sources of uncertainties — composite plate. . .	13
3.1	Nomenclature for dimensions and stacking sequence of the composite plate	38
4.1	Comparison of results from a Monte Carlo simulation with the present approximation Change of SD of deflection at the centre of the plate (0.5a, 0.5b), with SD of input RVs. [0°] laminate, AR=1.5, all sides simply supported Graphite/Epoxy . .	60

- 4.2 SD of input RVs 10 % of mean, $[90^\circ]$ laminate, $AR=1.0$, all sides simply supported. Distribution of mean of deflection and SD of deflection across $\frac{1}{4}^{th}$ of the plate. Graphite/Epoxy 60
- 4.3 Sensitivity of SD of deflection to SD of input RV E_{22} . SD of all other input RVs kept zero. $[90^\circ]$ laminate, $AR=1.0$, all sides simply supported. Graphite/Epoxy 61
- 4.4 Sensitivity of SD of deflection to SD of input RV ν_{12} . SD of all other input RVs kept zero. $[90^\circ]$, $AR=1.0$, all sides simply supported. Graphite/Epoxy . . . 61
- 4.5 Sensitivity of SD of deflection to SD of input RV G_{12} . SD of all other input RVs kept zero. $[90^\circ]$ laminate, $AR=1.0$, all sides simply supported. Graphite/Epoxy . . . 62
- 4.6 Sensitivity of SD of deflection to SD of input RV E_{11} . SD of all other input RVs kept zero. $[90^\circ]$ laminate, $AR=1.0$, all sides simply supported. Graphite/Epoxy. . . 62
- 4.7 Change in SD of system parameter a_{11} , with SD of input RVs $[90^\circ]$ laminate, all sides simply supported. Graphite/Epoxy 63
- 4.8 Change in SD of system parameter a_{13} , with SD of input RVs $[90^\circ]$ laminate, all sides simply supported. Graphite/Epoxy . 63
- 4.9 Change in SD of system parameter a_{31} , with SD of input RVs $[90^\circ]$ laminate, all sides simply supported. Graphite/Epoxy . 64
- 4.10 Change in SD of system parameter a_{33} , with SD of input RVs $[90^\circ]$ laminate, all sides simply supported. Graphite/Epoxy . 64

4 11	[90°] laminate, AR=0.5, all sides simply supported	Change in SD of deflection with SD of input RVs	Graphite/Epoxy	65
4 12	Change in SD of deflection, with SD of input RVs	[90°] laminate, AR=1, all sides simply supported	Graphite/Epoxy	65
4.13	[90°] laminate, AR=2, all sides simply supported,	Change in SD of deflection with SD of input RVs	Graphite/Epoxy	66
4 14	[90°] laminate, AR=3, all sides simply supported	Change in SD of deflection with SD of input RVs	Graphite/Epoxy	66
4 15	[90°] laminate, AR=4, all sides simply supported	Change in SD of deflection with SD of input RVs	Graphite/Epoxy	67
4 16	[90°] laminate, AR=5, all sides simply supported	Change in SD of deflection with SD of input RVs	Graphite/Epoxy	67
4 17	Variation of SD of deflection w at (0.5a,0.5b), with fiber orientation for different SDs of input RVs	AR=1, all edges of the plate simply supported	Graphite/Epoxy	68
4 18	Variation of SD of deflection w at (0.5a,0.5b), with aspect ratio a/b of the plate for various input RV SDs	Stacking sequence [90°] laminate, all edges of the plate simply supported	Graphite/Epoxy	68
4.19	[0°] laminate, AR=1, all sides simply supported	Change in SD of deflection with SD of input RVs	Graphite/Epoxy	69
4 20	[90°/0°] _s laminate, AR=1, all sides simply supported	Change in SD of deflection with SD of input RVs.	Graphite/Epoxy	69

4.21	$[0^\circ/90^\circ]_s$ laminate, $AR=1$, all sides simply supported	Change in SD of deflection with SD of input RVs	Graphite/Epoxy	70
4.22	$[45^\circ]$ laminate, $AR=1$, all sides simply supported	Change in SD of deflection with SD of input RVs	Graphite/Epoxy	70
4.23	$[45^\circ/0^\circ]_s$ laminate, $AR=1$, all sides simply supported	Change in SD of deflection with SD of input RVs	Graphite/Epoxy	71
4.24	$[0^\circ/45^\circ/90^\circ/-45^\circ]_s$ laminate, $AR=1$, all sides simply supported	Change in SD of deflection with SD of input RVs	Graphite/Epoxy	71
4.25	$[-45^\circ/45^\circ]_s$ laminate, $AR=1$, all sides simply supported	Change in SD of deflection with SD of input RVs	Graphite/Epoxy	72
4.26	$[60^\circ]$ laminate, $AR=1$, all sides simply supported	Change in SD of deflection with SD of input RVs	Graphite/Epoxy	72
4.27	Test case Glass/Epoxy composite	Change in SD of deflection, with SD of input RVs	$[90^\circ]$ laminate, $AR=0.5$, all sides simply supported,	73
4.28	Test case Glass/Epoxy composite	Change in SD of deflection, with SD of input RVs.	$[90^\circ]$ laminate, $AR=1.0$, all sides simply supported	73
4.29	Test case Glass/Epoxy composite.	Change in SD of deflection, with SD of input RVs	$[90^\circ]$ laminate, $AR=2.0$, all sides simply supported	74

4.30	Test case Glass/Epoxy composite Variation of SD of deflection w at (0.5a, 0.5b), with aspect ratio a/b of the plate for various input RVs SDs Stacking sequence $[90^\circ]$, all edges of the plate simply supported	74
4.31	SD of input RVs 10 % of mean, $[90^\circ]$ laminate, AR=1.0, all sides clamped Distribution of mean of deflection and SD of deflection across the full plate Graphite/Epoxy	75
4.32	$[0^\circ]$ laminate, AR=1, all sides clamped Change in SD of deflection with SD of input RVs Graphite/Epoxy	75
4.33	$[90^\circ]$ laminate, AR=1, all sides clamped Change in SD of deflection with SD of input RVs Graphite/Epoxy	76
4.34	$[90^\circ/0^\circ]_s$ laminate, AR=1, all sides clamped Change in SD of deflection with SD of input RVs Graphite/Epoxy	76
4.35	$[0^\circ/90^\circ]_s$ laminate, AR=1, all sides clamped Change in SD of deflection with SD of input RVs Graphite/Epoxy	77
4.36	$[45^\circ]$ laminate, AR=1, all sides clamped Change in SD of deflection with SD of input RVs Graphite/Epoxy	77
4.37	$[45^\circ/0^\circ]_s$ laminate, AR=1, all sides clamped Change in SD of deflection with SD of input RVs Graphite/Epoxy	78
4.38	$[60^\circ]$ laminate, AR=1, all sides clamped Change in SD of deflection with SD of input RVs Graphite/Epoxy.	78
4.39	$[-45^\circ/45^\circ]_s$ laminate, AR=1, all sides clamped Change in SD of deflection with SD of input RVs Graphite/Epoxy	79

4.40	$[0^\circ/45^\circ/90^\circ/-45^\circ]$, laminate, $AR=1$, all sides clamped Change in SD of deflection with SD of input RVs Graphite/Epoxy	79
4.41	Variation of SD of deflection w at $(0.5a, 0.5b)$, with fiber orientation for different SDs of input RVs $AR=1$, all edges of the plate clamped Graphite/Epoxy	80
5.1	Normalized SD of natural frequencies ω^2 , plotted against SD of input RVs The present approximation compared with results from a Monte Carlo simulation $[90^\circ]$ laminate, $AR=1.0$ Graphite/Epoxy	99
5.2	$[90^\circ]$ laminate, $AR=1$, all sides simply supported, sensitivity of SD of normalized natural frequencies ω^2 to SD of input RV E_{11} . SD of all other input RVs kept zero Graphite/Epoxy	99
5.3	$[90^\circ]$ laminate, $AR=1$, all sides simply supported, sensitivity of SD of normalized natural frequencies ω^2 to SD of input RV E_{22} SD of all other input RVs kept zero. Graphite/Epoxy	100
5.4	$[90^\circ]$ laminate, $AR=1$, all sides simply supported, sensitivity of SD of normalized natural frequencies ω^2 to SD of input RV ν_{12} SD of all other input RVs kept zero Graphite/Epoxy	100
5.5	$[90^\circ]$ laminate, $AR=1$, all sides simply supported, sensitivity of SD of normalized natural frequencies ω^2 to SD of input RV G_{12} SD of all other input RVs kept zero Graphite/Epoxy	101

5.6	[90°] laminate, AR=1, all sides simply supported	Variation of SD of normalized natural frequencies ω^2 with for different modes	
	Results for variation of SD of E_{11} alone	Graphite/Epoxy	101
5.7	[90°] laminate, AR=1, all sides simply supported	Variation of SD of normalized natural frequencies ω^2 with for different modes	
	Results for variation of SD of E_{22} alone	Graphite/Epoxy	102
5.8	[90°] laminate, AR=1, all sides simply supported	Variation of SD of normalized natural frequencies ω^2 with for different modes	
	Results for variation of SD of ν_{12} alone	Graphite/Epoxy	102
5.9	[90°] laminate, AR=1, all sides simply supported	Variation of SD of normalized natural frequencies ω^2 with for different modes	
	Results for variation of SD of G_{12} alone	Graphite/Epoxy	103
5.10	[90°] laminate, AR=0.5, all sides simply supported	Variation of SD of normalized natural frequencies ω^2 with SD of input RVs	
	Graphite/Epoxy	103
5.11	[90°] laminate, AR=1, all sides simply supported	Variation of SD of normalized natural frequencies ω^2 with SD of input RVs	
	Graphite/Epoxy	104
5.12	[90°] laminate, AR=2, all sides simply supported	Variation of SD of normalized natural frequencies ω^2 with SD of input RVs	
	Graphite/Epoxy	104

5.13	[90°] laminate, AR=3, all sides simply supported	Variation of SD of normalized natural frequencies ω^2 with SD of input RVs	
	Graphite/Epoxy	.	105
5.14	[90°] laminate, AR=4, all sides simply supported	Variation of SD of normalized natural frequencies ω^2 with SD of input RVs	
	Graphite/Epoxy	.	105
5.15	[90°] lamina, AR=5, all sides simply supported	Variation of SD of normalized natural frequencies ω^2 with SD of input RVs	
	Graphite/Epoxy	.	106
5.16	[90°] laminate, AR=1, all sides simply supported	Variation of SD of normalized natural frequencies ω^2 with change in aspect ratio, for different modes	
	SD of input RVs 10 % of mean		
	Graphite/Epoxy	106
5.17	[90°] laminate, all sides simply supported	Variation of SD of normalized fundamental frequency ω^2 with change in aspect ratio, for different SDs of input RVs	
	Graphite/Epoxy	.	107
5.18	AR=1, all sides simply supported	Variation of SD of normalized first natural frequency ω^2 with change fiber orientation, for different SDs of input RVs.	
	Graphite/Epoxy	.	107
5.19	[90°/0°] _s laminate, AR=1, all sides simply supported	Variation of SD of normalized natural frequencies ω^2 with SD of input RVs	
	Graphite/Epoxy	108

5.20	$[0^\circ/90^\circ]$, laminate, $AR=1$, all sides simply supported	Variation of SD of normalized natural frequencies ω^2 with SD of input RVs	
	Graphite/Epoxy	.	108
5.21	$[0^\circ]$ laminate, $AR=1$, all sides simply supported	Variation of SD of normalized natural frequencies ω^2 with SD of input RVs	
	Graphite/Epoxy		109
5.22	$[45^\circ]$ laminate, $AR=1$, all sides simply supported	Variation of SD of normalized natural frequencies ω^2 with SD of input RVs	
	Graphite/Epoxy	.	109
5.23	$[45^\circ/0^\circ]$, laminate, $AR=1$, all sides simply supported	Variation of SD of normalized natural frequencies ω^2 with SD of input RVs	
	Graphite/Epoxy	110
5.24	$[60^\circ]$ laminate, $AR=1$, all sides simply supported	Variation of SD of normalized natural frequencies ω^2 with SD of input RVs	
	Graphite/Epoxy	110
5.25	$[-45^\circ/45^\circ]_s$ laminate, $AR=1$, all sides simply supported	Variation of SD of normalized fundamental frequency ω^2 with SD of input RVs.	
	Graphite/Epoxy	111
5.26	$[0^\circ/45^\circ/90^\circ/-45^\circ]_s$ laminate, $AR=1$, all sides simply supported	Variation of SD of normalized fundamental frequency ω^2 with SD of input RVs	
	Graphite/Epoxy.	111

5.27	Test case Glass/Epoxy composite [90°] laminate, AR=0.5, all sides simply supported Variation of SD of normalized natural frequencies ω^2 with SD of input RVs .	112
5.28	Test case Glass/Epoxy composite [90°] laminate, AR=1.0, all sides simply supported Variation of SD of normalized natural frequency ω^2 with SD of input RVs .	112
5.29	Test case glass/epoxy composite [90°] laminate, AR=2.0, all sides simply supported Variation of SD of normalized natural frequencies ω^2 with SD of input RVs . . .	113
5.30	Test case glass/epoxy composite [90°] laminate, all sides simply supported Variation of SD of normalized fundamental frequency ω^2 with change in aspect ratio, for different SDs of input RVs	113
5.31	[45°] laminate, AR=1, all sides clamped Variation of SD of normalized fundamental frequency ω^2 with SD of input RVs Graphite/Epoxy	114
5.32	[60°] laminate, AR=1, all sides clamped Variation of SD of normalized fundamental frequency ω^2 with SD of input RVs Graphite/Epoxy	114
5.33	[45°/0°] _s laminate, AR=1, all sides clamped Variation of SD of normalized fundamental frequency ω^2 with SD of input RVs. Graphite/Epoxy	115

5.34	$[-45^\circ/45^\circ]_s$ laminate, $AR=1$, all sides clamped	Variation of SD of normalized fundamental frequency ω^2 with SD of input RVs	
	Graphite/Epoxy		115
5.35	$[90^\circ]$ laminate, $AR=1$, all sides clamped	Variation of SD of normalized fundamental frequency ω^2 with SD of input RVs	
	Graphite/Epoxy		116
5.36	$[0^\circ/45^\circ/90^\circ/-45^\circ]_s$ laminate, $AR=1$, all sides clamped	Variation of SD of normalized fundamental frequency ω^2 with SD of input RVs	
	Graphite/Epoxy		116
5.37	$AR=1$, all sides clamped	Variation of SD of normalized first natural frequency ω^2 with change fiber orientation, for different SDs of input RVs	
	Graphite/Epoxy		117
6.1	$[90^\circ]$ laminate, Normalized SD of buckling load N_{cr} , plotted against the aspect ratio	For various input parameter SDs Compared with results from a Monte Carlo simulation	
	All sides simply supported	Graphite/Epoxy	135
6.2	Normalized mean buckling load N_{cr} , plotted against the aspect ratio a/b	$[90^\circ]$ laminate All sides simply supported	
	Graphite/Epoxy		135
6.3	$[90^\circ]$ laminate, all sides simply supported	Sensitivity of SD of normalized buckling load N_{cr} to SD of input RV E_{11} . SD of all other input RVs kept zero.	
	Graphite/Epoxy.		136

6 4	[90°] laminate, all sides simply supported Sensitivity of SD of normalized buckling load N_{cr} to SD of input RV E_{22} SD of all other input RVs kept zero Graphite/Epoxy .	136
6 5	[90°] laminate, all sides simply supported Sensitivity of SD of normalized buckling load N_{cr} to SD of input RV ν_{12} SD of all other input RVs kept zero Graphite/Epoxy . .	137
6 6	[90°] laminate, all sides simply supported Sensitivity of SD of normalized buckling load N_{cr} to SD of input RV G_{12} SD of all other input RVs kept zero Graphite/Epoxy	137
6.7	Normalized mean buckling load N_{cr} , plotted against the AR [0°] laminate All sides simply supported Graphite/Epoxy	138
6.8	Normalized mean buckling load N_{cr} , plotted against the AR [90°/0°] _s laminate All sides simply supported Graphite/Epoxy	138
6 9	Normalized mean buckling load N_{cr} , plotted against the AR [0°/90°] _s lamina All sides simply supported Graphite/Epoxy	139
6 10	Normalized SD of buckling load N_{cr} , plotted against the aspect ratio a/b [90°] laminate, for various input parameter SDs All-sides simply supported Graphite/Epoxy	139
6 11	Normalized SD of buckling load N_{cr} , plotted against the aspect ratio a/b [90°/0°] _s laminate For various input parameter SDs All sides simply supported Graphite/Epoxy.	140

6.12	SD of normalized buckling load N_{cr} , plotted against the aspect ratio a/b $[0^\circ]$ laminate For various input parameter SDs All sides simply supported Graphite/Epoxy	140
6.13	SD of normalized buckling load N_{cr} , plotted against the aspect ratio a/b $[0^\circ/90^\circ]_s$ laminate For various input parameter SDs All sides simply supported Graphite/Epoxy	141
6.14	SD of normalized buckling load N_{cr} , plotted against the SD of input RVs $[45^\circ]$ laminate, $AR=1$ All sides simply supported Graphite/Epoxy	141
6.15	SD of normalized buckling load N_{cr} , plotted against the SD of input RVs $[45^\circ/0^\circ]_s$ laminate, $AR=1$ All sides simply supported Graphite/Epoxy	142
6.16	SD of normalized buckling load N_{cr} , plotted against the SD of input RVs $[0^\circ/45^\circ/90^\circ/-45^\circ]_s$ laminate, $AR=1$ All sides simply supported Graphite/Epoxy	142
6.17	SD of normalized buckling load N_{cr} , plotted against the SD of input RVs $[-45^\circ/45^\circ]_s$ laminate, $AR=1$ All sides simply supported Graphite/Epoxy	143
6.18	SD of normalized buckling load N_{cr} , plotted against the SD of input RVs $[60^\circ]_s$ laminate, $AR=1$. All sides simply supported Graphite/Epoxy	143

6 19	Test case Glass/Epoxy composite	Normalized mean buckling load N_{cr} , plotted against the aspect ratio a/b	[90°] laminate	
	All sides simply supported	.		144
6 20	Test case Glass/Epoxy composite	[90°] laminate, Normalized SD of buckling load N_{cr} , plotted against the aspect ratio	For various input parameter SDs	All sides simply supported . 144
6.21	SD of normalized buckling load N_{cr} , plotted against the SD of input RVs	[90°] laminate, $AR=1$	All sides clamped	
	Graphite/Epoxy	.	.	145
6 22	SD of normalized buckling load N_{cr} , plotted against the SD of input RVs	[0°] laminate, $AR=1$	All sides clamped	
	Graphite/Epoxy	.	.	145
6 23	SD of normalized buckling load N_{cr} , plotted against the SD of input RVs	[90°/0°] _s laminate, $AR=1$	All sides clamped	
	Graphite/Epoxy	.	.	146
6 24	SD of normalized buckling load N_{cr} , plotted against the SD of input RVs	[0°/90°] _s laminate, $AR=1$	All sides clamped	
	Graphite/Epoxy	.	.	146
6.25	SD of normalized buckling load N_{cr} , plotted against the SD of input RVs	[45°] laminate, $AR=1$	All sides clamped	
	Graphite/Epoxy	.	.	147

- 6.26 SD of normalized buckling load N_{cr} , plotted against the SD of input RVs $[45^\circ/0^\circ]_s$ laminate, $AR=1$ All sides clamped Graphite/Epoxy . . . 147
- 6.27 SD of normalized buckling load N_{cr} , plotted against the SD of input RVs $[-45^\circ/45^\circ]_s$ laminate, $AR=1$ All sides clamped Graphite/Epoxy . . . 148
- 6.28 SD of normalized buckling load N_{cr} , plotted against the SD of input RVs $[0^\circ/45^\circ/90^\circ/-45^\circ]_s$ laminate, $AR=1$ All sides clamped Graphite/Epoxy . . . 148
- 6.29 SD of normalized buckling load N_{cr} , plotted against the SD of input RVs $[60^\circ]$ laminate, $AR=1$ All sides clamped Graphite/Epoxy . . . 149

List of Tables

1.1	Variation of reported unidirectional properties for a widely used Graphite/Epoxy system, from five sources (Sources Major Air-frame Company Reports)	7
4.1	Mean of Primary Random Variables	52
5.1	Mean of natural frequencies ω^2 , for different aspect ratios $[90^\circ]$ lamina, all sides simply supported Graphite/Epoxy	97
5.2	Mean of natural frequencies ω^2 , for different stacking sequences Square plate, all sides simply supported Graphite/Epoxy	97
5.3	Mean of natural frequencies ω^2 , for different aspect ratios $[90^\circ]$ lamina, all sides simply supported Glass/Epoxy	98
5.4	Mean of fundamental frequency ω^2 , for different stacking sequences. Square plate, all sides clamped Graphite/Epoxy	98
6.1	Mean of normalized critical buckling load N_{cr} , for different stacking sequences Square plate, all sides simply supported Graphite/Epoxy	134

6.2	Mean of normalized critical buckling load N_{cr} , for different stack-	
	ling sequences	
	Square plate, all sides clamped	Graphite/Epoxy
		134

Chapter 1

INTRODUCTION

Research on new materials is an exciting, rapidly changing field. This is mainly because of their applications in aerospace industries which demand better materials. New alloys, plastics, composites etc. are always being presented as candidate materials. These materials, because of their superior performance in terms of their strength, stiffness, strength to weight ratio, stiffness to weight ratio, tailorable properties etc. throw open new possibilities and challenges for the analyst/designer. Fiber reinforced and advanced composites form an important part of this new challenge.

1.1 FIBER REINFORCED COMPOSITES

Composite materials may be defined as that class of materials in which there are two or more chemically distinct constituents on a macro scale, having a distinct interface separating them. A broad spectrum of

materials come under this definition

Polymer matrix composite materials with their well known advantages at normal temperatures have found widespread use in various engineering structures. In view of the fact that composites have high strength to weight ratio, stiffness to weight ratio, excellent fatigue resistance, and much better thermal expansion characteristics compared to metals, they outperform conventional structural materials.

The fundamental difference between composites and conventional structural materials is that composites are basically heterogeneous materials, though we treat them as homogeneous at macro level. This is an added advantage for the designer in terms of optimization of structural response. The design of the structure can be interlinked with the design of the composites used, to produce optimized structures with much superior performance than structures employing conventional materials.

Fiber reinforced composite materials have structurally superior quality fibers bonded together by a low performance matrix material. Reinforcement material is introduced in the composite in either discontinuous/chopped form or continuous form. The building block for a structure is a lamina. However, a lamina being very thin, cannot be employed for withstanding external loads. For this reason, laminae are stacked together to make a laminate. Multi-ply laminates employing continuous fiber composites are the most important class among composites for structural applications.

The fibers that are used currently are glass, carbon, graphite, aramid, and boron. Glass fibre composites are widely used and their processing technology is highly developed because of low cost. They are being used in many structures like ship hulls, antennas, sports goods etc. Carbon/graphite fibers have superior stiffness, better fatigue strength, low thermal expansion coefficients, and good heat resistance. Their performance is good under compressive as well as tensile loads. Carbon fibers are being widely introduced into aerospace industry because of the above advantages they offer. Kevlar fibre (aramid) composites have very high tensile strength combined with low density, high toughness, and high tensile modulus. However, they have low compressive strength. In view of this, they are not suitable in situations where compressive stresses are likely to develop. Composites with boron fiber, exhibit excellent compressive as well as tensile load bearing characteristics, and are used primarily for aerospace applications. In certain situations hybrid composites are employed to take advantage of the superior properties of different types of fibers. In many cases, they result in weight and cost savings when compared to structures made up of one type of fiber only.

1.2 MANUFACTURING OF COMPOSITES

The manufacturing/processing techniques employed for composites is very much different from that used for conventional materials like metals. Normally, manufacturing of a continuous fiber reinforced composite structure, like a plate, involves

- Designing the laminate layup sequence taking into consideration the application and the loads involved
- Actual laying up, with the design fiber orientation and the individual lamina thickness
- Curing, using a specified curing cycle, depending on the structure and the fiber and matrix materials involved.

Each stage of manufacturing of composites involves processes which can often be difficult to control to a great accuracy resulting in variability in the material properties. The main sources of this property variability in composites can be listed as follows [1]:

- inherent and production-related fiber and matrix property variability,
- variations in intermediate materials (e.g., prepregs, sheet molding compounds);
- variations in fabrication processes;

- local and overall variations in fiber volume fraction,
- variations in fiber orientation resulting from various sources such as resin flow and poor initial placement,
- voids

Depending on the structure and the materials utilized, a wide variety of processes like hand layup, filament winding, pultrusion etc are employed for the manufacturing of composites. The mechanical and physical properties of composites depend on the basic building blocks—the fiber and the matrix material—as well as the various processing related factors like fiber volume fraction, spatial distribution and orientation of fibers, void fraction, interfacial bond characteristics etc. In resin–matrix composites, the properties of matrix material are strongly dependent on processing conditions [1]. The influence of processing conditions has been brought out clearly by Maekawa et al. [2]. The difference in various properties of laminates processed under similar conditions are shown in Figure 1.1 [2]. Fiber–matrix interface properties of composites are strongly dependent on the processing of fibers and the curing cycle of the composite. The strength of the fiber matrix interface plays an important role in determining the properties of the manufactured composite. Thus, owing to the inherent uncertainties involved in manufacturing/processing techniques of composites, the end product can have significant variations in the properties about the de-

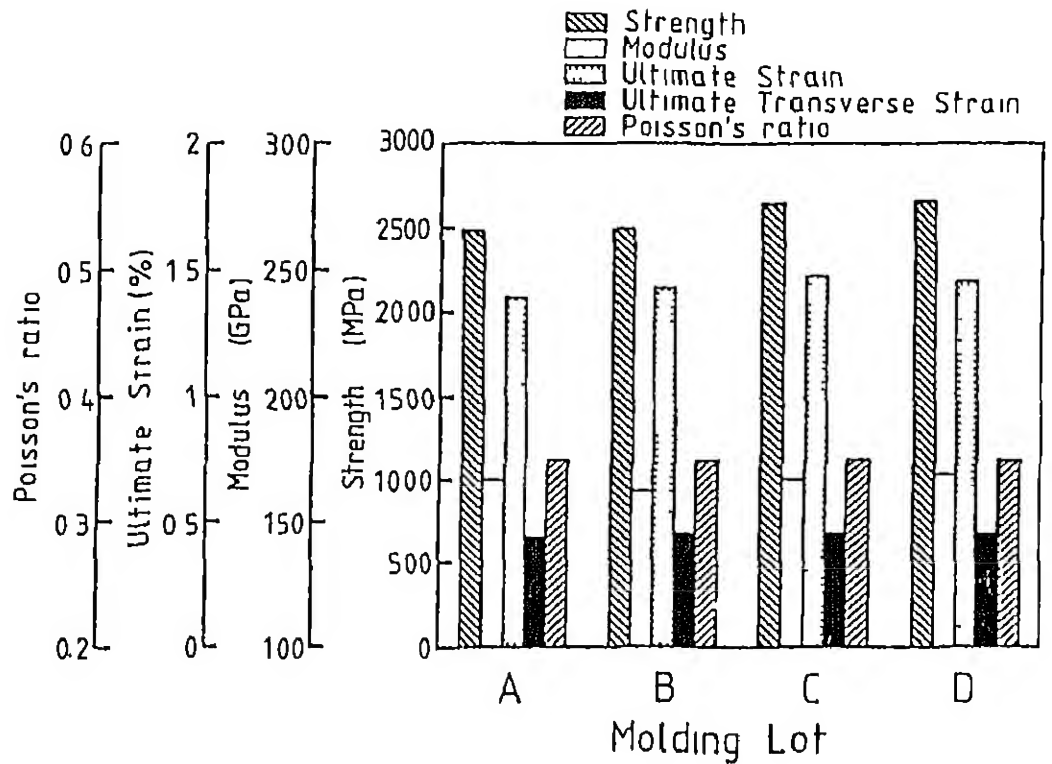


Figure 1.1. Influence of molding lot series on four mechanical characteristics of a CFRP laminate

sign values. Experimental data from various sources [1] endorse these observations (Table 1.1). It is interesting to note that experimental data from different divisions of the same company show this deviation in mechanical properties. Non-standard testing methods could be one reason for such property variability. But even the carefully fabricated materials show such property variation [1], indicating a more inherent cause. The variability in characteristics of the basic building blocks of laminates — the fiber and the matrix materials — may add to the dispersion in the properties of the end product. There are a large number of parameters that control the basic material characteristics (like elastic

Table 11. Variation of reported unidirectional properties for a widely used Graphite/Epoxy system, from five sources (Sources Major Airframe Company Reports)

Property	1	2*	3*	4	5	Max Diff %
Elastic Constants ($\times 10^6$ psi)						
Long tensile modulus	20.8	18.1	21	20.6	18.5	16
Long compr modulus	18.6	14.5	21	19.8	18.5	45
Trans tensile modulus	1.9	1.8	1.7	1.3	1.6	46
In-plane shear modulus	0.85	—	0.65	0.8	0.65	31
Poisson's ratio (dimensionless)	0.30	—	—	0.32	0.25	28
Strength Properties ($\times 10^3$ psi)						
Long tension	274	190	180	164	169	67
Long compression	280	126	180	126	162	122
Trans tension	9.5	5.2	8	5.4	6.0	83
Trans. compression	39	—	30	21	25	86
In-plane shear	17.3	—	12	8.4	—	106
Interlaminar shear	—	13.5	13	—	7.1	90

* Divisions of the same company

moduli, Poisson's ratio etc.) of composites. Sometimes these can cause considerable scatter in the observed experimental data [1], as shown in Figure 1.2. The reference also gives plenty of examples of uncertainties in composite material properties like tensile strength, tensile modulus etc.

A set of experimental observations described by Maekawa et al. [2] graphically describes the kind of scatter usually observed in experimental data — Figure 1.3. An analysis of the above results indicate that some of the properties of the composite materials as a function of the elastic

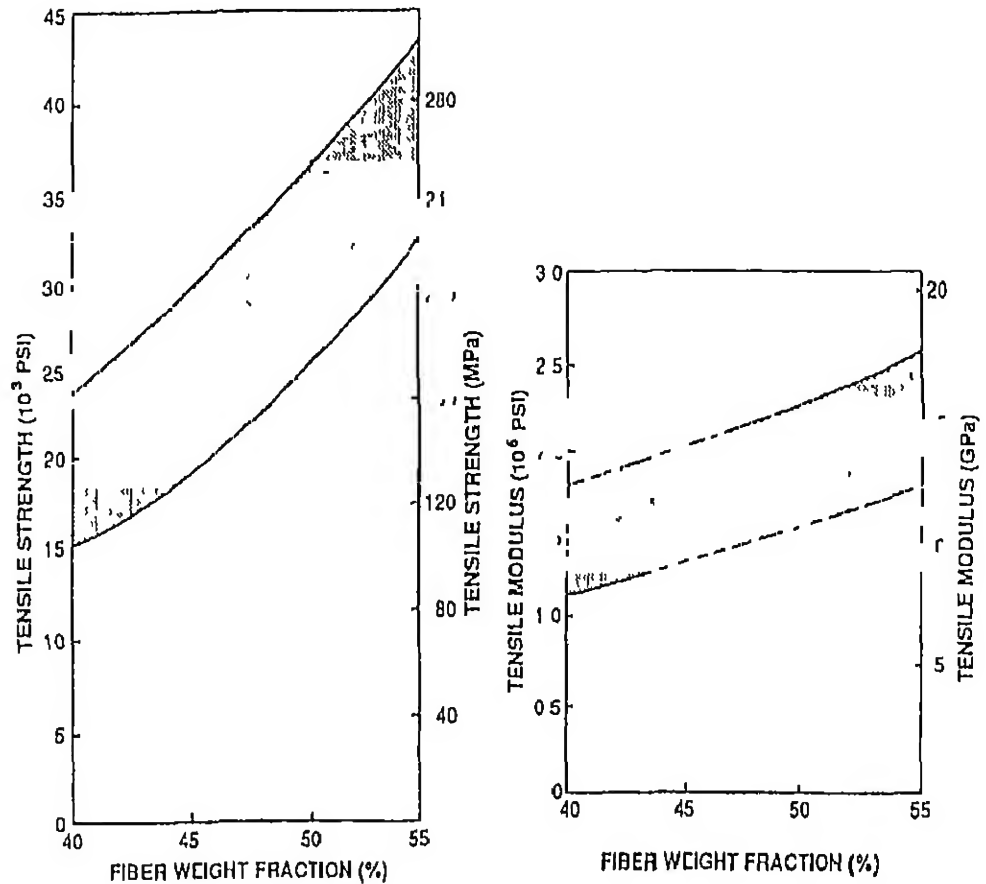


Figure 12 Tensile strength and tensile modulus of E-glass woven roving/polyester hand-layup laminates

modulus, may be closely approximated by Gaussian distributions.

1.3 SYSTEM MODELLING FOR DESIGN AND ANALYSIS

Normally, conventional methods of design and analysis of structures, models the system by assuming the various parameters involved — like system characteristics, boundary conditions etc — to be deterministic. Usually during the modelling of the structure, an empirical term called

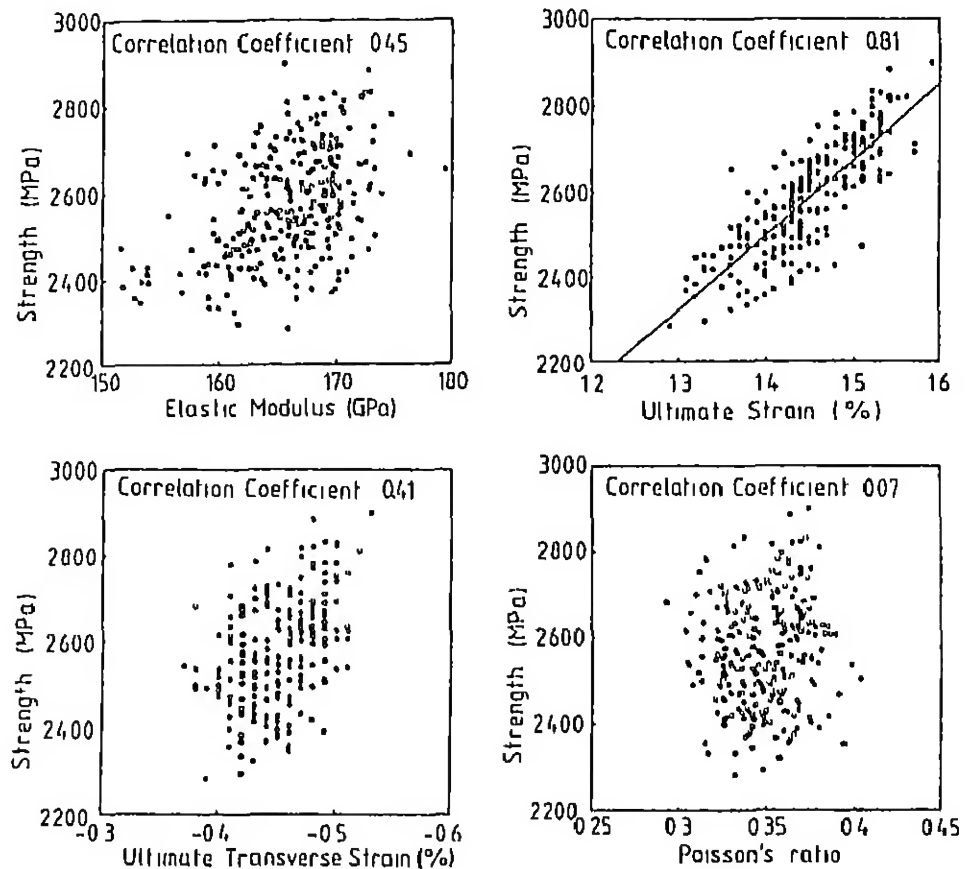


Figure 1.3 Correlation between tensile strength and four mechanical characteristics

the factor of safety is introduced at different stages. It is expected that the factor of safety covers the risks associated with the actual property variability in the structure.

In practice, however, the system parameters are seldom deterministic. Most of these parameters can be appropriately expressed in a probabilistic sense only. Thus, we can have a different class of problem modelling in which the parameters involved in the analysis are either deterministic or probabilistic or a combination of the two. This aspect is illustrated in Figure 1.4. When parameters like modulus, density, Poisson's ratio etc.

Different Types of Problems

System characteristics } Deterministic
 Boundary conditions } or
 Loading { Static } Probabilistic
 { Dynamic }

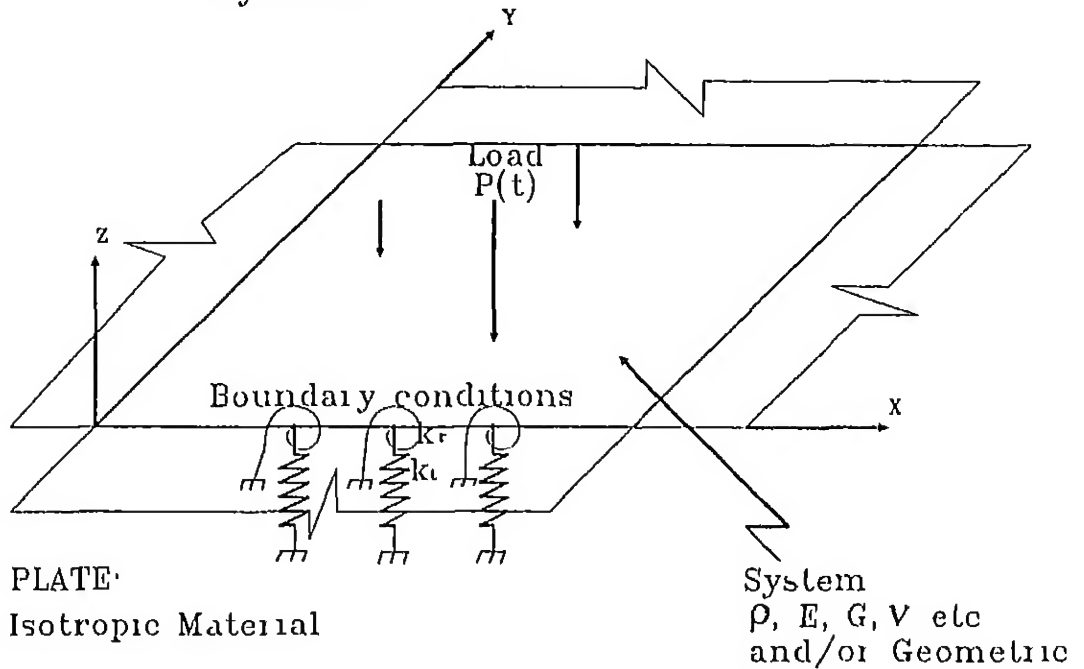


Figure 1 4 Different types of problems, with randomness in parameters — isotropic plate

are uncertain, the derived response parameters like deflections, natural frequencies, buckling loads, stresses, strains etc. are also random, being functions of these basic random material parameters. Randomness in material parameters/system parameters induce randomness in the free and forced response of structures. Depending on the sensitivity of the response parameter to the input random variables and the statistics of the input random variables, the statistics of the response parameter can vary. In certain structures this can cause mode localization [3]. Further, the risk of failure of the structures and its performance characteristics

can be evaluated accurately only by adopting a probabilistic approach of analysis. As brought out earlier, all these observations are more pertinent to composite structures in comparison to conventional metallic materials. It may further be argued that a simple factor of safety term introduced during the design process cannot take into account the intricate effects of property variability found in composites. The allowable design stresses (like tensile yield stress, tensile ultimate stress etc.) of conventional structural materials (like aluminium, steel etc.) can usually be expected to be very close to their respective mean values. This happens, because the scatter in these properties is confined to a very narrow domain about the mean value, owing to the effective control of the manufacturing/fabrication processes which has fewer parameters, in comparison to composites. However, in the case of composites, the allowable design stresses will normally be much less than the respective mean values, due to the widely scattered data [1]. A behavior similar to this can also be expected in the case of basic composite material characteristics like elastic modulus, Poisson's ratio etc.

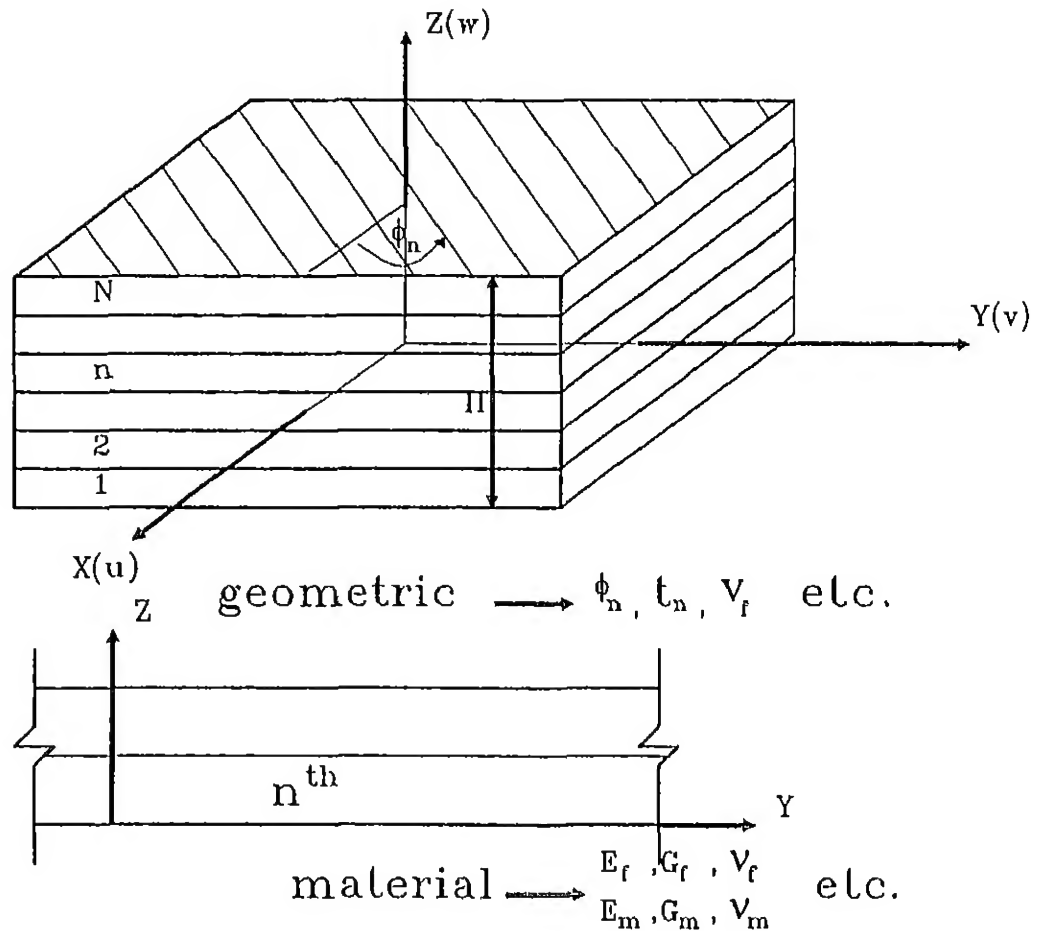
Composite materials are likely to be used extensively in primary and secondary structures in aeronautical and space projects, like advanced aircraft, helicopter, space stations etc. Computer simulation of some of the proposed configurations of such aeronautical and large outer-space installations often show closely packed/overlapping natural frequencies of some of the components. In such cases, even the slightest shift in

characteristics of the components can have pronounced effects on the response of the structure

Many results are available on the distribution of ultimate tensile strength of fiber reinforced composites [4, 5, 6]. Similar results on the variability of the elastic modulus, Poisson's ratio etc. is limited. Maekawa et al. [2] gave some experimental results on the distribution of various composite laminate properties like Poisson's ratio, strength, modulus etc. The detailed studies they conducted bring out the effect of curing, processing etc. on the material parameters of composites and their reliability. As discussed before, uncertainties in several factors like the fiber volume fraction, fiber orientation, void fraction, fiber-matrix interface parameters etc. can have significant effect on the response of fiber reinforced composites. The uncertainties in the factors mentioned above are in turn reflected on the characteristics of the lamina stiffness parameters like the longitudinal modulus, transverse modulus, Poisson's ratio, shear modulus etc. These can be treated as primary variables, since these are the basic parameters that are usually considered for formulating any structural analysis problem. Different factors and uncertainties which can affect on the response of composites are illustrated in Figure 1.5. These considerations indicate the need for more accurate probabilistic approach in the analysis of these sensitive composite structures.

Apart from randomness in material parameters, there could be ran-

COMPOSITE LAMINATES



Randomness in System Parameters

- 1) Fiber volume fraction v_f
- 2) Fiber orientation ϕ_n
- 3) Lamina thickness t_n
- 4) Basic fiber and matrix properties
 E_f, G_f, v_f & E_m, G_m, v_m

Figure 1.5: Various sources of uncertainties — composite plate

domness in loading, geometry and boundary conditions as indicated in Figure 1.4. All these can affect the response of the structure.

1.4 ANALYSIS OF COMPOSITES

Literature on the analysis of composite structures, with a probabilistic approach using parameter uncertainties is limited. The general formulation/solution techniques available are

1. Perturbation techniques
2. Monte Carlo simulation
3. Stochastic finite element method

In perturbation formulation, the random parameters involved are expressed in the form of a truncated asymptotic expansion, *by introducing a small parameter*. This kind of approximation is valid only when the randomness is much smaller than the mean value of the random variable. This condition, however, is satisfied in most of the engineering problems and hence, the approach can generally be adopted for almost all practical engineering situations. The expanded forms of the terms are introduced into the system equations. The deterministic part and the random part of the solution can be separated from these expanded system equations. These two solutions can be combined to get the complete solution of the problem as the characteristics of the response.

In the case of Monte Carlo simulation, a random sample of the system parameters is generated first. This is used to calculate the response, by repeated numerical experiments. From the results of a large number of such samples, statistics of the unknowns can be found. The sample size is dependent on the nature of random variables and the problem considered. Complex problems which are otherwise very difficult or impossible to solve using other techniques can be solved using Monte Carlo simulation. This is a computation intensive technique. Usually the only limiting factor for the problems is the computing resources available. It is normally used as a tool for validating results obtained through other methods.

Usually real life structures are so complex that it is impossible to analyze them with conventional analytical techniques. More so, in the case of structures with randomness in their system parameters. In stochastic FEM, the randomness in parameters is taken into account at the element level itself [7]. Normally, the basic formulation techniques employed to take into account the randomness in finite element equations are the perturbation technique or Monte Carlo simulation or a combination of these two. The main advantage with this approach is that it is possible to handle more realistic structures.

1.5 MOTIVATION

The discussion in the previous sections clearly demonstrates the importance of structural analysis problems with parameter randomness. This type of analysis will be of much importance in the case of composites, where there is a wide dispersion in structural system parameters. Not much work has been done in the case of composites, in this area. Hence the motivation for the present study.

1.6 LAYOUT OF THE THESIS

The thesis comprises of eight chapters. The first chapter gives an introduction to the problem. A brief overview of the area of study, the issues involved and the motivation for the present work is described. A brief review of the pertinent literature available is presented in chapter two. A description of the general methodology adopted is given in chapter three. Chapters four, five and six discuss specific problems related to static analysis, free vibration, and buckling of composite plates, along with the results. Chapter seven describes the general conclusions, limitations of the present work, and suggestions for further research. Chapter eight briefly describes a method to take into account the coupling of basic material parameters.

17 SUMMARY

The system parameters of structures composed of composite materials are often much more uncertain in comparison to those made of conventional materials. Judging from the available test results it appears that the real life values have a wide dispersion. Commonly, for conventional methods of analysis of composites, all the parameters that describe the system are considered to be deterministic. Thus the results, so obtained do not reflect the effects of the real life uncertainty of the parameters involved and may predict the system behavior inaccurately. For more sensitive applications like aerospace structures, the problem of analysis of composites with uncertain parameters call for a probabilistic approach.

The pertinent literature available in this area and related fields is reviewed in the next chapter.

Chapter 2

LITERATURE SURVEY

2.1 INTRODUCTION

A considerable volume of literature exists for problems related to structures with uncertainties in geometric and loading parameters. However, very little literature is available for composite materials in this area. This may be due to the fact that there are a large number of parameters that affect the response of composite. Furthermore, the interactive effects of various parameters are not clearly understood. The available literature may be broadly classified into two groups

- 1 Problems involving structural or material uncertainties for structures made of isotropic materials
- 2 Problems involving structural or material uncertainties for structures made of composite materials (generally anisotropic)

2.2 ISOTROPIC MATERIALS

Several studies [8] exist for structures made of conventional materials. In these, the basic material parameters and/or other parameters of the structure under consideration (like geometry, boundary conditions, loading etc.) are modelled to be random variables (RV).

A general treatment of probability theory and its applications to theory of structures can be found in [9]. This provides detailed information about problems related to static and dynamic behavior of structures with system parameter randomness.

Ibrahim [3] has presented a comprehensive review of the various approaches and solution techniques for structural dynamics problems with parameter uncertainties. Many problems related to random eigenvalues, random responses etc. of discrete and continuous systems have been discussed. The review also includes results of experimental investigations and discussions on the effect of these types of problems on areas such as design optimization, reliability analysis, sensitivity of structural performance to parameter uncertainties etc.

Vaicaitis [10] has discussed the free vibration analysis of beams with flexural rigidity (EI) and mass (ρA) as RVs, along the axis of the beam. Various types of distributions for the random parameters have been considered. The formulation of the problem uses a two variable perturbation expansion for the deflection. Natural frequency and normal

mode results for a clamped beam, obtained by using Monte Carlo simulation have also been presented. The accuracy of the method used has been found to increase with higher frequencies. It has been found that for a beam with random characteristics, the frequencies and normal modes deviate significantly from that for a beam with uniform characteristics.

Astill et al. [11] have studied stress wave propagation through a structure with random geometric and material properties under impact loading. Different concrete structures have been used as examples. The Monte Carlo approach has been employed to solve the problem. The technique proposed has been demonstrated to be compatible with Finite Element Method.

A scheme for finding probability distribution function of eigenvalues of simple structural systems (like bars, strings, shafts etc) governed by the stochastic wave equation has been suggested by Manohar and Iyengar [12]. The stochastic averaging method employed can take into account randomness in mass, stiffness and boundary conditions.

A beam-column, supported by torsional springs at ends has been studied by Shinozuka and Astill [13]. The free vibration with random variations in spring constants, axial force, distributions of material and geometric properties have been considered. Statistical properties of eigenvalues have been found using a perturbation formulation. These results were compared with results from a Monte Carlo simulation. The

perturbation approximation has been shown to be acceptable for cases where the statistical variation of properties have a limited range

A general approach for solving the statistics of the eigenvalues has been presented by Collins and Thomson [14]. The method can take into account correlation between matrix elements and can provide statistics of eigenvalues and eigenvectors. Linear equations for dynamic systems have been formulated for finding the statistics of eigenvalues and eigenvectors. The approach has been verified by an independent Monte Carlo simulation.

The influence of damping uncertainty on the frequency response of a multi degree-of-freedom dynamic system has been studied by Caravani and Thomson [15]. A statistical linear model that allows a probabilistic description of the response in terms of second-order statistics has been presented. A hypothesis regarding the statistical correlation of damping coefficients has also been presented. Validation of the presented linear model, has been done by Monte Carlo simulation. The technique is applicable to different forms of damping and other system parameters.

Chen and Soroka [16] have studied the response of a multi degree-of-freedom dynamic system with statistical properties, to deterministic excitation. The formulation employs a perturbation technique. A numerical example has been presented to illustrate the determination of response statistics using the procedure given. To show the effect of system property variations, the results have been compared with the

response of the system without considering structural property variations. It was found that the probabilistic response always provides larger response values than the deterministic response. In yet another paper [17] they have looked into the case of impulse response of an analogous system employing similar technique. Statistical moments of the impulse response function have been obtained.

The free vibrations of a slender bar with slightly different characteristics from those of a uniform bar has been studied by Mok and Murray [18]. A simple, approximate solution obtained by ignoring the higher order terms and their products, of the varying parameters like area of cross section, elastic modulus, density etc. has been presented. Experimental results, presented for free-free flexural vibrations have been shown to agree well with the theoretical predictions.

Grigoriu [19] has described methods for calculating probabilistic characteristics of the eigenvalues of stochastic symmetric matrices. The formulation has been obtained by developing approximate expressions for eigenvalues and eigenvectors, using a perturbation technique. Several examples from dynamics and elasticity have been solved using the method and the results have been compared with exact solutions.

Weighted integral method has been used by Deodatis and Shinozuka [20, 21] for calculating the response variability and reliability of stochastic frame structures. Energy approach along with FEM has been employed for solving the problems. Illustrative examples for finding the stochastic

displacement field of a beam element with random material properties have been given

Bucher and Bienner [22] have described a method for the analysis of structural systems with random properties subjected to dynamic loading. They have used the weighted integral technique. Mass and stiffness terms have been expanded in terms of weighted integrals. Monte Carlo simulation and response surface method have been used to determine the threshold exceedence probabilities of the response.

A procedure for analyzing structures with random stress-strain behavior has been presented by Millwater et al. [23]. The uncertainties in stress-strain behavior of a structure has been simulated by letting parameters like Elastic modulus, stress at yield etc. to be random variables. The approach has been used to evaluate structural reliability of complex stochastic structures by employing a finite element scheme.

Chen and Zhang [24] have described a method to determine the response sensitivity for complex stochastic structures subjected to arbitrary deterministic excitation. The probabilistic problem has been converted into a deterministic one using a perturbation technique. The response sensitivity has been calculated with respect to parameters like beam cross-sectional area, plate thickness etc.

A technique for computing the instantaneous transient response statistics of an undamped linear multi degree of freedom system subjected to arbitrary deterministic excitation, when random uncertainties

are introduced into the stiffness matrix, has been described by Piasthofer and Beadle [25]. Perturbation technique has been used to model the uncertainties. The response uncertainty has been presented as a function of the model uncertainty for an impulsive excitation function.

Bliven and Soong [26] have presented a method for analysis of natural frequencies of elastic beams having randomly varying characteristics. The method is based on a lumped parameter model. The randomness may be due to material inhomogeneities or geometrical imperfections. Statistics of natural frequencies of a simply supported beam have been calculated with randomly varying stiffness with position along the beam.

Zhang and Chen [27] have studied multi degree of freedom systems with uncertainties in mass and stiffness matrix elements. The formulation for free vibration analysis has been carried out by using a first order perturbation expansion of the uncertain parameters. Statistical properties of eigenvalues and eigenvectors have been found for beam and truss problems. The technique employed is simple and general, and can be applied to some problems related to composite materials.

Beams with arbitrary boundary conditions have been studied by Low [28]. The formulation takes into account the effect from neighboring structures and boundary conditions, and incorporates them into the frequency equation. Energy approach has been used. Exact roots of the equations have been found by a simple search method. Some experimental results are provided to validate the approach used.

Vanmarcke and Grigoriu [29] have presented results on their study of beams with random rigidity variations along the axis. Static analysis of a cantilever beam with a uniformly distributed load and concentrated load on the tip has been performed using FEM. Random elastic characteristics of each element has been represented by the local spatial average over the element, with correlation function represented by a parameter called *scale of fluctuation*. Second order statistics of deflection have been evaluated using the procedure

A general procedure for formulating problems involving random fields, using probabilistic FEM has been described by Liu et al [30]. The random field has been discretized into a mean vector and a co-variance matrix. To reduce computational effort, the above correlated vector has been transformed into an uncorrelated vector using an eigenvalue orthogonalisation. The method has been applied to several problems, including a two-dimensional plane-stress beam bending problem. An independent Monte Carlo simulation has been employed to check the results. In another paper Liu et al [31] have described a finite element method applicable to truss structures for the determination of the probabilistic distribution of the dynamic response of truss structures owing to material and geometric effects.

A solution for free vibration of thin rectangular plates resting on non-uniform lateral elastic edge supports has been obtained by Gorman [32]. A method of superposition has been used. The stiffness of elastic

supports may have any desired distribution along the edges including discontinuities and local concentrations. Results have been presented for square and rectangular plates.

All the investigations mentioned above are confined to elastic isotropic materials.

2.3 COMPOSITE MATERIALS

Limited literature is available for the response structures made of composite materials, with randomness in system properties.

Two papers by Martin and Leissa [33, 34] treat plane elasticity, static and dynamic analysis of composite lamina with variable fiber spacing. The fiber volume fraction has been assumed to vary according to some given functions. This results in variation of elements of stiffness matrix across the width of the lamina. The plane stress problem of such a lamina is governed by a partial differential equation with variable coefficients. The Ritz method has been used for general formulation. Several free vibration problems have also been solved. The non-uniform distribution of fibers is found to increase the buckling load by as much as 38 percent and the fundamental frequency by 21 percent.

Nakagiri et al. [35] have studied fiber reinforced composite plates undergoing free vibration, with uncertainties in stacking sequence. Fiber orientation and thickness of the individual lamina have been consid-

ered as the basic uncertain parameters. Mean centered second order perturbation expansion of stiffness matrix has been used for formulation of the problem. The eigenvalue statistics has been obtained by successively solving the series of equations obtained from the perturbation formulation. The problems have been solved using FEM.

Engelstad and Reddy [36] have described a probabilistic micromechanics –based non–linear analysis procedure to predict the variability in the properties of metal–matrix composites. Monte Carlo simulation, with assumed probabilistic distributions of properties—like fiber, matrix and interphase properties, volume and void ratios, strengths, fiber misalignment etc — have been used to predict the statistics of resultant lamina properties.

The problem of maximization of critical buckling load of an angle–ply laminated plate, when the properties of the plate are known to be scattered around some values, has been discussed by Adali et al [37]. Convex analysis approach has been employed to determine the material properties producing the minimum buckling load. The results have been given for uniaxial and biaxial loadings, with various aspect ratios.

2.4 OBSERVATIONS

The perturbation method seems to be common for analysis of structures with parameter uncertainties. In general Monte Carlo simulation seems to be the choice for checking the validity of the proposed analysis/method. Some prefer techniques like the weighted integral method. In some cases the above approaches are implemented using finite element methods. In most of the cases the solutions have been attempted using first order approximations, due to the complexity of the resulting equations. Introduction of randomness in system parameters was found to result in significant deviations of the solutions from the mean values.

2.5 OBJECTIVES

From the review of pertinent literature, it is observed that not much information is available on analysis of composite beams, plates and shells, with parameter uncertainties. Techniques for finding the response of different types of composite laminates with randomness in system properties are not available in the literature. In this thesis an attempt is made to study the response of orthotropic and midplane symmetric laminates under static, dynamic and inplane compressive loads. In Chapter 3 a general method that can be used for analyzing composite materials with parameter uncertainties, based on the perturbation technique is derived.

Chapter 3

GENERAL FORMULATION

3.1 INTRODUCTION

This chapter gives an account of the broad character of the problem and a general approach and formulation for problems in structural analysis involving random material parameters. It has been discussed in previous chapters that it is very difficult to closely control the geometric/material characteristics of composites. For the present formulation, the basic lamina characteristics like the longitudinal modulus, transverse modulus, Poisson's ratio, shear modulus etc. are considered to be random in nature. All other system parameters are treated as deterministic.

3.2 GENERAL NATURE OF THE PROBLEM

The mathematical statement of a structural analysis problem usually involves three sets of parameters:

- 1 Terms describing the known system parameters
- 2 Terms describing the known forcing function
- 3 Terms describing the unknown response function

In general, the governing equations of any structural analysis problem can be expressed as

$$[L_{ij}] \{A_i\} = \{q_i\} \quad (3.1)$$

Where $[L_{ij}]$ is the linear/nonlinear system matrix involving the known system parameters, $\{A_i\}$ is the unknown response vector, and $\{q_i\}$ is the given forcing vector on the structure

If the system parameters are random variables, the above equation is transformed to

$$[L_{ij}^R] \{A_i^R\} = \{q_i\} \quad (3.2)$$

Where $[L_{ij}^R]$ is the random system matrix, $\{A_i^R\}$ is the random response vector, and $\{q_i\}$ is the forcing vector. L_{ij}^R can be expressed as known functions of a set of primary RVs b_i^R . A_i^R are unknown and also functions of b_i^R and, hence are random in nature. The characteristics of the primary random variables are assumed to be completely known. The forcing vector $\{q_i\}$ can be either random or deterministic in nature. For the purposes of the study, it has been assumed to be deterministic. The problem, therefore, is to find the statistics of A_i^R when the statistics of the primary RVs b_i^R are known.

3.3 SYSTEM PROPERTY RANDOMNESS

The randomness in system properties are taken into account using a perturbation technique. It is assumed here that all the primary variables are independent random variables. In actual practice this need not be true. For example, the fiber volume fraction affects all properties. However this is done to keep the resulting equations simple/solvable, since a system involving a number of dependent random variables will give rise to a highly coupled system of equations. This is justified as a first approximation in the case of composites where the governing equations are much more complicated than those for a system involving isotropic materials.

Any random variable can be expressed as a zero mean random variable superimposed over a mean. This can be expressed as

$$\text{random variable} = \text{mean} + \text{zero mean random variable} \quad (3.3)$$

$$\text{i.e. } RV^R = RV^d + RV^r \quad (3.4)$$

The random variables in Equation 3.2, can be represented in the form given above. Similarly the basic random variables can also be expressed in this manner. Thus we have

$$\begin{aligned} L_{ij}^R &= L_{ij}^d + L_{ij}^r \\ A_i^R &= A_i^d + A_i^r \\ b_i^R &= b_i^d + b_i^r \end{aligned} \quad (3.5)$$

For many practical engineering situations the random component (RV') is generally small compared to the mean (RV^d) Equation 3.5 therefore, can again be expressed as

$$\begin{aligned} L_{ij}^R &= L_{ij}^d + \epsilon L_{ij}' \\ A_i^R &= A_i^d + \epsilon A_i' \\ b_i^R &= b_i^d + \epsilon b_i^r \end{aligned} \quad (3.6)$$

Here ϵ is a scaling parameter, small in magnitude. No generality is lost in using the same value of ϵ in all the cases. The remaining factor in the random term can absorb varying levels of this term. Using Taylor series expansion, some of the terms of Equation 3.6, can be expanded as

$$\begin{aligned} L_{ij}^r &= \sum_i \frac{\partial L_{ij}^d}{\partial b_i^R} b_i \\ A_i' &= \sum_i \frac{\partial A_i^d}{\partial b_i^R} b_i \end{aligned} \quad (3.7)$$

Assuming b_i to be small in magnitude, the second and higher order terms are neglected here. This assumption sets a limit to the range of applications of the approach being outlined. This assumption is justified if the randomness is small compared to the mean value. Substituting for the terms of Equation 3.2 from Equation 3.6 we get.

$$[L_{ij}^d + \epsilon L_{ij}^r] \{A_i^d + \epsilon A_i'\} = \{q_i\} \quad (3.8)$$

Equation 3.8, can again be further expanded as:

$$[L_{ij}^d] \{A_i^d\} + \epsilon [L_{ij}^d] \{A_i'\} + \epsilon [L_{ij}^r] \{A_i^d\} + \epsilon^2 [L_{ij}^r] \{A_i'\} = \{q_i\} \quad (3.9)$$

Collecting coefficients of different powers of ϵ from Equation 3.9, we get

$$\epsilon^0 \rightarrow [L_{ij}^d] \{A_i^d\} = \{q_i\} \quad (3.10)$$

$$\epsilon^1 \rightarrow [L_{ij}^d] \{A_i^d\} + [L_{ij}^r] \{A_i^d\} = \{0\} \quad (3.11)$$

Confining to first order perturbation, the smaller terms of $O(\epsilon^2)$ and higher order are neglected here. Equation 3.10, represents the deterministic part and Equation 3.11, represents the random part of the system of equations. The Taylor series approximations for $\{A_i^d\}$ and $[L_{ij}^r]$ from Equation 3.7, are now substituted in Equation 3.11. This results in

$$\sum_i [L_{ij}^d] \left\{ \frac{\partial A_i^d}{\partial b_l^R} b_l^R \right\} + \left[\frac{\partial L_{ij}^d}{\partial b_l^R} b_l^R \right] \{A_i^d\} = \{0\} \quad (3.12)$$

Since the variables b_l^R are assumed to be independent of each other, their coefficients in Equation 3.12, can be equated for each l . Hence we get

$$[L_{ij}^d] \left\{ \frac{\partial A_i^d}{\partial b_l^R} \right\} + \left[\frac{\partial L_{ij}^d}{\partial b_l^R} \right] \{A_i^d\} = \{0\}, \quad l = 1, 2, \quad (3.13)$$

$\{A_i^d\}$ can be found by solving Equation 3.10. The random part of system of Equations 3.13, can now be solved for the only unknown $\left\{ \frac{\partial A_i^d}{\partial b_l^R} \right\}$, for each l . Thus an approximation of the random response can be found as:

$$A_i^R = A_i^d + \epsilon A_i^r \quad (3.14)$$

Here A_i^d is given by Equation 3.7. Statistics of the response can be found using Equation 3.7 and Equation 3.14. Thus the variance and hence the standard deviation (SD) of the response can be evaluated as

$$Var(A_i^R) = \sum_l E \left[\left(\epsilon \frac{\partial A_i^d}{\partial b_l^R} b_l \right)^2 \right] \quad (3.15)$$

The above technique is general in nature. This can be used to solve a variety of problems related to analysis of structures, involving random system parameters.

3.4 ANALYSIS OF LAMINATED COMPOSITE PLATES

The analysis presented here is based on the Classical Laminate Theory (CLT), with the following basic assumptions

- Plate deflections are small compared to its thickness
- Thickness of the plate is small compared to its other dimensions
- The mid plane of the plate remains neutral and is not stretched
- Points of the plate lying initially on a normal-to-the-midplane, remains like that
- Normal stresses in the transverse direction can be neglected.

For the present analysis the elastic properties of a composite lamina are selected as the basic variables and are assumed to be independent

random variables. These random variables b_i^R — elastic moduli, Poisson's ratio etc — can be represented as

$$\begin{aligned}
 b_1^R &= E_{11}^R \\
 b_2^R &= E_{22}^R \\
 b_3^R &= \mu_{12}^R \\
 b_4^R &= G_{12}^R \\
 b_5^R &= G_{23}^R
 \end{aligned} \tag{3.16}$$

If Q_{ij} are the reduced stiffness matrix terms, the simplified relationships between the reduced stiffness matrix terms and the basic lamina properties are given by [38]

$$\begin{aligned}
 Q_{11} &= \frac{E_{11}}{(1 - \mu_{12}\mu_{21})} \\
 Q_{22} &= \frac{E_{22}}{(1 - \mu_{12}\mu_{21})} \\
 Q_{12} &= \frac{\mu_{21}E_{11}}{(1 - \mu_{12}\mu_{21})} = \frac{\mu_{12}E_{22}}{(1 - \mu_{12}\mu_{21})} \\
 Q_{21} &= Q_{12} \\
 Q_{66} &= G_{12} \\
 Q_{44} &= G_{23} \\
 Q_{55} &= G_{13} = G_{12}
 \end{aligned} \tag{3.17}$$

Equations 3.17, can be individually expanded to represent them in an infinite series form. Thus we get:

$$\overline{Q}_{55} = U_6 - U_7 \cos 2\theta \quad (3.20)$$

where the invariant terms U_i are defined as linear combinations of the reduced stiffness matrix terms Q_{ij} as

$$\begin{aligned} U_1 &= \frac{1}{8}[3Q_{11} + 3Q_{22} + 2Q_{33} - 4Q_{66}] \\ U_2 &= \frac{1}{2}[Q_{11} - Q_{22}] \\ U_3 &= \frac{1}{8}[Q_{11} + Q_{22} - 2Q_{33} - 4Q_{66}] \\ U_4 &= \frac{1}{8}[Q_{11} + Q_{22} + 6Q_{33} - 4Q_{66}] \\ U_5 &= \frac{1}{8}[Q_{11} + Q_{22} - 2Q_{33} + 4Q_{66}] \\ U_6 &= \frac{1}{2}[Q_{44} + Q_{55}] \\ U_7 &= \frac{1}{2}[Q_{44} - Q_{55}] \end{aligned} \quad (3.21)$$

The Equations 3.20 can be written in a convenient and compact form like

$$(\overline{Q}_{ij})_k = \sum_{q=1}^7 (C_{ijq})_k U_q \quad (3.22)$$

where $(C_{ijq})_k$ are known functions of θ_k , the fiber orientation and U_q are the invariant functions defined in Equations 3.21. Again these invariant functions can be expressed in the following form

$$U_q = \sum_{i=1}^6 \sum_{j=1}^6 a_{qij} Q_{ij} \quad (3.23)$$

Here a_{qij} are known constants

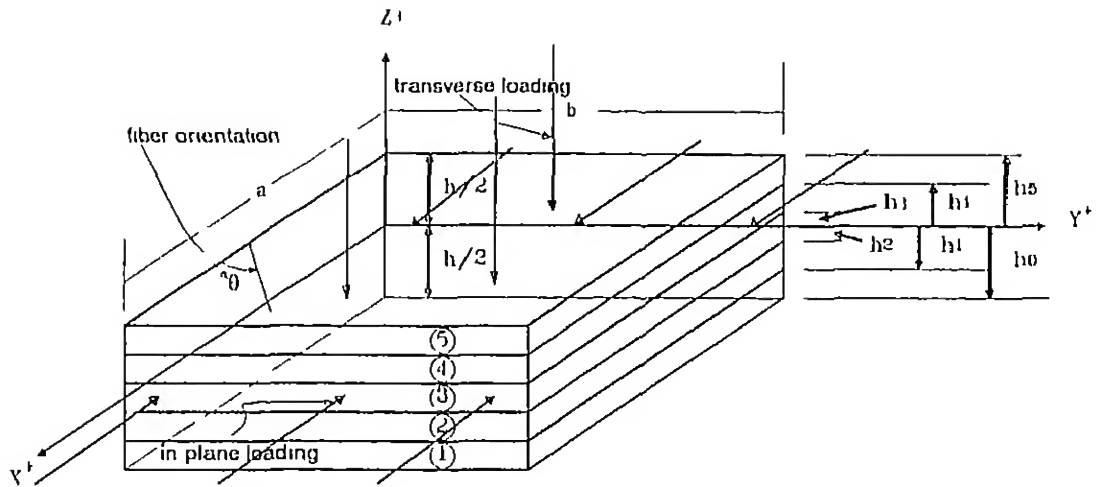


Figure 3.1 Nomenclature for dimensions and stacking sequence of the composite plate

The elements of the extensional stiffness matrix A_{ij} , coupling stiffness matrix B_{ij} and bending stiffness matrix D_{ij} [38] are given by

$$\begin{aligned} A_{ij} &= \sum_{k=1}^{N_{lay}} (\bar{Q}_{ij})_k (h_k - h_{k-1}) \\ B_{ij} &= \frac{1}{2} \sum_{k=1}^{N_{lay}} (\bar{Q}_{ij})_k (h_k^2 - h_{k-1}^2) \\ D_{ij} &= \frac{1}{3} \sum_{k=1}^{N_{lay}} (\bar{Q}_{ij})_k (h_k^3 - h_{k-1}^3) \quad i, j = 1, 2 \text{ and } 6 \end{aligned} \quad (3.24)$$

where h_k is the thickness of the k^{th} lamina, in the laminate given in Figure 3.1. For the sake of clarity only one inplane load transverse load is shown in the figure. However in general all inplane loads and/or bending loads may be acting on the plate.

The solution \mathcal{U} , of a structural analysis problem involving fiber reinforced composites will in general, be a function of the stiffness matrix terms of A_{ij} , B_{ij} and D_{ij} as given by.

$$\mathcal{U} = \mathcal{F}(A_{ij}, B_{ij}, D_{ij}) \quad (3.25)$$

So, the expectation of \mathcal{U} will be a function of expectations of the stiffness matrix elements – $E[A_{ij}]$, $E[B_{ij}]$ and $E[D_{ij}]$. This may be expressed

as

$$E[\mathcal{V}] = \mathcal{F}(E[A_{ij}], E[B_{ij}], E[D_{ij}]) \quad (3.26)$$

Here as a simplification, we consider only those problems which do not involve the cross terms between different stiffness matrix elements. The unknown expectations in Equation 3.26 can be found with the help of the special compact forms of the equations already defined. Thus the expectation of the stiffness matrix elements – $E[A_{ij}]$, $E[B_{ij}]$ and $E[D_{ij}]$ are given by

$$\begin{aligned} E[A_{ij}] &= \sum_{k=1}^{N_{lay}} E[(\overline{Q}_{ij})_k] (h_k - h_{k-1}) \\ E[B_{ij}] &= \frac{1}{2} \sum_{k=1}^{N_{lay}} E[(\overline{Q}_{ij})_k] (h_k^2 - h_{k-1}^2) \\ E[D_{ij}] &= \frac{1}{3} \sum_{k=1}^{N_{lay}} E[(\overline{Q}_{ij})_k] (h_k^3 - h_{k-1}^3) \end{aligned} \quad (3.27)$$

In the above equations, the expectation of $(\overline{Q}_{ij})_k$ is given by

$$E[(\overline{Q}_{ij})_k] = \sum_{q=1}^7 (C_{ijq})_k E[U_q] \quad (3.28)$$

Again, here the $E[U_q]$ terms – the expectation of invariant functions – are given by.

$$E[U_q] = \sum_{i=1}^6 \sum_{j=1}^6 a_{qij} E[Q_{ij}] \quad (3.29)$$

$E[Q_{ij}]$ are given by

$$E[Q_{ij}] = \sum_{n=0}^{\infty} f_{ij} \left\{ \prod_{l=1}^5 E[(b_l)^{|e_{ijl}(n)|}] \right\} \quad (3.30)$$

The set of primary random variables b_l , for the present study are the basic material properties – elastic moduli, Poisson's ratio etc. These are

defined by Equation 3.16. The derivatives of the stiffness matrix terms with respect to b_l^R are required, for solving the Equations 3.13. These can be defined in a form, similar to Equations 3.27 to 3.30. Thus we have

$$\begin{aligned}\frac{\partial E[A_{ij}]}{\partial b_l^R} &= \sum_{k=1}^{N_{lay}} \frac{\partial E[(\bar{Q}_{ij})_k]}{\partial b_l^R} (h_k - h_{k-1}) \quad l = 1, 2, \dots, 5 \\ \frac{\partial E[B_{ij}]}{\partial b_l^R} &= \frac{1}{2} \sum_{k=1}^{N_{lay}} \frac{\partial E[(\bar{Q}_{ij})_k]}{\partial b_l^R} (h_k^2 - h_{k-1}^2) \\ \frac{\partial E[D_{ij}]}{\partial b_l^R} &= \frac{1}{3} \sum_{k=1}^{N_{lay}} \frac{\partial E[(\bar{Q}_{ij})_k]}{\partial b_l^R} (h_k^3 - h_{k-1}^3)\end{aligned}\quad (3.31)$$

As an example for the case of $b_l = E_{11}$ we get

$$\begin{aligned}\frac{\partial E[A_{ij}]}{\partial E_{11}^R} &= \sum_{k=1}^{N_{lay}} \frac{\partial E[(\bar{Q}_{ij})_k]}{\partial E_{11}^R} (h_k - h_{k-1}) \\ \frac{\partial E[B_{ij}]}{\partial E_{11}^R} &= \frac{1}{2} \sum_{k=1}^{N_{lay}} \frac{\partial E[(\bar{Q}_{ij})_k]}{\partial E_{11}^R} (h_k^2 - h_{k-1}^2) \\ \frac{\partial E[D_{ij}]}{\partial E_{11}^R} &= \frac{1}{3} \sum_{k=1}^{N_{lay}} \frac{\partial E[(\bar{Q}_{ij})_k]}{\partial E_{11}^R} (h_k^3 - h_{k-1}^3)\end{aligned}$$

In the above equations the terms $\frac{\partial E[(\bar{Q}_{ij})_k]}{\partial b_l^R}$ are given by

$$\frac{\partial E[(\bar{Q}_{ij})_k]}{\partial b_l^R} = \sum_{q=1}^7 (C_{ijq})_k \frac{\partial E[U_q]}{\partial b_l^R} \quad (3.32)$$

Here the $\frac{\partial E[U_q]}{\partial b_l^R}$ terms are given by

$$\frac{\partial E[U_q]}{\partial b_l^R} = \sum_{i=1}^6 \sum_{j=1}^6 a_{qij} \frac{\partial E[Q_{ij}]}{\partial b_l^R} \quad (3.33)$$

and $\frac{\partial E[Q_{ij}]}{\partial b_l^R}$ are given by

$$\frac{\partial E[Q_{ij}]}{\partial b_l^R} = \sum_{n=0}^{\infty} f_{ijn} \left\{ \prod_{k=1}^5 E[(b_k)^{e_{ijn}(n)}] \right\} \quad (3.34)$$

With the help of the above equations, the mean and the variance of the response can be found out.

3.5 SUMMARY

A general approach for the analysis of composite laminated plates with random system parameters is presented. This method

can be applied to a wide variety of problems, in static and dynamic analysis of composite structures

The approach presented here is used to solve some problems, related to analysis of fiber reinforced composite plates, in the next three chapters. The approach and assumptions used are validated by Monte Carlo simulations in each case.

Chapter 4

COMPOSITE PLATES — STATIC ANALYSIS

4.1 INTRODUCTION

In this chapter, we consider the problem of a laminated rectangular plate supported along the edges under transverse static loading. The geometry of the plate and the co-ordinate system used are defined in Figure 3.1. As stated earlier, we shall use the classical laminated plate theory for deriving the governing differential equations.

4.2 FORMULATION

Consider a rectangular laminated composite plate subjected to a transverse load $p(x, y)$. The governing equations of such a system in terms of displacements (u^0 , v^0 , and w) and the stiffness matrix terms (A_{ij} , B_{ij} and D_{ij}) are given by [40]

$$\begin{aligned}
& A_{11} \frac{\partial^2 u^0}{\partial x^2} + 2A_{16} \frac{\partial^2 u^0}{\partial x \partial y} + A_{66} \frac{\partial^2 u^0}{\partial y^2} + A_{16} \frac{\partial^2 v^0}{\partial x^2} \\
& + (A_{12} + A_{66}) \frac{\partial^2 v^0}{\partial x \partial y} + A_{26} \frac{\partial^2 v^0}{\partial y^2} - B_{11} \frac{\partial^3 w}{\partial x^3} \\
& - 3B_{16} \frac{\partial^3 w}{\partial x^2 \partial y} - (B_{12} + 2B_{66}) \frac{\partial^3 w}{\partial x \partial y^2} - B_{26} \frac{\partial^3 w}{\partial y^3} = 0 \quad (4.1)
\end{aligned}$$

$$\begin{aligned}
& A_{16} \frac{\partial^2 u^0}{\partial x^2} + (A_{12} + A_{66}) \frac{\partial^2 u^0}{\partial x \partial y} + A_{26} \frac{\partial^2 u^0}{\partial y^2} + A_{66} \frac{\partial^2 v^0}{\partial x^2} \\
& + 3A_{26} \frac{\partial^2 v^0}{\partial x \partial y} + A_{22} \frac{\partial^2 v^0}{\partial y^2} - B_{16} \frac{\partial^3 w}{\partial x^3} - (B_{12} + 2B_{66}) \frac{\partial^3 w}{\partial x^2 \partial y} \\
& - 3B_{26} \frac{\partial^3 w}{\partial x \partial y^2} - B_{22} \frac{\partial^3 w}{\partial y^3} = 0 \quad (4.2)
\end{aligned}$$

$$\begin{aligned}
& D_{11} \frac{\partial^4 w}{\partial x^4} + 4D_{16} \frac{\partial^4 w}{\partial x^3 \partial y} + 2(D_{12} + 2D_{66}) \frac{\partial^4 w}{\partial x^2 \partial y^2} + 4D_{26} \frac{\partial^4 w}{\partial x \partial y^3} \\
& + D_{22} \frac{\partial^4 w}{\partial y^4} - B_{11} \frac{\partial^3 u^0}{\partial x^3} - 3B_{16} \frac{\partial^3 u^0}{\partial x^2 \partial y} - (B_{12} + 2B_{66}) \frac{\partial^3 u^0}{\partial x \partial y^2} \\
& - B_{26} \frac{\partial^3 u^0}{\partial y^3} - B_{16} \frac{\partial^3 v^0}{\partial x^3} - (B_{12} + 2B_{66}) \frac{\partial^3 v^0}{\partial x^2 \partial y} \\
& - 3B_{26} \frac{\partial^3 v^0}{\partial x \partial y^2} - B_{22} \frac{\partial^3 v^0}{\partial y^3} = p(x, y) \quad (4.3)
\end{aligned}$$

Equations 4.1, 4.2 and 4.3 can be simplified based on stacking sequence

4.3 SPECIALLY ORTHOTROPIC LAMINATED PLATE

In specially orthotropic laminates all the elements of $[B]$ matrix are identically zero, $A_{16} = A_{26} = 0$ and $D_{16} = D_{26} = 0$. The only nonzero stiffness matrix terms present are D_{11} , D_{22} , D_{12} and D_{66} . In view of this, Equations 4.1 and 4.2 are not coupled to equation 4.3. Since we are interested in only bending deflection, Equations for u^0 and v^0 are not considered

For specially orthotropic plates subjected to transverse loads, Equation 4.3 reduces to the following form

$$D_{11} \frac{\partial^4 w}{\partial x^4} + 2(D_{12} + 2D_{66}) \frac{\partial^4 w}{\partial x^2 \partial y^2} + D_{22} \frac{\partial^4 w}{\partial y^4} = p(x, y) \quad (4.4)$$

4.3.1 Simply Supported Plate

The boundary conditions for deflection w , when all the four sides of the plate are simply supported are given by the following set of equations

along $x = 0$ and $x = a$ for all y

$$\begin{aligned} w &= 0 \\ M_x &= -D_{11} \frac{\partial^2 w}{\partial x^2} - D_{12} \frac{\partial^2 w}{\partial y^2} \\ &= 0 \end{aligned} \quad (4.5)$$

along $y = 0$ and $y = b$ for all x

$$\begin{aligned} w &= 0 \\ M_y &= -D_{12} \frac{\partial^2 w}{\partial x^2} - D_{22} \frac{\partial^2 w}{\partial y^2} \\ &= 0 \end{aligned} \quad (4.6)$$

Navier's method can be applied to solve the Equation 4.4, for the above set of boundary conditions. A series approximation for the deflection of the plate, $w(x, y)$ is written as:

$$w(x, y) = \sum_{m=1}^{\infty} \sum_{n=1}^{\infty} a_{mn} X_m(x) Y_n(y) \quad (4.7)$$

where $X_m(x)$ and $Y_n(y)$ are functions that satisfy the set of boundary conditions given by Equations 4.5 and 4.6. In terms of beam characteristic functions, Equation 4.7 can be rewritten as

$$w(x, y) = \sum_{m=1}^{\infty} \sum_{n=1}^{\infty} a_{mn} \sin \frac{m\pi x}{a} \sin \frac{n\pi y}{b} \quad (4.8)$$

The transverse load distribution $p(x, y)$ can also be similarly expressed as

$$p(x, y) = \sum_{m=1}^{\infty} \sum_{n=1}^{\infty} q_{mn} \sin \frac{m\pi x}{a} \sin \frac{n\pi y}{b} \quad (4.9)$$

When Equations 4.8 and 4.9 are substituted in the governing equation 4.4, we get.

$$\sum_{m=1}^{\infty} \sum_{n=1}^{\infty} \left[D_{11} \left(\frac{m\pi x}{a} \right)^4 + 2(D_{12} + 2D_{66}) \left(\frac{m\pi x}{a} \right)^2 \left(\frac{n\pi y}{b} \right)^2 + D_{22} \left(\frac{n\pi y}{b} \right)^4 \right] a_{mn} = q_{mn} \quad (4.10)$$

Equation 4.10 is of the form

$$\sum_{m=1}^{\infty} \sum_{n=1}^{\infty} L_{mn} a_{mn} = q_{mn} \quad (4.11)$$

where

$$L_{mn} = D_{11}\lambda_m^4 + 2(D_{12} + 2D_{66})\lambda_m^2\lambda_n^2 + D_{22}\lambda_n^4$$

with $\lambda_m = \frac{m\pi x}{a}$ and $\lambda_n = \frac{n\pi y}{b}$

The expectation of L_{mn} is

$$E[L_{mn}] = E[D_{11}]\lambda_m^4 + 2(E[D_{12}] + 2E[D_{66}])\lambda_m^2\lambda_n^2 + E[D_{22}]\lambda_n^4 \quad (4.12)$$

Where $E[D_{ij}]$, the expectation of D_{ij} , is defined by Equation 3.27. The basic random variables b_i^R are assumed to be independent. Here they are defined by Equation 3.16. From Equation 4.12, taking derivatives with respect to each of the basic random variables, b_i^R we get:

$$\frac{\partial E[L_{mn}]}{\partial b_i^R} = \frac{\partial E[D_{11}]}{\partial b_i^R} \lambda^4 + 2 \left(\frac{\partial E[D_{12}]}{\partial b_i^R} + 2 \frac{\partial E[D_{66}]}{\partial b_i^R} \right) \lambda_m^2 \lambda_n^2 + \frac{\partial E[D_{22}]}{\partial b_i^R} \lambda_n^4 \quad (4.13)$$

The derivatives that appear in Equation 4.13 are defined by Equations 3.31.

Thus, with the help of the expressions defined above and using Equations 3.10, 3.13, 3.14 and 3.15, the mean and variance of the response $w^R(x, y)$ can be found out, provided the statistics of the basic random variables b_i^R are known.

4.3.2 Clamped Plate

For a plate clamped on all edges, the differential equation cannot be solved using a variable separable technique, since boundary conditions have odd ordered derivatives in it, while the differential equation has even order derivatives. Hence energy approach is used here, to obtain an approximate solution. The simplified energy criterion for this problem with lateral load $p(x, y)$ is.

$$\text{Total potential, } \Pi_p = U + W = \text{stationary value} \quad (4.14)$$

Where U is the strain energy and W is the work done by external loads. The total potential, Π_p , for a plate undergoing only bending can

be written as

$$\begin{aligned}
 \Pi_p &= U + W = \frac{1}{2} \int_0^b \int_0^a \left[D_{11} \left(\frac{\partial^2 w}{\partial x^2} \right)^2 + 2D_{12} \frac{\partial^2 w}{\partial x^2} \frac{\partial^2 w}{\partial y^2} \right. \\
 &\quad \left. + D_{22} \left(\frac{\partial^2 w}{\partial y^2} \right)^2 + 4D_{66} \left(\frac{\partial^2 w}{\partial x \partial y} \right)^2 - p(x, y)w \right] dx dy \\
 &= \text{stationary value}
 \end{aligned} \tag{4.15}$$

All the four edges of the rectangular plate considered here are clamped. The boundary conditions along these edges are defined by the equations

along $x = 0$ and $x = a$ for all y

$$w = 0$$

$$\frac{\partial w}{\partial x} = 0 \tag{4.16}$$

along $y = 0$ and $y = b$ for all x

$$w = 0$$

$$\frac{\partial w}{\partial y} = 0 \tag{4.17}$$

Rayleigh–Ritz method is used to solve Equation 4.15. A series approximation for the deflection of the plate $w(x, y)$ can be defined as

$$w(x, y) = \sum_{m=1}^M \sum_{n=1}^N a_{mn} X_m(x) Y_n(y) \tag{4.18}$$

The functions $X_m(x)$ and $Y_n(y)$, that satisfy the boundary conditions 4.16 and 4.17 are defined as follows

$$\begin{aligned}
 X_m(x) &= (x^2 - ax)^2 x^{(m-1)} \\
 Y_n(y) &= (y^2 - by)^2 y^{(n-1)}
 \end{aligned}
 \tag{4.19}$$

Substituting Equation 4.18 in 4.15 and applying the conditions given by Equations 4.16 and 4.17, we get $M \times N$ algebraic equations as

$$\begin{aligned}
 \sum_{i=1}^M \sum_{j=1}^N &\left\{ D_{11} \int_0^a \frac{d^2 X_i}{dx^2} \frac{d^2 X_m}{dx^2} dx \int_0^b Y_j Y_n dy \right. \\
 &+ D_{12} \left[\int_0^a X_m \frac{d^2 X_i}{dx^2} dx \int_0^b Y_j \frac{d^2 Y_n}{dy^2} dy + \int_0^a X_i \frac{d^2 X_m}{dx^2} dx \int_0^b Y_n \frac{d^2 Y_j}{dy^2} dy \right] \\
 &+ D_{22} \int_0^a X_i X_m dx \int_0^b \frac{d^2 Y_j}{dy^2} \frac{d^2 Y_n}{dy^2} dy + 4D_{66} \int_0^a \frac{dX_i}{dx} \frac{dX_m}{dx} dx \int_0^b \frac{dY_j}{dy} \frac{dY_n}{dy} dy \Big\} a_{mn} \\
 &= \int_0^b \int_0^a p(x, y) X_m Y_n dx dy \\
 m &= 1, 2, \dots, M \text{ and } n = 1, 2, \dots, N
 \end{aligned}
 \tag{4.20}$$

The system of $M \times N$ equations that we get after substituting Equation 4.19 in 4.20 is of a form similar to 4.11. This can be transformed and solved for the unknowns a_{ij}^R as already described.

4.4 MIDPLANE SYMMETRIC LAMINATED PLATE

We now consider plates with only bending-twisting coupling. The stiffness matrix terms present in the governing equation for $w(x, y)$ are $-D_{11}$, D_{22} , D_{12} , D_{00} , D_{10} and D_{20} . Here again, we do not consider full equations along u^0 and v^0 since elements of $[B]$ matrix are identically zero.

4.4.1 Simply Supported Plate

For midplane symmetric laminates, subjected to transverse static loads the Equation 4.3 reduce to the form

$$\begin{aligned} D_{11} \frac{\partial^4 w}{\partial x^4} + 4D_{16} \frac{\partial^4 w}{\partial x^3 \partial y} + 2(D_{12} + 2D_{66}) \frac{\partial^4 w}{\partial x^2 \partial y^2} \\ + 4D_{26} \frac{\partial^4 w}{\partial x \partial y^3} + D_{22} \frac{\partial^4 w}{\partial y^4} = p(x, y) \end{aligned} \quad (4.21)$$

The boundary conditions for the present case where all the four edges are simply supported are

along $x = 0$ and $x = a$ for all y

$$\begin{aligned} w &= 0 \\ M_x &= -D_{11} \frac{\partial^2 w}{\partial x^2} - 2D_{66} \frac{\partial^2 w}{\partial x \partial y} - D_{12} \frac{\partial^2 w}{\partial y^2} \\ &= 0 \end{aligned} \quad (4.22)$$

along $y = 0$ and $y = b$ for all x

$$\begin{aligned} w &= 0 \\ M_y &= -D_{12} \frac{\partial^2 w}{\partial x^2} - 2D_{26} \frac{\partial^2 w}{\partial x \partial y} - D_{22} \frac{\partial^2 w}{\partial y^2} \\ &= 0 \end{aligned} \quad (4.23)$$

Closed form solution for Equation 4.21 is not feasible because of the presence of odd ordered derivatives in governing equation and the boundary conditions. We formulate the problem in terms of the total potential Π_p , and solve it by employing Rayleigh–Ritz technique. Thus

the total potential Π_p , for the plate is.

$$\begin{aligned}\Pi_p &= U + W = \frac{1}{2} \int_0^b \int_0^a \left[D_{11} \left(\frac{\partial^2 w}{\partial x^2} \right)^2 + 2D_{12} \frac{\partial^2 w}{\partial x^2} \frac{\partial^2 w}{\partial y^2} + D_{22} \left(\frac{\partial^2 w}{\partial y^2} \right)^2 \right. \\ &\quad \left. + 4 \left(D_{16} \frac{\partial^2 w}{\partial x^2} + D_{26} \frac{\partial^2 w}{\partial y^2} \right) + 4D_{66} \left(\frac{\partial^2 w}{\partial x \partial y} \right)^2 - 2p(x, y)w \right] dx dy \\ &= \text{stationary value}\end{aligned}\quad (4.24)$$

A series solution of the form of Equation 4.18, that satisfies the boundary conditions specified by Equation 4.22 and 4.23 can be assumed here for solving Equation 4.24. Thus we get

$$\begin{aligned}&\sum_{i=1}^M \sum_{j=1}^N \left\{ D_{11} \int_0^a \frac{d^2 X_i}{dx^2} \frac{d^2 X_m}{dx^2} dx \int_0^b Y_j Y_n dy \right. \\ &\quad \left. + D_{12} \left[\int_0^a X_m \frac{d^2 X_i}{dx^2} dx \int_0^b Y_j \frac{d^2 Y_n}{dy^2} dy + \int_0^a X_i \frac{d^2 X_m}{dx^2} dx \int_0^b Y_n \frac{d^2 Y_j}{dy^2} dy \right] \right. \\ &\quad \left. + D_{22} \int_0^a X_i X_m dx \int_0^b \frac{d^2 Y_j}{dy^2} \frac{d^2 Y_n}{dy^2} dy + 4D_{66} \int_0^a \frac{dX_i}{dx} \frac{dX_m}{dx} dx \int_0^b \frac{dY_j}{dy} \frac{dY_n}{dy} dy \right. \\ &\quad \left. + 2D_{16} \left[\int_0^a \frac{d^2 X_i}{dx^2} \frac{dX_m}{dx} dx \int_0^b Y_j \frac{dY_n}{dy} dy + \int_0^a \frac{dX_i}{dx} \frac{d^2 X_m}{dx^2} dx \int_0^b Y_n \frac{dY_j}{dy} dy \right] \right. \\ &\quad \left. + 2D_{26} \left[\int_0^a X_m \frac{dX_i}{dx} dx \int_0^b \frac{dY_j}{dy} \frac{d^2 Y_n}{dy^2} dy + \int_0^a X_i \frac{dX_m}{dx} dx \int_0^b \frac{d^2 Y_j}{dy^2} \frac{dY_n}{dy} dy \right] \right\} a_{mn} \\ &= \int_0^b \int_0^a p(x, y) X_m Y_n dx dy \\ &m = 1, 2, \dots, M \text{ and } n = 1, 2, \dots, N\end{aligned}\quad (4.25)$$

$M \times N$ linear simultaneous equations obtained from Equation 4.25 is of the form specified by Equation 4.11. These set of equations can be solved for finding the statistics of the unknowns a_{mn} , if the statistics of the basic random variables b_i^R are known. The approximating functions given by Equation 4.8 are again used for solving the problem.

4.4.2 Clamped Plate

Here, again the governing equations and boundary conditions are given by Equations 4.21, 4.16 and 4.17 respectively. We once again use the energy approach along with Rayleigh–Ritz technique satisfying the boundary conditions given by Equations 4.16 and 4.17.

4.5 NUMERICAL RESULTS

Experimental data regarding the distribution of basic composite material parameters is very limited in open literature. Analysis of some of the available experimental data [2] show that the distribution of Poisson's ratio, Elastic modulus etc. may be closely approximated by a Gaussian distribution. For the present analysis, distribution of all the random variables are assumed to be Gaussian. The knowledge of the distribution of the basic random variables is required for the Monte Carlo simulation approach. However, the perturbation approach needs only the mean and SD of the variables. Table 4.1 gives the assumed mean values of all the primary random variables b_i^R used.

4.5.1 Validation of the Technique

Validation of the proposed perturbation technique, for the static problem is carried out for the case of a rectangular Graphite/Epoxy plate, with aspect ratio 1.5 by comparing the SD of deflection obtained with the

Table 4.1 Mean of Primary Random Variables [39]

Random Variable	Graphite/Epoxy	Glass/Epoxy
E_{11}	181.0 GPa	53.78 GPa
E_{22}	10.3 GPa	17.93 GPa
ν_{12}	0.28	0.25
G_{12}	7.17 GPa	8.963 GPa
G_{23}	0.717 GPa	0.89 GPa

results of Monte Carlo simulation. All the four edges are assumed to be simply supported with each lamina having fibers oriented along X-axis. The plate is loaded by a uniformly distributed load.

Results are computed for different sets of SDs for input RVs, to find the SD of deflection at the center of the plate. The ratio $\frac{SD}{Mean}$ are assumed to be same for all the four primary RVs.

Monte Carlo simulation solution is also obtained for the same problem. Two different random number generation techniques are combined to generate the random samples with specified mean and SD for the system parameters required for the solution. This is done to reduce any bias in the random samples generated. The total number of samples used in simulation is 15000. Figure 4.1 shows the comparison of the proposed approach with the results obtained from Monte Carlo simulation. For the range of SD of input RVs considered the results from the present approximation comes very close to the Monte Carlo simulation results.

The results show that the first order perturbation technique adopted for the present analysis is sufficient to give accurate results, under the assumptions made for the analysis of the problem for the level of variations considered in the basic random variables

4.5.2 Simply Supported Rectangular Plate

Results have been computed for rectangular plates simply supported along all the four edges. The entire calculations are carried out for plates of constant thickness, h

First some results for Graphite/Epoxy laminates are discussed. Towards the end some results for Glass/Epoxy laminates are also examined. Graphite/Epoxy composites have $\frac{E_{11}}{E_{22}}$ ratio around 18. While for Glass/Epoxy composites it is of the order of 3.

Plots showing variation of Mean of deflection and SD of deflection for one quarter of a plate are given in Figure 4.2. The results are for a $[90^\circ]$ lamina, with aspect ratio of 1.0. All the input RVs were assumed to have SD equal to 10 percent of their mean values. The nature of variation of SD across the plate is similar to the variation of mean across the plate. Points having higher magnitude of deflection have proportionately higher values of SD.

Figure 4.3 to 4.6 gives similar plots for the other basic RVs — the transverse modulus E_{22} , the Poisson's ratio ν_{12} and the shear modulus G_{12} and longitudinal modulus E_{11} . In all these cases SD of one of the

RVs is changed and SD of all other RVs are kept zero

All the four plots show a linear relationship between SD of the input RV and SD of deflection w at a point on the plate. It is observed that as we go towards the center of the plate the effect of input RV on the response reduces. Relation between distribution of mean of deflection across the plate and SD of deflection across the plate is not linear. The nature of this varies with the basic random variable that we consider. The maximum effect on the SD of deflection is due to change in E_{11} . The effect of G_{12} and E_{22} respectively, comes next. Variation in SD of ν_{12} has the least effect on deflection. Thus, if we consider a combination of effects of all the basic random variables, the net effect of them on the SD of deflection will be a complex combination of effects due to each one of them. The above observation implies that experiments for evaluation of E_{11} should be performed very precisely.

Figures 4.7 to 4.10 show the variation of SD of coefficients a_{mn} — in Equation 4.7 — with the change in SD of input RVs. The results are for a $[90^\circ]$ lamina, with AR as a parameter. The plots show a linear trend. Increase in aspect ratio beyond a certain level doesn't seem to affect the results. As indicated by Figure 4.7, the first coefficient of the series a_{11} is affected most by the change in SD of input RVs.

Figure 4.11 gives the effect of SD of primary RVs on the SD of deflection w , at four different locations for an aspect ratio of 0.5. Figures 4.12 to 4.16 are for aspect ratios 1.0, 2.0, 3.0, 4.0 and 5.0 respectively.

at different locations. They also indicate a similar behavior. The effect of increasing aspect ratio is to increase the SD of deflection. This effect dominant at low AR, slows down with increase in AR. Beyond a limit, the aspect ratio doesn't seem to have much effect on the SD of deflection.

Figure 4.17 shows the variation of SD of deflection w at the center of the plate, with fiber orientation. The results are presented for different levels of SD of input RVs, ranging from 1 percent to 15 percent of the mean. At lower levels of input SD of RV, change in fiber orientation has practically no effect on the SD of deflection. At higher levels of SD of input RVs the fiber orientation seems to affect the SD of deflection. Fiber orientations which results in stiffer plates seem to have lower levels of SD of deflection.

Variation of SD of deflection at the center of a plate, with the plate aspect ratio (a/b) is shown in Figure 4.18 for $[90^\circ]$ stacking sequence. Results are presented for different levels of SD of input RVs ranging from 1 percent of mean to 15 percent of mean. The plate is assumed to be simply supported along all the four edges. As with the case of change in stacking sequence, here also change in aspect ratio doesn't have much effect on the SD of deflection at low levels of SD of input RVs. As the SD of input RVs is increased we can observe that there is significant influence of change in aspect ratio on the SD of deflection, at the initial stages of the curve. But beyond a limit the result stabilizes.

and further change in aspect ratio doesn't seem have any effect on the SD

Change in SD of deflection with SD of input RVs is shown in Figures 4.19, 4.20 and 4.21 for laminates having stacking sequences $[0^\circ]$, $[90^\circ/0^\circ]_s$, and $[0^\circ/90^\circ]_s$ respectively. The results are for simply supported square plates. These plots are similar to Figure 4.12 — the results for a $[90^\circ]$ square plate. It may be noted here that all these plates have the same thickness and size.

Figure 4.22 and 4.23 show the plot of SD of deflection w against the SD of input RVs for $[45^\circ]$ and $[45^\circ/0^\circ]_s$ plates. The plates compared here are square plates with identical thickness. These plots are almost identical — indicating that the middle 0° layers in the second plate does not have any noticeable influence on the result. Results for $[0^\circ/45^\circ/90^\circ/-45^\circ]_s$, $[-45^\circ/45^\circ]_s$ and $[60^\circ]$ laminates are given in Figures 4.24, 4.25 and 4.26 respectively. The plots indicate a similarity in the behavior pattern in all the cases.

Now some typical results for a Glass/Epoxy composite are considered. Table 4.1 lists the mean values of primary random variables used. The variation of SD of deflection at different locations of the plate, with the SD of input RVs is given by Figures 4.27, 4.28 and 4.29, for aspect ratios 0.5, 1.0 and 2.0 respectively. The results are for rectangular laminates having $[90^\circ]$ stacking sequence, with all the four sides simply supported. The SD values are much larger than that for the

Graphite/Epoxy laminates having similar configuration, given by Figures 4.11, 4.12 and 4.13. This behavior can be expected since the stiffness of Glass/Epoxy laminates are much less than that for Graphite/Epoxy laminates.

Figure 4.30 shows the sensitivity of SD of deflection at the midpoint of a $[90^\circ]$ lamina, to change in aspect ratio. The lamina is assumed to be simply supported on all the four edges. Here the behavior is similar to the corresponding plot for Graphite/Epoxy given by Figure 4.18 except at the initial portions of the curves, corresponding to low aspect ratios. At AR 1.0 the SD of deflection dips to a minimum value, after which it gradually increases, with a tendency to reach a plateau at some high values of aspect ratio. Here also, at low levels of SD of input RVs, change in AR do not have much influence on the SD of deflection.

4.5.3 Clamped Rectangular Plate

Here we consider rectangular plates with all the four sides clamped. All the plates considered here are assumed to have the same thickness. The results presented are for a Graphite/Epoxy composite, specifications of which are given in Table 4.1.

The variation of mean of deflection and SD of deflection across the full plate, when all the edges are clamped is given by Figure 4.31. The results are for a $[90^\circ]$ square lamina, with SD of all the input RVs set to 10 percent of their mean values. The nature of variation of the SD across

the plate is similar to that of mean. Figures 4.32, 4.33, 4.34 and 4.35 show SD of deflection w against the change in SD of input RVs at various points across the plate, for $[0^\circ]$, $[90^\circ]$, $[90^\circ/0^\circ]_s$ and $[0^\circ/90^\circ]_s$ laminates. All the laminates under consideration have the same thickness and platform dimensions. The plots show identical trends of variation of deflection SD with the changes in the input SD. The SD of deflection w , like the mean value is considerably lower than the corresponding values for similar plates with simply supported boundary conditions as described in the last section.

Results for $[45^\circ]$ and $[45^\circ/0^\circ]_s$ square plates are given in Figures 4.36 and 4.37 respectively. Unlike the results for similar plates with simply supported boundary conditions as discussed in the last section, here the plots show different trends. Here $[45^\circ/0^\circ]_s$ laminate shows a higher level of SD compared with the $[45^\circ]$ lamina. Hence we can see that the middle 0° layers do have an influence on the SD of deflection for the present case.

Figures 4.38, 4.39 and 4.40 show the variation of SD of deflection with the SD of input RVs, of laminates $[60^\circ]$, $[-45^\circ/45^\circ]_s$ and $[0^\circ/45^\circ/90^\circ/-45^\circ]_s$. All of them show linear trends, with $[-45^\circ/45^\circ]_s$ stacking sequence showing the minimum SD. This again shows the dominating influence of the outer plies, for laminates in the bending mode.

The influence of change in fiber orientation on the SD of deflection

at the center of a square plate is shown in Figure 4.41. The results are presented for various levels of SD of input RVs. The trend here is similar to that given in Figure 4.17. At low levels of SD of input RVs, the SD of deflection is not influenced much by the change in fiber orientation. Fiber orientations which results in stiffer plates seem to have lower levels of SD of deflection.

4.6 SUMMARY

Application of the perturbation technique described in Chapter 3 to the problem of deflection of rectangular plates with randomness in basic material properties is demonstrated. In this chapter the formulation of the problem for various configurations of boundary conditions, stacking sequences, aspect ratios etc. have been presented. Results for various combinations of parameters involved have been presented. The first order perturbation formulation and some of the associated assumptions made have been validated by an independent Monte Carlo simulation.

This analysis shows that the first order perturbation technique adopted for the displacement response is sufficient to give accurate results for the problem discussed. In practice the overall effect is dependent on the extent of randomness exhibited by each one of the input random variables. The maximum effect on SD of deflection is mainly due to change in E_{11} . It is therefore necessary that experiments for evaluation of E_{11} should be performed very precisely to get accurate displacement response estimation. Most of the results show a linear trend for the range of variations considered. The Monte-Carlo simulation also exhibits a similar behavior. Hence we may conclude that, apart from the effect of linear perturbation analysis, the response relations themselves are linear in nature for the problem considered here. Fiber orientations which results in stiffer plates gives lower SD of deflection. In general, at low levels of SD of input RVs, change in AR, fiber orientation etc. doesn't have much influence on the SD of deflection. The outer plies, in general have a dominating influence on SD of deflection.

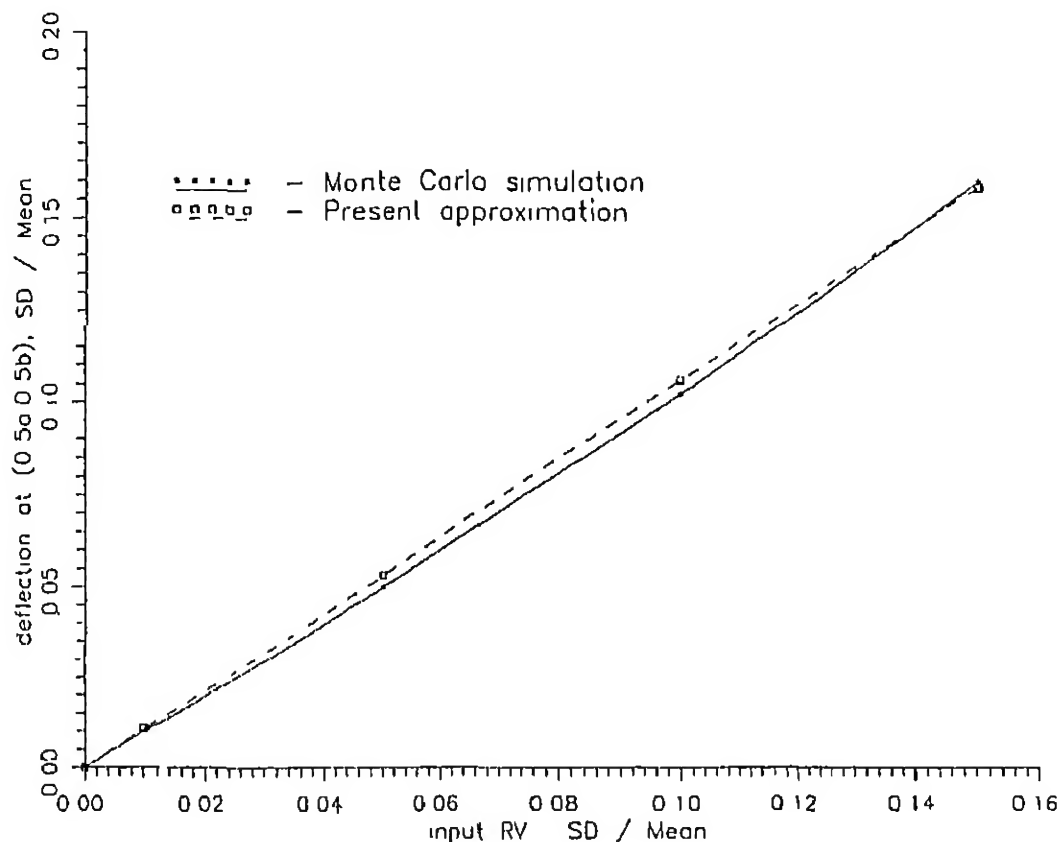


Figure 4.1: Comparison of results from a Monte Carlo simulation with the present approximation. Change of SD of deflection at the centre of the plate (0.5a, 0.5b), with SD of input RVs $[0^\circ]$ laminate, AR=1.5, all sides simply supported. Graphite/Epoxy

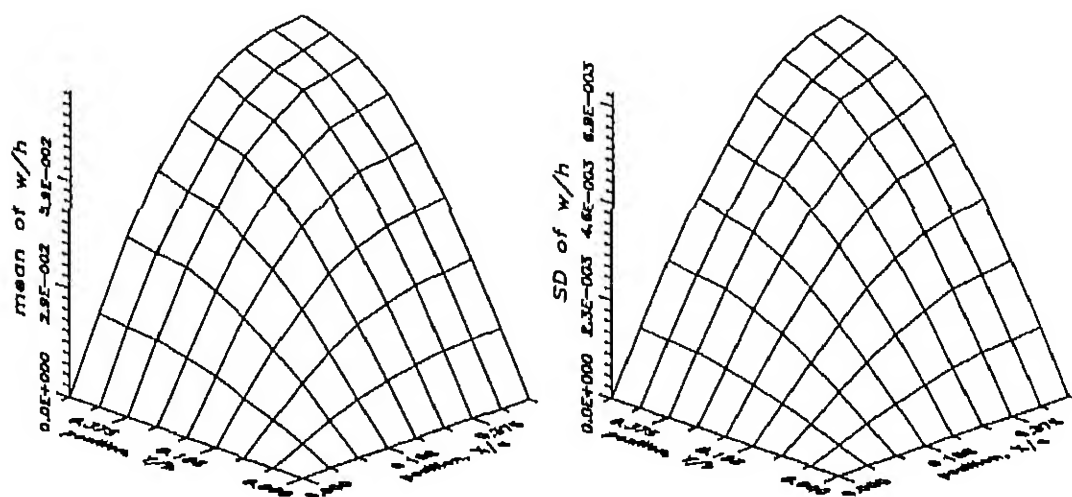


Figure 4.2: SD of input RVs 10 % of mean, $[90^\circ]$ laminate, AR=1.0, all sides simply supported. Distribution of mean of deflection and SD of deflection across $\frac{1}{4}^{th}$ of the plate. Graphite/Epoxy

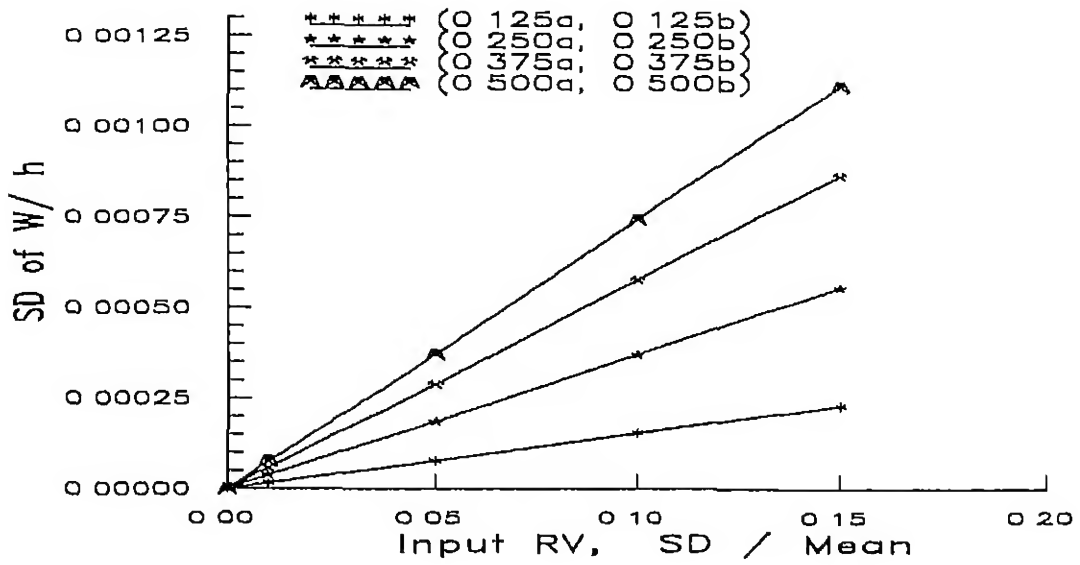


Figure 4.3 Sensitivity of SD of deflection to SD of input RV E_{22} SD of all other input RVs kept zero $[90^\circ]$ laminate, AR=1.0, all sides simply supported Graphite/Epoxy

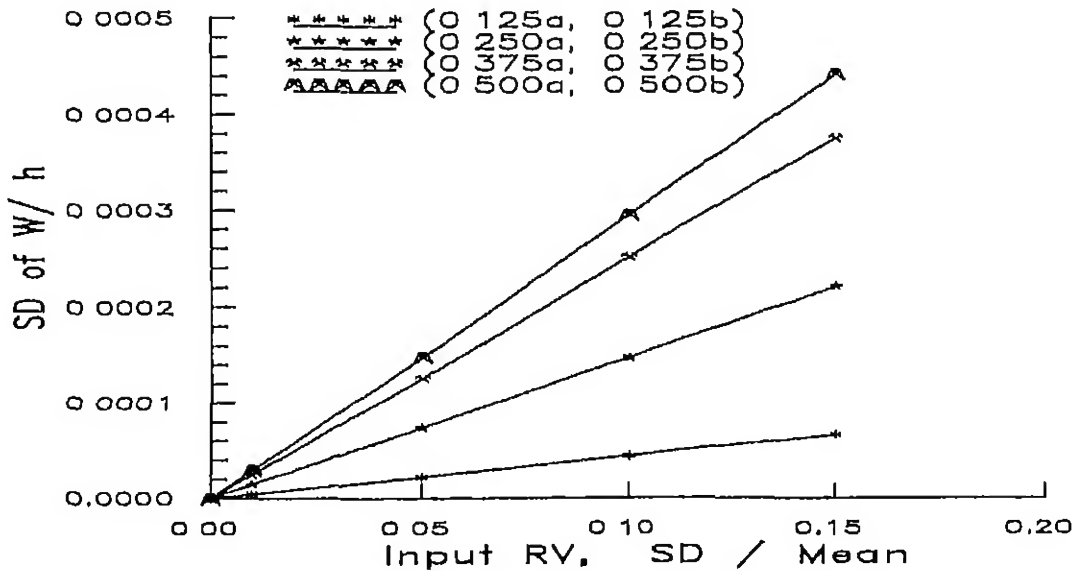


Figure 4.4: Sensitivity of SD of deflection to SD of input RV ν_{12} SD of all other input RVs kept zero $[90^\circ]$, AR=1.0, all sides simply supported Graphite/Epoxy

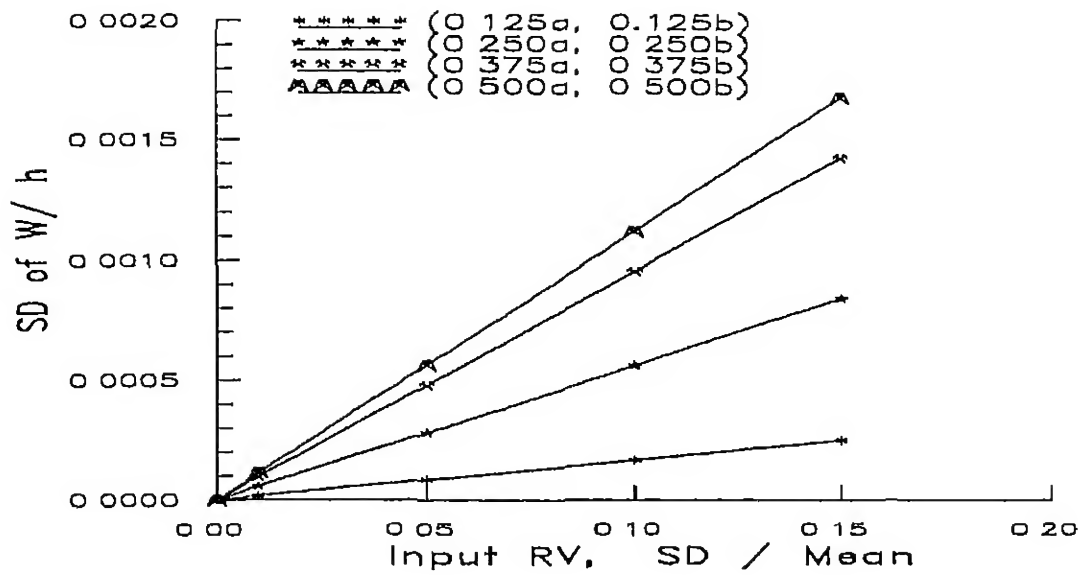


Figure 4.5 Sensitivity of SD of deflection to SD of input RV G_{12} SD of all other input RVs kept zero $[90^\circ]$ laminate, AR=1.0, all sides simply supported Graphite/Epoxy

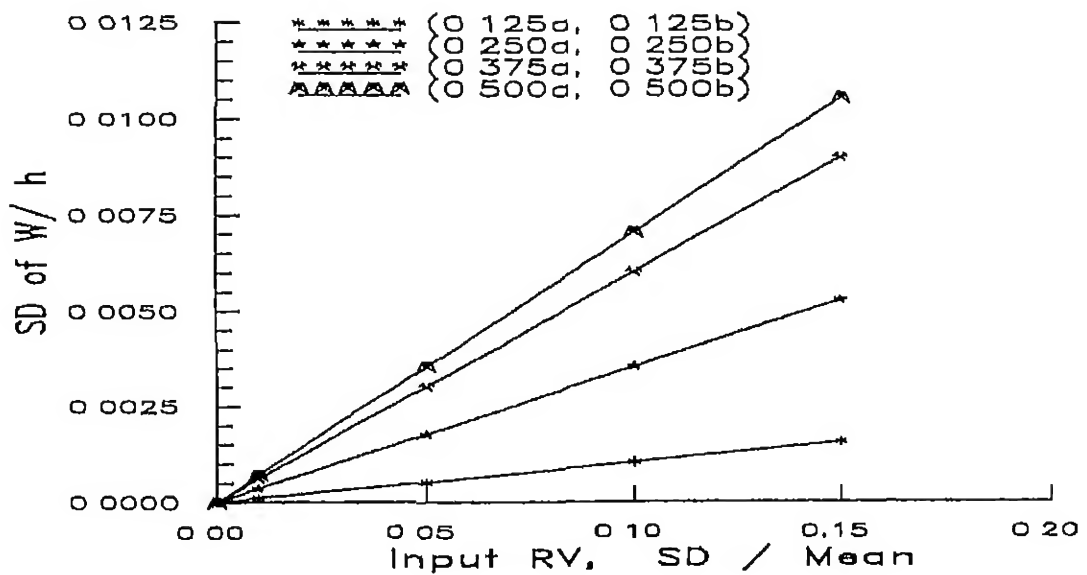


Figure 4.6: Sensitivity of SD of deflection to SD of input RV E_{11} SD of all other input RVs kept zero. $[90^\circ]$ laminate, AR=1.0, all sides simply supported Graphite/Epoxy

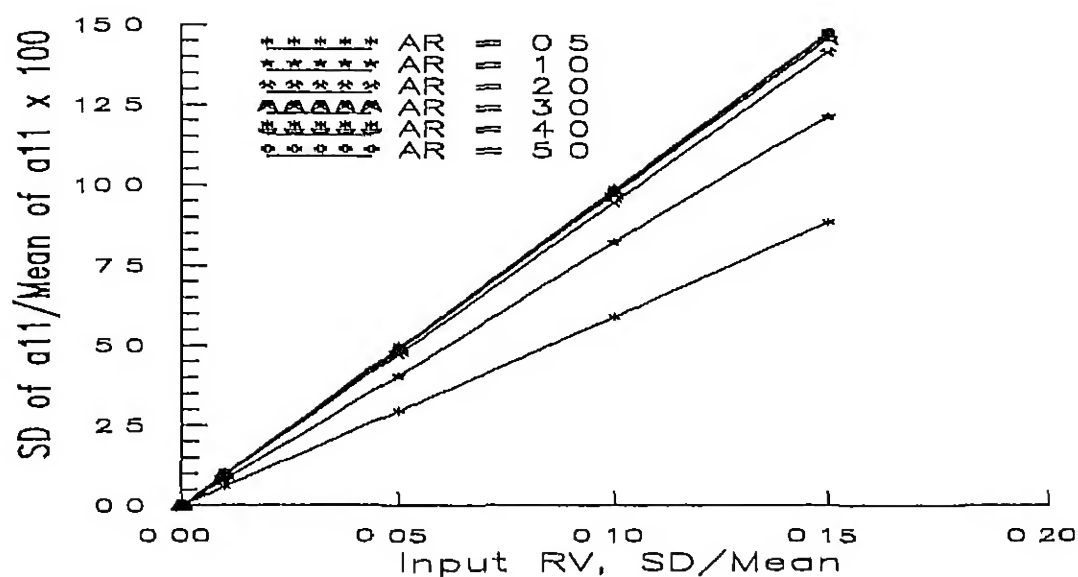


Figure 4.7 Change in SD of system parameter a_{11} , with SD of input RVs $[90^\circ]$ laminate, all sides simply supported Graphite/Epoxy

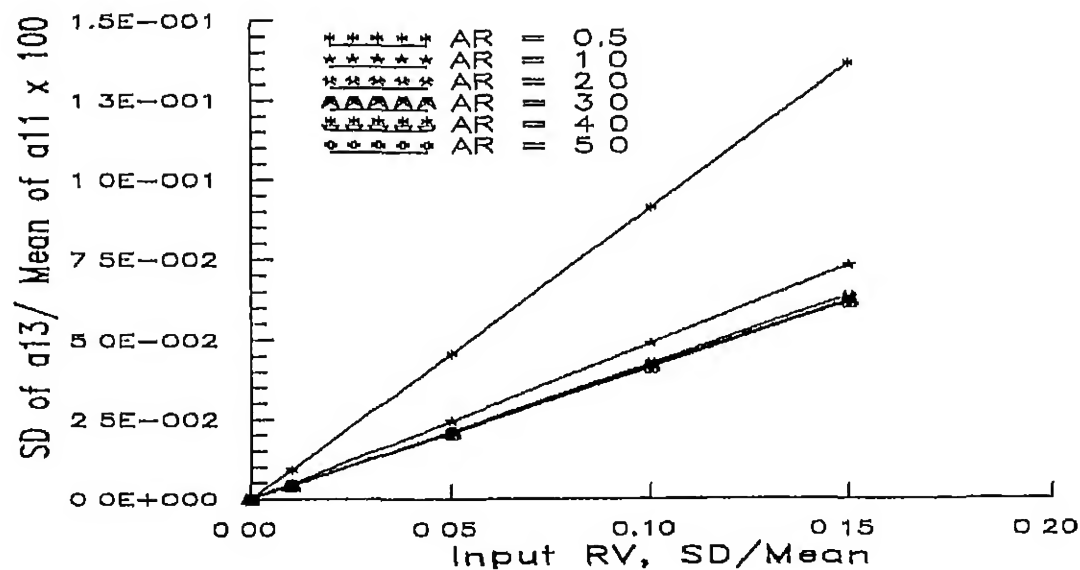


Figure 4.8: Change in SD of system parameter a_{13} , with SD of input RVs $[90^\circ]$ laminate, all sides simply supported Graphite/Epoxy

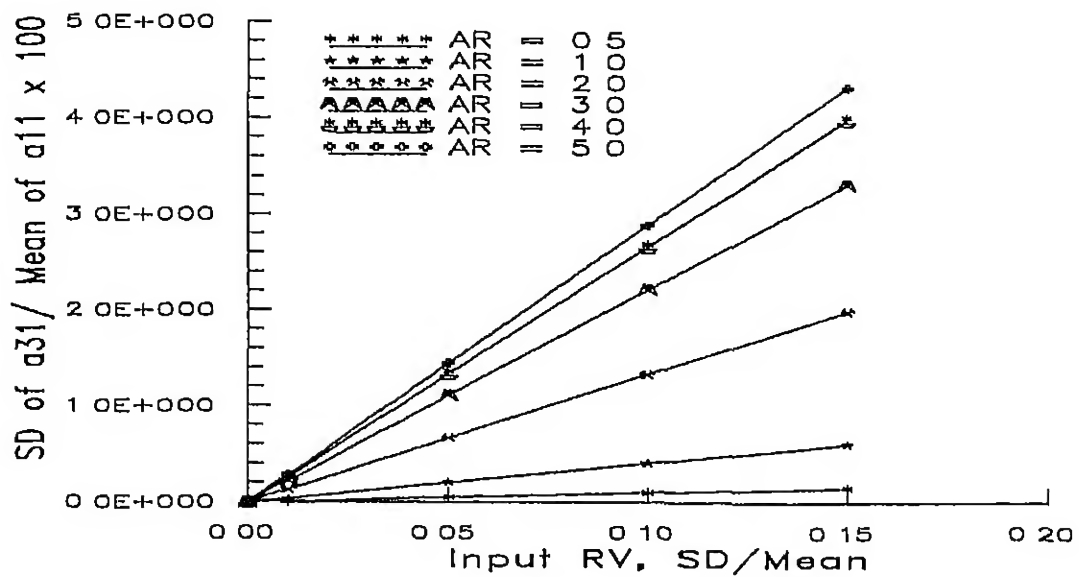


Figure 4.9 Change in SD of system parameter a_{31} , with SD of input RVs $[90^\circ]$ laminate, all sides simply supported Graphite/Epoxy

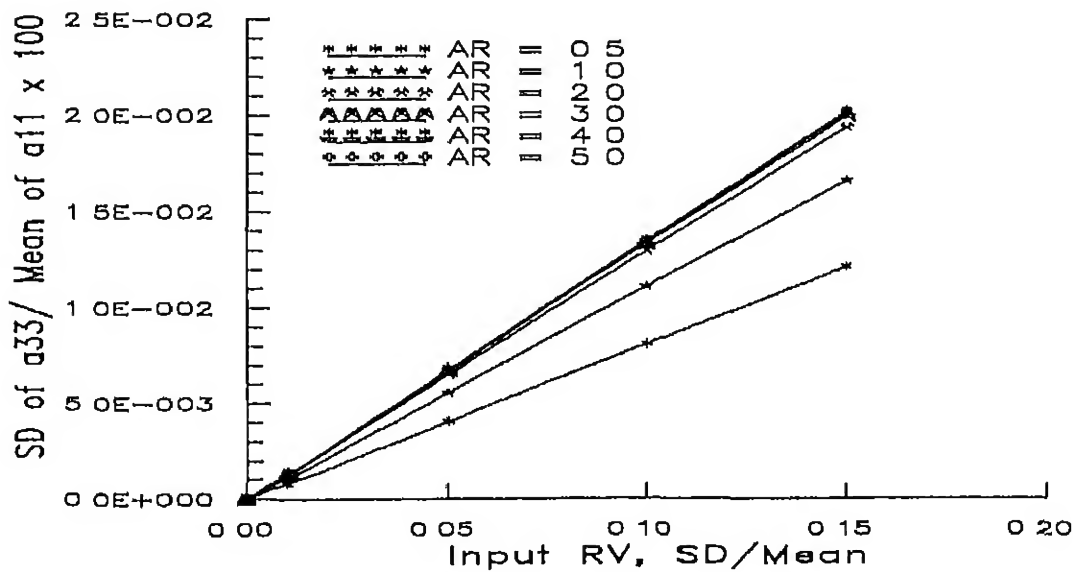


Figure 4.10 Change in SD of system parameter a_{33} , with SD of input RVs $[90^\circ]$ laminate, all sides simply supported Graphite/Epoxy

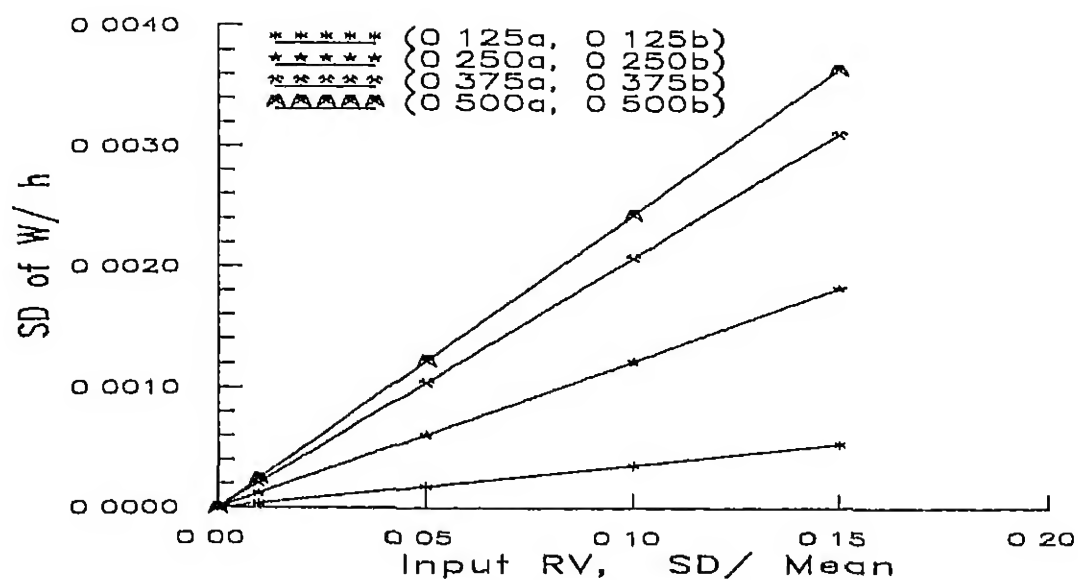


Figure 4.11 $[90^\circ]$ laminate, $AR=0.5$, all sides simply supported Change in SD of deflection with SD of input RVs Graphite/Epoxy

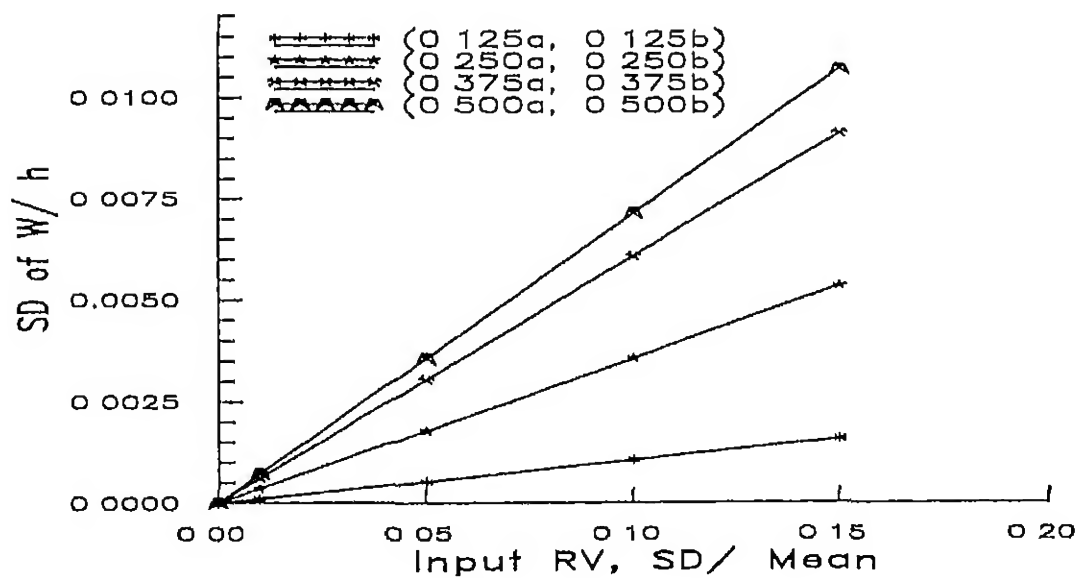


Figure 4.12: Change in SD of deflection, with SD of input RVs $[90^\circ]$ laminate, $AR=1$, all sides simply supported Graphite/Epoxy

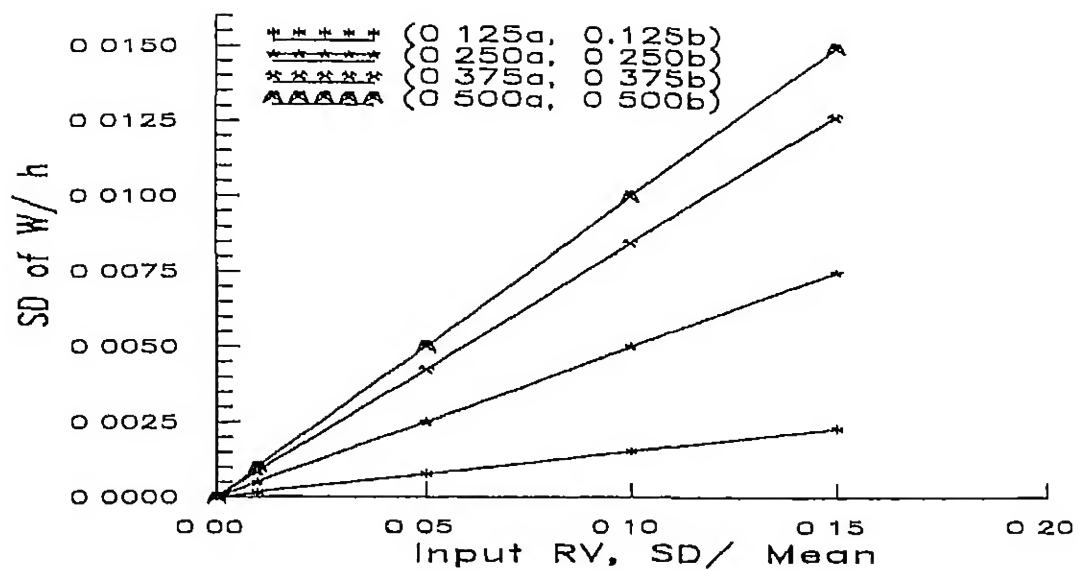


Figure 4.13 $[90^\circ]$ laminate, $AR=2$, all sides simply supported, Change in SD of deflection with SD of input RVs Graphite/Epoxy

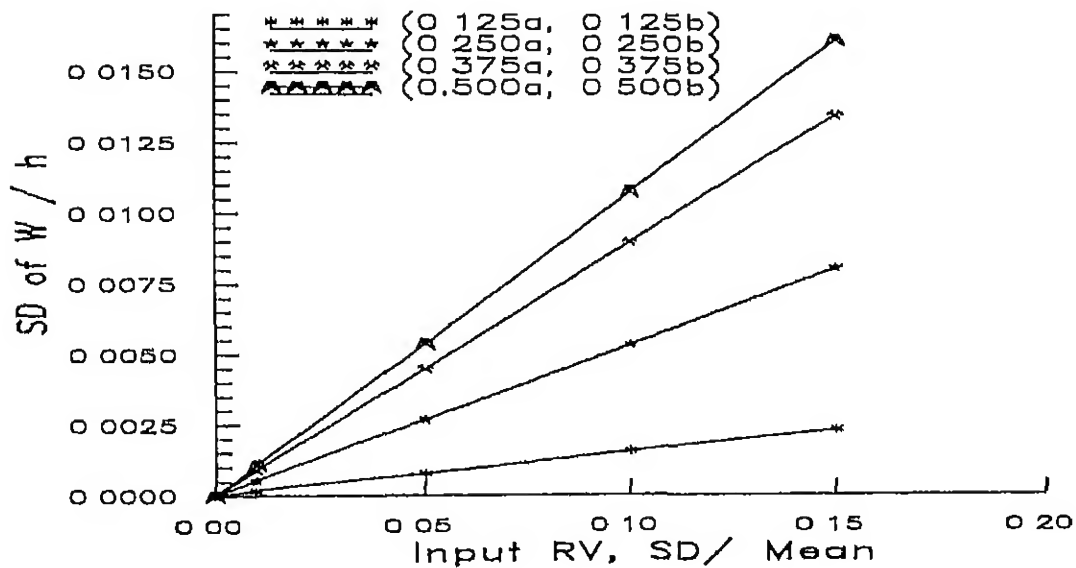


Figure 4.14. $[90^\circ]$ laminate, $AR=3$, all sides simply supported. Change in SD of deflection with SD of input RVs Graphite/Epoxy

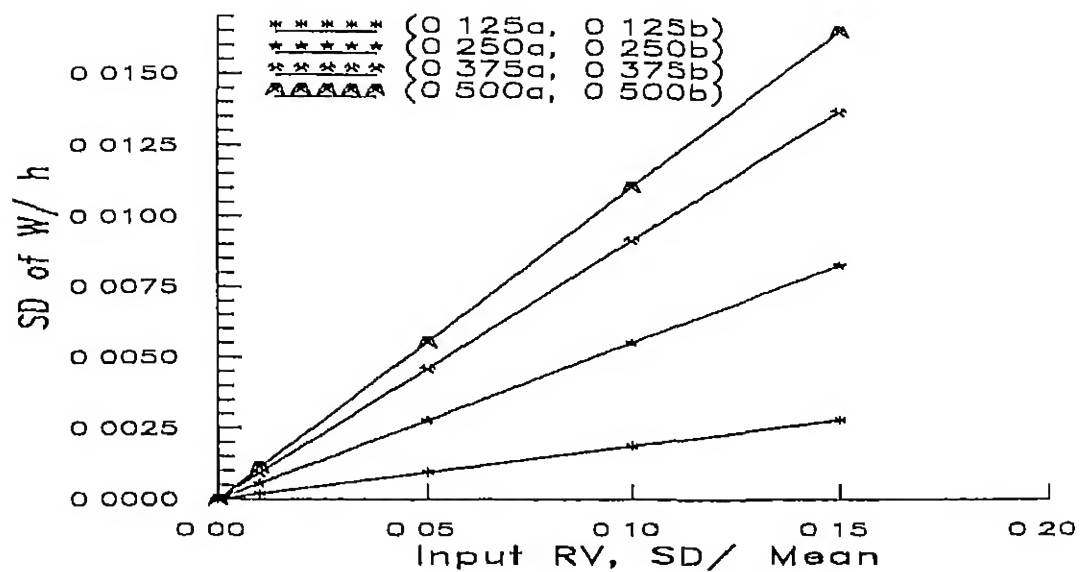


Figure 4.15 $[90^\circ]$ laminate, $AR=4$, all sides simply supported Change in SD of deflection with SD of input RVs Graphite/Epoxy

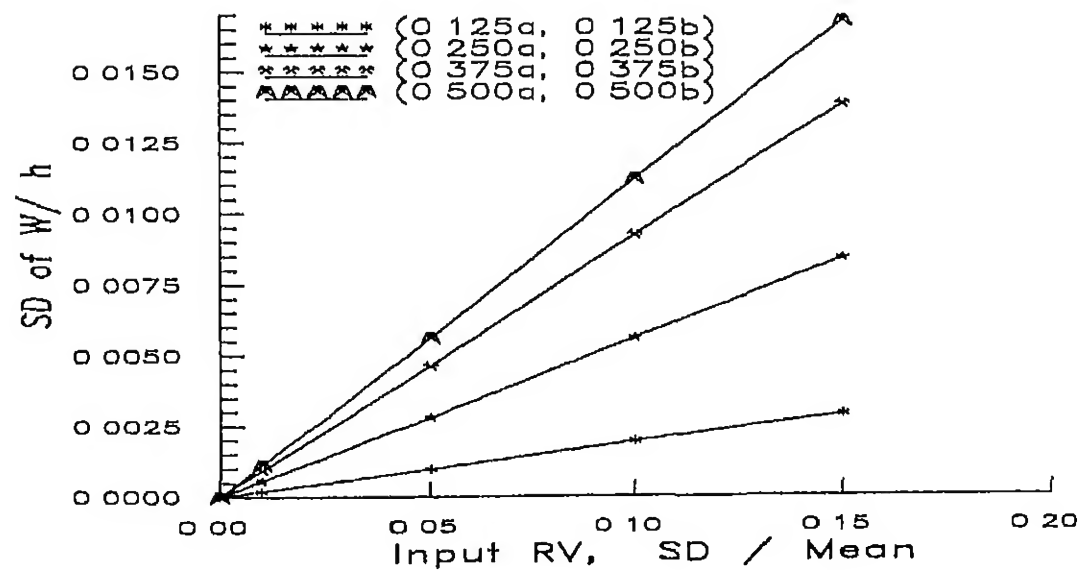


Figure 4.16: $[90^\circ]$ laminate, $AR=5$, all sides simply supported. Change in SD of deflection with SD of input RVs. Graphite/Epoxy

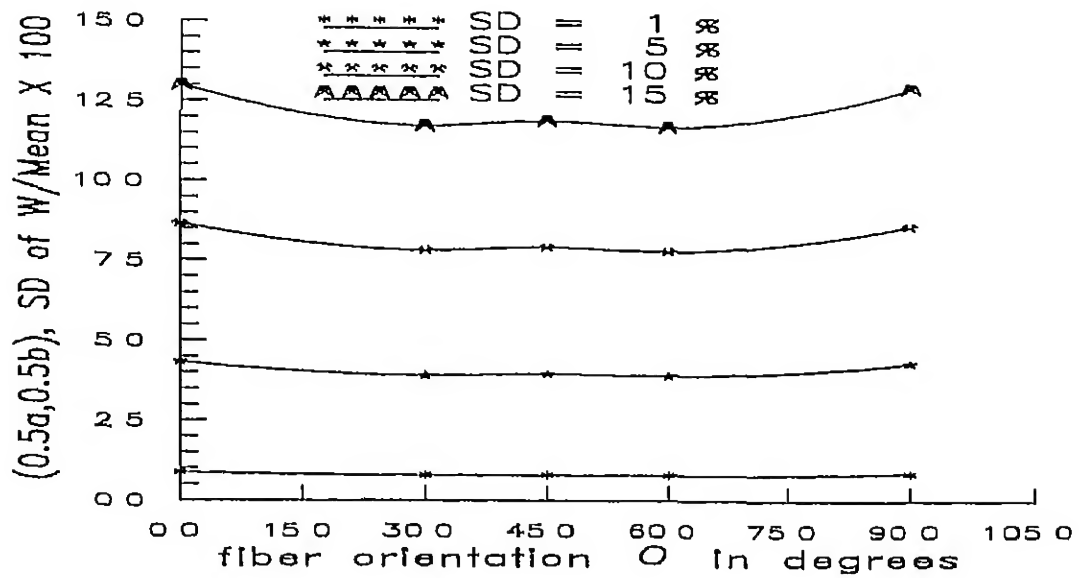


Figure 4.17 Variation of SD of deflection w at $(0.5a, 0.5b)$, with fiber orientation for different SDs of input RVs AR=1, all edges of the plate simply supported Graphite/Epoxy

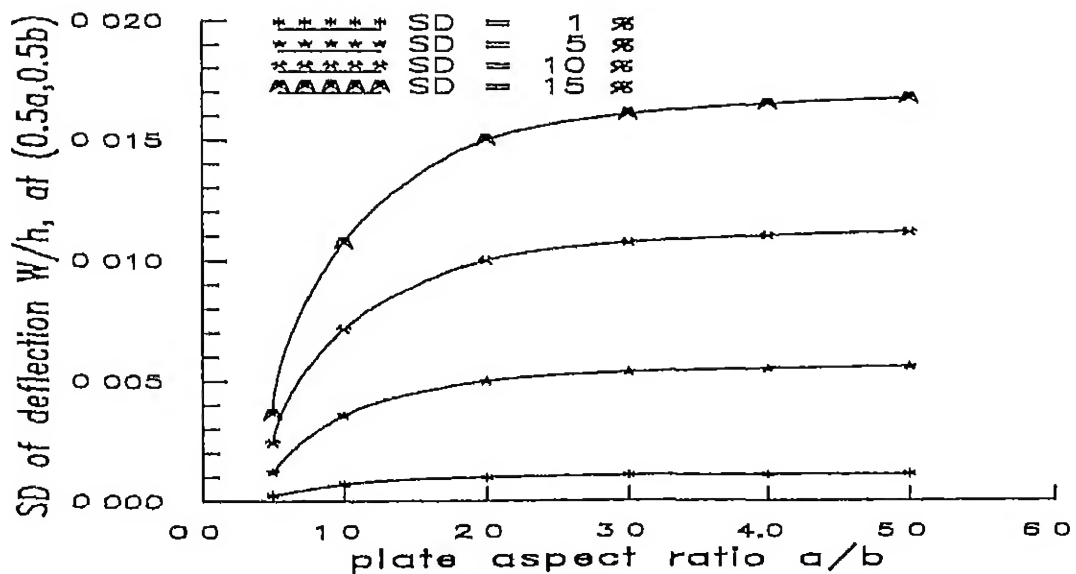


Figure 4.18: Variation of SD of deflection w at $(0.5a, 0.5b)$, with aspect ratio a/b of the plate for various input RV SDs Stacking sequence $[90^\circ]$ laminate, all edges of the plate simply supported Graphite/Epoxy

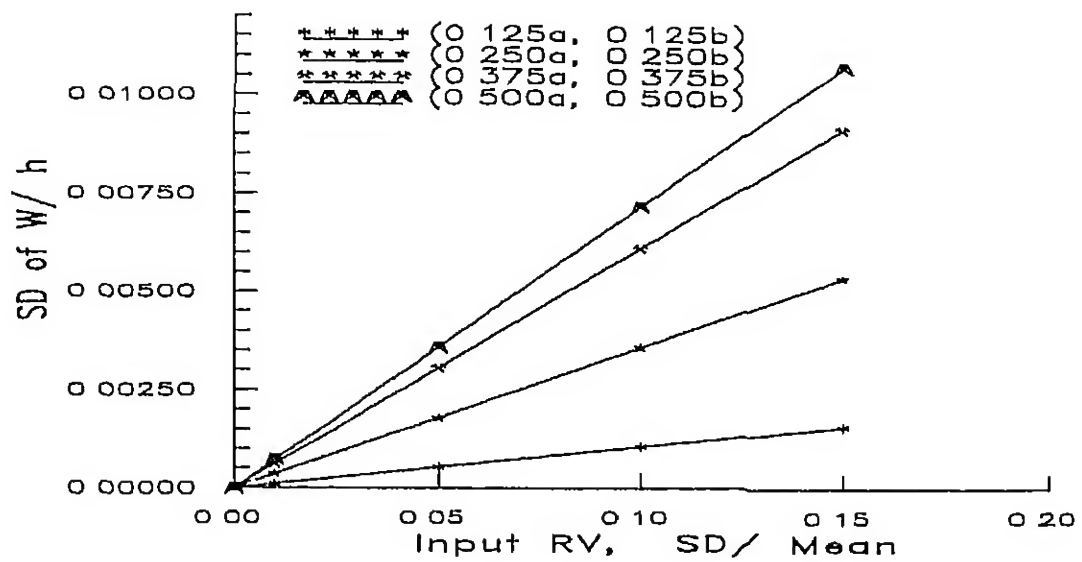


Figure 4 19 $[0^\circ]$ laminate, AR=1, all sides simply supported Change in SD of deflection with SD of input RVs Graphite/Epoxy

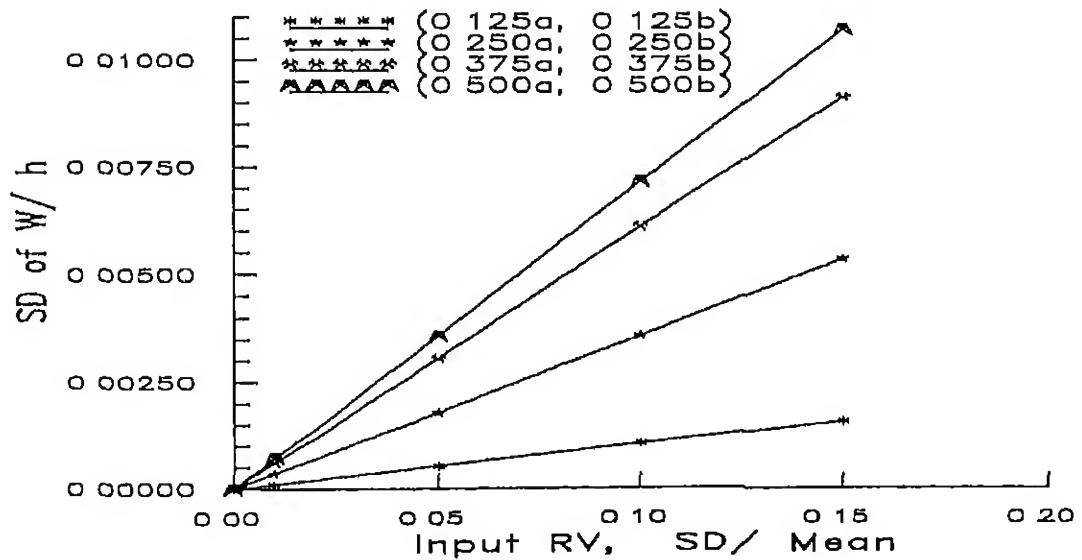


Figure 4 20: $[90^\circ/0^\circ]_s$ laminate, AR=1, all sides simply supported Change in SD of deflection with SD of input RVs Graphite/Epoxy

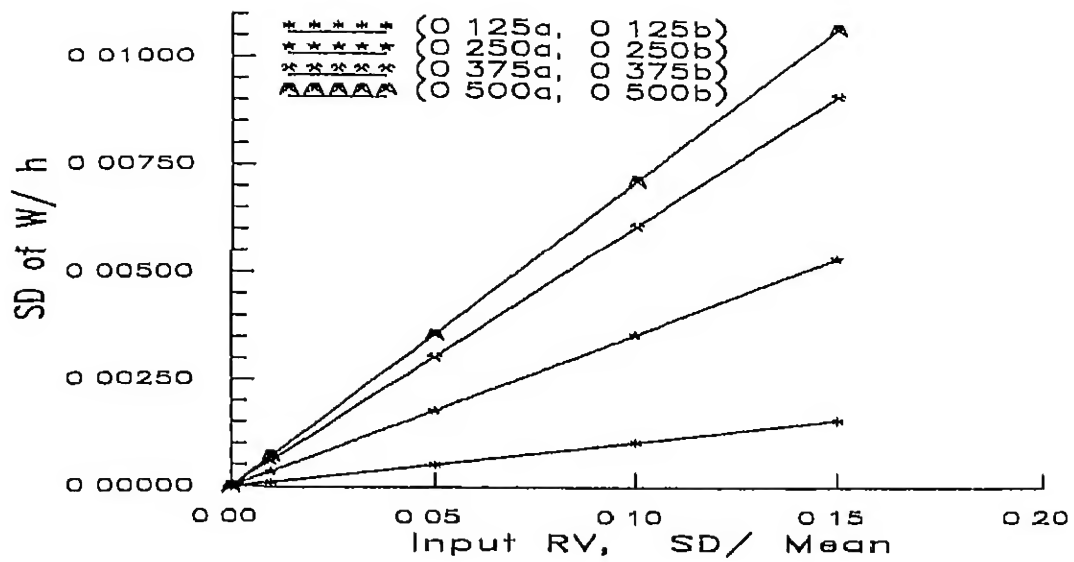


Figure 4.21 $[0^\circ/90^\circ]_s$ laminate, AR=1, all sides simply supported Change in SD of deflection with SD of input RVs Graphite/Epoxy

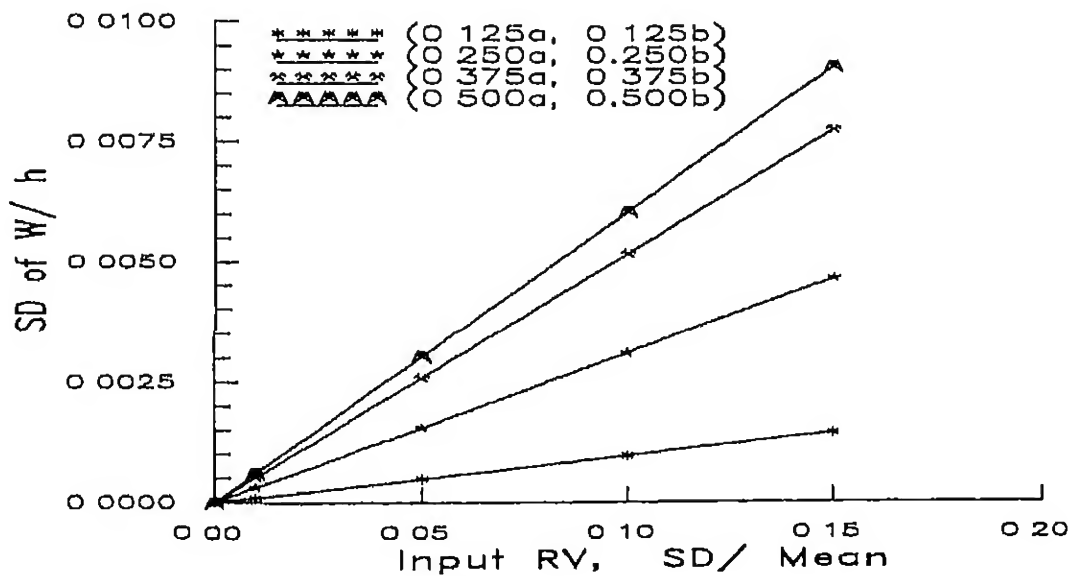


Figure 4.22: $[45^\circ]$ laminate, AR=1, all sides simply supported Change in SD of deflection with SD of input RVs Graphite/Epoxy

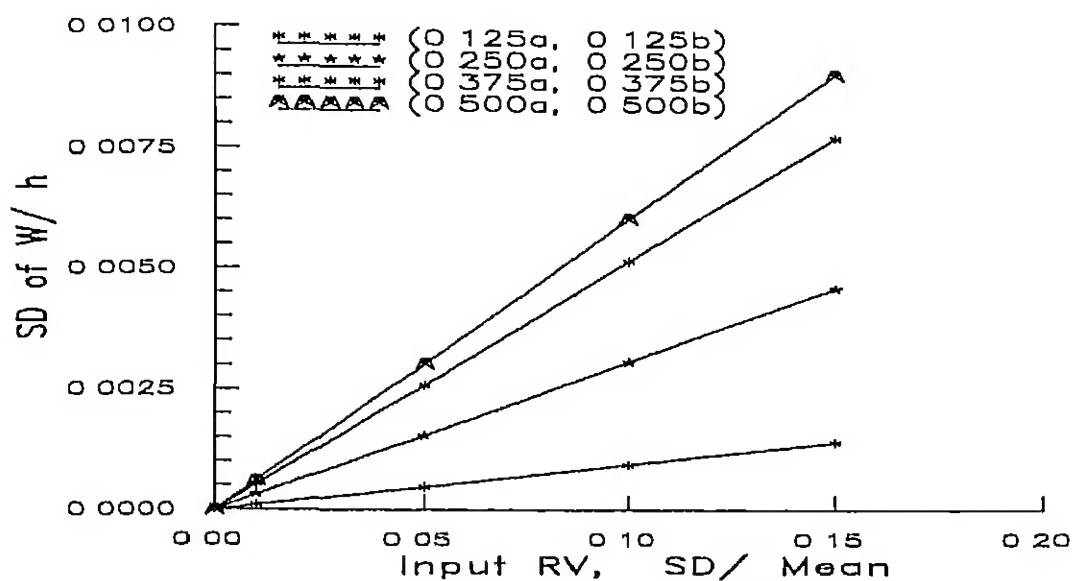


Figure 4.23 $[45^\circ/0^\circ]_s$ laminate, AR=1, all sides simply supported Change in SD of deflection with SD of input RVs Graphite/Epoxy

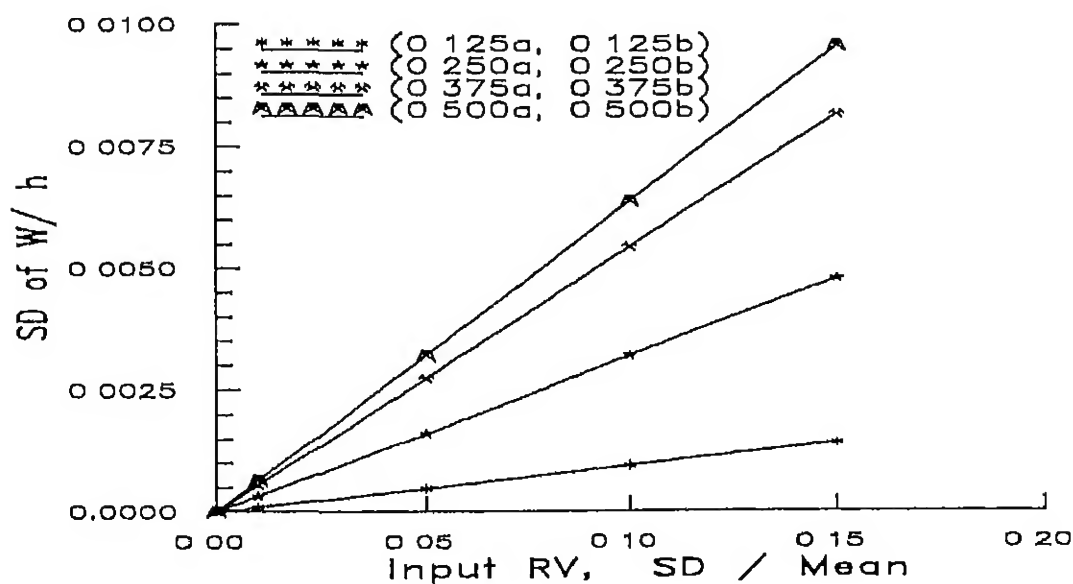


Figure 4.24: $[0^\circ/45^\circ/90^\circ/-45^\circ]_s$ laminate, AR=1, all sides simply supported Change in SD of deflection with SD of input RVs Graphite/Epoxy

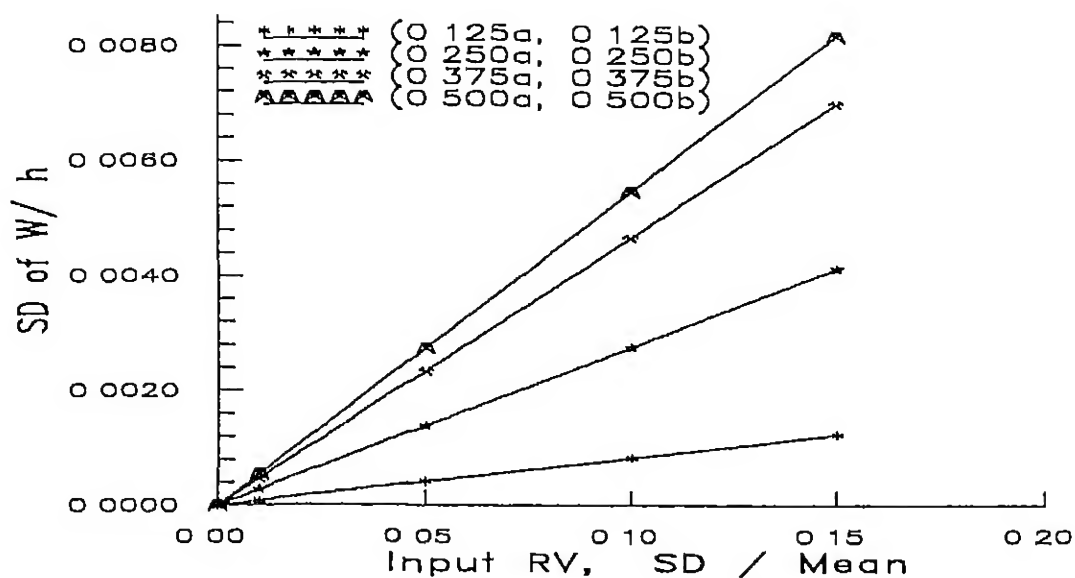


Figure 4.25. $[-45^\circ/45^\circ]$ laminate, $AR=1$, all sides simply supported Change in SD of deflection with SD of input RVs Graphite/Epoxy

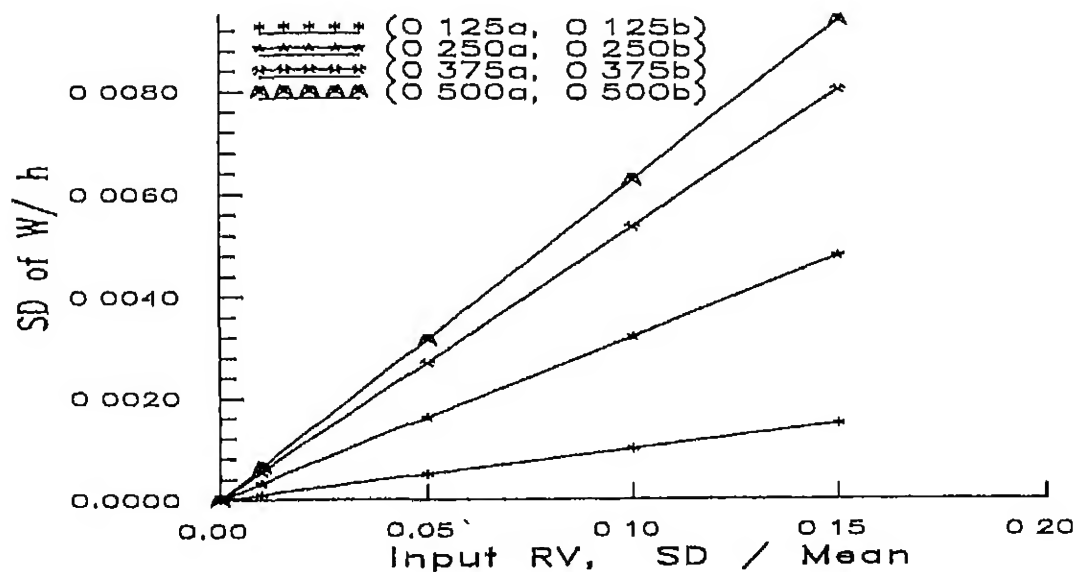


Figure 4.26. $[60^\circ]$ laminate, $AR=1$, all sides simply supported Change in SD of deflection with SD of input RVs. Graphite/Epoxy

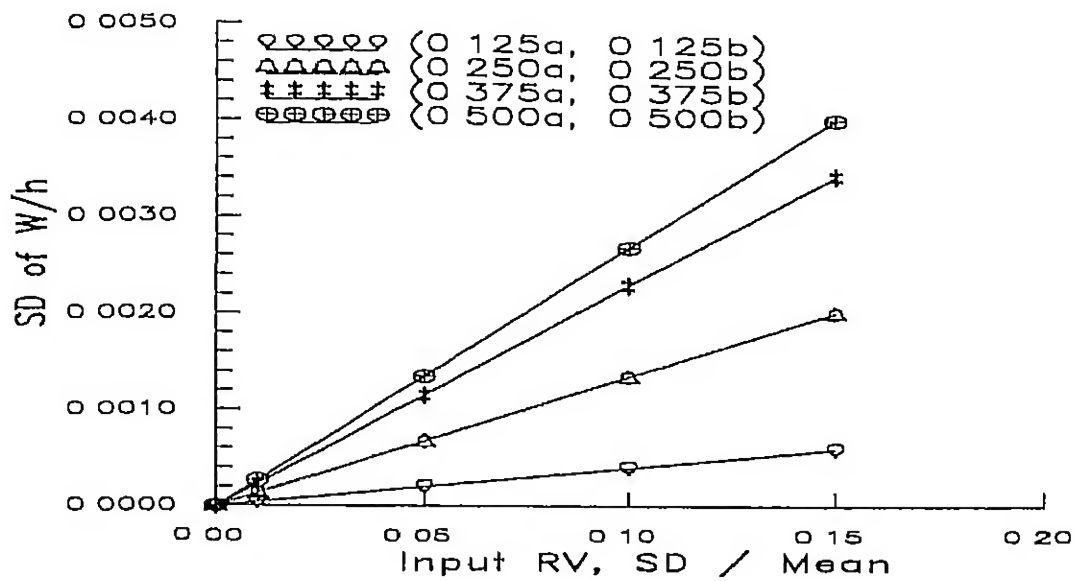


Figure 4.27: Test case Glass/Epoxy composite Change in SD of deflection, with SD of input RVs [90°] laminate, AR=0.5, all sides simply supported

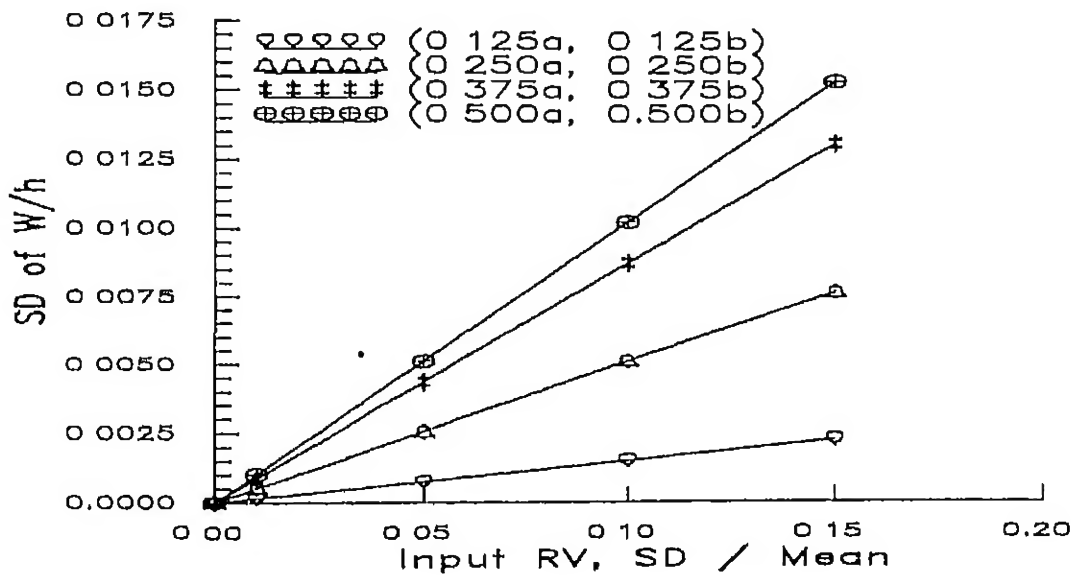


Figure 4.28: Test case Glass/Epoxy composite Change in SD of deflection, with SD of input RVs [90°] laminate, AR=1.0, all sides simply supported

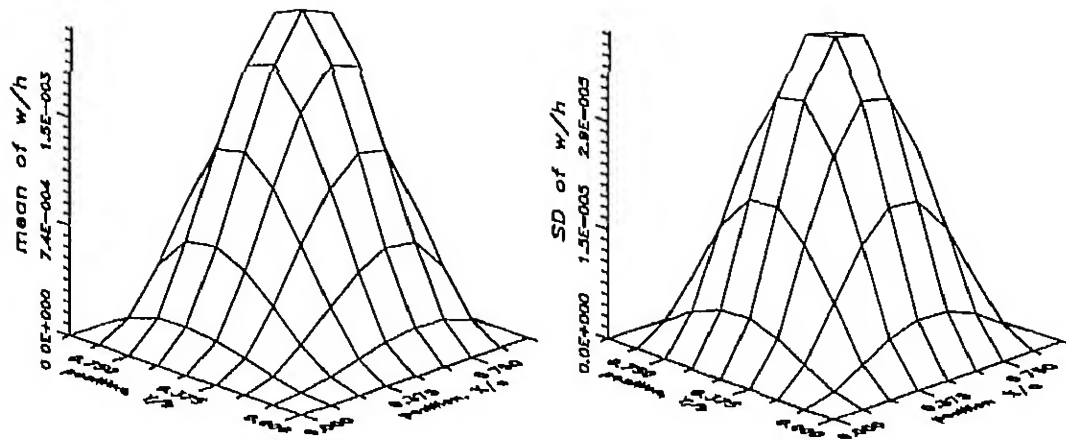


Figure 4.31 SD of input RVs 10 % of mean, $[90^\circ]$ laminate, $AR=1.0$, all sides clamped Distribution of mean of deflection and SD of deflection across the full plate Graphite/Epoxy

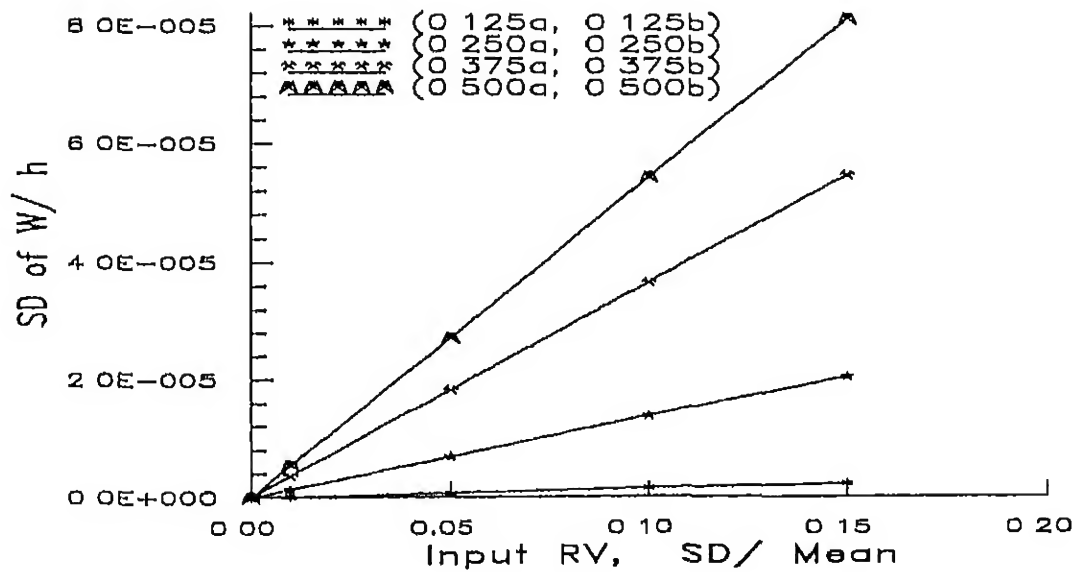


Figure 4.32. $[0^\circ]$ laminate, $AR=1$, all sides clamped Change in SD of deflection with SD of input RVs Graphite/Epoxy

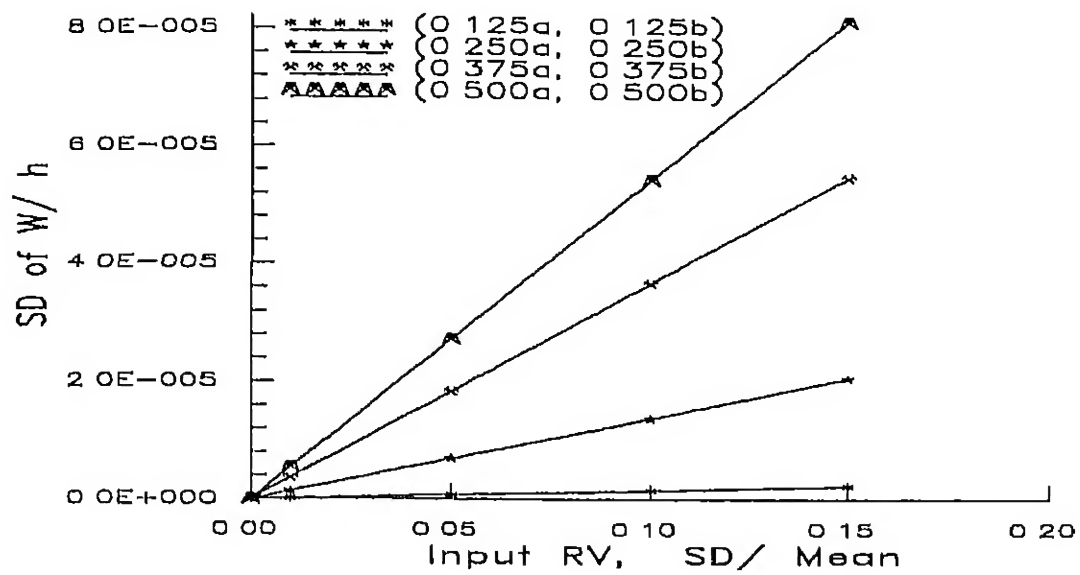


Figure 4.33 $[90^\circ]$ laminate, $AR=1$, all sides clamped Change in SD of deflection with SD of input RVs Graphite/Epoxy

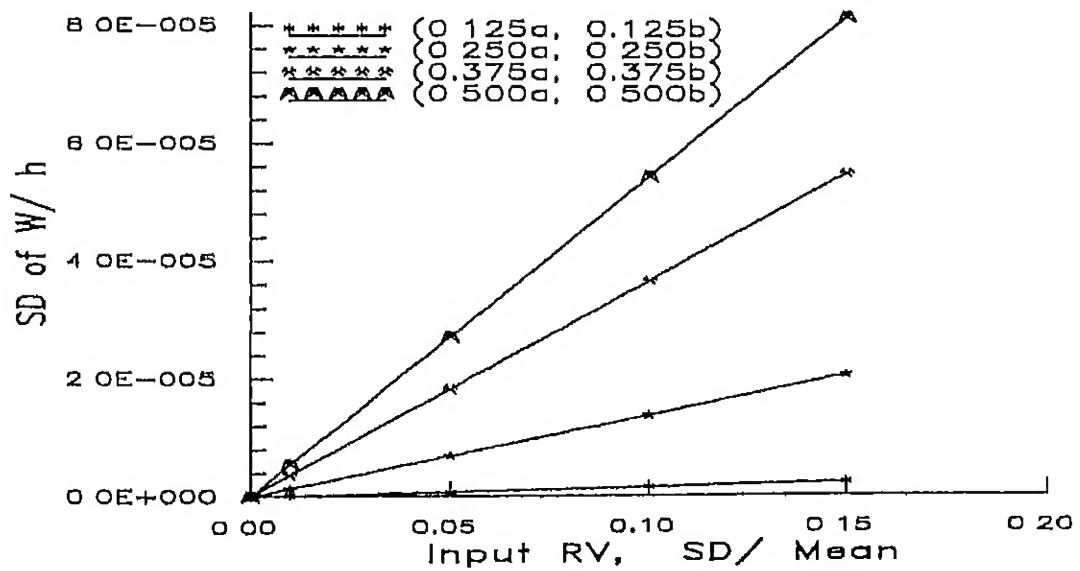


Figure 4.34. $[90^\circ/0^\circ]$ laminate, $AR=1$, all sides clamped Change in SD of deflection with SD of input RVs Graphite/Epoxy

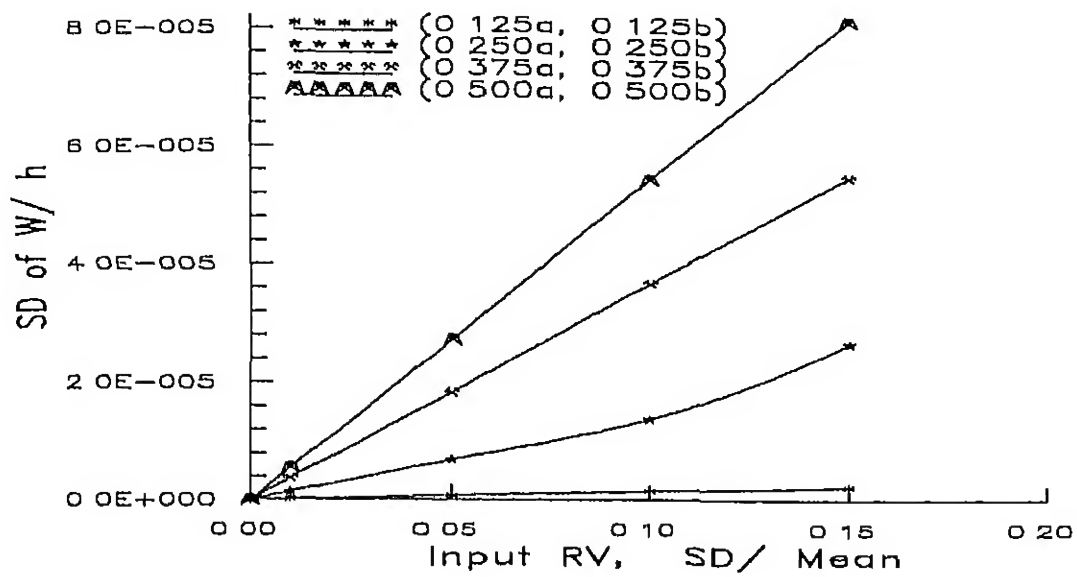


Figure 4.35. $[0^\circ/90^\circ]$ laminate, AR=1, all sides clamped Change in SD of deflection with SD of input RVs Graphite/Epoxy

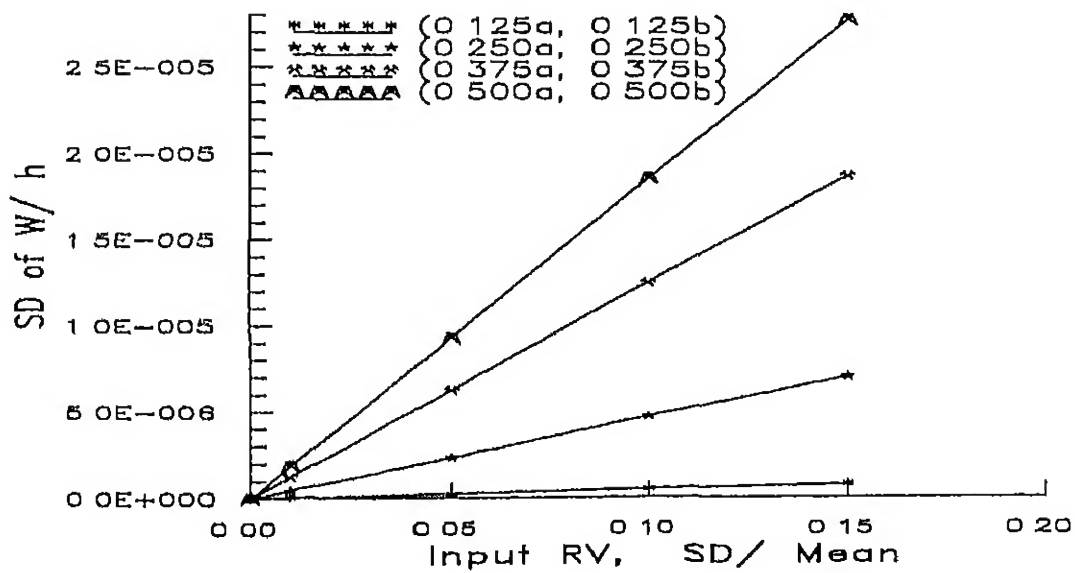


Figure 4.36. $[45^\circ]$ laminate, AR=1, all sides clamped Change in SD of deflection with SD of input RVs. Graphite/Epoxy.

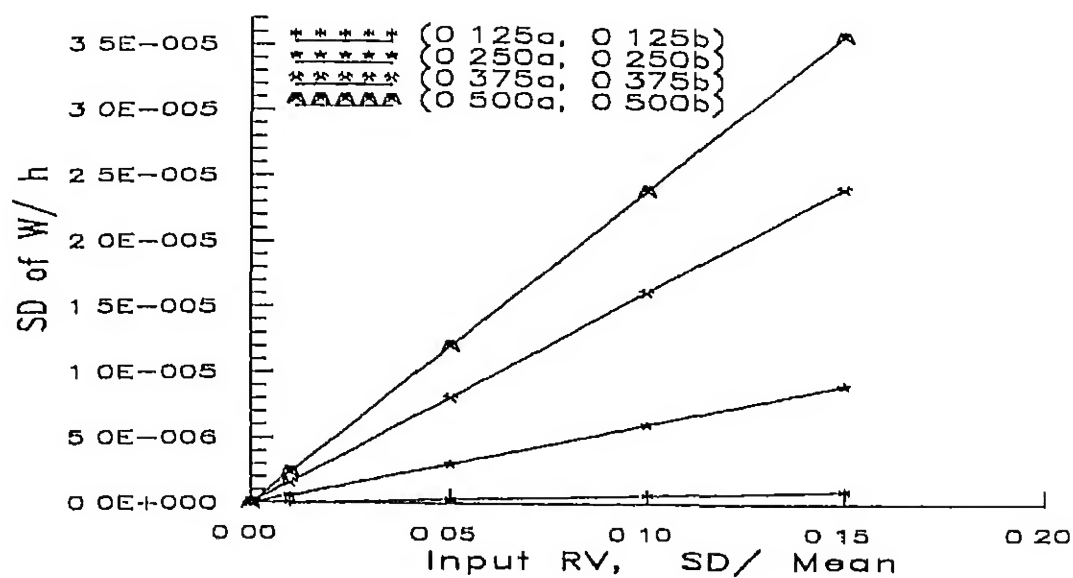


Figure 4.37. [45°/0°], laminate, AR=1, all sides clamped Change in SD of deflection with SD of input RVs Graphite/Epoxy

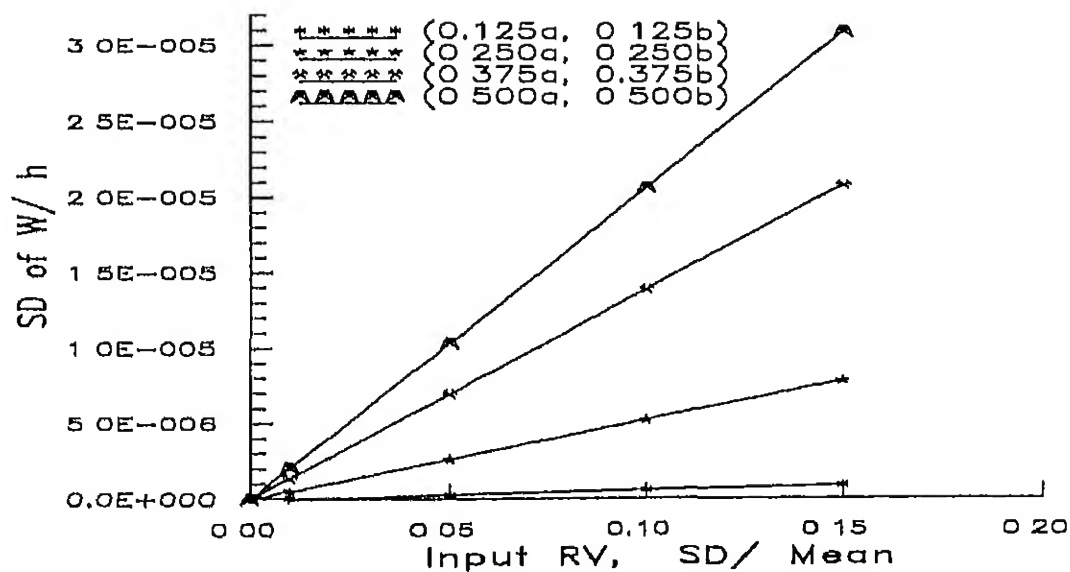


Figure 4.38. [60°] laminate, AR=1, all sides clamped Change in SD of deflection with SD of input RVs Graphite/Epoxy

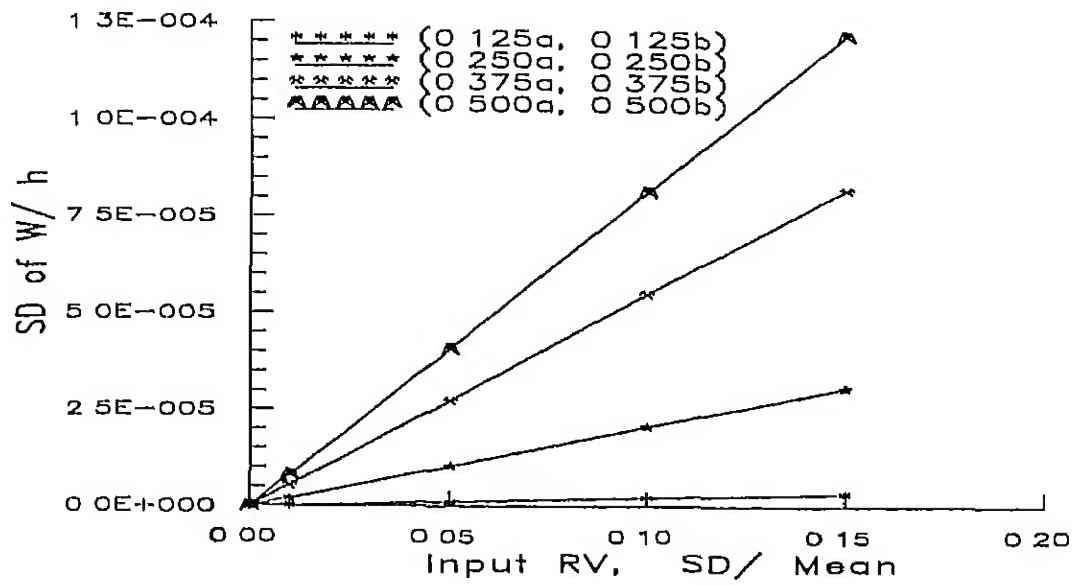


Figure 4.39 $[-45^\circ/45^\circ]$, laminate, AR=1, all sides clamped Change in SD of deflection with SD of input RVs Graphite/Epoxy

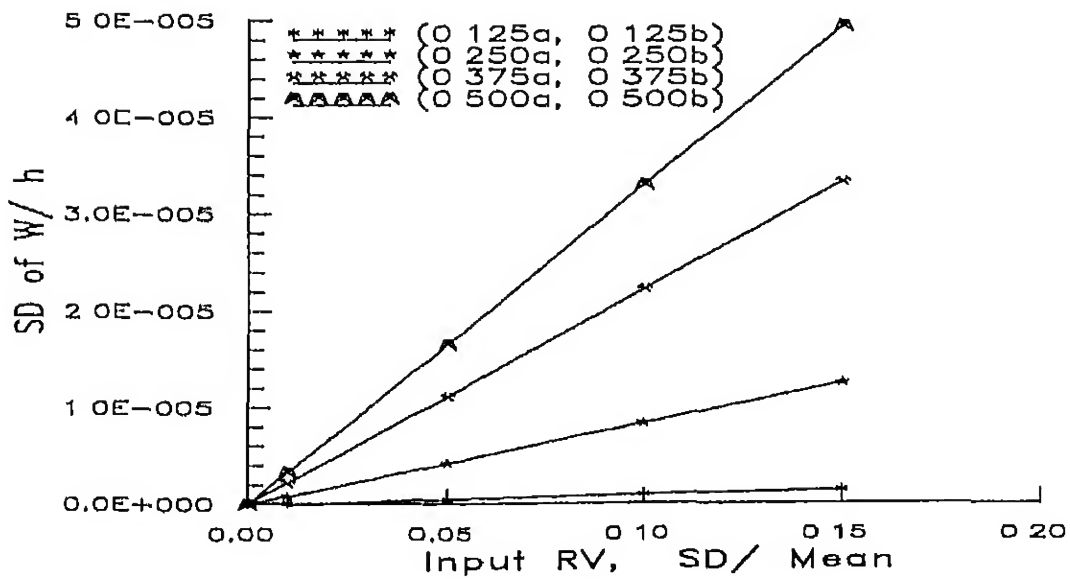


Figure 4.40: $[0^\circ/45^\circ/90^\circ/-45^\circ]$, laminate, AR=1, all sides clamped Change in SD of deflection with SD of input RVs Graphite/Epoxy

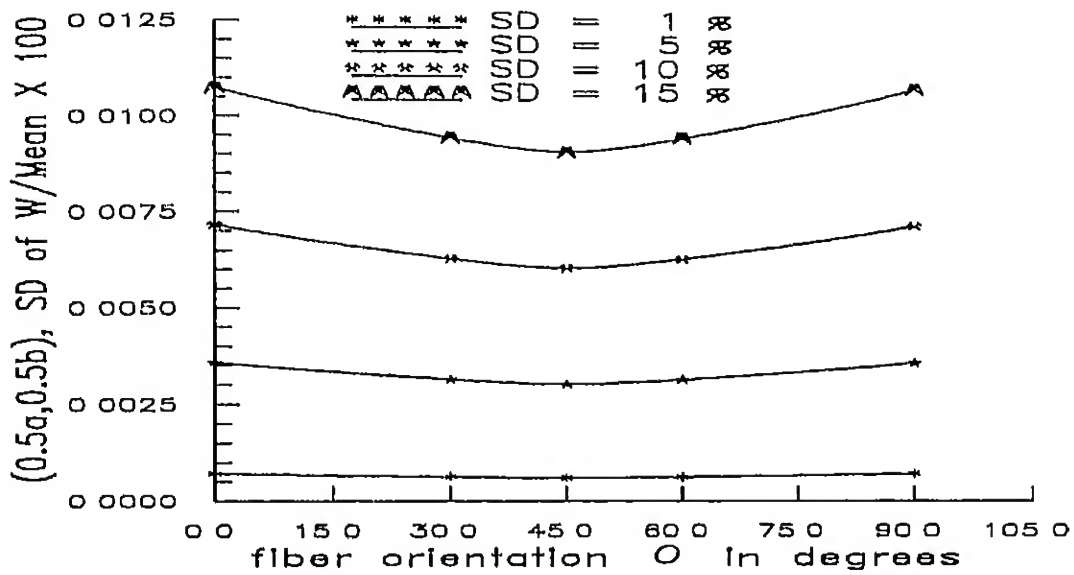


Figure 4.41: Variation of SD of deflection w at $(0.5a, 0.5b)$, with fiber orientation for different SDs of input RVs. $AR=1$, all edges of the plate clamped Graphite/Epoxy

Chapter 5

COMPOSITE PLATES — FREE VIBRATION ANALYSIS

5.1 INTRODUCTION

The problem of rectangular plates undergoing free vibrations is considered in this chapter. The classical laminated plate theory is used to obtain the governing equations. The randomness in basic material parameters is introduced later, using the techniques described in Chapter 3. The geometry of the plate is defined by Figure 3.1.

5.2 FORMULATION

Consider a rectangular laminated composite plate undergoing free oscillations. The governing equations of such a system in terms of displacements (u^0 , v^0 , and w) and the stiffness matrix terms (A_{ij} , B_{ij} , and

D_{17}) is given by [40]

$$\begin{aligned}
 & A_{11} \frac{\partial^2 u^0}{\partial t^2} + 2A_{16} \frac{\partial^2 u^0}{\partial x \partial y} + A_{66} \frac{\partial^2 u^0}{\partial y^2} + A_{16} \frac{\partial^2 v^0}{\partial x^2} \\
 & + (A_{12} + A_{66}) \frac{\partial^2 v^0}{\partial x \partial y} + A_{26} \frac{\partial^2 v^0}{\partial y^2} - B_{11} \frac{\partial^3 w}{\partial x^3} \\
 & - 3B_{16} \frac{\partial^3 w}{\partial x^2 \partial y} - (B_{12} + 2B_{66}) \frac{\partial^3 w}{\partial x \partial y^2} - B_{26} \frac{\partial^3 w}{\partial y^3} = \rho \frac{\partial^2 u^0}{\partial t^2} \quad (5.1)
 \end{aligned}$$

$$\begin{aligned}
 & A_{16} \frac{\partial^2 u^0}{\partial x^2} + (A_{12} + A_{66}) \frac{\partial^2 u^0}{\partial x \partial y} + A_{26} \frac{\partial^2 u^0}{\partial y^2} + A_{66} \frac{\partial^2 v^0}{\partial x^2} \\
 & + 3A_{26} \frac{\partial^2 v^0}{\partial x \partial y} + A_{22} \frac{\partial^2 v^0}{\partial y^2} - B_{16} \frac{\partial^3 w}{\partial x^3} - (B_{12} + 2B_{66}) \frac{\partial^3 w}{\partial x^2 \partial y} \\
 & - 3B_{26} \frac{\partial^3 w}{\partial x \partial y^2} - B_{22} \frac{\partial^3 w}{\partial y^3} = \rho \frac{\partial^2 v^0}{\partial t^2} \quad (5.2)
 \end{aligned}$$

$$\begin{aligned}
 & D_{11} \frac{\partial^4 w}{\partial x^4} + 4D_{16} \frac{\partial^4 w}{\partial x^3 \partial y} + 2(D_{12} + 2D_{66}) \frac{\partial^4 w}{\partial x^2 \partial y^2} + 4D_{26} \frac{\partial^4 w}{\partial x \partial y^3} \\
 & + D_{22} \frac{\partial^4 w}{\partial y^4} - B_{11} \frac{\partial^3 u^0}{\partial x^3} - 3B_{16} \frac{\partial^3 u^0}{\partial x^2 \partial y} - (B_{12} + 2B_{66}) \frac{\partial^3 u^0}{\partial x \partial y^2} \\
 & - B_{26} \frac{\partial^3 u^0}{\partial y^3} - B_{16} \frac{\partial^3 v^0}{\partial x^3} - (B_{12} + 2B_{66}) \frac{\partial^3 v^0}{\partial x^2 \partial y} \\
 & - 3B_{26} \frac{\partial^3 v^0}{\partial x \partial y^2} - B_{22} \frac{\partial^3 v^0}{\partial y^3} + \rho \frac{\partial^2 w}{\partial t^2} = 0 \quad (5.3)
 \end{aligned}$$

Equations 5.1, 5.2 and 5.3 can be simplified based on stacking sequence.

5.3 SPECIALLY ORTHOTROPIC LAMINATED PLATE

In specially orthotropic laminates all the elements of $[B]$ matrix are identically zero. Other coupling terms like A_{16}, A_{26} and D_{16}, D_{26} are also absent. The only stiffness matrix terms present are D_{11}, D_{22}, D_{12} and D_{66} . Again here we are concerned only with the transverse oscillations of the plate. Owing to these simplifications several terms drop out from

the general equations given above and result in a simplified governing equation as

$$D_{11} \frac{\partial^4 w}{\partial x^4} + 2(D_{12} + 2D_{66}) \frac{\partial^4 w}{\partial x^2 \partial y^2} + D_{22} \frac{\partial^4 w}{\partial y^4} + \rho \frac{\partial^2 w}{\partial t^2} = 0 \quad (5.4)$$

Closed form solution for Equation 5.4 can be found only for the case of some specialized boundary conditions

5.3.1 Simply Supported Plate

Here, we consider rectangular composite plates with all the four sides simply supported. Even though closed form solution can be found for the Equation 5.4 with this boundary condition, we try to attempt the solution using energy formulation. The simplified energy criterion for this problem assuming no lateral or in-plane loads is

$$\text{Total potential, } \Pi_p = U + T = \text{stationary value} \quad (5.5)$$

Where U is the strain energy and T is the kinetic energy. Thus for the present case is:

$$\begin{aligned} \Pi_p &= U + T = \frac{1}{2} \int_0^b \int_0^a \left[D_{11} \left(\frac{\partial^2 w}{\partial x^2} \right)^2 + 2D_{12} \frac{\partial^2 w}{\partial x^2} \frac{\partial^2 w}{\partial y^2} \right. \\ &\quad \left. + D_{22} \left(\frac{\partial^2 w}{\partial y^2} \right)^2 + 4D_{66} \left(\frac{\partial^2 w}{\partial x \partial y} \right)^2 - \rho \omega^2 w^2 \right] dx dy \\ &= \text{stationary value} \end{aligned} \quad (5.6)$$

The boundary conditions along the edges of the plate for the case when all the four edges of the plate are simply supported are defined by

along $x = 0$ and $x = a$ for all y

$$\begin{aligned} w &= 0 \\ M_x &= -D_{11} \frac{\partial^2 w}{\partial x^2} - D_{12} \frac{\partial^2 w}{\partial y^2} \\ &= 0 \end{aligned} \quad (5.7)$$

along $y = 0$ and $y = b$ for all x

$$\begin{aligned} w &= 0 \\ M_y &= -D_{12} \frac{\partial^2 w}{\partial x^2} - D_{22} \frac{\partial^2 w}{\partial y^2} \\ &= 0 \end{aligned} \quad (5.8)$$

The Rayleigh–Ritz technique can be used to solve Equation 5.6 for the boundary conditions specified by Equations 5.7 and 5.8. A series approximation for the transverse deflection $w(x, y)$, satisfying the boundary conditions can be defined as:

$$w(x, y) = \sum_{m=1}^M \sum_{n=1}^N a_{mn} X_m(x) Y_n(y) \quad (5.9)$$

Here $X_m(x)$ and $Y_n(y)$ are eigen-functions that satisfy the set of boundary conditions considered. Substituting Equation 5.9 in 5.6 and applying the conditions given by Equations 5.7 and 5.8 we get $M \times N$ homogeneous

algebraic equations

$$\begin{aligned}
 \sum_{i=1}^M \sum_{j=1}^N \left\{ D_{11} \int_0^a \frac{d^2 X_i}{dx^2} \frac{d^2 X_m}{dx^2} dx \int_0^b Y_j Y_n dy \right. \\
 + D_{12} \left[\int_0^a X_m \frac{d^2 X_i}{dx^2} dx \int_0^b Y_j \frac{d^2 Y_n}{dy^2} dy + \int_0^a X_i \frac{d^2 X_m}{dx^2} dx \int_0^b Y_n \frac{d^2 Y_j}{dy^2} dy \right] \\
 + D_{22} \int_0^a X_i X_m dx \int_0^b \frac{d^2 Y_j}{dy^2} \frac{d^2 Y_n}{dy^2} dy + 4D_{66} \int_0^a \frac{dX_i}{dx} \frac{dX_m}{dx} dx \int_0^b \frac{dY_j}{dy} \frac{dY_n}{dy} dy \\
 \left. - \rho \omega_{mn}^2 \int_0^a X_i X_m dx \int_0^b Y_j Y_n dy \right\} a_{ij} = 0 \\
 m = 1, 2, \dots, M \text{ and } n = 1, 2, \dots, N
 \end{aligned} \quad (5.10)$$

The approximating function given by Equation 5.9 for deflection $w(x, y)$ satisfying Equations 5.7 and 5.8 is assumed as:

$$w(x, y) = \sum_{m=1}^{\infty} \sum_{n=1}^{\infty} a_{mn} \sin \frac{m\pi x}{a} \sin \frac{n\pi y}{b} \quad (5.11)$$

Equation 5.11 can now be substituted in 5.10 to get the set of $M \times N$ equations for the present case. Equations 5.10 are of the form of Equations 3.2 described in Chapter 3. The procedure described in Chapter 3 can now be applied here to incorporate the randomness in basic material parameters and convert the above equation to the form of Equation 3.1. These equations can be solved for the random eigenvalues ω_{mn}^R , using the random response $w^R(x, y)$, given by.

$$w^R(x, y) = \sum_{m=1}^M \sum_{n=1}^N a_{mn}^R \sin \frac{m\pi x}{a} \sin \frac{n\pi y}{b} \quad (5.12)$$

5.3.2 Clamped Plate

Here all the four edges of the rectangular plate considered are assumed to be clamped. The boundary conditions are defined by the equations

along $x = 0$ and $x = a$ for all y

$$\begin{aligned} w &= 0 \\ \frac{\partial w}{\partial x} &= 0 \end{aligned} \quad (5.13)$$

along $y = 0$ and $y = b$ for all x

$$\begin{aligned} w &= 0 \\ \frac{\partial w}{\partial y} &= 0 \end{aligned} \quad (5.14)$$

For these boundary conditions closed form solution of Equation 5.4 is difficult. Again solution of the problem by energy methods is attempted. The approximating function for $w(x, y)$ — the transverse deflection of the plate — is again assumed as:

$$w(x, y) = \sum_{m=1}^M \sum_{n=1}^N a_{mn} X_m(x) Y_n(y) \quad (5.15)$$

The functions $X_m(x)$ and $Y_n(y)$, that satisfy the boundary conditions 5.13 and 5.14 are defined again as follows:

$$\begin{aligned} X_m(x) &= (x^2 - ax)^2 x^{(m-1)} \\ Y_n(y) &= (y^2 - by)^2 y^{(n-1)} \end{aligned} \quad (5.16)$$

The governing equation for this case is also given by Equations 5.10. Using the same procedure as carried out in the last section, it can

be shown that, the resulting equation is of the form of Equation 3.2 from Chapter 3. The random approximating function for deflection is assumed to have the form

$$w^R(x, y) = \sum_{m=1}^M \sum_{n=1}^N a_{mn}^R X_m(x) Y_n(y) \quad (5.17)$$

Using this, Equation 5.10 can be solved as described in the last section, for the random eigenvalues, resulting from the randomness in basic material parameters.

5.4 MIDPLANE SYMMETRIC LAMINATED PLATE

Bending-twisting are the only coupling terms that are present in midplane symmetric angle-ply laminates. D_{11} , D_{22} , D_{12} , D_{66} , D_{16} and D_{26} are the stiffness matrix terms present in the governing equation. In Equation 5.3 we are concerned only with the w terms, further $[B]$ matrix terms are zero. This results in a much simplified governing equation

5.4.1 Simply Supported Plate

For midplane symmetric laminates Equation 5.3 takes the following form:

$$\begin{aligned} D_{11} \frac{\partial^4 w}{\partial x^4} + 4D_{16} \frac{\partial^4 w}{\partial x^3 \partial y} + 2(D_{12} + 2D_{66}) \frac{\partial^4 w}{\partial x^2 \partial y^2} \\ + 4D_{26} \frac{\partial^4 w}{\partial x \partial y^3} + D_{22} \frac{\partial^4 w}{\partial y^4} - \rho \frac{\partial^2 w}{\partial t^2} = 0 \end{aligned} \quad (5.18)$$

The boundary conditions are again given by Equations 4.22 and 4.23. The approximating function for $w(x, y)$ can again be assumed to be of the form of Equation 5.11. Again, closed form solution of this Equation 5.18 is not feasible. If, solution of the problem is attempted using energy formulation, the total potential energy Π_p for the plate is

$$\begin{aligned} \Pi_p = U + T = & \frac{1}{2} \int_0^b \int_0^a \left[D_{11} \left(\frac{\partial^2 w}{\partial x^2} \right)^2 + 2D_{12} \frac{\partial^2 w}{\partial x^2} \frac{\partial^2 w}{\partial y^2} \right. \\ & + D_{22} \left(\frac{\partial^2 w}{\partial y^2} \right)^2 + 4D_{66} \left(\frac{\partial^2 w}{\partial x \partial y} \right)^2 + 4D_{16} \frac{\partial^2 w}{\partial x \partial y} \frac{\partial^2 w}{\partial x^2} \\ & \left. + 4D_{26} \frac{\partial^2 w}{\partial x \partial y} \frac{\partial^2 w}{\partial y^2} - \rho \omega^2 w^2 \right] dx dy \\ & = \text{stationary value} \end{aligned} \quad (5.19)$$

The approximating function given by Equation 5.11 along with Equation 5.19 is used to find the governing equations — using Rayleigh–Ritz technique. Hence we get

$$\begin{aligned} \sum_{i=1}^M \sum_{j=1}^N \left\{ D_{11} \int_0^a \frac{d^2 X_i}{dx^2} \frac{d^2 X_m}{dx^2} dx \int_0^b Y_j Y_n dy \right. \\ + D_{12} \left[\int_0^a X_m \frac{d^2 X_i}{dx^2} dx \int_0^b Y_j \frac{d^2 Y_n}{dy^2} dy + \int_0^a X_i \frac{d^2 X_m}{dx^2} dx \int_0^b Y_n \frac{d^2 Y_j}{dy^2} dy \right] \\ + D_{22} \int_0^a X_i X_m dx \int_0^b \frac{d^2 Y_j}{dy^2} \frac{d^2 Y_n}{dy^2} dy + 4D_{66} \int_0^a \frac{dX_i}{dx} \frac{dX_m}{dx} dx \int_0^b \frac{dY_j}{dy} \frac{dY_n}{dy} dy \\ + 2D_{16} \left[\int_0^a \frac{d^2 X_i}{dx^2} \frac{dX_m}{dx} dx \int_0^b dY_j \frac{dY_n}{dy} dy + \int_0^a \frac{dX_i}{dx} \frac{d^2 X_m}{dx^2} dx \int_0^b Y_n \frac{dY_j}{dy} dy \right] \\ + 2D_{26} \left[\int_0^a X_m \frac{dX_i}{dx} dx \int_0^b \frac{dY_j}{dy} \frac{d^2 Y_n}{dy^2} dy + \int_0^a X_i \frac{dX_m}{dx} dx \int_0^b \frac{d^2 Y_j}{dy^2} \frac{dY_n}{dy} dy \right] \\ \left. - \rho \omega_m^2 \int_0^a X_i X_m dx \int_0^b Y_j Y_n dy \right\} a_{ij} = 0 \\ m = 1, 2, \dots, M \text{ and } n = 1, 2, \dots, N \end{aligned} \quad (5.20)$$

This set of $M \times N$ homogeneous simultaneous equations can be expressed in the form of Equation 3.8 given in Chapter 3. The derived equations for finding the mean and variance of the eigen values can be expressed in the form of Equations 3.10 and 3.11. For a non-trivial solution of these equations, coefficients a_{ij} cannot be zero. Hence rest of the terms in these system of equations must go to zero. This condition will give a set of equations that form an eigenvalue problem. When solved, these sets of equations yield mean and variance of normal mode frequencies.

5.4.2 Clamped Plate

The clamped boundary conditions are specified by the Equations 5.13 and 5.14. The approximating function assumed is again given by Equations 5.15 and 5.16. The governing equations for the conventional problem is once again given by Equations 5.20. The randomness is incorporated in these equations as described in Chapter 3.

5.5 NUMERICAL RESULTS

Results have been obtained for some typical problems to study the effect of variation in material property characteristics on the natural frequencies of rectangular composite plates. All the plate configurations discussed are assumed to have the same total thickness. For the problems studied, the basic material properties like the longitudinal modulus, transverse modulus, shear modulus etc. are considered to be random variables. The randomness in material properties is handled using the perturbation technique discussed in Chapter 3 and earlier sections in this chapter. The assumed mean values of the random variables used are given in Table 4.1 of Chapter 4.

5.5.1 Validation of the Technique

Validation of the perturbation technique used, for the present problem was done by comparing it with the results from a Monte Carlo simulation study. The basic random variables are assumed to be Gaussian for this purpose. Since solving Equation 5.11 using Monte Carlo simulation is computationally expensive, an one term approximation of the equation was used for validation. (Results obtained by solving the full set of equation is given later)

Figure 5.1 shows the results from the Monte Carlo simulation, compared with the present approximation for a $[90^\circ]$ square Graphite/Epoxy plate with all the four sides simply supported. The ratio $\frac{SD}{Mean}$ are assumed to be the same for all the four primary random variables. Random samples of the primary RVs with specified characteristics were generated for simulation, as described in Chapter 4. Here the SD of fundamental and higher natural frequencies ω^2 are plotted against the change in SD of input RVs. As indicated by the plots, for the range of SD of input RVs considered both the results are quite close. One may, therefore, conclude that the present approximation employing first order perturbation gives sufficiently accurate results for the free vibration problem under consideration.

5.5.2 Simply Supported Rectangular Plate

In this section we consider free vibration of thin rectangular composite plates simply supported along all the four edges. Except when indicated, all the input RVs are assumed to have the same SD. All the plates under consideration are assumed to have the same thickness h . Most of the results are for Graphite/Epoxy plates. Towards the end some results for plates made of Glass/Epoxy composite are also presented. This is done to investigate the effect of modular ratio since the ratio of $\frac{E_{11}}{E_{22}}$ is more for Graphite/Epoxy material, in comparison with Glass/Epoxy.

The mean values of natural frequencies for a $[90^\circ]$ lamina simply supported along all the edges is given in Table 5.1, for various aspect ratios. Table 5.2 gives mean of natural frequencies for a square laminate, with various stacking sequences. Figure 5.2 gives the plot of variation of SD of natural frequencies ω^2 of a $[90^\circ]$ square lamina with variation in SD of longitudinal modulus E_{11} . SD of all other RVs are assumed to be zero. Figures 5.3, 5.4 and 5.5 show similar results for the other RVs — E_{22} the transverse modulus, ν_{12} the Poisson's ratio and G_{12} the shear modulus. The SD of natural frequencies are affected most by the change in SD of the longitudinal modulus E_{11} . The fundamental frequency is most affected by changes in E_{11} , E_{22} and ν_{12} . We can see that the influence of SD of input RVs on SD of natural frequencies diminishes, as we consider higher and higher modes for the above three cases. We

can further observe a flattening trend for this effect, as indicated by Figures 5.6 , 5.7 and 5.8. In the case of G_{12} , the fundamental frequency is least affected by the change in SD of input RV. The higher modes are progressively affected more by the change in SD of G_{12} . Here also there is a flattening trend for this effect as indicated by Figure 5.9. If we consider the magnitude of effect on the SD of natural frequencies by the SD each of the input RVs — E_{11} , G_{12} , E_{22} and ν_{12} respectively show progressively less and less influence on the SD of the natural frequencies.

Figure 5.10 shows the influence of simultaneous change in the SD of input RVs on the SD of the natural frequencies. Here all the basic RVs are assumed to have the same level of SD. The results are for a $[90^\circ]$ lamina with aspect ratio 0.5. All the four sides are assumed to be simply supported. The first natural frequency is affected least. Higher and higher modes are progressively affected more by the change in SD of input RVs. Figures 5.11 , 5.12 , 5.13 , 5.14 and 5.15 give corresponding results for aspect ratios 1.0, 2.0, 3.0, 4.0 and 5.0 respectively. In all these cases, except for the aspect ratio and SD of input RVs all other parameters remain the same.

The influence of change in aspect ratio on the SD of natural frequencies is shown by Figure 5.16 . Here all the input RVs are assumed to have a SD equal to 10% of their mean value. The results are for a $[90^\circ]$ lamina. The nature of variation of the SD of frequencies at low aspect

ratios is strongly dependent on the mode we are considering. But the result seems to reach plateau as we approach higher aspect ratios. At aspect ratios above 2.0, the SD of first mode frequency is the largest, with gradually decreasing values for the higher modes compared to the first mode shown in the figure. At low aspect ratios this pattern is not present.

Figure 5.17 illustrates the influence of change in aspect ratio on the SD of fundamental frequency at different SDs of input RVs, with all of them having the same SD. When the SD of input RVs is low the change in aspect ratio doesn't seem to affect the SD of natural frequencies ω^2 . As the SD of input RVs is increased, the influence of change in aspect ratio increases. The change in aspect ratio doesn't seem to affect the SD of ω^2 beyond a limit, depending on the SD of input RVs.

The influence of fiber orientation on the SD of fundamental frequency is illustrated in Figure 5.18 – for a square plate. The influence of variation in SD of input RVs is also shown. Here also for low levels of SD of input RVs, change in fiber orientation does not have much effect on the SD of natural frequencies. For higher levels of SD of input RVs the SD of ω^2 rises to a maximum value at 45° fiber orientation and then again drops down.

Results for the case of a $[90^\circ/0^\circ]_s$ square plate is shown in Figure 5.19 for several frequencies. The results shown here are almost identical to result as given by Figure 5.11 for a $[90^\circ]$ lamina with the same dimensions.

and thickness. Figures 5.20 and 5.21 gives similar results for $[0^\circ/90^\circ]_s$ and $[0^\circ]$ laminates.

Figures 5.22 and 5.23 shows the results for $[45^\circ]$ and $[45^\circ/0^\circ]_s$ laminates. The plots for different modes are closely packed together in both the cases. The 0° layers in the second case doesn't seem to have much influence on the output SD.

Results for $[60^\circ]$, $[-45^\circ/45^\circ]_s$ and $[0^\circ/45^\circ/90^\circ/-45^\circ]_s$ laminate configurations are shown in Figures 5.24, 5.25 and 5.26 respectively for a square plate. In Figures 5.25 and 5.26 only the fundamental frequency is given, as other frequencies are very close.

Some results for a typical Glass/Epoxy composite are now presented. Table 5.3 gives mean values of natural frequencies for a $[90^\circ]$ lamina, simply supported along all the four edges. The result is given for different aspect ratios. Figures 5.27, 5.28 and 5.29 give the variation of SD of natural frequencies with the SD of input RVs for aspect ratios 0.5, 1.0 and 2.0 respectively. The results are for a $[90^\circ]$ lamina, simply supported on all the four edges. The magnitude of SD of the natural frequencies are comparable to those for a similar Graphite/Epoxy configuration given by Figures 5.10, 5.11 and 5.12, except for the order of rate of change for the SD of the frequencies.

Influence of the change in aspect ratio of the plate on the SD of natural frequencies is shown by Figure 5.30, for different levels of SD of input RVs. The result is for a $[90^\circ]$ lamina with all the sides simply

supported. At low levels of SD of input RVs the change in aspect ratio has practically no effect on the SD of first natural frequency. At higher levels of SD of input RVs the response SD dips to the lowest value at AR 1.0, to to again increase to higher values. All the response curves ultimately reach a plateau and further increase in aspect ratio doesn't seem to have much effect on the SD of first natural frequency.

5.5.3 Clamped Rectangular Plate

Here we consider rectangular plates with all the four sides clamped. All the plates are assumed to have the same thickness.

Even though the numerical values are different, the trend here also is similar to the simply supported boundary condition examples discussed in the last section. The mean values of fundamental frequencies for square laminates with various stacking sequences are given in Table 5.4. The results for variation in SD of ω^2 with SD of input RV are shown in Figures 5.31, 5.32, 5.33, 5.34, 5.35 and 5.36 for the first natural frequency for different stacking sequences for a plate with aspect ratio 1.0. In all these cases the higher modes are closely packed along with the fundamental frequency. All of them show linear behavior. Figure 5.37 illustrates the influence of variation in fiber orientation on the SD of the fundamental frequency for a square plate, for different SDs of input RVs.

The rate of change as well as the order of change of the the natural

frequencies with change in SD of input RVs is dependent on the the stacking sequence and the boundary conditions of the plate i.e. for different configurations they vary differently. This can be important when the plates are subjected to an excitation which approaches the range of variation of the natural frequencies.

5.6 SUMMARY

Application of the perturbation technique described in Chapter 3, to problems free vibration of rectangular plates has been discussed. Formulation and results are presented for problems with clamped and simply supported boundary conditions, having various combinations of stacking sequence and aspect ratio. The method has been validated for the present class of problems by an independent Monte Carlo simulation, which shows excellent agreement with the results from the present technique.

The perturbation approximation gives sufficiently accurate results for the problem under consideration. In general the SD of natural frequencies are affected most by the change in E_{11} . The nature of influence of the input RVs are strongly dependent on the mode of vibration and the extent of randomness of the variable under consideration. The nature of variation of SD of normal mode frequencies is strongly dependent on the mode under consideration at low aspect ratios. Change in aspect ratio beyond a limit doesn't seem to affect the SD of natural frequencies. At low levels of SD of input RVs change in aspect ratio, fiber orientation etc. doesn't seem to have much effect on the SD of natural frequencies. SD of natural frequencies have a maximum value for a laminate with 45° fiber orientation. The outer plies of laminates have a dominating influence on the SD of natural frequencies. In general the results show a linear behavior for the change in SD of natural frequencies with the SD of the input RVs. The rate of change and order of change of natural frequencies with change in SD of input RVs is strongly dependent on the stacking sequence and the boundary conditions.

Table 5.1 Mean of natural frequencies ω^2 , for different aspect ratios $[90^\circ]$ lamina, all sides simply supported Graphite/Epoxy

AR	1 st	2 nd	3 rd	4 th
0.5	0.15044E-02	0.32505E-02	0.61606E-02	0.10235E-01
1.0	0.10679E-02	0.15044E-02	0.22319E-02	0.32505E-02
2.0	0.95878E-03	0.10679E-02	0.12498E-02	0.15044E-02
3.0	0.93857E-03	0.98707E-03	0.10679E-02	0.11811E-02
4.0	0.93149E-03	0.95878E-03	0.10042E-02	0.10679E-02
5.0	0.92822E-03	0.94568E-03	0.97478E-03	0.10155E-02

Table 5.2. Mean of natural frequencies ω^2 , for different stacking sequences Square plate, all sides simply supported Graphite/Epoxy

Stacking Sequence	1 st	2 nd	3 rd	4 th
$[90^\circ/0^\circ]_s$	0.959E-03	0.139E-02	0.212E-02	0.314E-02
$[0^\circ/90^\circ]_s$	0.306E-03	0.743E-03	0.147E-02	0.248E-02
$[45^\circ]$	0.123E-02	0.309E+00	0.393E+00	0.411E+00
$[60^\circ]$	0.130E-02	0.361E+00	0.402E+00	0.431E+00
$[45^\circ/0^\circ]_s$	0.110E-02	0.277E+00	0.352E+00	0.369E+00
$[-45^\circ/45^\circ]_s$	0.123E-02	0.318E+00	0.393E+00	0.410E+00
$[0^\circ/45^\circ/90^\circ/-45^\circ]_s$	0.616E-03	0.177E+00	0.190E+00	0.210E+00

Table 5.3 Mean of natural frequencies ω^2 , for different aspect ratios $[90^\circ]$ lamina, all sides simply supported Glass/Epoxy

ω^2	AR=0.5	AR=1.0	AR=2.0
1 st	0.10062E-02	0.46055E-03	0.32412E-03
2 nd	0.31890E-02	0.10062E-02	0.46055E-03
3 rd	0.68269E-02	0.19157E-02	0.68792E-03
4 th	0.73687E-02	0.31890E-02	0.10062E-02

Table 5.4 Mean of fundamental frequency ω^2 , for different stacking sequences Square plate, all sides clamped Graphite/Epoxy

Stacking Sequence	ω^2
$[90^\circ]$	0.118E-04
$[90^\circ/0^\circ]_s$	0.118E-04
$[0^\circ/90^\circ]_s$	0.118E-04
$[45^\circ]$	0.378E-04
$[60^\circ]$	0.334E-04
$[45^\circ/0^\circ]_s$	0.346E-04
$[-45^\circ/45^\circ]_s$	0.662E-05
$[0^\circ/45^\circ/90^\circ/-45^\circ]_s$	0.193E-04

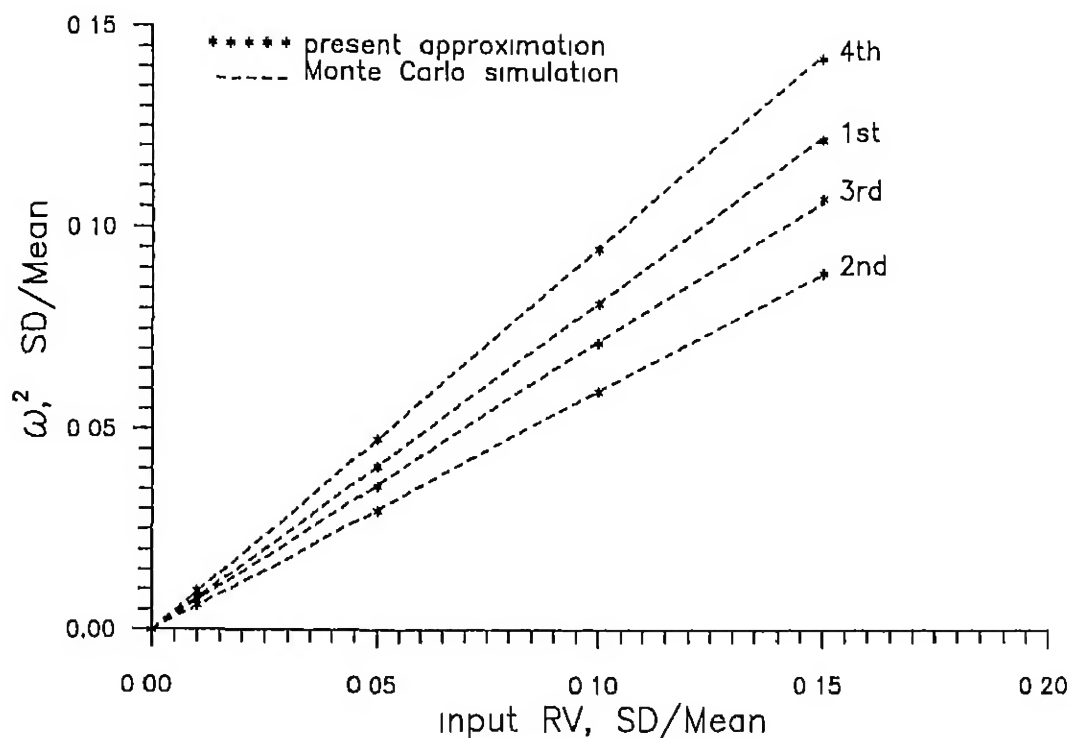


Figure 5.1. Normalized SD of natural frequencies ω^2 , plotted against SD of input RVs. The present approximation compared with results from a Monte Carlo simulation. $[90^\circ]$ laminate, AR=1.0 Graphite/Epoxy

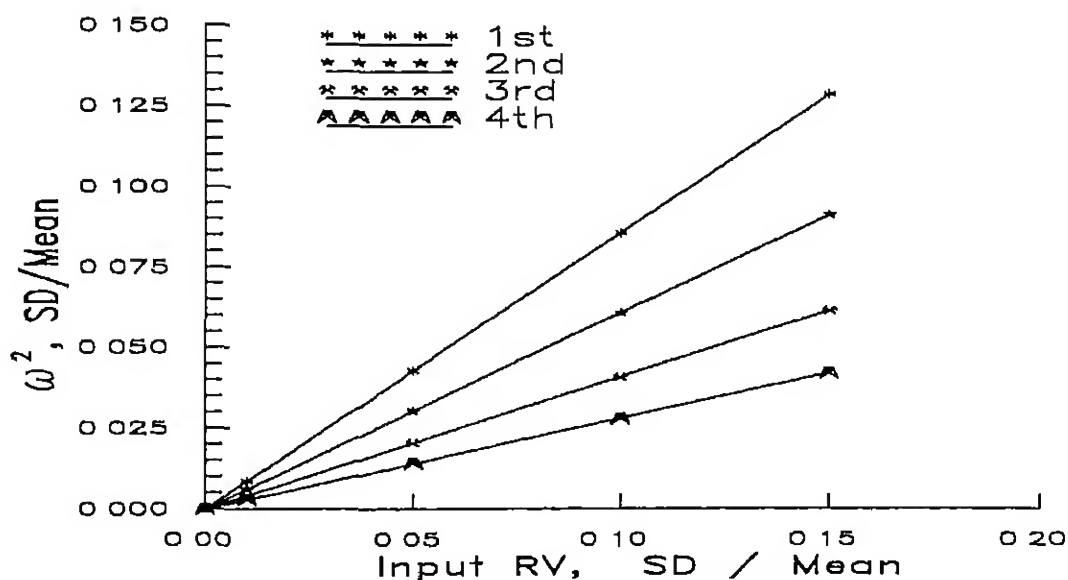


Figure 5.2. $[90^\circ]$ laminate, AR=1, all sides simply supported, sensitivity of SD of normalized natural frequencies ω^2 to SD of input RV E_{11} . SD of all other input RVs kept zero. Graphite/Epoxy

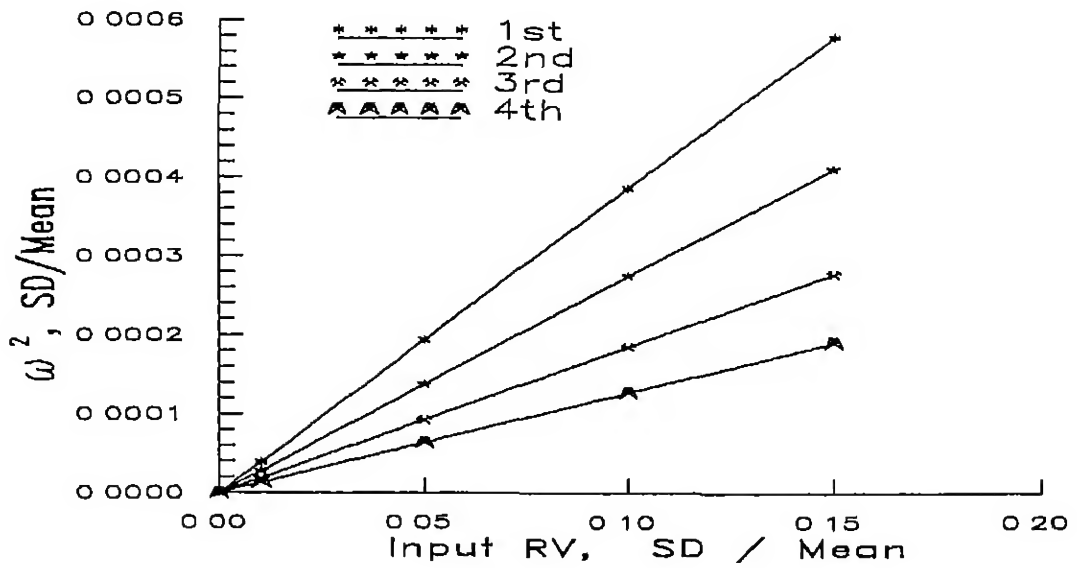


Figure 5.3 $[90^\circ]$ laminate, $AR=1$, all sides simply supported, sensitivity of SD of normalized natural frequencies ω^2 to SD of input RV E_{22} . SD of all other input RVs kept zero Graphite/Epoxy

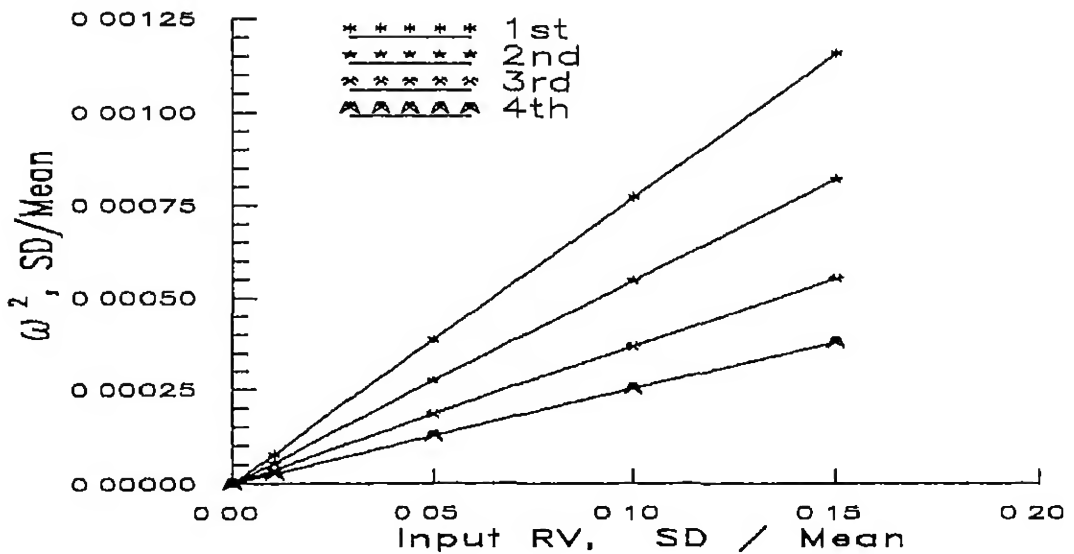


Figure 5.4: $[90^\circ]$ laminate, $AR=1$, all sides simply supported, sensitivity of SD of normalized natural frequencies ω^2 to SD of input RV ν_{12} . SD of all other input RVs kept zero Graphite/Epoxy

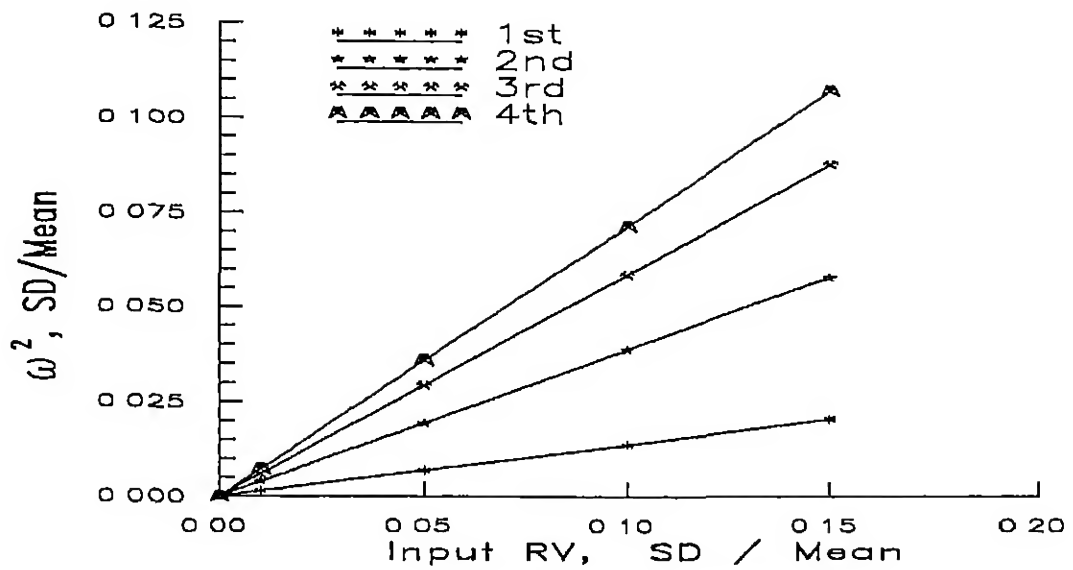


Figure 5.5 $[90^\circ]$ laminate, $AR=1$, all sides simply supported, sensitivity of SD of normalized natural frequencies ω^2 to SD of input RV G_{12} SD of all other input RVs kept zero Graphite/Epoxy

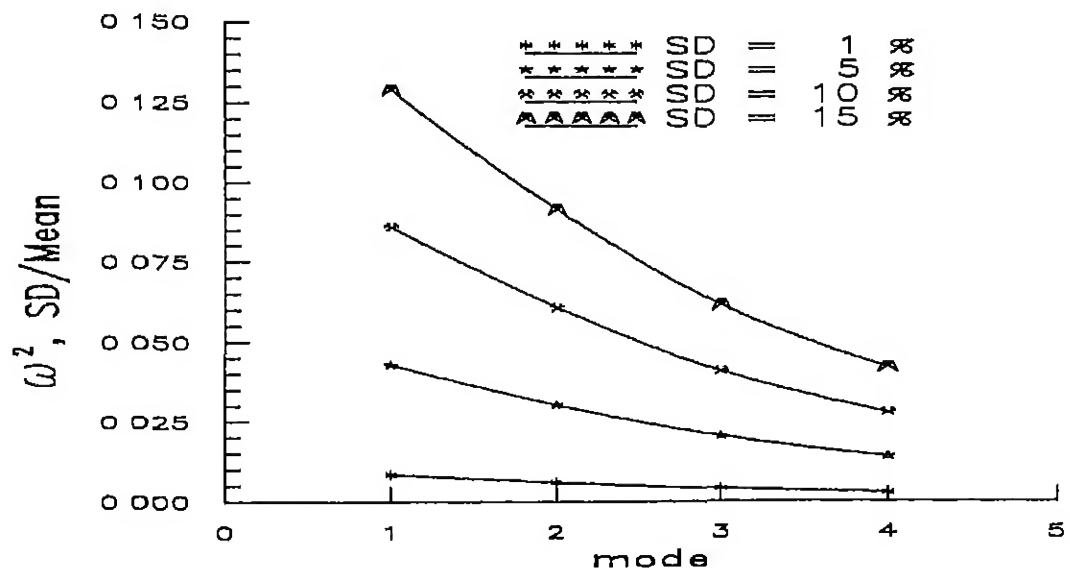


Figure 5.6 $[90^\circ]$ laminate, $AR=1$, all sides simply supported Variation of SD of normalized natural frequencies ω^2 with for different modes Results for variation of SD of E_{11} alone Graphite/Epoxy

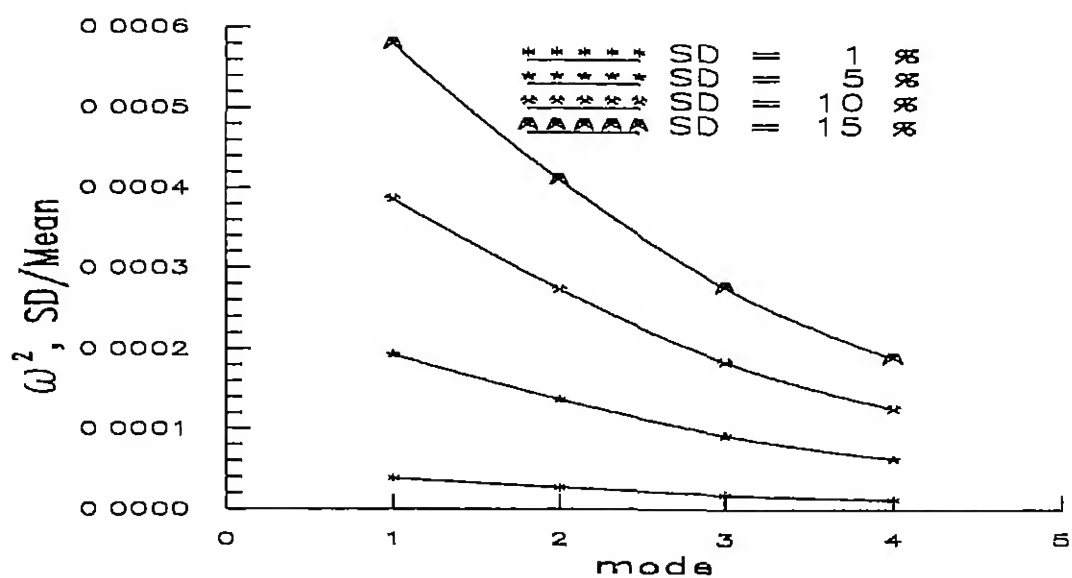


Figure 5.7 [90°] laminate, AR=1, all sides simply supported Variation of SD of normalized natural frequencies ω^2 with for different modes Results for variation of SD of E_{22} alone Graphite/Epoxy

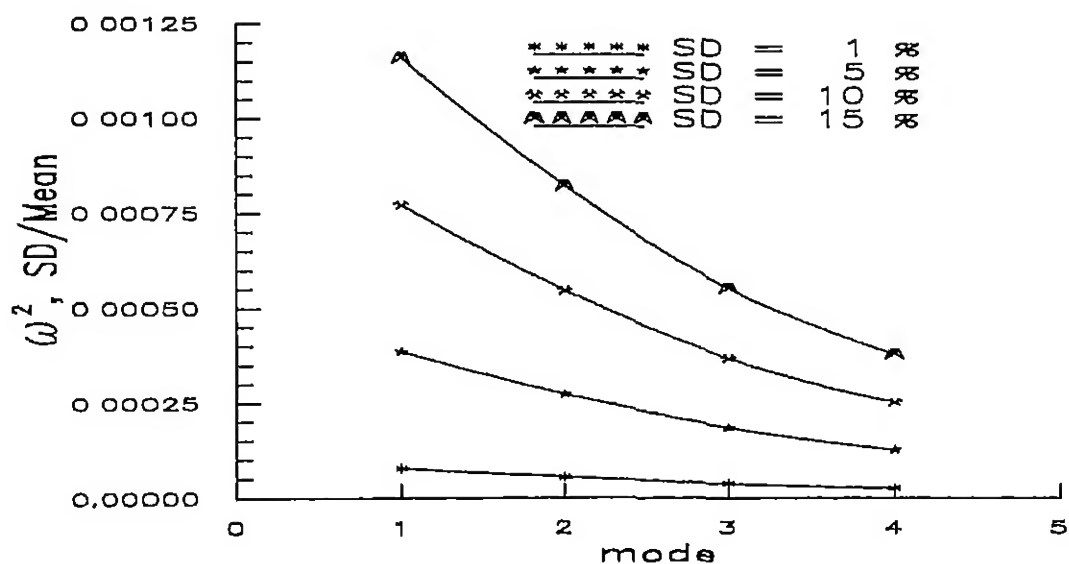


Figure 5.8 [90°] laminate, AR=1, all sides simply supported Variation of SD of normalized natural frequencies ω^2 with for different modes Results for variation of SD of ν_{12} alone Graphite/Epoxy

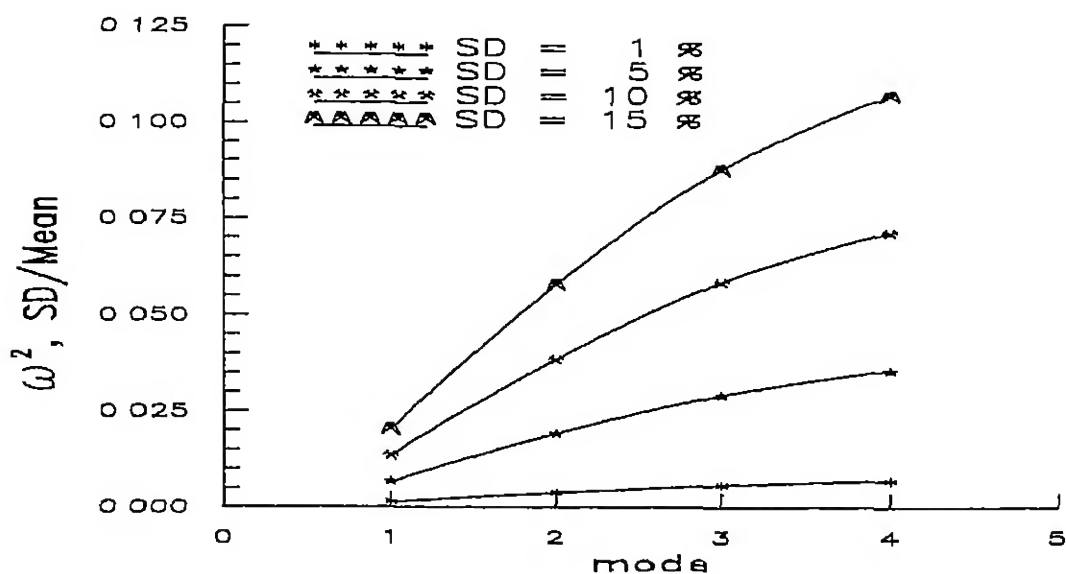


Figure 5.9 $[90^\circ]$ laminate, $AR=1$, all sides simply supported Variation of SD of normalized natural frequencies ω^2 with for different modes Results for variation of SD of G_{12} alone Graphite/Epoxy

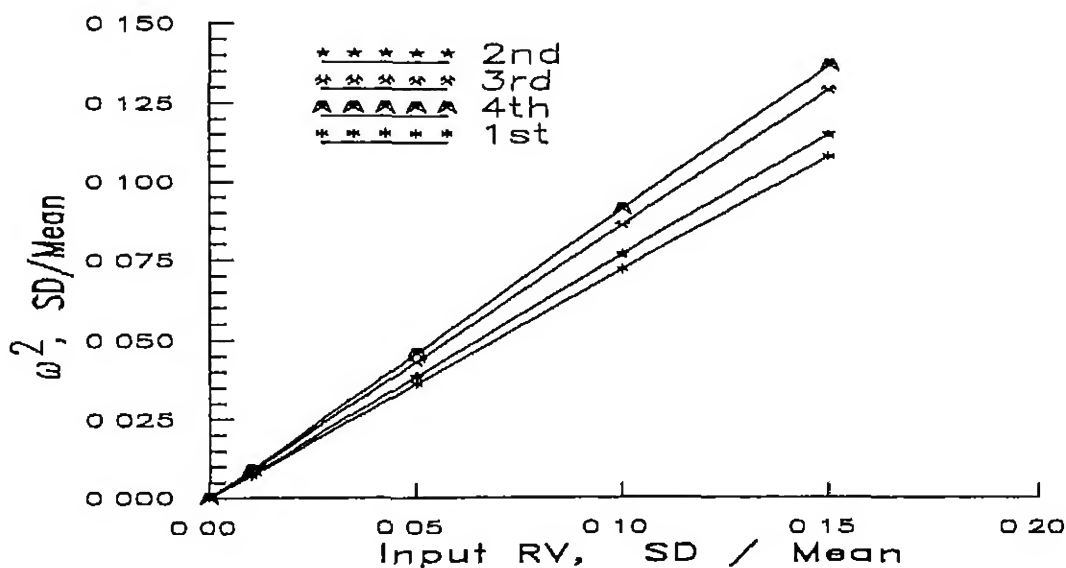


Figure 5.10 $[90^\circ]$ laminate, $AR=0.5$, all sides simply supported Variation of SD of normalized natural frequencies ω^2 with SD of input RVs Graphite/Epoxy

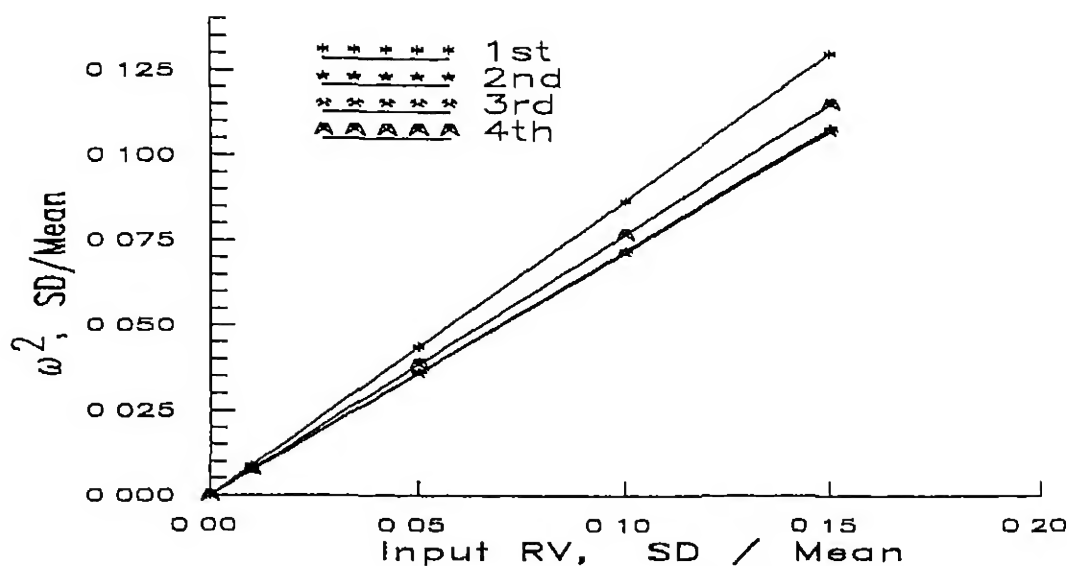


Figure 5.11 $[90^\circ]$ laminate, $AR=1$, all sides simply supported Variation of SD of normalized natural frequencies ω^2 with SD of input RVs Graphite/Epoxy

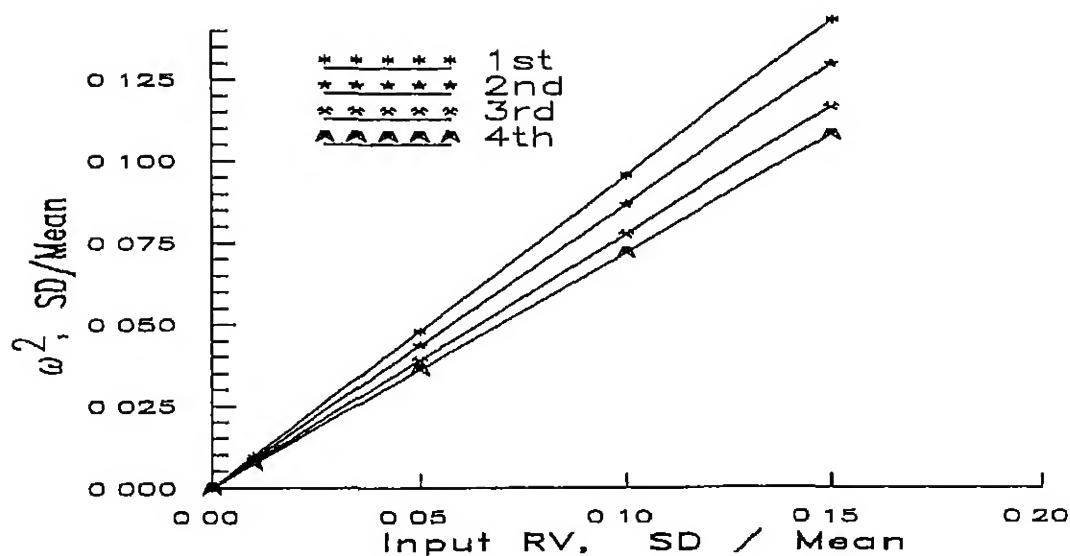


Figure 5.12. $[90^\circ]$ laminate, $AR=2$, all sides simply supported Variation of SD of normalized natural frequencies ω^2 with SD of input RVs Graphite/Epoxy

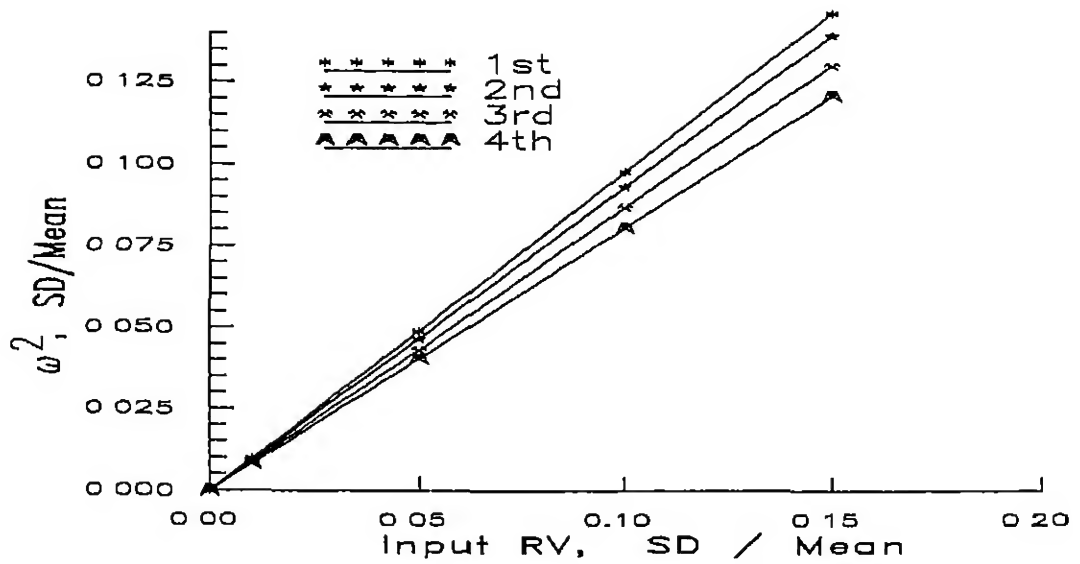


Figure 5.13 $[90^\circ]$ laminate, $AR=3$, all sides simply supported Variation of SD of normalized natural frequencies ω^2 with SD of input RVs Graphite/Epoxy

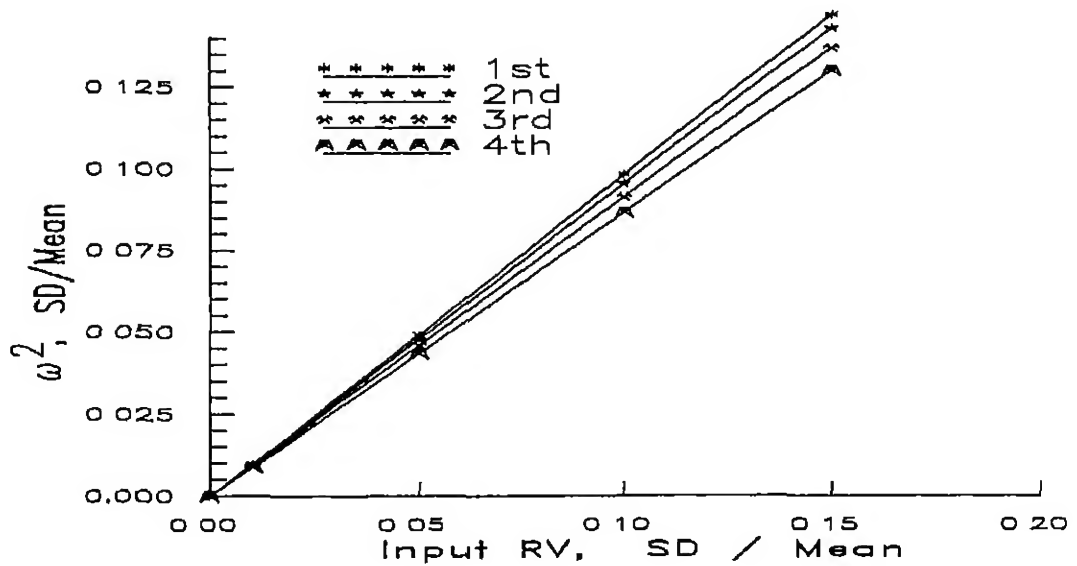


Figure 5.14 $[90^\circ]$ laminate, $AR=4$, all sides simply supported Variation of SD of normalized natural frequencies ω^2 with SD of input RVs Graphite/Epoxy

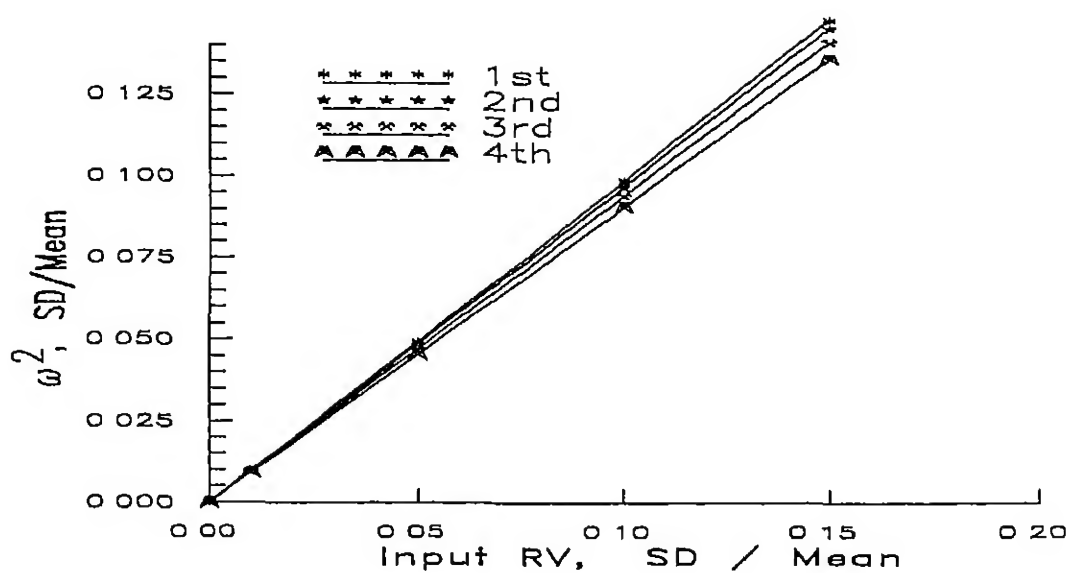


Figure 5.15 [90°] lamina, AR=5, all sides simply supported Variation of SD of normalized natural frequencies ω^2 with SD of input RVs Graphite/Epoxy

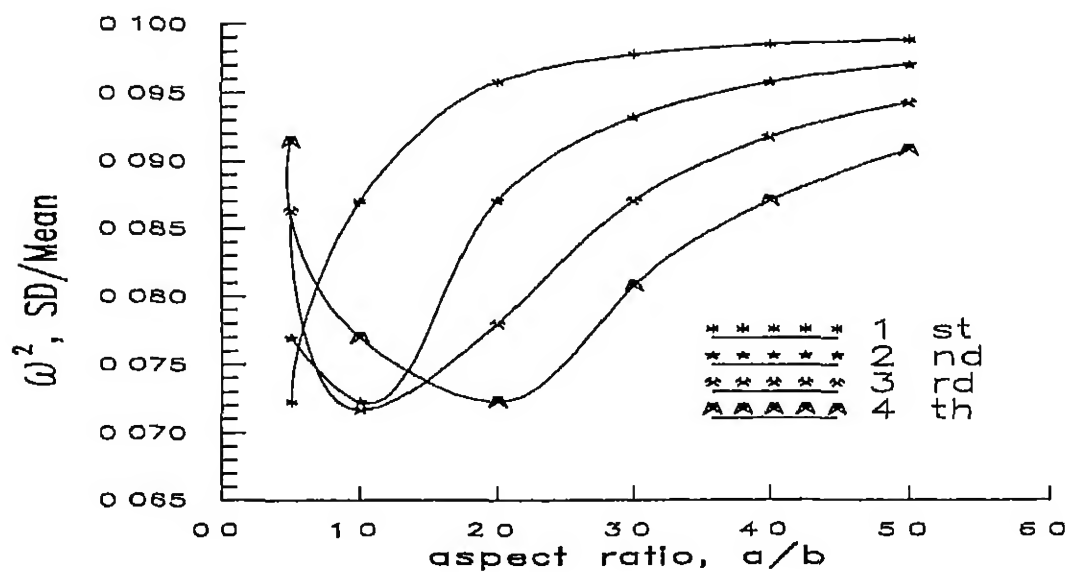


Figure 5.16: [90°] laminate, AR=1, all sides simply supported Variation of SD of normalized natural frequencies ω^2 with change in aspect ratio, for different modes SD of input RVs 10 % of mean Graphite/Epoxy

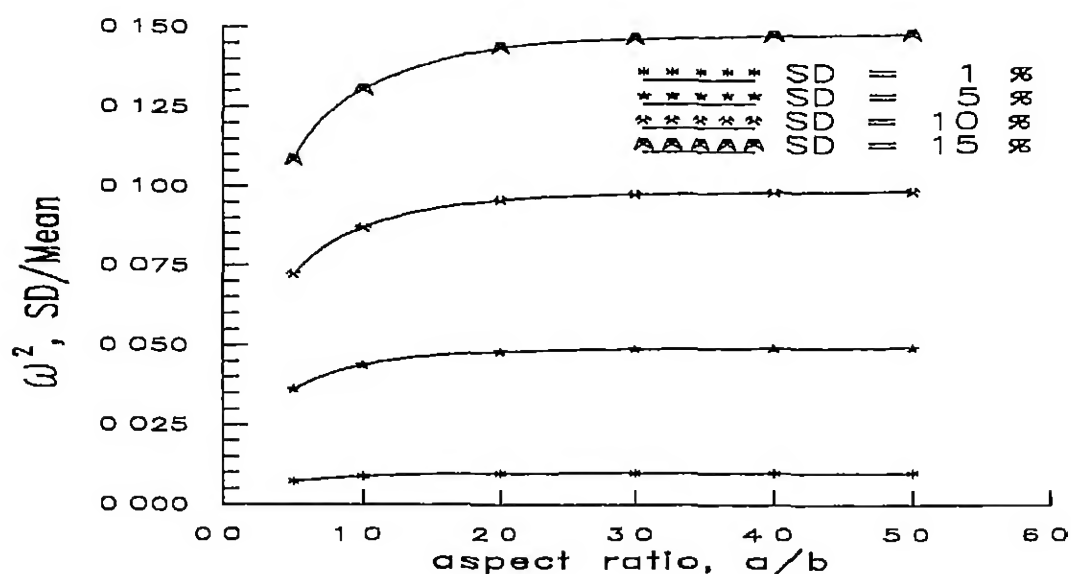


Figure 5.17. $[90^\circ]$ laminate, all sides simply supported Variation of SD of normalized fundamental frequency ω^2 with change in aspect ratio, for different SDs of input RVs Graphite/Epoxy

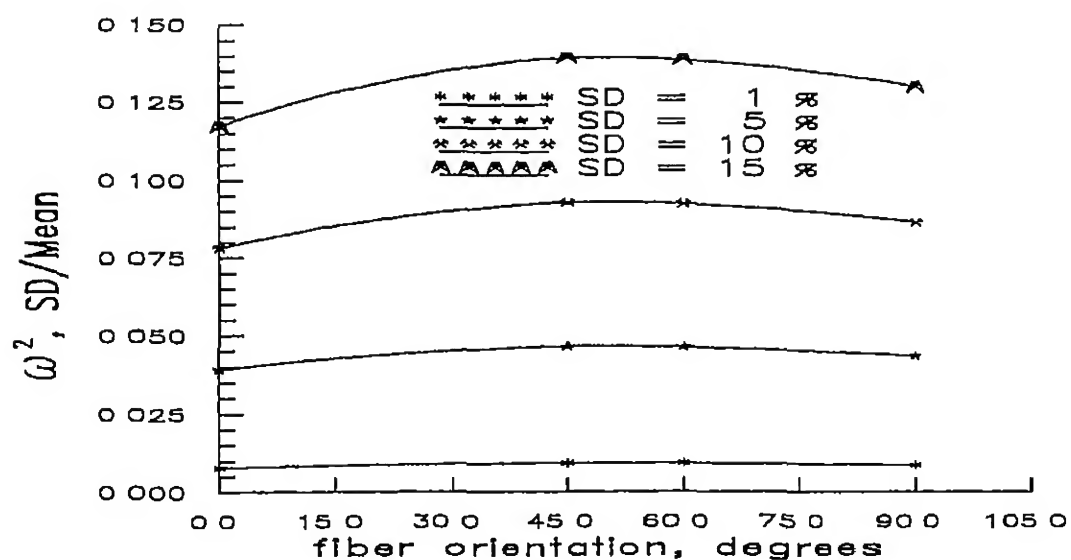


Figure 5.18. $AR=1$, all sides simply supported Variation of SD of normalized first natural frequency ω^2 with change fiber orientation, for different SDs of input RVs Graphite/Epoxy

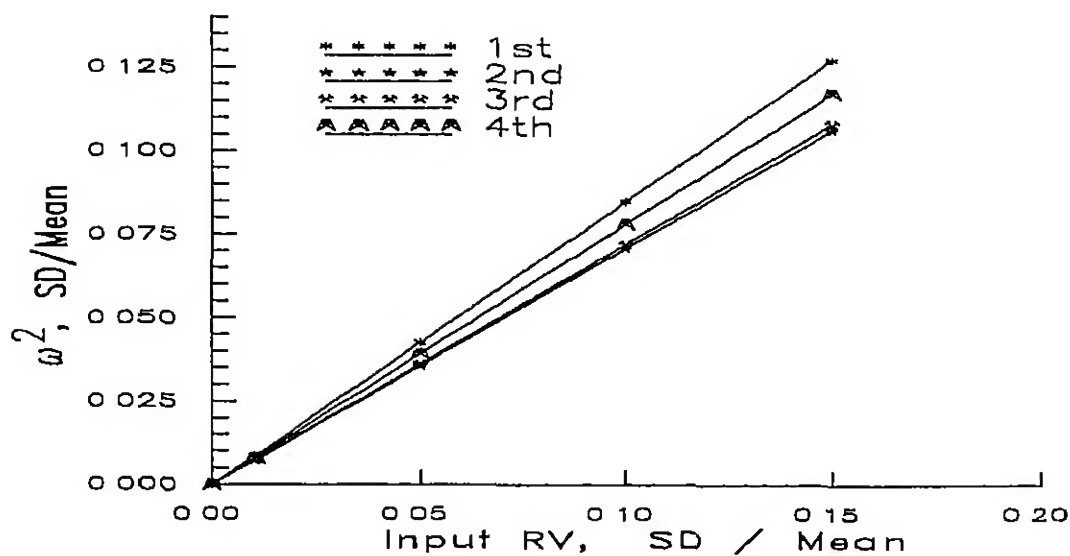


Figure 5.19 $[90^\circ/0^\circ]$, laminate, AR=1, all sides simply supported Variation of SD of normalized natural frequencies ω^2 with SD of input RVs Graphite/Epoxy

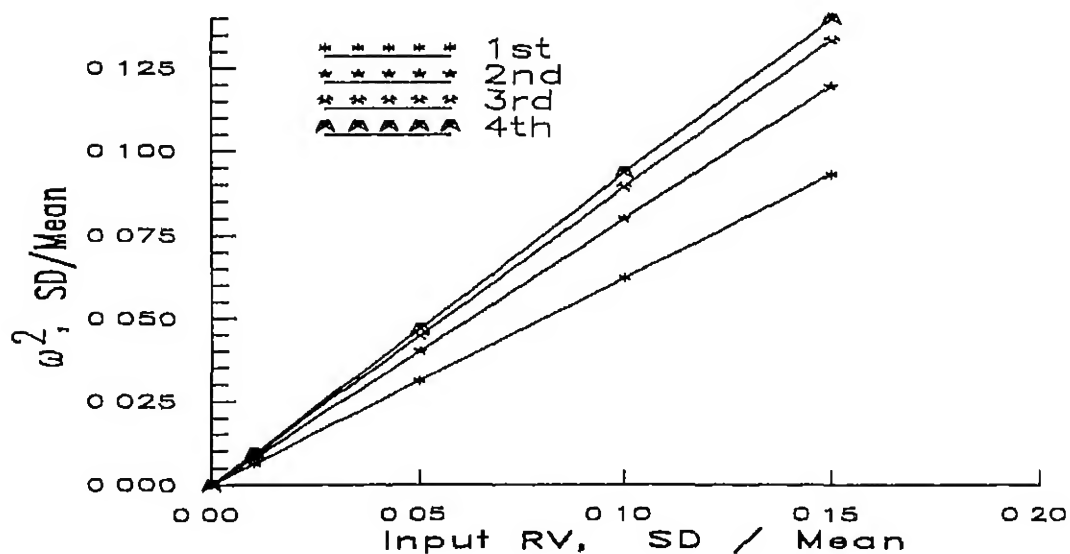


Figure 5.20. $[0^\circ/90^\circ]$, laminate, AR=1, all sides simply supported Variation of SD of normalized natural frequencies ω^2 with SD of input RVs Graphite/Epoxy

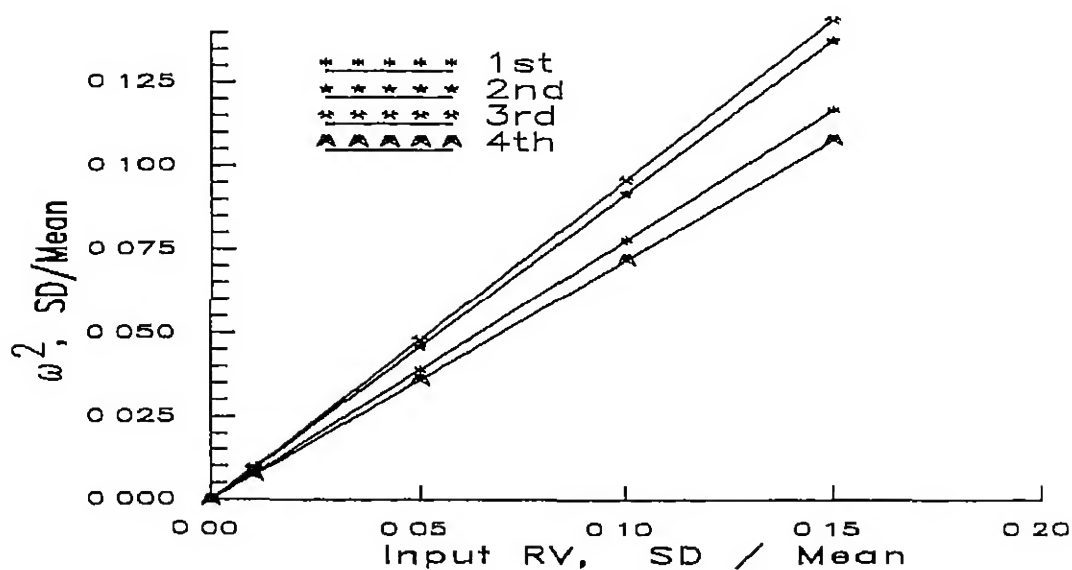


Figure 5.21 $[0^\circ]$ laminate, AR=1, all sides simply supported Variation of SD of normalized natural frequencies ω^2 with SD of input RVs Graphite/Epoxy

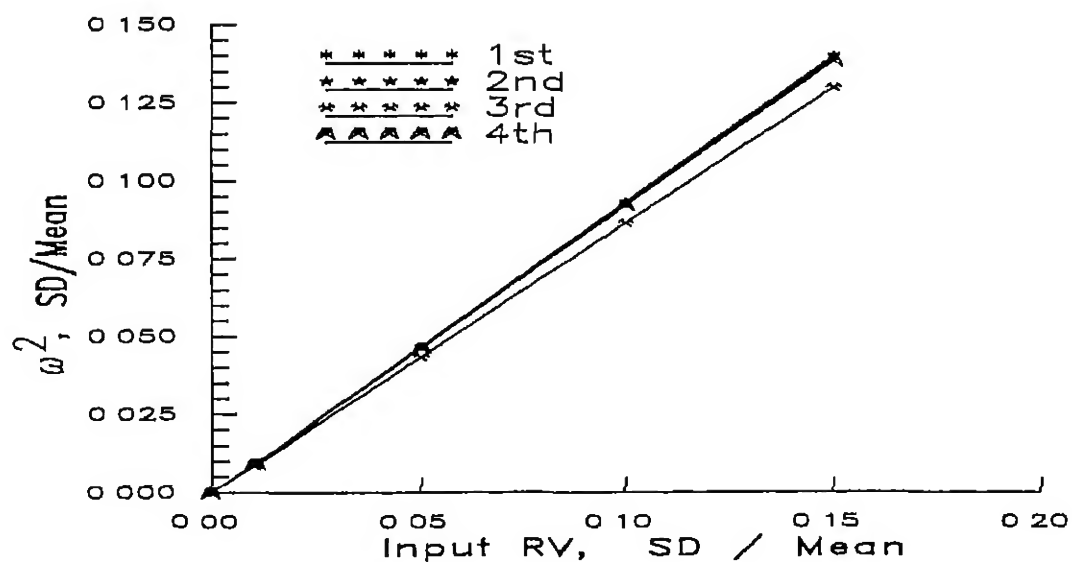


Figure 5.22 $[45^\circ]$ laminate, AR=1, all sides simply supported Variation of SD of normalized natural frequencies ω^2 with SD of input RVs Graphite/Epoxy

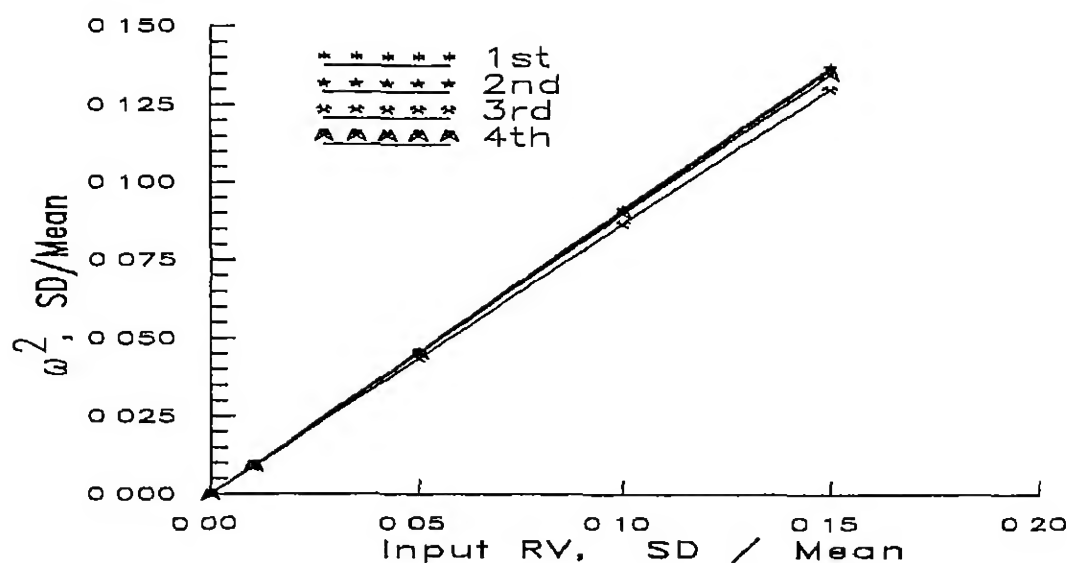


Figure 5.23 $[45^\circ/0^\circ]_8$ laminate, $AR=1$, all sides simply supported Variation of SD of normalized natural frequencies ω^2 with SD of input RVs Graphite/Epoxy

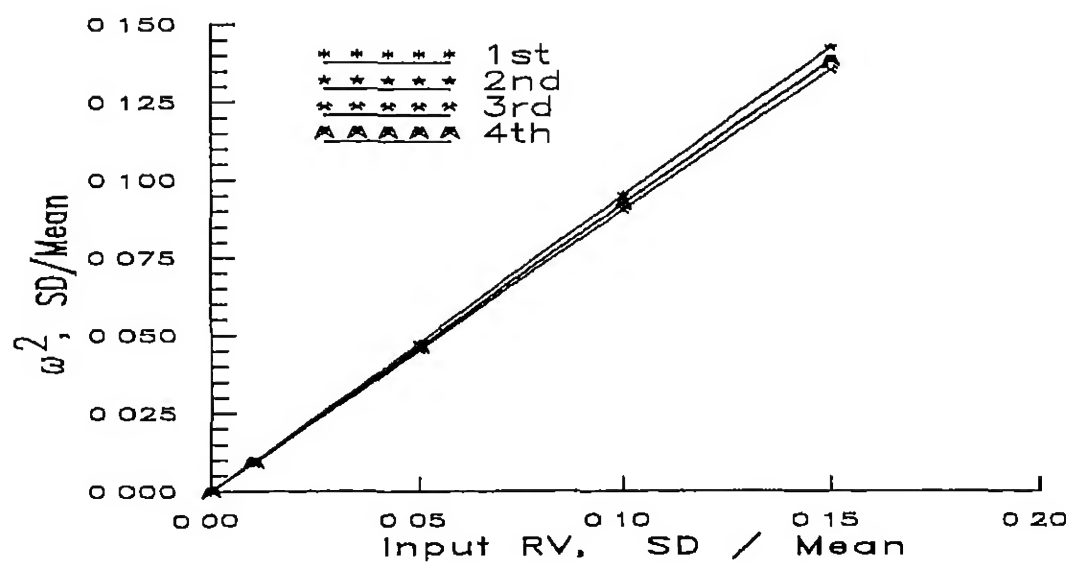


Figure 5.24 $[60^\circ]$ laminate, $AR=1$, all sides simply supported Variation of SD of normalized natural frequencies ω^2 with SD of input RVs Graphite/Epoxy

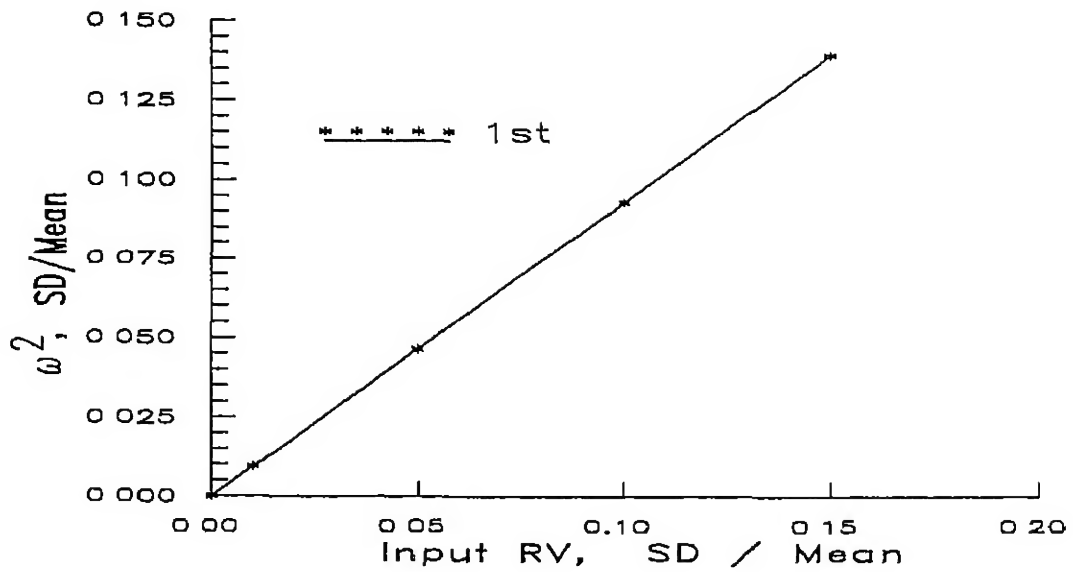


Figure 5.25 $[-45^\circ/45^\circ]_s$ laminate, $AR=1$, all sides simply supported Variation of SD of normalized fundamental frequency ω^2 with SD of input RVs Graphite/Epoxy

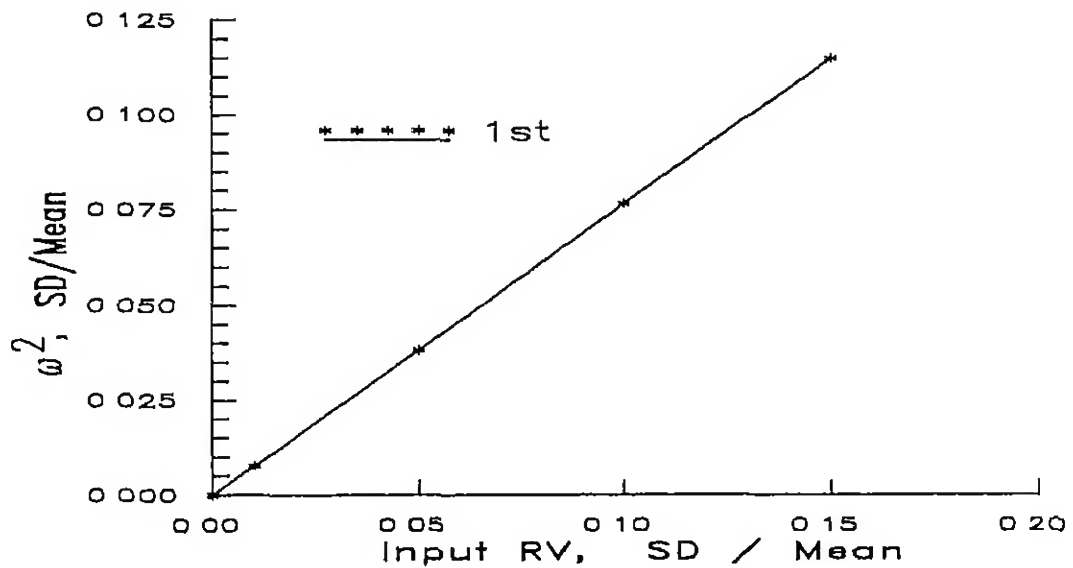


Figure 5.26 $[0^\circ/45^\circ/90^\circ/-45^\circ]_s$ laminate, $AR=1$, all sides simply supported Variation of SD of normalized fundamental frequency ω^2 with SD of input RVs Graphite/Epoxy

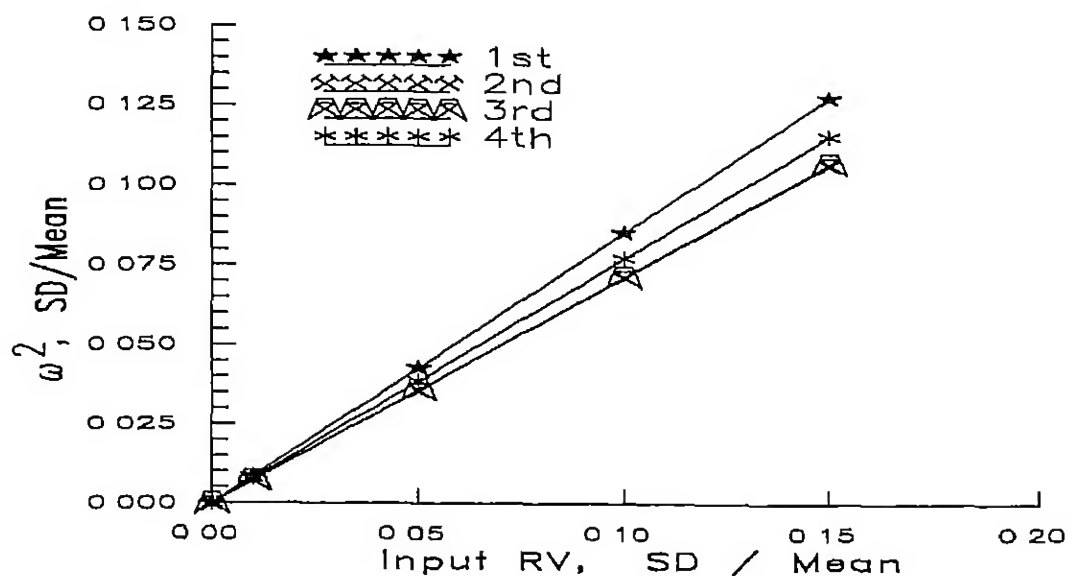


Figure 5.29 Test case glass/epoxy composite $[90^\circ]$ laminate, $AR=2.0$, all sides simply supported. Variation of SD of normalized natural frequencies ω^2 with SD of input RVs

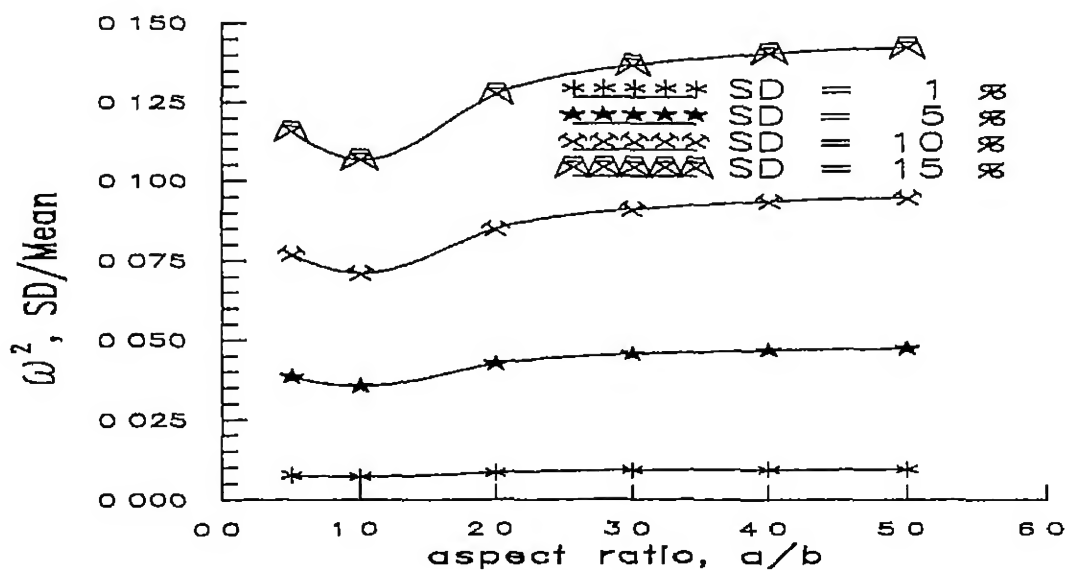


Figure 5.30. Test case glass/epoxy composite. $[90^\circ]$ laminate, all sides simply supported. Variation of SD of normalized fundamental frequency ω^2 with change in aspect ratio, for different SDs of input RVs

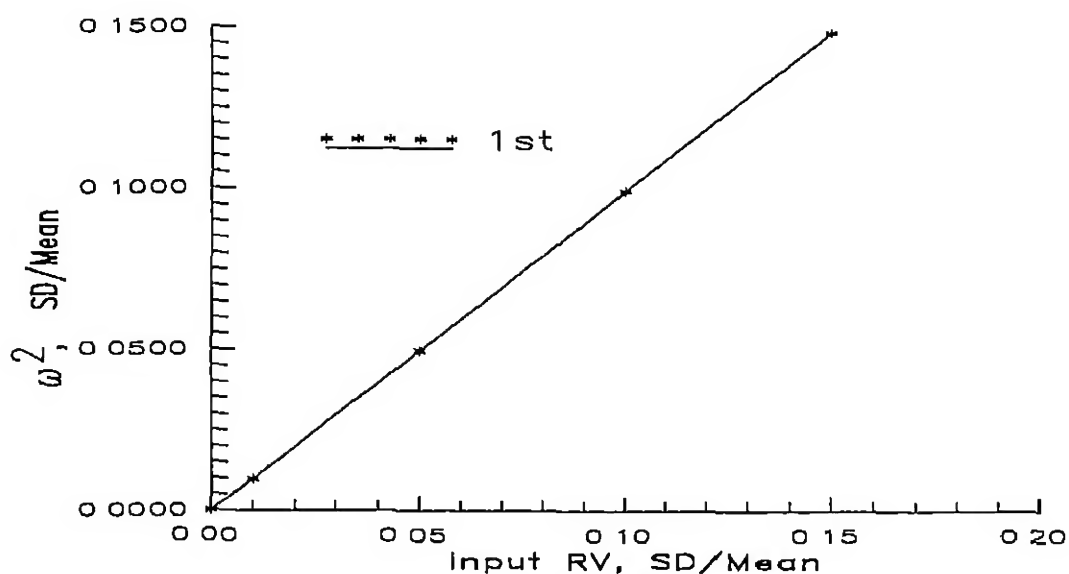


Figure 5.31 $[45^\circ]$ laminate, AR=1, all sides clamped Variation of SD of normalized fundamental frequency ω^2 with SD of input RVs Graphite/Epoxy

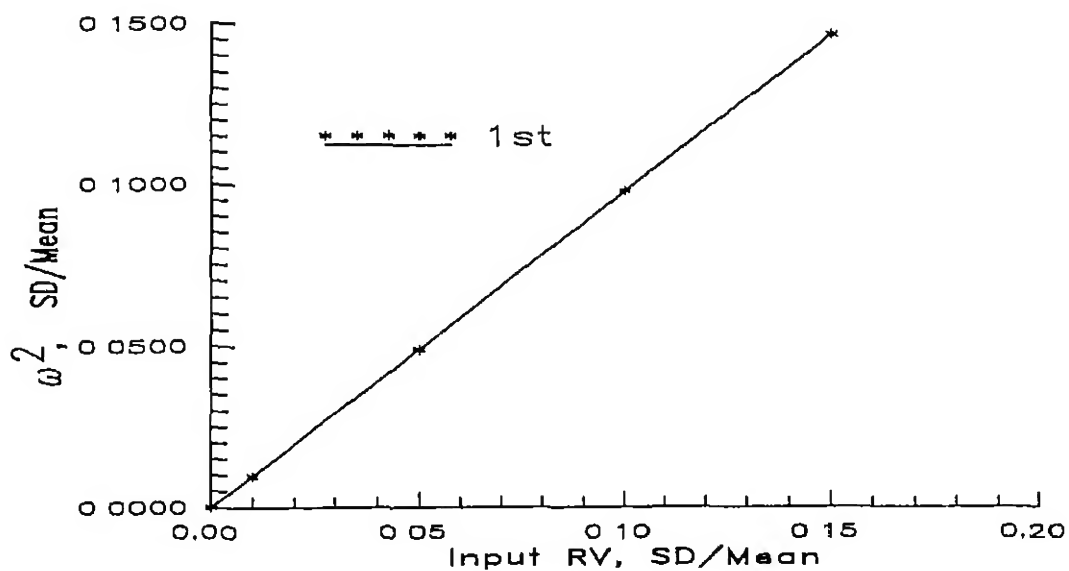


Figure 5.32 $[60^\circ]$ laminate, AR=1, all sides clamped Variation of SD of normalized fundamental frequency ω^2 with SD of input RVs Graphite/Epoxy

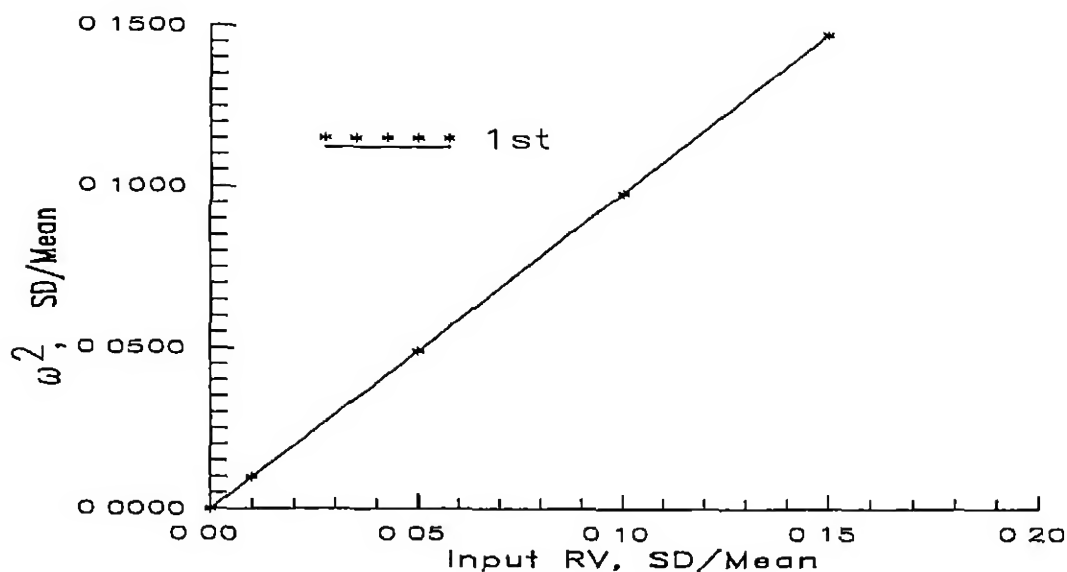


Figure 5.33 $[45^\circ/0^\circ]_s$ laminate, AR=1, all sides clamped Variation of SD of normalized fundamental frequency ω^2 with SD of input RVs Graphite/Epoxy

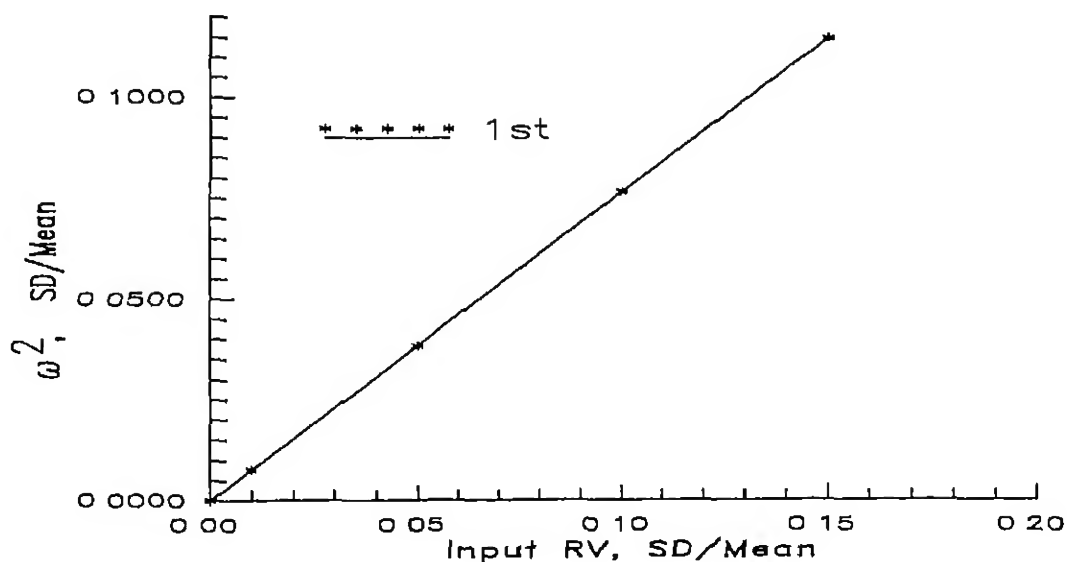


Figure 5.34. $[-45^\circ/45^\circ]_s$ laminate, AR=1, all sides clamped Variation of SD of normalized fundamental frequency ω^2 with SD of input RVs Graphite/Epoxy

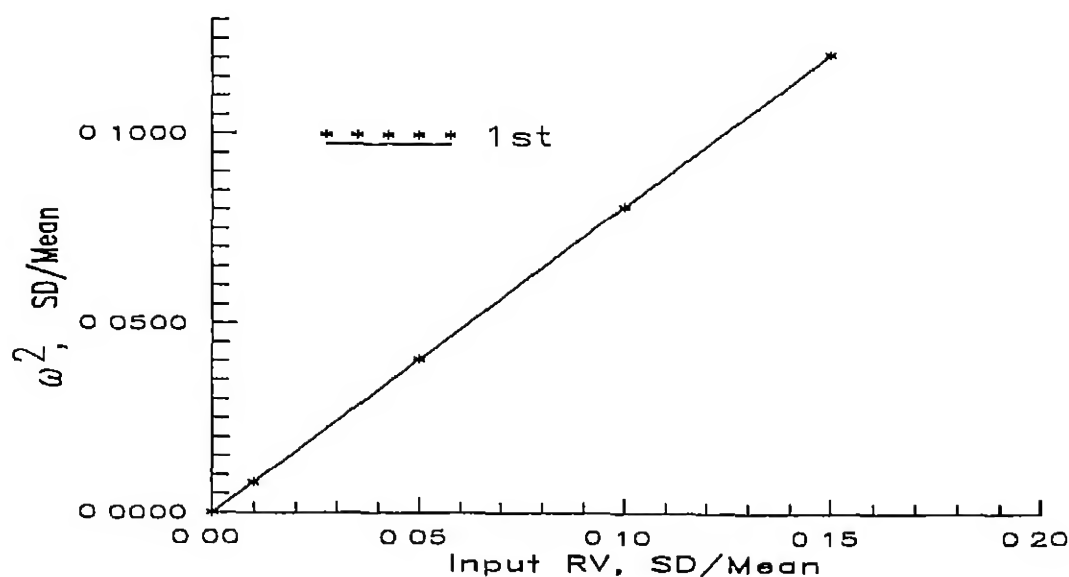


Figure 5.35 $[90^\circ]$ laminate, $AR=1$, all sides clamped Variation of SD of normalized fundamental frequency ω^2 with SD of input RVs Graphite/Epoxy

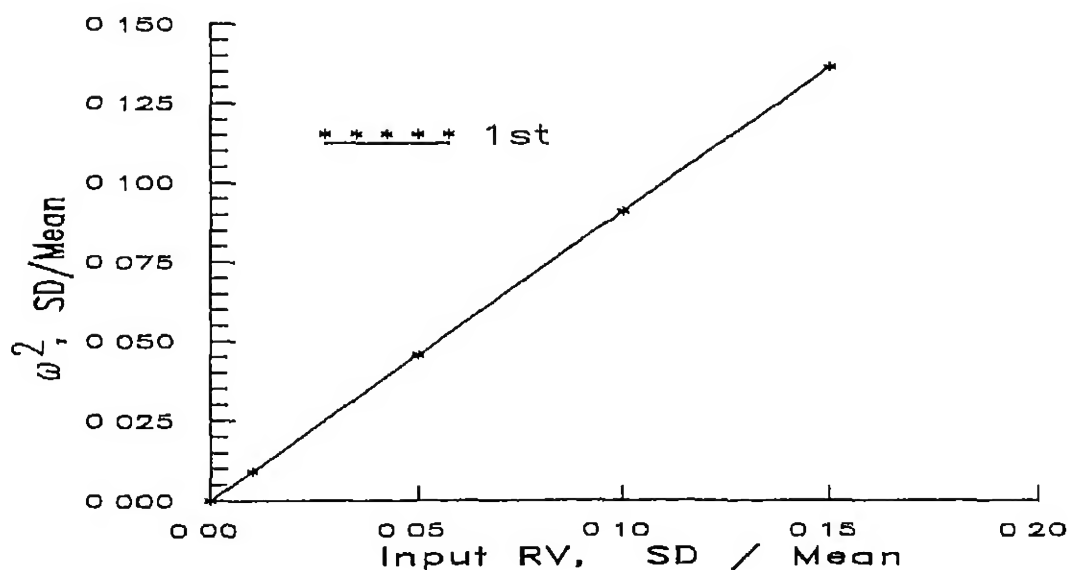


Figure 5.36 $[0^\circ/45^\circ/90^\circ/-45^\circ]_s$ laminate, $AR=1$, all sides clamped Variation of SD of normalized fundamental frequency ω^2 with SD of input RVs Graphite/Epoxy

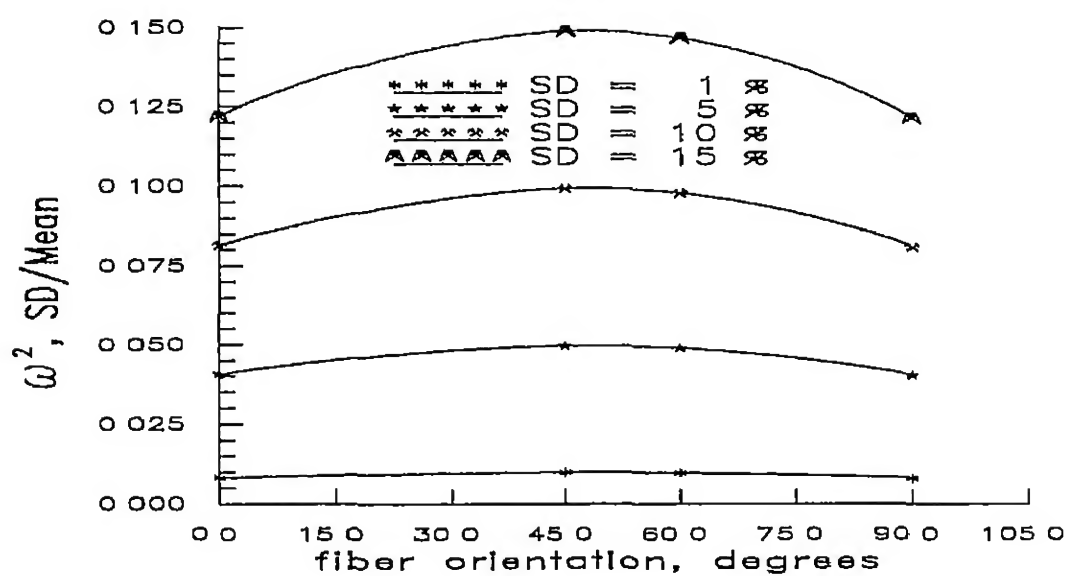


Figure 5.37 AR=1, all sides clamped Variation of SD of normalized first natural frequency ω^2 with change fiber orientation, for different SDs of input RVs Graphite/Epoxy

Chapter 6

COMPOSITE PLATES — BUCKLING ANALYSIS

6.1 INTRODUCTION

The aim of this chapter is to investigate the effect of material property randomness on the initial buckling characteristics of rectangular composite plates. The geometry of the plate and the co-ordinate system used are given in Figure 3.1. The classical laminated plate theory is used for the basic formulation, to arrive at the governing equations for the problem.

6.2 FORMULATION

Consider a rectangular laminated composite plate subjected to uniform inplane compressive and shear loads. The plates considered are supported along all the four edges. The governing equations for such a system in terms of displacements (u^o , v^o and w) and the stiffness matrix

terms (A_{ij} , B_{ij} and D_{ij}) are given by [40] These are

$$\begin{aligned} & A_{11} \frac{\partial^2 u^0}{\partial x^2} + 2A_{16} \frac{\partial^2 u^0}{\partial x \partial y} + A_{66} \frac{\partial^2 u^0}{\partial y^2} + A_{16} \frac{\partial^2 v^0}{\partial x^2} \\ & + (A_{12} + A_{66}) \frac{\partial^2 v^0}{\partial x \partial y} + A_{26} \frac{\partial^2 v^0}{\partial y^2} - B_{11} \frac{\partial^3 w}{\partial x^3} \\ & - 3B_{16} \frac{\partial^3 w}{\partial x^2 \partial y} - (B_{12} + 2B_{66}) \frac{\partial^2 w}{\partial x \partial y^2} - B_{26} \frac{\partial^3 w}{\partial y^3} = 0 \end{aligned} \quad (6.1)$$

$$\begin{aligned} & A_{16} \frac{\partial^2 u^0}{\partial x^2} + (A_{12} + A_{66}) \frac{\partial^2 u^0}{\partial x \partial y} + A_{26} \frac{\partial^2 u^0}{\partial y^2} + A_{66} \frac{\partial^2 v^0}{\partial x^2} \\ & + 3A_{26} \frac{\partial^2 v^0}{\partial x \partial y} + A_{22} \frac{\partial^2 v^0}{\partial y^2} - B_{16} \frac{\partial^3 w}{\partial x^3} - (B_{12} + 2B_{66}) \frac{\partial^3 w}{\partial x^2 \partial y} \\ & - 3B_{26} \frac{\partial^3 w}{\partial x \partial y^2} - B_{22} \frac{\partial^3 w}{\partial y^3} = 0 \end{aligned} \quad (6.2)$$

$$\begin{aligned} & D_{11} \frac{\partial^4 w}{\partial x^4} + 4D_{16} \frac{\partial^4 w}{\partial x^3 \partial y} + 2(D_{12} + 2D_{66}) \frac{\partial^4 w}{\partial x^2 \partial y^2} + 4D_{26} \frac{\partial^4 w}{\partial x \partial y^3} \\ & + D_{22} \frac{\partial^4 w}{\partial y^4} - B_{11} \frac{\partial^3 u^0}{\partial x^3} - 3B_{16} \frac{\partial^3 u^0}{\partial x^2 \partial y} - (B_{12} + 2B_{66}) \frac{\partial^3 u^0}{\partial x \partial y^2} \\ & - B_{26} \frac{\partial^3 u^0}{\partial y^3} - B_{16} \frac{\partial^3 v^0}{\partial x^3} - (B_{12} + 2B_{66}) \frac{\partial^3 v^0}{\partial x^2 \partial y} \\ & - 3B_{26} \frac{\partial^3 v^0}{\partial x \partial y^2} - B_{22} \frac{\partial^3 v^0}{\partial y^3} = N_x \frac{\partial^2 w}{\partial x^2} + 2N_{xy} \frac{\partial^2 w}{\partial x \partial y} + N_y \frac{\partial^2 w}{\partial y^2} \end{aligned} \quad (6.3)$$

Equations 6.1, 6.2 and 6.3 can be simplified based on stacking sequence

6.3 SPECIALLY ORTHOTROPIC LAMINATED PLATE

For the case of specially orthotropic laminates the entire $[B]$ matrix elements reduce to zero. Other coupling terms like $A_{16} = A_{26} = 0$ and $D_{16} = D_{26} = 0$ also vanish. So the only stiffness matrix terms present are D_{11} , D_{22} , D_{12} and D_{66} . Hence, for the present case, the general equations given by Equations 6.1, 6.2 and 6.3 are reduced to the form

$$\begin{aligned}
& D_{11} \frac{\partial^4 w}{\partial x^4} + 2(D_{12} + 2D_{66}) \frac{\partial^4 w}{\partial x^2 \partial y^2} + D_{22} \frac{\partial^4 w}{\partial y^4} \\
& = N_x \frac{\partial^2 w}{\partial x^2} + 2N_{xy} \frac{\partial^2 w}{\partial x \partial y} + N_y \frac{\partial^2 w}{\partial y^2}
\end{aligned} \tag{6.4}$$

We consider the case of uniform compressive load applied along two opposite edges, in the X-direction. Hence Equation 6.4 further reduces to the form

$$D_{11} \frac{\partial^4 w}{\partial x^4} + 2(D_{12} + 2D_{66}) \frac{\partial^4 w}{\partial x^2 \partial y^2} + D_{22} \frac{\partial^4 w}{\partial y^4} = N_x \frac{\partial^2 w}{\partial x^2} \tag{6.5}$$

6.3.1 Simply Supported Plate

The boundary conditions for the case when all the four sides of the plate are simply supported are defined by the following set of equations

along $x = 0$ and $x = a$ for all y

$$\begin{aligned}
w &= 0 \\
M_x &= -D_{11} \frac{\partial^2 w}{\partial x^2} - D_{12} \frac{\partial^2 w}{\partial y^2} \\
&= 0
\end{aligned} \tag{6.6}$$

along $y = 0$ and $y = b$ for all x

$$\begin{aligned}
w &= 0 \\
M_y &= -D_{12} \frac{\partial^2 w}{\partial x^2} - D_{22} \frac{\partial^2 w}{\partial y^2} \\
&= 0
\end{aligned} \tag{6.7}$$

A series approximation for the deflection of the plate, $w(x, y)$ is written as:

$$w(x, y) = \sum_{m=1}^{\infty} \sum_{n=1}^{\infty} a_{mn} X_m(x) Y_n(y) \quad (6.8)$$

where $X_m(x)$ and $Y_n(y)$ are functions that satisfies the set of boundary conditions considered given by Equations 6.6 and 6.7. In terms of beam characteristic functions, Equation 6.8 is rewritten as

$$w(x, y) = \sum_{m=1}^{\infty} \sum_{n=1}^{\infty} a_{mn} \sin \frac{m\pi x}{a} \sin \frac{n\pi y}{b} \quad (6.9)$$

If Equation 6.9 is substituted in the governing Equation 6.5 and simplified, the expression for the initial buckling load is obtained in the form [40]

$$N_o = \frac{\pi^2}{m^2 a^2} [D_{11} m^4 + 2(D_{12} + 2D_{66}) m^2 n^2 R^2 + D_{22} n^4 R^4] \quad (6.10)$$

Equation 6.10 reduces to the critical buckling load expression when $n = 1$. That is

$$N_{cr} = \frac{\pi^2}{m^2 a^2} [D_{11} m^4 + 2(D_{12} + 2D_{66}) m^2 R^2 + D_{22} R^4] \quad (6.11)$$

Equation 6.11 is of the form of Equation 3.2 described in Chapter 3. At this stage we introduce the effect of randomness in material properties on the system response. The procedure described in Chapter 3 is now applied here to incorporate the randomness in basic material parameters and convert the above equation to the form of Equation 3.1. These equations are then solved for the random critical buckling load N_{cr}^R ,

using the random response $w^R(x, y)$, given by

$$w^R(x, y) = \sum_{m=1}^M \sum_{n=1}^N a_{mn}^R \sin \frac{m\pi x}{a} \sin \frac{n\pi y}{b} \quad (6.12)$$

The mean and variance of the random critical buckling load N_{cr}^R can be found, provided the statistics of the basic random variables b_i^R are known

6.3.2 Clamped Plate

For the case of a plate clamped on all the edges it is difficult to solve the governing Equation 6.5 in closed form. So the energy method is used here to formulate the problem and to find an approximate solution. Simplified energy criterion for the present problem, with inplane compressive loads is given by

$$\text{Total potential } \Pi_p = U + W = \text{stationary value} \quad (6.13)$$

Where U is the strain energy, W is the work done by the external loads

For the present case total potential Π_p is given by

$$\begin{aligned} \Pi_p = U + W &= \frac{1}{2} \int_0^b \int_0^a \left[D_{11} \left(\frac{\partial^2 w}{\partial x^2} \right)^2 + 2D_{12} \frac{\partial^2 w}{\partial x^2} \frac{\partial^2 w}{\partial y^2} \right. \\ &\quad \left. + D_{22} \left(\frac{\partial^2 w}{\partial y^2} \right)^2 + 4D_{66} \left(\frac{\partial^2 w}{\partial x \partial y} \right)^2 + N_x \left(\frac{\partial^2 w}{\partial x^2} \right)^2 \right] dx dy \\ &= \text{stationary value} \end{aligned} \quad (6.14)$$

The boundary conditions for the case when all the sides are clamped are given by

along $x = 0$ and $x = a$ for all y

$$w = 0$$

$$\frac{\partial w}{\partial x} = 0 \quad (6.15)$$

along $y = 0$ and $y = b$ for all x

$$w = 0$$

$$\frac{\partial w}{\partial y} = 0 \quad (6.16)$$

We employ Rayleigh–Ritz technique to solve the Equation 6.14 for the boundary conditions specified by Equations 6.15 and 6.16. A series approximating function for $w(x, y)$ satisfying the boundary conditions given by Equations 6.15 and 6.16 can be defined as

$$w(x, y) = \sum_{m=1}^M \sum_{n=1}^N a_{mn} X_m(x) Y_n(y) \quad (6.17)$$

with $X_m(x)$ and $Y_n(y)$ that satisfy the boundary conditions given by

$$X_m(x) = (x^2 - ax)^2 x^{(m-1)}$$

$$Y_n(y) = (y^2 - by)^2 y^{(n-1)} \quad (6.18)$$

Substituting Equation 6.17 in Equation 6.14 and applying the conditions given by Equations 6.15 and 6.16 we get the following set of $M \times N$ equations

$$\begin{aligned}
& \sum_{i=1}^M \sum_{j=1}^N \left\{ D_{11} \int_0^a \frac{d^2 X_i}{dx^2} \frac{d^2 X_m}{dx^2} dx \int_0^b Y_j Y_n dy \right. \\
& \quad + D_{12} \left[\int_0^a X_m \frac{d^2 X_i}{dx^2} dx \int_0^b Y_j \frac{d^2 Y_n}{dy^2} dy + \int_0^a X_i \frac{d^2 X_m}{dx^2} dx \int_0^b Y_n \frac{d^2 Y_j}{dy^2} dy \right] \\
& \quad + D_{22} \int_0^a X_i X_m dx \int_0^b \frac{d^2 Y_j}{dy^2} \frac{d^2 Y_n}{dy^2} dy + 4D_{66} \int_0^a \frac{dX_i}{dx} \frac{dX_m}{dx} dx \int_0^b \frac{dY_j}{dy} \frac{dY_n}{dy} dy \\
& \quad \left. + N_x \int_0^a \frac{dX_i}{dx} \frac{dX_m}{dx} dx \int_0^b Y_j Y_n dy \right\} a_{mn} = 0 \\
& m = 1, 2, \dots, M \text{ and } n = 1, 2, \dots, N
\end{aligned} \tag{6.19}$$

Equation 6.19 can once again be expressed in the form of Equation 3.2 described in Chapter 3. The effect of randomness in primary random variables can be introduced in Equation 6.19 using the techniques described in Chapter 3. The characteristics of random critical buckling load N_{cr}^R can now be found, if the statistics of input random variables b_i^R are known.

6.4 MIDPLANE SYMMETRIC LAMINATED PLATE

Midplane symmetric laminates have the bending-twisting coupling terms present in the governing equations. The coupling stiffness matrix terms $[B]$ are identically zero. The stiffness matrix terms D_{11} , D_{12} , D_{22} , D_{66} , D_{16} and D_{26} are present in the governing equation.

6.4.1 Simply Supported Plate

For midplane symmetric laminated plates the Equation 6.3 reduces to the following form

$$\begin{aligned}
 & D_{11} \frac{\partial^4 w}{\partial x^4} + 4D_{16} \frac{\partial^4 w}{\partial x^3 \partial y} + 2(D_{12} + 2D_{66}) \frac{\partial^4 w}{\partial x^2 \partial y^2} \\
 & + 4D_{26} \frac{\partial^4 w}{\partial x \partial y^3} + D_{22} \frac{\partial^4 w}{\partial y^4} \\
 & = N_x \frac{\partial^2 w}{\partial x^2}
 \end{aligned} \tag{6.20}$$

The boundary conditions when all the four sides are simply supported are given by Equations 4.22 and 4.23. Since closed form solution of Equation 6.20 is difficult for this set of boundary conditions, we attempt a solution of the problem by energy method. Here the total potential Π_p can be expressed in the following form

$$\begin{aligned}
 \Pi_p = U + W &= \frac{1}{2} \int_0^b \int_0^a \left[D_{11} \left(\frac{\partial^2 w}{\partial x^2} \right)^2 + 2D_{12} \frac{\partial^2 w}{\partial x^2} \frac{\partial^2 w}{\partial y^2} \right. \\
 & + D_{22} \left(\frac{\partial^2 w}{\partial y^2} \right)^2 + 4D_{16} \frac{\partial^2 w}{\partial x^2} \frac{\partial^2 w}{\partial x \partial y} + 4D_{26} \frac{\partial^2 w}{\partial y^2} \frac{\partial^2 w}{\partial x \partial y} \\
 & \left. + 4D_{66} \left(\frac{\partial^2 w}{\partial x \partial y} \right)^2 + N_x \left(\frac{\partial^2 w}{\partial x^2} \right)^2 \right] dx dy \\
 & = \text{stationary value}
 \end{aligned} \tag{6.21}$$

The approximating function for $w(x, y)$ satisfying the boundary conditions can be assumed again in the form of Equation 6.9. From these equations applying Rayleigh–Ritz method we get a set of $M \times N$ linear equations as:

$$\begin{aligned}
& \sum_{i=1}^M \sum_{j=1}^N \left\{ D_{11} \int_0^a \frac{d^2 X_i}{dx^2} \frac{d^2 X_m}{dx^2} dx \int_0^b Y_j Y_n dy \right. \\
& + D_{12} \left[\int_0^a X_m \frac{d^2 X_i}{dx^2} dx \int_0^b Y_j \frac{d^2 Y_n}{dy^2} dy + \int_0^a X_i \frac{d^2 X_m}{dx^2} dx \int_0^b Y_n \frac{d^2 Y_j}{dy^2} dy \right] \\
& + D_{22} \int_0^a X_i X_m dx \int_0^b \frac{d^2 Y_j}{dy^2} \frac{d^2 Y_n}{dy^2} dy + 4D_{66} \int_0^a \frac{dX_i}{dx} \frac{dX_m}{dx} dx \int_0^b \frac{dY_j}{dy} \frac{dY_n}{dy} dy \\
& + 2D_{16} \left[\int_0^a \frac{d^2 X_i}{dx^2} \frac{dX_m}{dx} dx \int_0^b Y_j \frac{dY_n}{dy} dy + \int_0^a \frac{dX_i}{dx} \frac{d^2 X_m}{dx^2} dx \int_0^b Y_n \frac{dY_j}{dy} dy \right] \\
& + 2D_{26} \left[\int_0^a X_m \frac{dX_i}{dx} dx \int_0^b \frac{dY_j}{dy} \frac{d^2 Y_n}{dy^2} dy + \int_0^a X_i \frac{dX_m}{dx} dx \int_0^b \frac{d^2 Y_j}{dy^2} \frac{dY_n}{dy} dy \right] \\
& \left. + N_x \int_0^a \frac{dX_i}{dx} \frac{dX_m}{dx} dx \int_0^b Y_j Y_n dy \right\} a_{mn} = 0 \\
& m = 1, 2, \dots, M \text{ and } n = 1, 2, \dots, N
\end{aligned} \tag{6.22}$$

Equation 6.22 is of the form of Equation 3.2 discussed in Chapter 3. The effect due to randomness in basic material parameters can now be introduced by assuming an approximating function as given below for the random process for deflection $w^R(x, y)$

$$w^R(x, y) = \sum_{m=1}^M \sum_{n=1}^N a_{mn}^R X_m(x) Y_n(y) \tag{6.23}$$

From Equation 6.22 and 6.23 employing the technique described in Chapter 3 statistics of the random critical buckling load N_{cr}^R can be found, provided the statistics of the primary random variables are known.

6.4.2 Clamped Plate

Here again the energy formulation along with the Rayleigh–Ritz technique is used to solve the problem. The total potential energy equation

and the derived governing equation are given by Equations 6.21 and 6.22 respectively. The boundary conditions for the case where all the four sides of a rectangular plate are clamped are given by Equations 6.15 and 6.16. Equations 6.17 and 6.18 give the approximating functions satisfying these boundary conditions. A series approximating function like Equation 6.23 is used to incorporate the randomness owing to the basic material characteristics. The characteristics of the random critical buckling load process N_{cr}^R is found using the procedure described in Chapter 3.

6.5 NUMERICAL RESULTS

The effect of randomness in material parameters on the buckling load and the mode shape is described in this section. We limit our discussion to rectangular plates. Thickness of the plates are taken to be the same irrespective of the change in laminate configurations. The mean values for the basic material parameters E_{11} , E_{22} , G_{12} and ν_{12} for Graphite/Epoxy composite are as given in Table 4.1. The randomness in these basic material parameters is incorporated by the perturbation technique described in Chapter 3. Bulk of the results presented are for a typical Graphite/Epoxy composite. Some results are given for a Glass/Epoxy composite system also.

6 5 1 Validation of the Technique

Validation of the present technique applied to the plate buckling problem is done by comparing the results obtained using the present technique with the results from an independent Monte Carlo simulation. The problem of a $[90^\circ]$ rectangular lamina with all the four sides simply supported, subjected to a uniformly distributed compressive load from two opposite X-edges is considered for this. The results are computed for a Graphite/Epoxy system. In Figure 6.1 SD of normalized buckling load N_{cr} ($N_{cr} = \frac{N_x b^2}{4D_{22}}$) is plotted against the aspect ratio for various SD of input RVs ranging from 1 percent to 15 percent of mean. Results from the present technique are compared with that from the Monte Carlo simulation. For the range of SD of input RVs considered results from the simulation are almost identical to those from the present approximation. Hence we can see that the first order perturbation approximation assumption for the random variables is valid for the present class of problems. One can further conclude that neglecting of the higher order terms does not introduce any significant error in the results.

6 5 2 Simply Supported Rectangular Plate

Numerical results are presented for initial buckling of laminated thin rectangular composite plates. The results are presented for a typical

Graphite/Epoxy system Here we consider plates with all the four sides simply supported The plates are assumed to be subjected to uniformly distributed compressive load from the pair of opposite X-edges

The mean of normalized critical buckling load N_{cr} plotted against the aspect ratio is given in Figure 6.2 for a $[90^\circ]$ lamina

Figure 6.3 shows the change in SD of normalized critical buckling load N_{cr} with the change in aspect ratio a/b The results are for a $[90^\circ]$ lamina Plots are given for various values of SD of E_{11} SD of all other basic material parameters are assumed to be zero Similar plots, for change in SD of E_{22} , ν_{12} and G_{12} , with SD of all the other RVs kept zero is given in Figures 6.4, 6.5 and 6.6 respectively SD of E_{11} and E_{22} has the maximum influence on the SD of buckling load N_{cr} SD of ν_{12} has the least influence on the buckling load In the case of G_{12} the SD of N_{cr} is independent of the aspect ratio It dependent only on the input SD For ν_{12} except at very low aspect ratios SD of N_{cr} is independent of aspect ratio But in the case of E_{11} and E_{22} there we can see abrupt jumps in the SD of N_{cr} as the aspect ratio of the plate is gradually increased In the first case SD of N_{cr} shows an increasing trend as the aspect ratio is increased. But in the case of E_{22} the trend is reversed and the SD of N_{cr} decreases for higher aspect ratios Further in both the cases for low levels of SD of input RVs, the SD of N_{cr} seems to be independent of the change in aspect ratio It may be noted here that E_{11} is a fiber dominated property, where as E_{22} is a matrix

dominated property

The ratio of SD to mean is assumed to be same for all the input RVs. The mean of normalized critical buckling load plotted against the aspect ratio, for laminate configurations $[0^\circ]$, $[90^\circ/0^\circ]_s$ and $[0^\circ/90^\circ]_s$ are given in Figure 6.7, 6.8 and 6.9 respectively. These indicate a trend similar to the results from a conventional deterministic analysis. Laminate configurations with the outer plies having higher stiffness in the load direction gives higher buckling loads.

Figure 6.10 shows the change of SD of N_{cr} with the aspect ratio for $[90^\circ]$ lamina. Different plots are given to show the change in SD of N_{cr} with the change in SD of input RVs b_f^R . The SD of N_{cr} has similar qualitative behavior with variation in aspect ratio and m , as the mean of N_{cr} . Increased randomness in the input is reflected in the increased level of SD of N_{cr} for the plate. Figure 6.11 shows the change of SD of N_{cr} with the aspect ratio for $[90^\circ/0^\circ]_s$ laminate. The general trend is similar in nature to the $[90^\circ]$ laminate. Figures 6.12 and 6.13 show corresponding results for $[0^\circ]$ and $[0^\circ/90^\circ]_s$ laminate configurations. The trend in the plot is similar to the plot of mean of N_{cr} . We can observe that the N_{cr} is less and less affected by the change in aspect ratio as the SD of input RVs is decreased. At 1 percent SD of the input RVs the N_{cr} is virtually unaffected by the change in aspect ratio of the plate. Thus, we may be able to set a limit for the SD of input RVs below which their influence on the aspect ratio can be neglected.

We can see that Figure 6 10 — where all the input RVs are assumed to have the same SD — is a combination of Figures 6 3, 6 4, 6 5 and 6 6. The nature of variation of each one of the four basic random variables is different. The combined nature of variation of the SD of N_{cr} will strongly depend on the magnitude and nature of contribution of the individual RVs.

The mean values of normalized critical buckling load N_{cr} for plates with various stacking sequences, having aspect ratio 1 0, are given in Table 6 1. All the plates are simply supported on the four edges. The results for laminates having stacking sequences $[45^\circ]$, $[45^\circ/0^\circ]_s$, $[0^\circ/45^\circ/90^\circ/-45^\circ]_s$ and $[-45^\circ/45^\circ]_s$ in the form of plots of SD of normalized critical buckling load against the SD of input RVs are given in Figures 6 14, 6 15, 6 16 and 6 17 respectively. The results are for square plates, when all the input RVs are assumed to have the same SD to mean ratio. The maximum buckling load is given by the $[45^\circ]$ lamina. We can see that, in the case of $[45^\circ/0^\circ]_s$ laminate the 0° layers don't have much effect on the SD of N_{cr} . The results in the case of $[0^\circ/45^\circ/90^\circ/-45^\circ]_s$ are similar to that for $[0^\circ]$ lamina given in Figure 6 12 earlier, again indicating the overall dominating influence of outer layers.

Figure 6 18 gives the SD of N_{cr} against SD of input RVs plot for a $[60^\circ]$ square lamina.

Now we examine some results for a typical Glass/Epoxy composite. Figure 6 19 shows the normalized mean buckling load plotted against

the aspect ratio. The SD of normalized buckling load plotted against the aspect ratio is given in Figure 6.20. Both the results are for a $[90^\circ]$ rectangular lamina with all the edges simply supported. The general trend for N_{cr} is similar in the two material systems. However, the Graphite/Epoxy mean critical buckling load plot given by Figure 6.2 shows lower buckling loads in comparison with that for Glass/Epoxy composite given by Figure 6.19. The corresponding plots for SD of N_{cr} also shows higher values for Graphite/Epoxy system. Here also, as observed earlier at low levels of SD of input RVs change in the aspect ratio do not have any effect on the SD of N_{cr} , except at very low values of aspect ratio.

6.5.3 Clamped Rectangular Plate

In this section we consider thin rectangular plates clamped along all the four edges, subjected to a uniformly distributed inplane buckling load along the pair of opposite X-edges.

Table 6.2 gives the mean values of N_{cr} for square plates clamped on all the four edges having various stacking sequences. Results for SD of N_{cr} for laminates having stacking sequences $[90^\circ]$, $[0^\circ]$, $[90^\circ/0^\circ]_s$ and $[0^\circ/90^\circ]_s$ are given in Figures 6.21, 6.22, 6.23 and 6.24 respectively. Here the SD of N_{cr} is plotted against the SD of input RVs. All the input RVs are assumed to have the same SD to mean ratio. We can clearly see that those configurations with outer laminas having higher bending

stiffness give higher values of SD of N_{cr}

Figures 6.25, 6.26, 6.27, 6.28 and 6.29 give SD of N_{cr} against SD of input RV plots for $[45^\circ]$, $[45^\circ/0^\circ]_s$, $[-45^\circ/45^\circ]_s$, $[0^\circ/45^\circ/90^\circ/-45^\circ]_s$ and $[60^\circ]$ laminate configurations. In all these cases we can see the dominating influence of the properties of the outer layer on the SD of N_{cr} .

6.6 SUMMARY

The perturbation technique described in Chapter 3 is applied to the problem of buckling of thin rectangular composite plates with randomness in material properties. The validation of the technique for the present set of problems is done by comparing the results obtained from an independent Monte Carlo simulation with the same boundary conditions. Stability characteristics for various laminate configurations with change in stacking sequence, aspect ratio and boundary conditions are presented.

The analysis shows that the first order perturbation approximation for RVs is valid for the present class of problems. In practice the nature of variation of SD of critical buckling load N_{cr} will depend on the magnitude and the nature of contribution of the individual RVs. The results show that below a limit of SD (around 1 percent of mean) of input RVs the aspect ratio doesn't have much influence on the buckling characteristics. Further it is observed that SD of critical buckling load is strongly dependent on the buckling mode shape, if we consider variation of RVs E_{11} and E_{22} alone. This indicates that for two different buckling modes having similar mean critical buckling load values, the SD of buckling load can have widely differing values. The outer plies in laminates, in general have a dominating influence on the SD of critical buckling load.

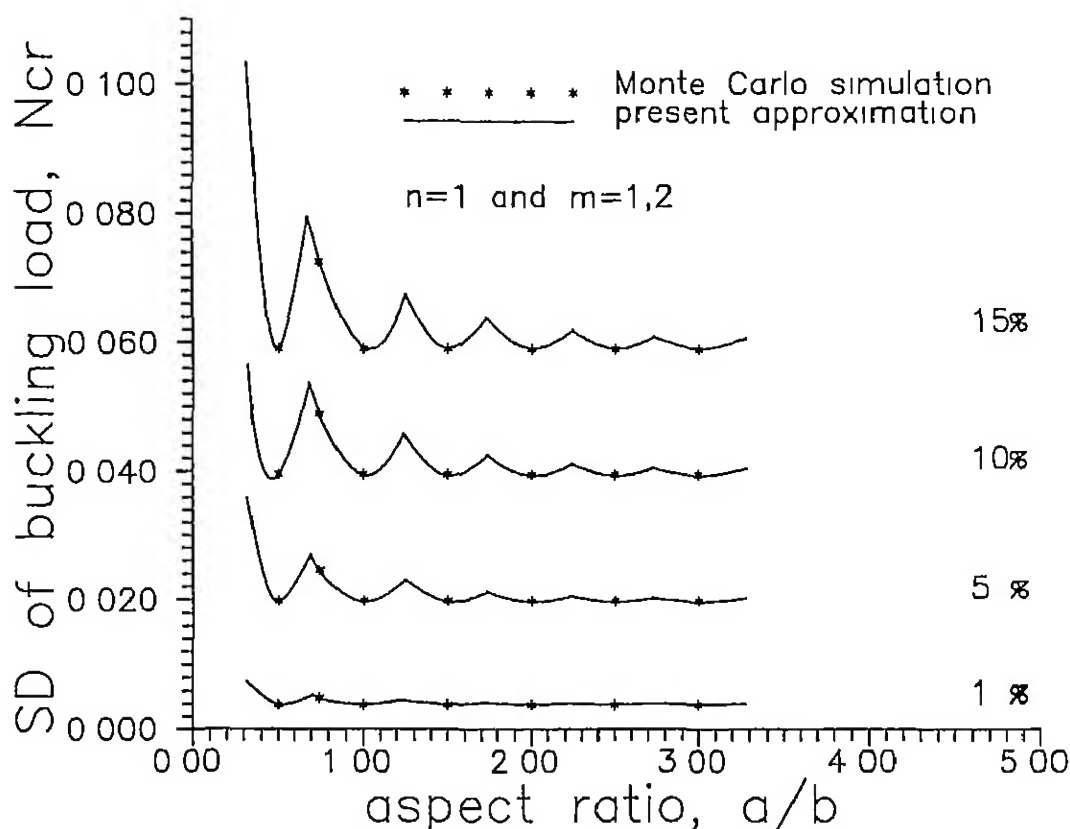


Figure 6.1 $[90^\circ]$ laminate, Normalized SD of buckling load N_{cr} , plotted against the aspect ratio. For various input parameter SDs. Compared with results from a Monte Carlo simulation. All sides simply supported. Graphite/Epoxy.

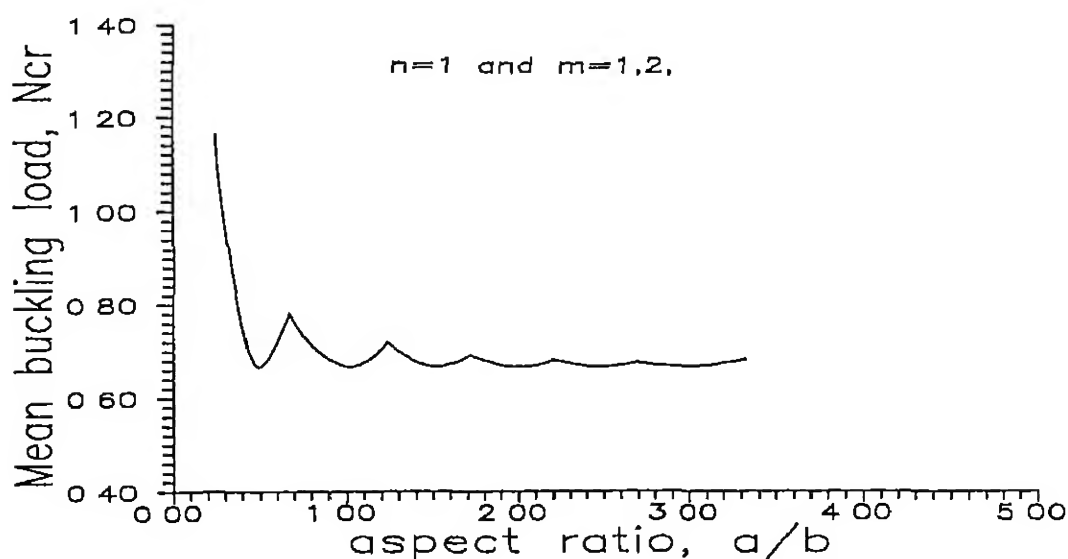


Figure 6.2 Normalized mean buckling load N_{cr} , plotted against the aspect ratio a/b $[90^\circ]$ laminate. All sides simply supported. Graphite/Epoxy.

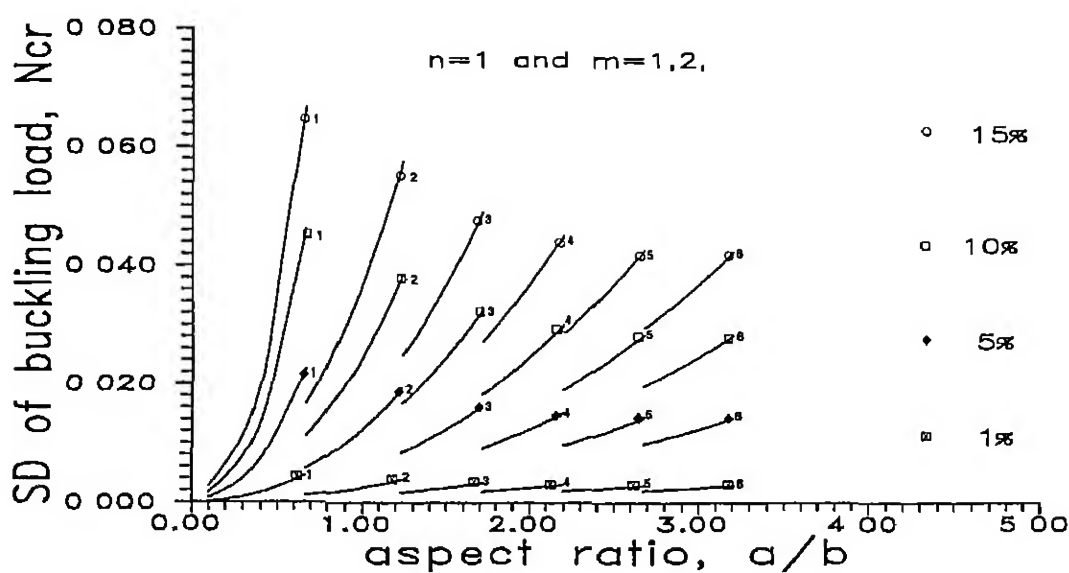


Figure 6.3 $[90^\circ]$ laminate, all sides simply supported Sensitivity of SD of normalized buckling load N_{cr} to SD of input RV E_{11} SD of all other input RVs kept zero Graphite/Epoxy

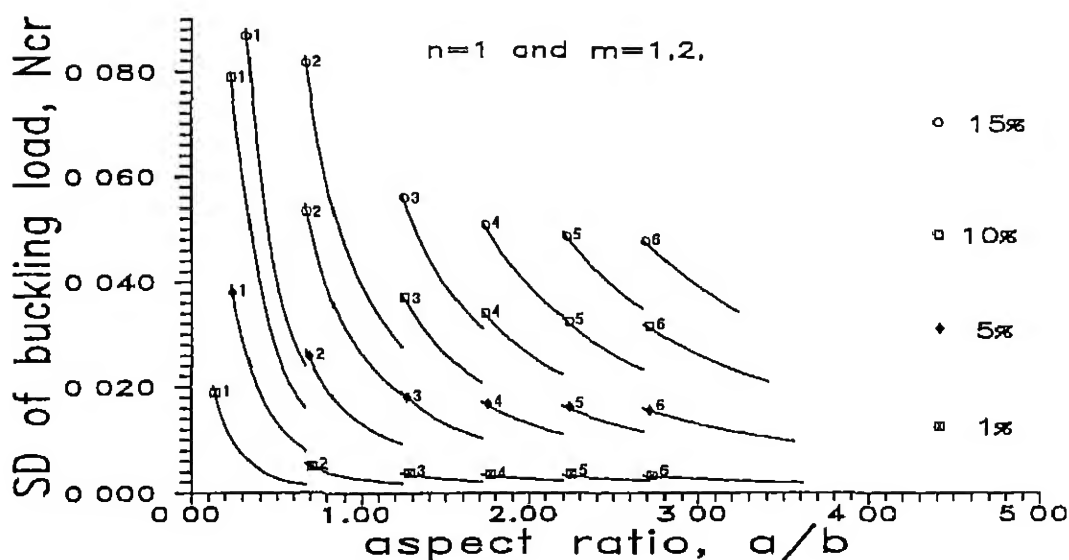


Figure 6.4 $[90^\circ]$ laminate, all sides simply supported Sensitivity of SD of normalized buckling load N_{cr} to SD of input RV E_{22} SD of all other input RVs kept zero Graphite/Epoxy

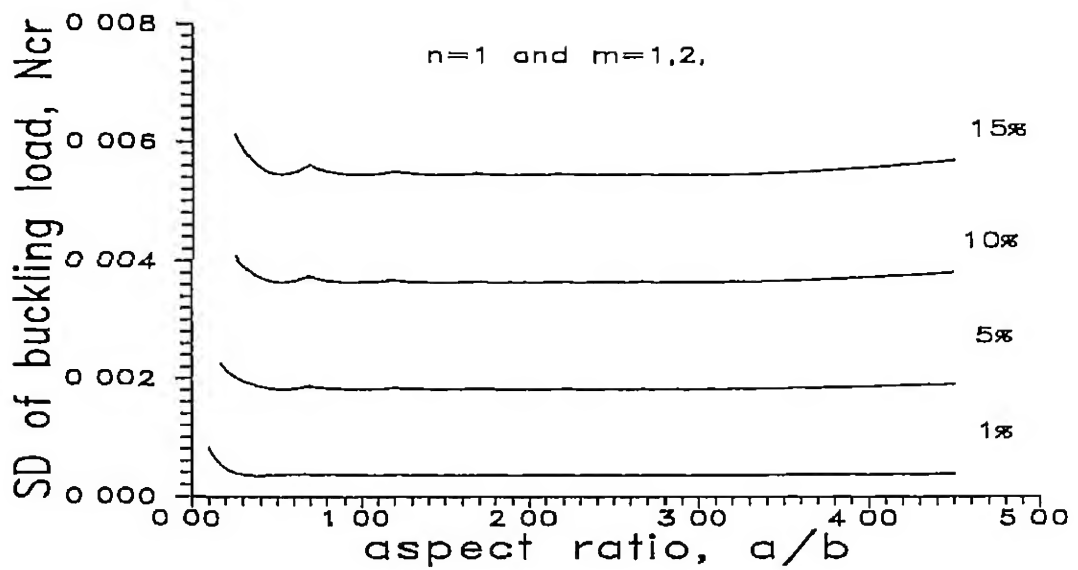


Figure 6.5 $[90^\circ]$ laminate, all sides simply supported Sensitivity of SD of normalized buckling load N_{cr} to SD of input RV ν_{12} SD of all other input RVs kept zero Graphite/Epoxy

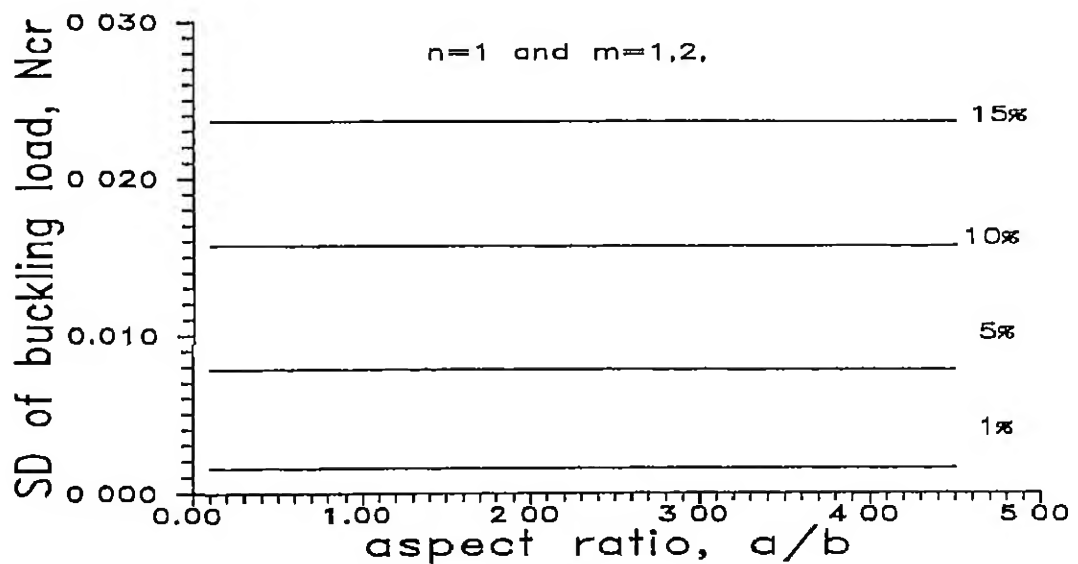


Figure 6.6. $[90^\circ]$ laminate, all sides simply supported Sensitivity of SD of normalized buckling load N_{cr} to SD of input RV G_{12} SD of all other input RVs kept zero Graphite/Epoxy

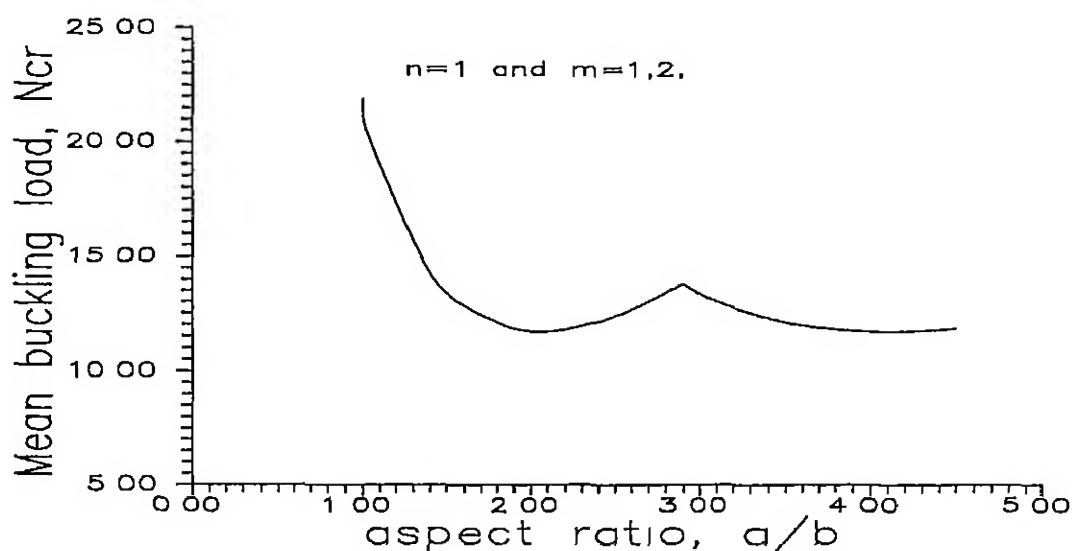


Figure 6.7. Normalized mean buckling load N_{cr} , plotted against the AR $[0^\circ]$ laminate All sides simply supported Graphite/Epoxy

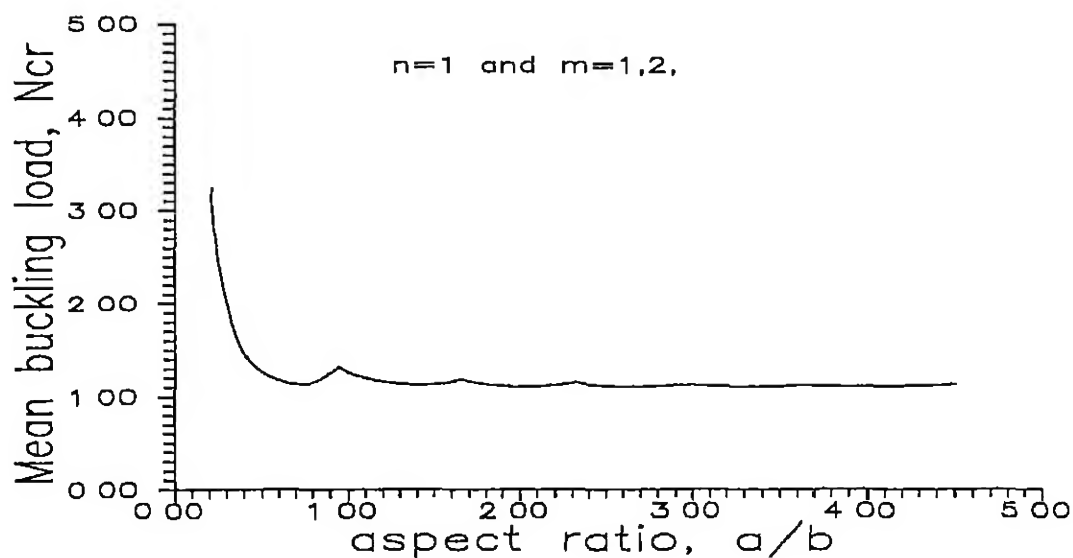


Figure 6.8 Normalized mean buckling load N_{cr} , plotted against the AR $[90^\circ/0^\circ]$, laminate All sides simply supported Graphite/Epoxy

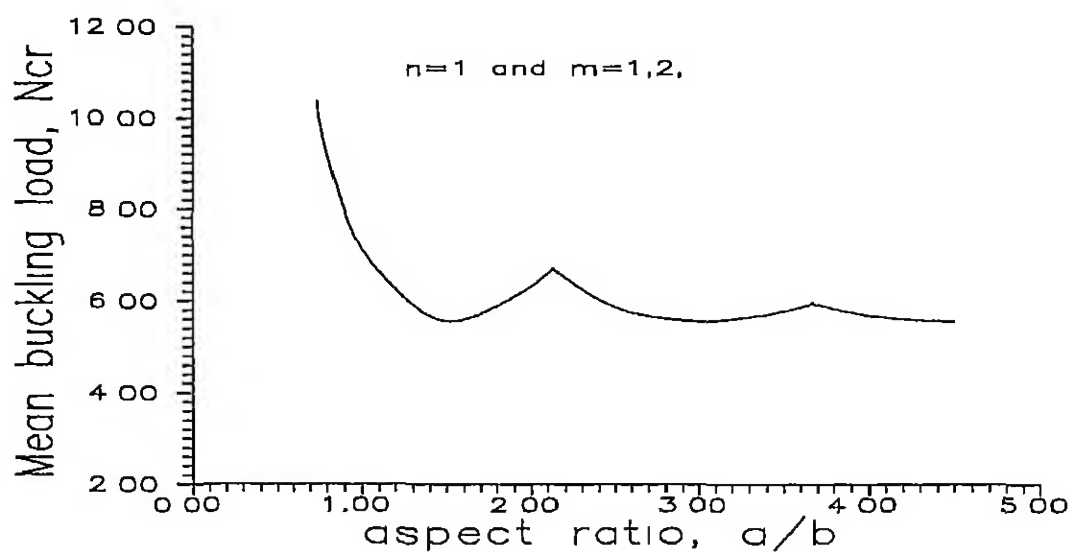


Figure 6.9 Normalized mean buckling load N_{cr} , plotted against the AR $[0^\circ/90^\circ]_s$ lamina. All sides simply supported. Graphite/Epoxy

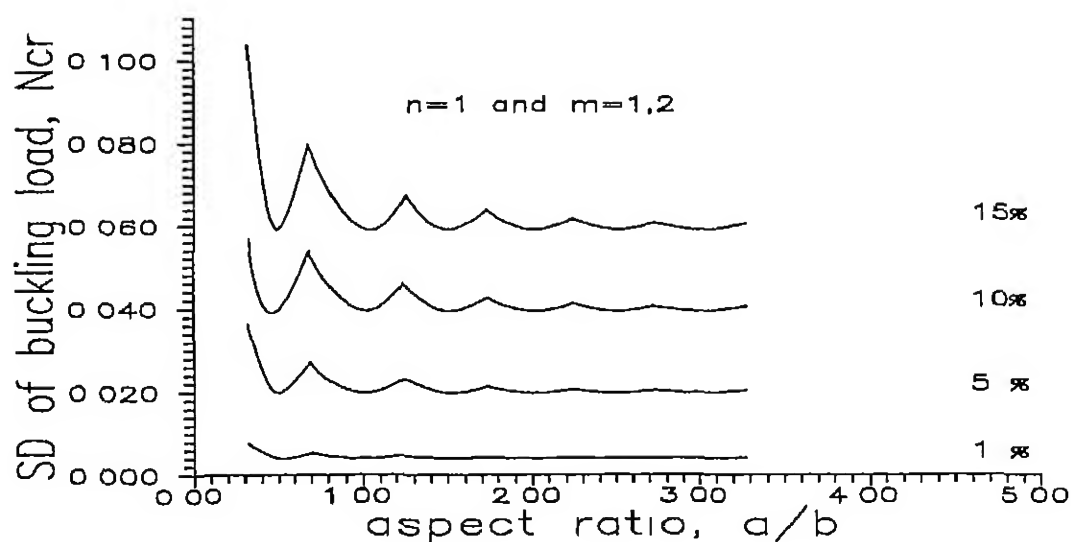


Figure 6.10 Normalized SD of buckling load N_{cr} , plotted against the aspect ratio a/b $[90^\circ]$ laminate, for various input parameter SDs. All sides simply supported. Graphite/Epoxy

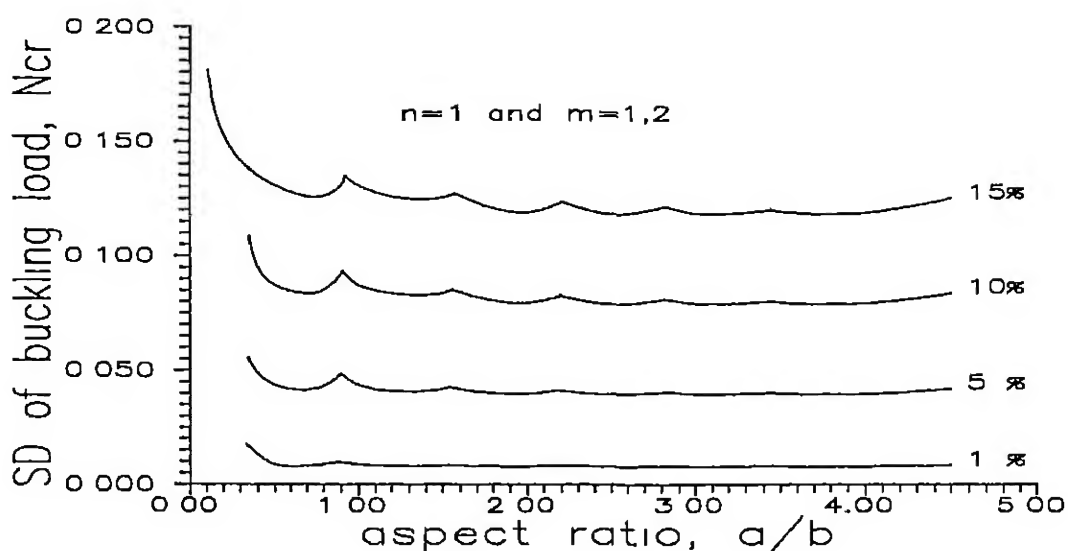


Figure 6 11. Normalized SD of buckling load N_{cr} , plotted against the aspect ratio a/b $[90^\circ/0^\circ]_s$ laminate For various input parameter SDs All sides simply supported Graphite/Epoxy

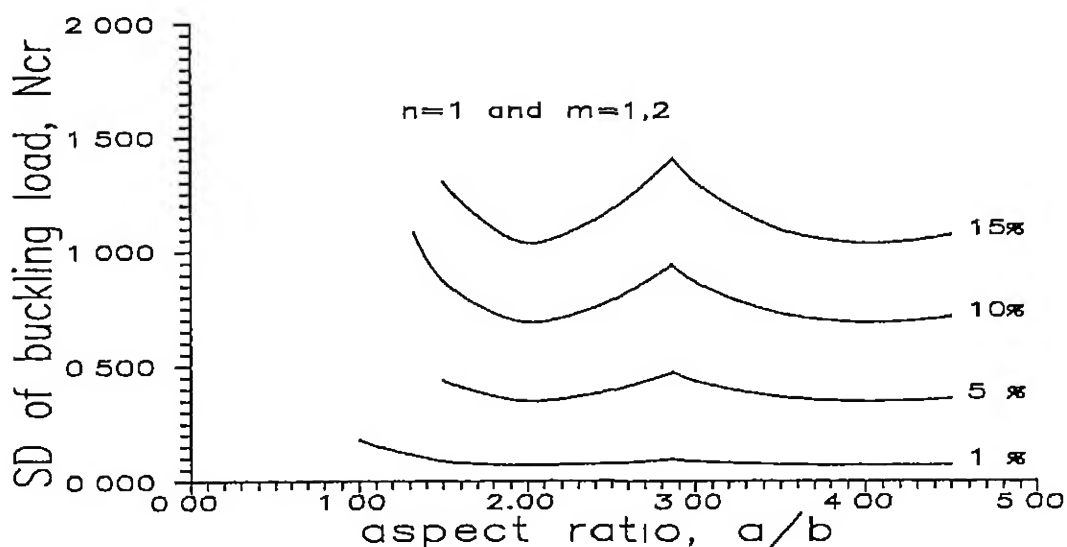


Figure 6 12 SD of normalized buckling load N_{cr} , plotted against the aspect ratio a/b $[0^\circ]$ laminate For various input parameter SDs All sides simply supported Graphite/Epoxy

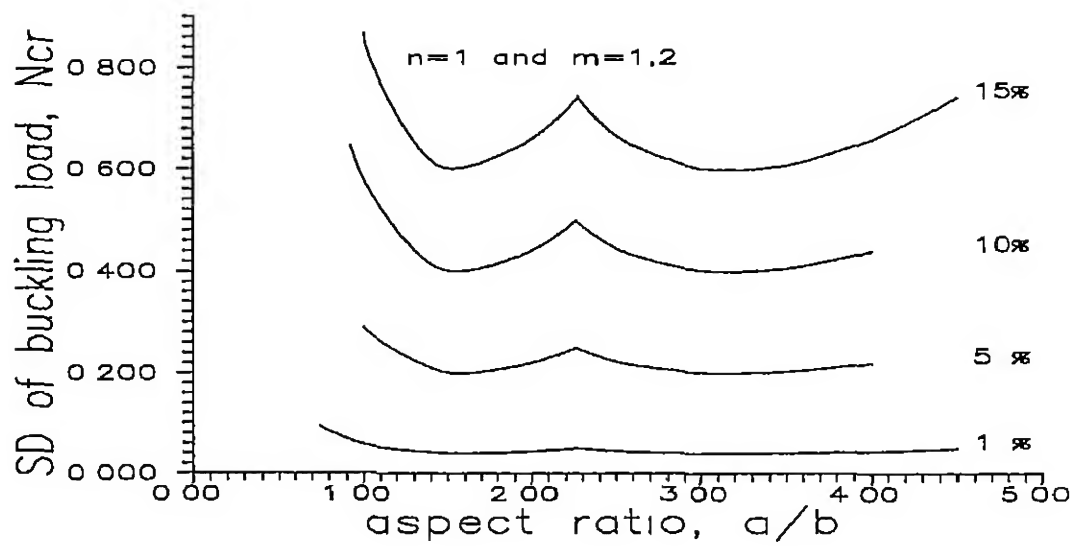


Figure 6.13 SD of normalized buckling load N_{cr} , plotted against the aspect ratio a/b $[0^\circ/90^\circ]_s$ laminate. For various input parameter SDs. All sides simply supported. Graphite/Epoxy.

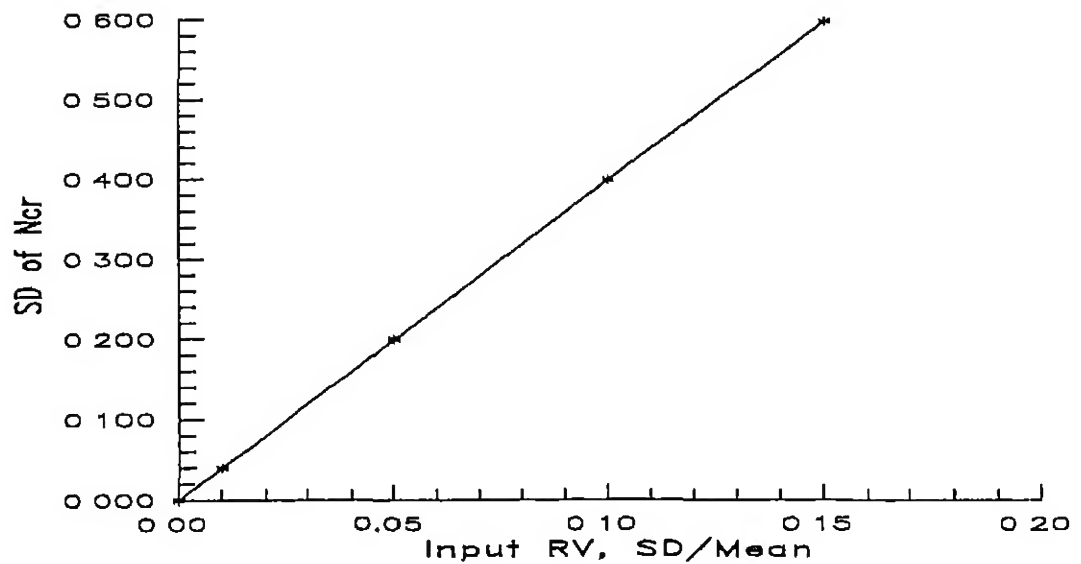


Figure 6.14 SD of normalized buckling load N_{cr} , plotted against the SD of input RVs $[45^\circ]$ laminate, $AR=1$. All sides simply supported. Graphite/Epoxy.

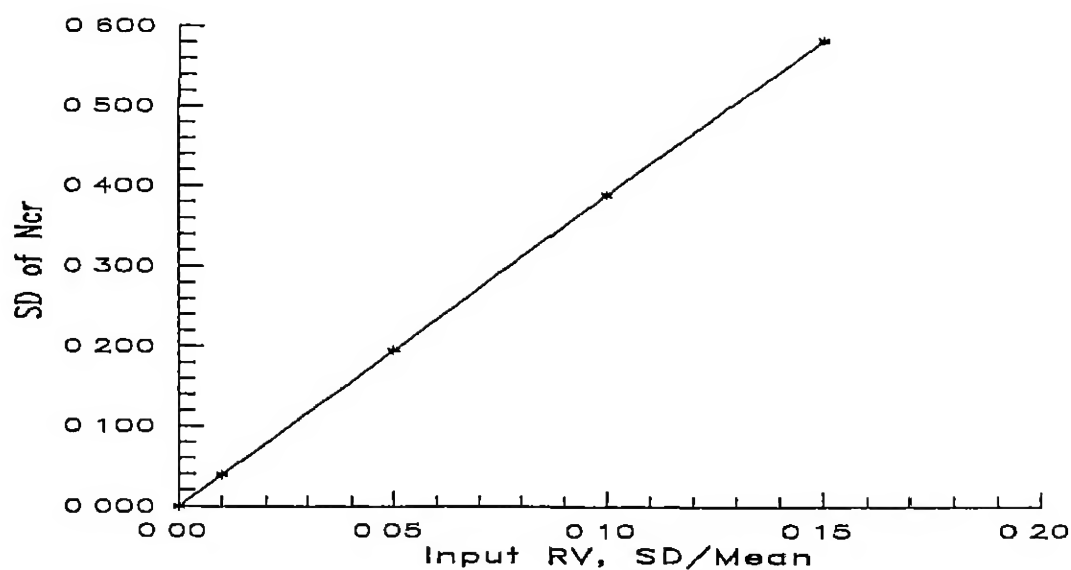


Figure 6.15 SD of normalized buckling load N_{cr} , plotted against the SD of input RVs $[45^\circ/0^\circ]_s$ laminate, $AR=1$ All sides simply supported Graphite/Epoxy

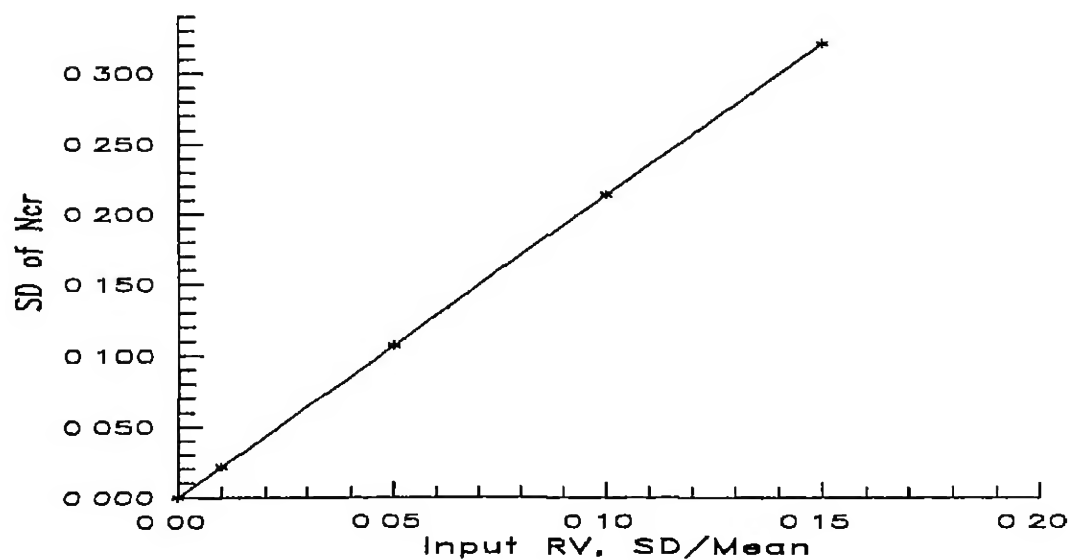


Figure 6.16 SD of normalized buckling load N_{cr} , plotted against the SD of input RVs $[0^\circ/45^\circ/90^\circ/-45^\circ]_s$ laminate, $AR=1$ All sides simply supported Graphite/Epoxy

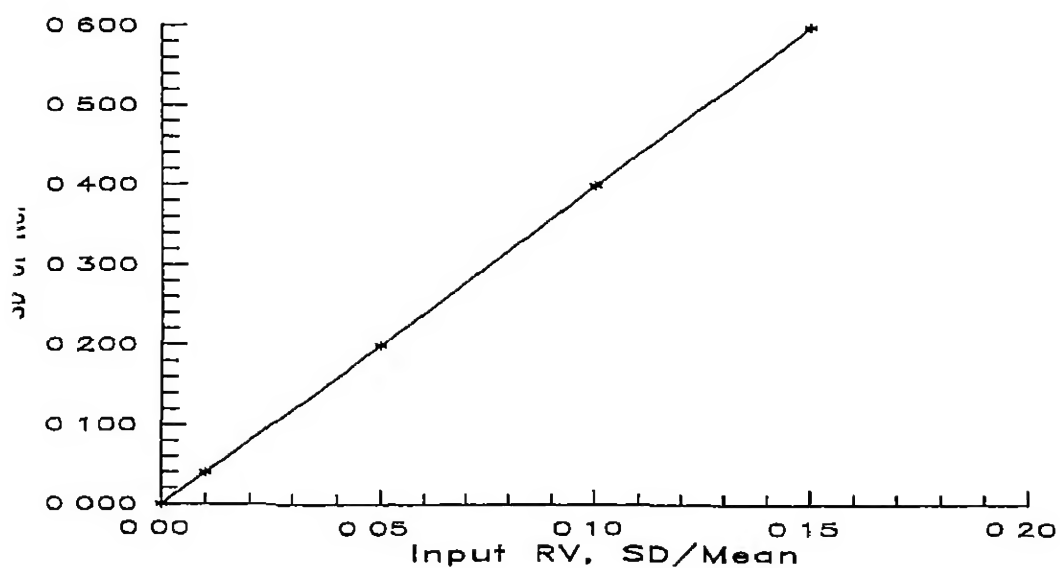


Figure 6.17 SD of normalized buckling load N_{cr} , plotted against the SD of input RVs $[-45^\circ/45^\circ]$, laminate, $AR=1$ All sides simply supported Graphite/Epoxy

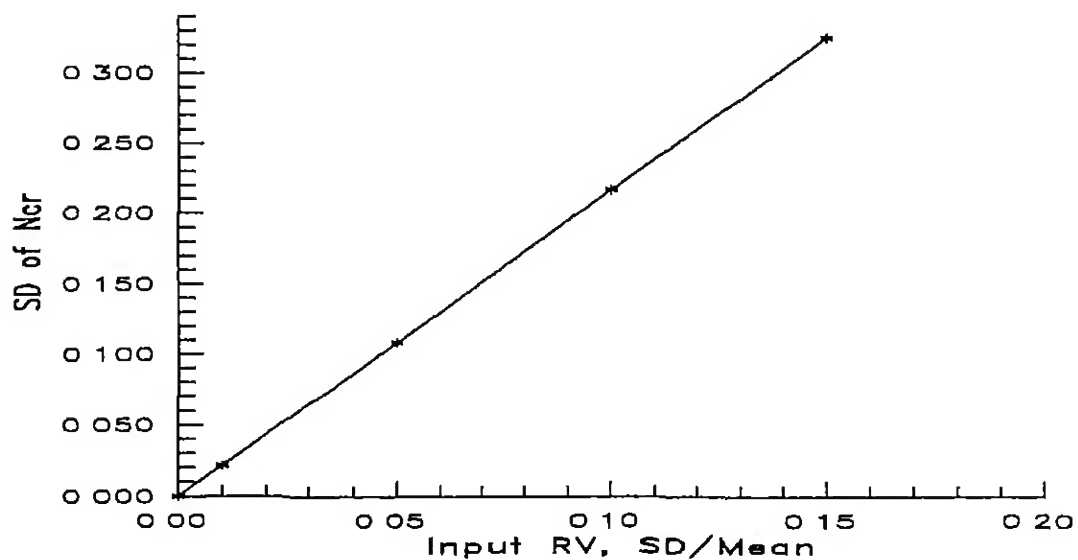


Figure 6.18 SD of normalized buckling load N_{cr} , plotted against the SD of input RVs $[60^\circ]$, laminate, $AR=1$ All sides simply supported Graphite/Epoxy

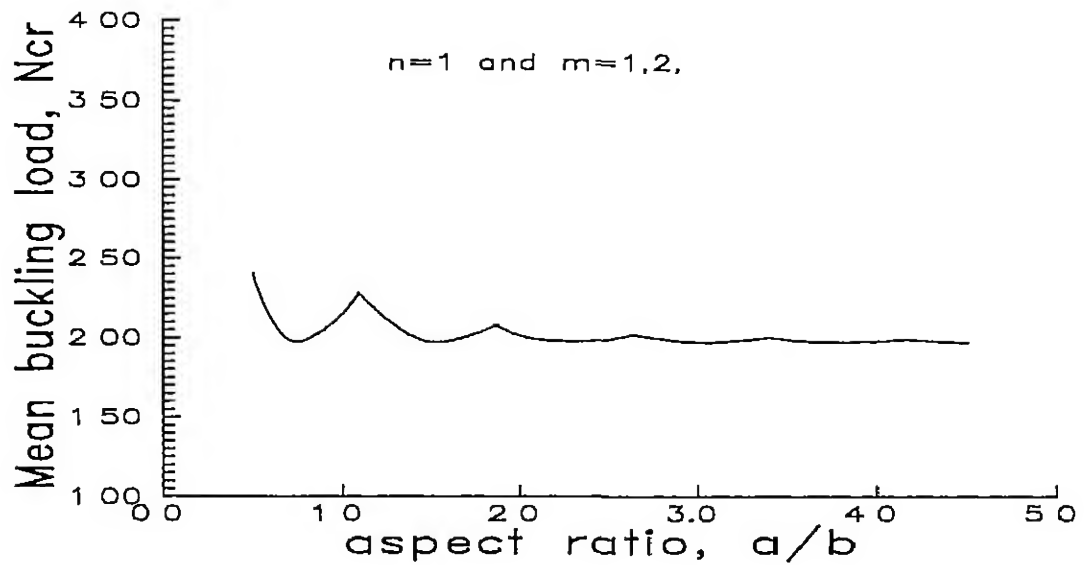


Figure 6 19 Test case Glass/Epoxy composite Normalized mean buckling load N_{cr} , plotted against the aspect ratio a/b $[90^\circ]$ laminate All sides simply supported

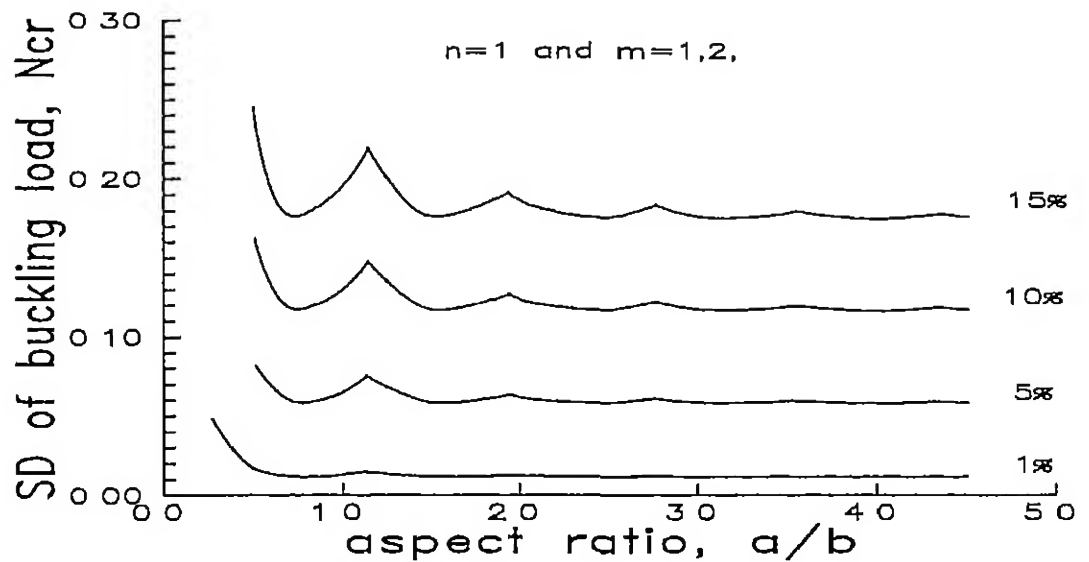


Figure 6 20: Test case Glass/Epoxy composite $[90^\circ]$ laminate, Normalized SD of buckling load N_{cr} , plotted against the aspect ratio. For various input parameter SDs All sides simply supported

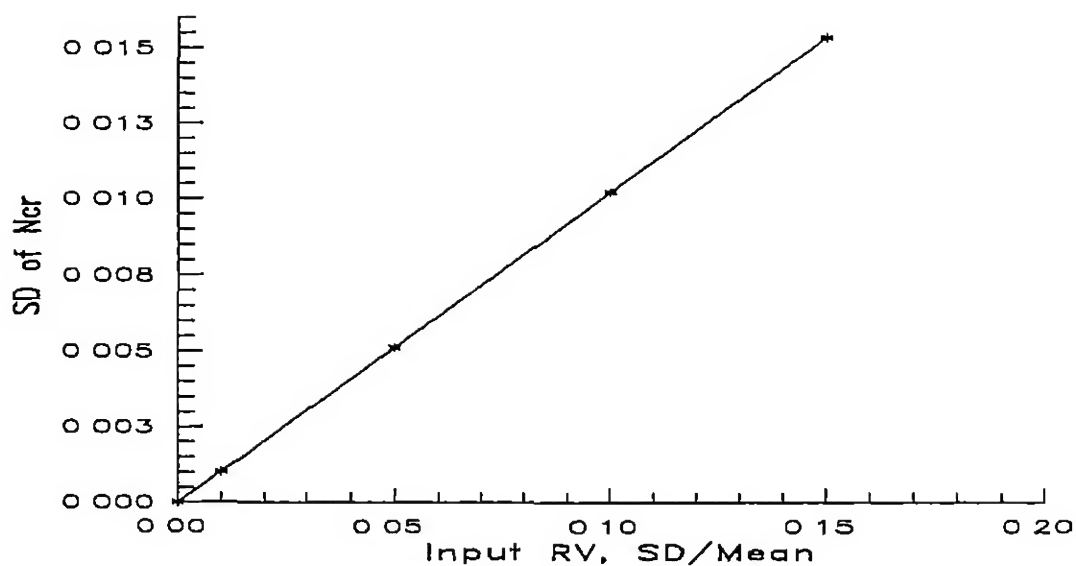


Figure 6.21 SD of normalized buckling load N_{cr} , plotted against the SD of input RVs $[90^\circ]$ laminate, $AR=1$ All sides clamped Graphite/Epoxy

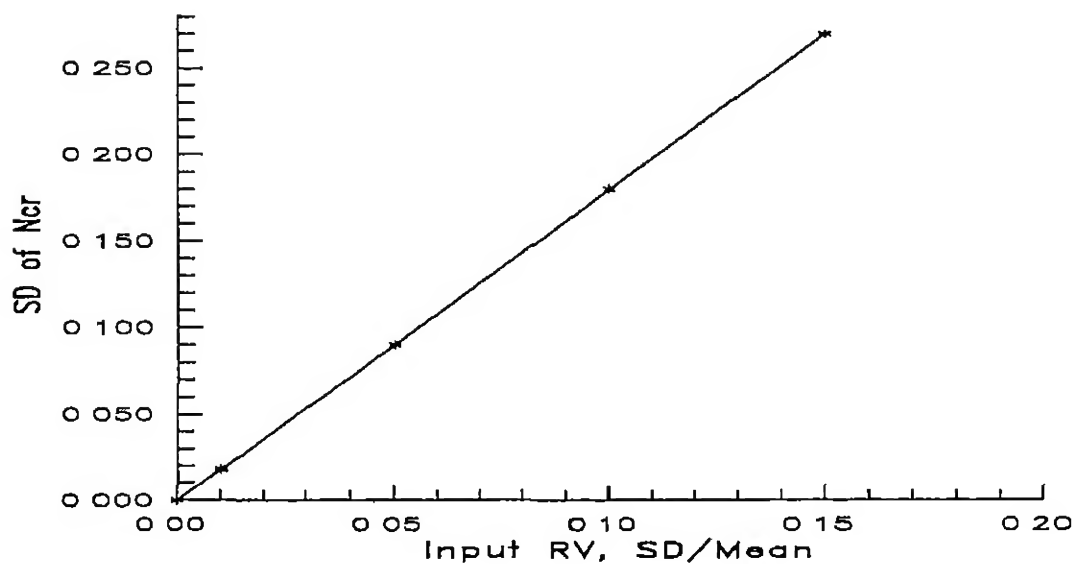


Figure 6.22 SD of normalized buckling load N_{cr} , plotted against the SD of input RVs $[0^\circ]$ laminate, $AR=1$ All sides clamped Graphite/Epoxy

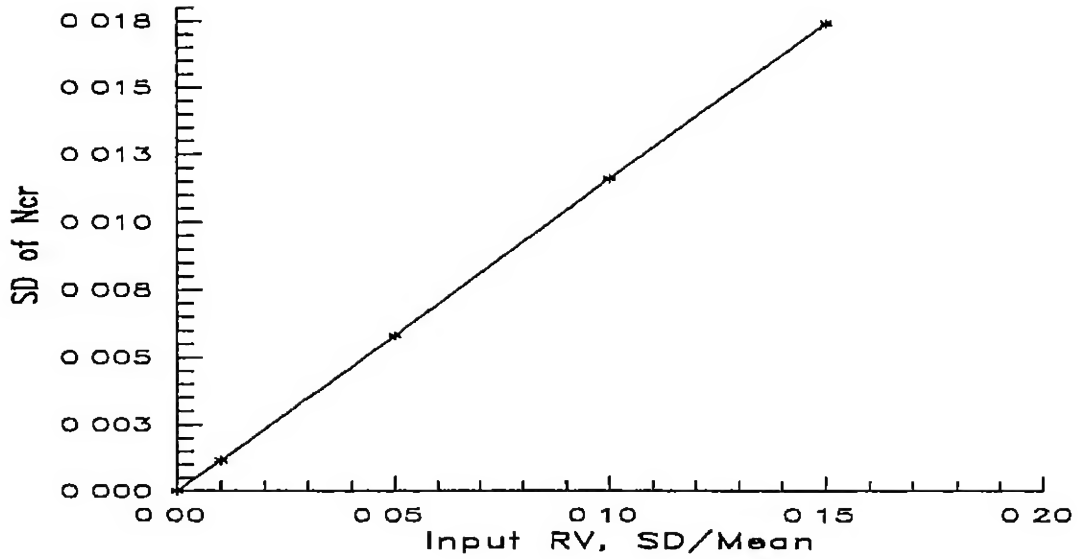


Figure 6.23 SD of normalized buckling load N_{cr} , plotted against the SD of input RVs $[90^\circ/0^\circ]_s$ laminate, $AR=1$ All sides clamped Graphite/Epoxy

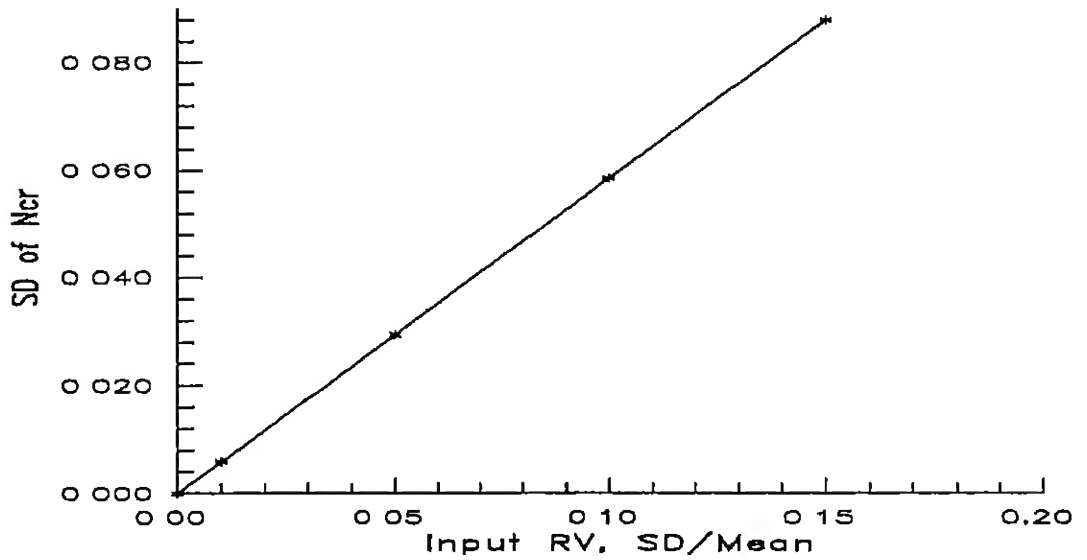


Figure 6.24. SD of normalized buckling load N_{cr} , plotted against the SD of input RVs $[0^\circ/90^\circ]_s$ laminate, $AR=1$ All sides clamped Graphite/Epoxy

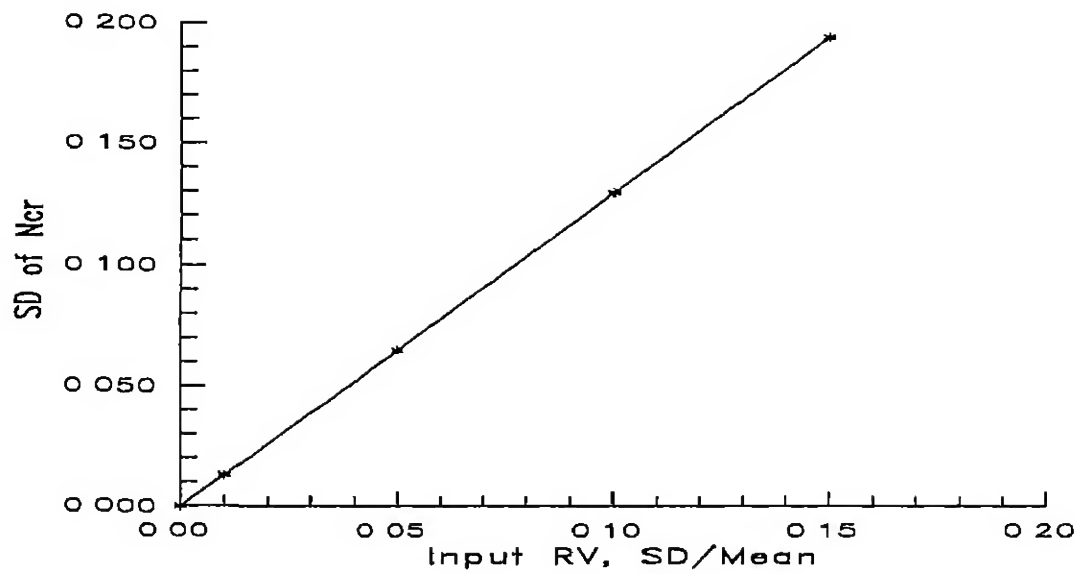


Figure 6.25 SD of normalized buckling load N_{cr} , plotted against the SD of input RVs $[45^\circ]$ laminate, $AR=1$ All sides clamped Graphite/Epoxy

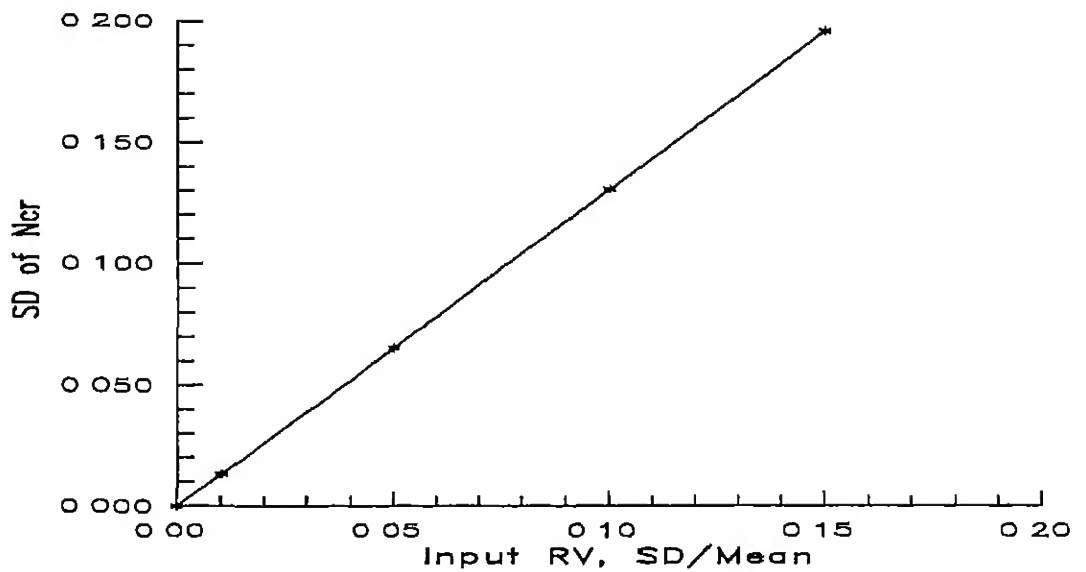


Figure 6.26 SD of normalized buckling load N_{cr} , plotted against the SD of input RVs $[45^\circ/0^\circ]$, laminate, $AR=1$ All sides clamped Graphite/Epoxy

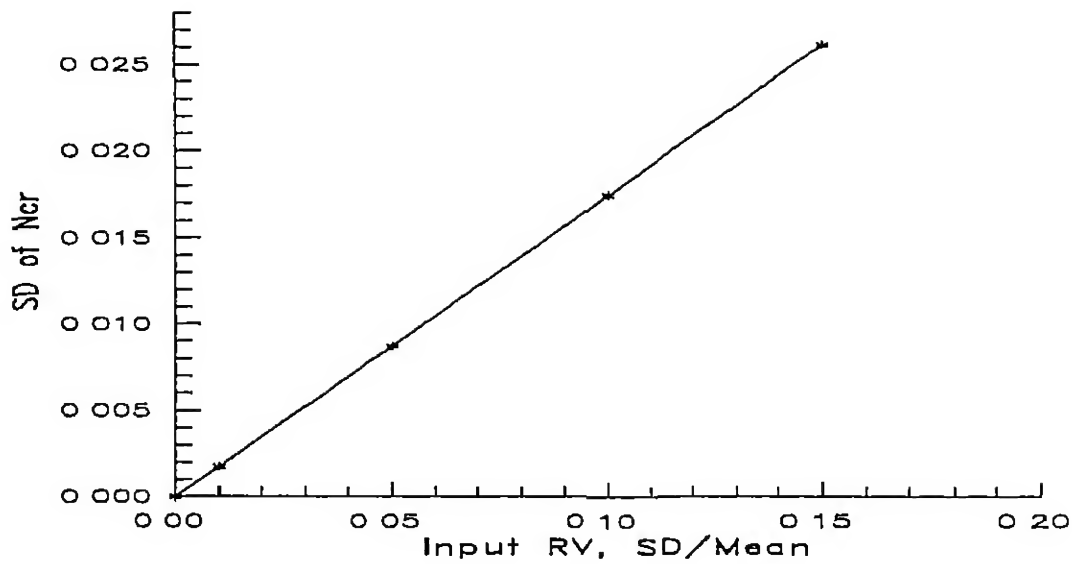


Figure 6.27 SD of normalized buckling load N_{cr} , plotted against the SD of input RVs $[-45^\circ/45^\circ]_s$ laminate, $AR=1$ All sides clamped Graphite/Epoxy

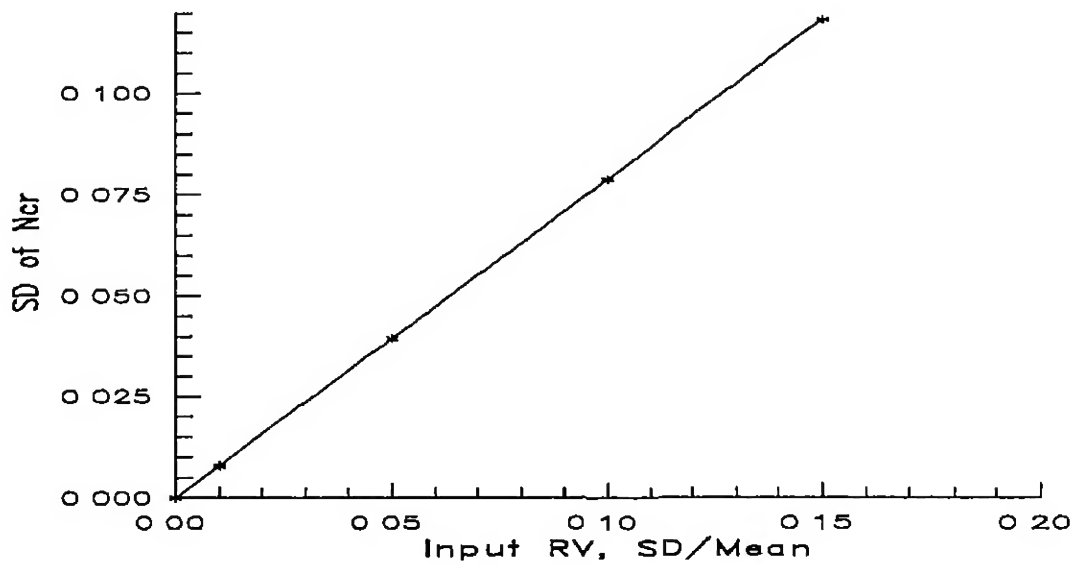


Figure 6.28 SD of normalized buckling load N_{cr} , plotted against the SD of input RVs $[0^\circ/45^\circ/90^\circ/-45^\circ]_s$ laminate, $AR=1$ All sides clamped Graphite/Epoxy

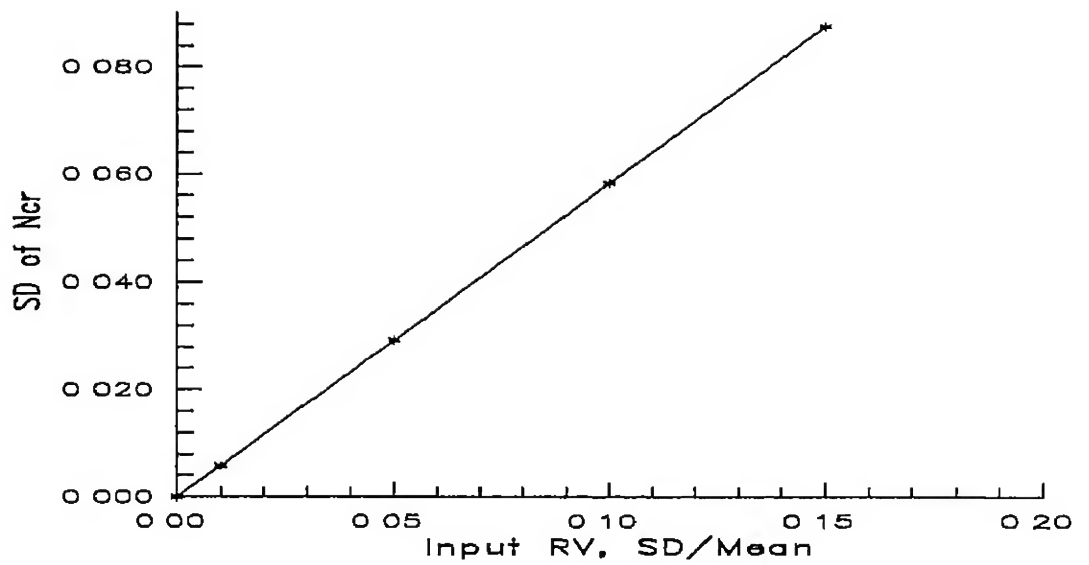


Figure 6.29 SD of normalized buckling load N_{cr} , plotted against the SD of input RVs $[60^\circ]$ laminate, $AR=1$ All sides clamped Graphite/Epoxy

Chapter 7

COUPLING OF BASIC MATERIAL PROPERTIES

7.1 INTRODUCTION

Randomness in composites can be the result of various factors like variation in fiber orientation, individual lamina thickness, fiber volume fraction, void fraction etc. Analysis of composites is normally based on the basic material properties like elastic modulus, Poisson's ratio etc. In this chapter we try to accommodate the coupling between basic material properties in the analysis by considering the fiber volume fraction as the primary random variable.

7.2 ANALYSIS

One of the basic simplifying assumptions used in the perturbation formulation presented in Chapter 3 is the independence of basic random variables. The random variables on which the formulation is based are

$$G_{12} = \frac{G_f G_m}{G_f V_m + G_m V_f} \quad (7.5)$$

Assuming that the void content in the composite material is nil, the matrix volume fraction can be expressed in terms of fiber volume fraction [41] as, $V_m = (1 - V_f)$. The above expressions for basic material parameters can be rewritten as

$$E_{11} = E_m + V_f(E_f - E_m) \quad (7.6)$$

$$E_{22} = \frac{E_f E_m}{E_f - V_f(E_f - E_m)} \quad (7.7)$$

$$\nu_{12} = \nu_m + V_f(\nu_f - \nu_m) \quad (7.8)$$

$$G_{12} = \frac{G_f G_m}{G_f - V_f(G_f - G_m)} \quad (7.9)$$

Now from Chapter 3 we have the expressions for the reduced stiffness matrix terms Q_{ij} in the infinite series form as

$$\begin{aligned} Q_{11} &= \sum_{n=0}^{\infty} E_{11}^{1-n} E_{22}^n \mu_{12}^{2n} \\ Q_{22} &= \sum_{n=0}^{\infty} E_{11}^{-n} E_{22}^{n+1} \mu_{12}^{2n} \\ Q_{12} &= \sum_{n=0}^{\infty} E_{11}^{-n} E_{22}^{n+1} \mu_{12}^{2n+1} \\ Q_{66} &= G_{12} \\ Q_{44} &= G_{23} \\ Q_{55} &= G_{12} \end{aligned} \quad (7.10)$$

If we substitute Equations 7 6, 7 7, 7 8 and 7 9 in Equations 7 10 and write in a compact form, the following expression is obtained

$$Q_{ij} = \sum_{n=0}^{\infty} f_{ij} V_f^{[g_{ij}(n)]} \left\{ \prod_{l=1}^6 (c_l)^{[h_{ijl}(n)]} \right\} \quad (7 11)$$

Here f_{ij} are constants and $h_{ijl}(n)$ are known functions of n , and c_l are the basic fiber and matrix material properties, given by E_f , G_f , ν_f , E_m , G_m and ν_m . $g_{ij}(n)$ are known functions of n

Consider the case when we study the effect on the system due to material parameter randomness. If the fiber volume fraction V_f^R is considered as the basic random variable, the coupling between various basic material properties such as elastic modulus, Poisson's ratio, shear modulus etc can be taken care of. Thus from Equation 7 11 the expectation of Q_{ij} can be found as.

$$E[Q_{ij}] = \sum_{n=0}^{\infty} f_{ij} E[V_f^{[g_{ij}(n)]}] \left\{ \prod_{l=1}^6 (c_l)^{[h_{ijl}(n)]} \right\} \quad (7 12)$$

Similarly expressions for other related quantities can also be developed. Hence the expectation of $[A_{ij}]$, $[B_{ij}]$ and $[D_{ij}]$ matrices can be expressed again in the form

$$\begin{aligned} E[A_{ij}] &= \sum_{k=1}^{N_{lay}} E[(\overline{Q}_{ij})_k] (h_k - h_{k-1}) \\ E[B_{ij}] &= \frac{1}{2} \sum_{k=1}^{N_{lay}} E[(\overline{Q}_{ij})_k] (h_k^2 - h_{k-1}^2) \\ E[D_{ij}] &= \frac{1}{3} \sum_{k=1}^{N_{lay}} E[(\overline{Q}_{ij})_k] (h_k^3 - h_{k-1}^3) \end{aligned} \quad (7 13)$$

Similarly, derivatives of these terms as given in Chapter 3 can be

developed in the following form

$$\frac{\partial E[Q_{ij}]}{\partial b_i^R} = \sum_{n=0}^{\infty} f_{ijl} E[V_f^{[g_{ijl}(n)]}] \left\{ \prod_{k=1}^6 (c_k)^{[e_{ijkl}(n)]} \right\} \quad (7.14)$$

Here f_{ijl} are constants and $e_{ijkl}(n)$ are known functions of n , and c_k are the basic fiber and matrix material properties, given by E_f , G_f , ν_f , E_m , G_m and ν_m . $g_{ijl}(n)$ are known functions of n

From this, similar derivative forms can be developed for $[A_{ij}]$, $[B_{ij}]$ and $[D_{ij}]$ also

$$\begin{aligned} \frac{\partial E[A_{ij}]}{\partial b_i^R} &= \sum_{k=1}^{N_{lay}} \frac{\partial E[(\bar{Q}_{ij})_k]}{\partial b_i^R} (h_k - h_{k-1}) \\ \frac{\partial E[B_{ij}]}{\partial b_i^R} &= \frac{1}{2} \sum_{k=1}^{N_{lay}} \frac{\partial E[(\bar{Q}_{ij})_k]}{\partial b_i^R} (h_k^2 - h_{k-1}^2) \\ \frac{\partial E[D_{ij}]}{\partial b_i^R} &= \frac{1}{3} \sum_{k=1}^{N_{lay}} \frac{\partial E[(\bar{Q}_{ij})_k]}{\partial b_i^R} (h_k^3 - h_{k-1}^3) \end{aligned} \quad (7.15)$$

Thus with the help of the above expressions the statistics of the unknown response can be found out, following the procedure outlined in Chapter 3, provided we know the the statistics of the fiber volume fraction

7.3 SUMMARY

A method for taking into account the effect of mutual coupling of the basic material parameters like E_{11} , E_{22} , ν_{12} and G_{12} in the analysis of composites is presented. This method can be used to solve problems similar to those discussed in the previous chapters. Thus the effect of

coupling of basic material parameters can be taken care of through the fiber volume fraction V_f

Chapter 8

GENERAL OBSERVATIONS AND CONCLUSIONS

8.1 INTRODUCTION

In chapters 1 to 6, we have discussed the importance of the present problem, the related work already done in this field and general formulation of the problem. Specific examples with results for problems related to static deflection, free vibration and initial buckling have been discussed. In this chapter we summarize some of the general observations and conclusions.

8.2 CONCLUSIONS

From the results discussed in the previous chapters it can be seen that the effect of randomness on the response of composites is a complex phenomenon dependent on a large number of parameters. The general conclusions that can be derived from the present study are

- The first order perturbation approximation gives sufficiently accurate results for the present class of problems, for the range of variation in the input SD considered
- At low levels of SD of input material parameters, change in fiber orientation, aspect ratio etc do not have much influence on the output SDs. Higher levels of SD of input RVs show progressively higher influence on the response
- The nature and magnitude of influence of each one of the primary random variables on the response SD is different
- In the case of unidirectional laminae, SD of E_{11} has the maximum influence on the SD of the response
- Stiffer laminate configurations show lesser SD of deflection and higher SD of natural frequencies – if other parameters remain unchanged
- The mode shape, in the case of natural frequencies and buckling loads has a dominating influence on the nature and magnitude of variation of the response SD with the SD of input material parameters
- In general if we consider bending mode, the outer plies of plate have an overall dominating influence on the SD of response.

8.3 LIMITATIONS

The main limitations of the present study can be summed up as follows

- The technique cannot be applied to problems where the randomness of the variables involved are very large, compared with the mean values
- The technique is difficult to apply in its present form, to problems with complicated shapes and/or boundary conditions
- The study is confined to the case of thin plates with small deformations
- Classical laminated plate theory is used throughout, neglecting transverse shear effects

8.4 SUGGESTIONS

The following problems can be attempted as an extension of the present work

- A method to handle coupled systems of equations, in the case of general composites
- Implementation of the present technique using finite element method, by which the effects due to randomness in system pa-

rameters can be taken care of at the element level itself. With this complex structural shapes can be handled easily.

- A technique to accommodate correlated basic random variables
- Problems with randomness in applied static or dynamic loading
- Problems where geometric parameters and boundary conditions are uncertain

REFERENCES

- [1] C Zweben, H.T Hahn and T-W Chou, *Mechanical behavior and properties of composite materials, Delaware composites design encyclopedia*, Vol 1, Technomic Lancaster, (1989)
- [2] Z Maekawa, H Hamada, A Yokoyama, S Ishibashi and T. Tanimoto, Reliability evaluation of unidirectional CFRP, *Proceedings of the 4th US-Japan Conference on Composite Materials*, Washington D C , (1988), pp 1025-1034
- [3] R A Ibrahim, Structural dynamics with parameter uncertainties, *Trans ASME, Applied Mechanics Reviews*, 40(3), (1987), pp 309-328
- [4] L F Tenn, *Statistical analysis of fibrous composite strength data, Test methods and design allowables for fibrous composites*, ASTM STP 734, American Society for Testing and Materials, (1981), pp 229-244

- [5] H Fukuda, TW Chou and K Kawata, Probabilistic approach on the strength of fibrous composites, Composite Materials, Proc Japan-US Conference, Tokyo, (1981), pp 181-193
- [6] Z Maekawa, H Hamada, K Lee and T Kitagawa, Reliability evaluation of mechanical properties of AS4/PEEK composites, Composites, 25(1), 1994, pp 37-45
- [7] M Kleiber and TD Hien, *The stochastic finite element method*, John Wiley & Sons, Chichester, (1992)
- [8] N.C Nigam and S Narayanan, *Applications of random vibrations*, Narosa Publishing House, New Delhi, (1994)
- [9] I Elishakoff, *Probabilistic methods in theory of structures*, John Wiley & Sons, New York, (1983)
- [10] R Vaicatis, Free vibrations of beams with random characteristics, J. Sound and Vibration, 35(1), (1975), pp.13-21
- [11] C J Astill, S B Nosseir and M Shinozuka, Impact loading on structures with random properties, J Structural Mechanics, 1(1), (1972), pp 63-77
- [12] C S Manohar and R N Iyengar, Natural frequencies of simple stochastic structural systems, Advances in structural

- testing, analysis & design Vol I, ICSTAD Proceedings, Bangalore, August (1990), pp 302–307
- [13] M Shinozuka and C J Astill, Random eigenvalue problems in structural analysis, *AIAA J* , 10(4), (1972), pp 656–462
- [14] J D Collins and WT Thomson, The eigenvalue problem for structural systems with statistical properties, *AIAA J* , 7(4), (1969), pp 642–648
- [15] P Caravani and WT Thomson, Frequency response of a dynamic system with statistical damping, *AIAA J* , 11(2), (1973), pp 170–173
- [16] PC Chen and WW Soroka, Multi-degree dynamic response of a system with statistical properties, *J Sound and Vibration*, 37(4), (1974), pp.547–556
- [17] PC Chen and WW Soroka, Impulse response of a dynamic system with statistical properties, *J Sound and Vibration*, 31(3), (1973), pp 309–314
- [18] C Mok and E A Murray, Free vibrations of a slender bar with nonuniform characteristics, *J of the Acoustical Society of America*, 40(2), (1965), pp 385–389

- [19] M Grigoriu, Eigenvalue problem for uncertain systems, Trans ASME Applied Mechanics Rev, 44(11) part2, (1991), pp S89-S95
- [20] G Deodatis, Weighted integral method I Stochastic stiffness matrix, ASCE J Engineering Mech, 117(8), (1991), pp 1851-1864
- [21] G Deodatis and M Shinozuka, Weighted integral method II Response variability and reliability, ASCE J Engineering Mech, 117(8), (1991), pp 1865-1877
- [22] C G Bucher and C E. Brenner, Stochastic response of uncertain systems, Archive of Applied Mechanics, 62, (1992), pp 507-516
- [23] H R Millwater, S V Harren and B H Thacker, Probabilistic analysis of structures involving random stress-strain behavior, Proc of AIAA 32nd Structures Structural Dynamics and Materials Conference, Baltimore, April (1991), pp 1236-1242
- [24] S Chen and Z Zhang, The response sensitivity analysis for the complex stochastic structures to arbitrary deterministic excitation, Advances in structural testing analysis

- and design, ICSTAD Proceedings, Bangalore, India, July (1990), pp 251–258
- [25] PH Prasthofer and CW Beadle, Dynamic response of structures with statistical uncertainties in their stiffness, *J Sound and Vibration*, 42(4), (1975), pp 477–493
- [26] DO Bliven and TT Soong, On frequencies of elastic beams with random imperfections, *J of the Franklin Institute*, 287(4), (1969), pp 297–304
- [27] Z Zhang and S Chen, The standard deviations of the eigensolutions for random MDOF systems, *Computers & Structures*, 39(6), (1991), pp 603–607
- [28] KH Low, A comprehensive approach for the eigenproblem of beams with arbitrary boundary conditions, *Computers & Structures*, 39(6), (1991), pp 671–678
- [29] E Vanmarcke and M Grigoriu, Stochastic finite element analysis of simple beams, *ASCE J of Engineering Mechanics*, 109(5), (1983), pp 1203–1214
- [30] WK Liu, T Belytschko and A Mani, Random field finite elements, *International J of Numerical Methods in Engineering*, 23, (1986), pp 1831–1845

- [31] WK Liu, T Belytschko and A Mani, Probabilistic finite elements for nonlinear structural dynamics, *Computer Methods in Applied Mechanics and Engineering*, 56, (1986), pp 61–81
- [32] D J Gorman, Free vibration analysis of rectangular plates with nonuniform lateral elastic edge support, *Trans ASME J of Applied Mechanics*, 60, (1993), pp 998–1003
- [33] A.F Martin and A W Leissa, Application of the Ritz method to plane elasticity problems for composite sheets with variable fibre spacing, *Int J Numerical Methods in Engineering*, 28, (1989), pp 1813–1825
- [34] A W Leissa and A F Martin, Vibration and buckling of rectangular composite plates with variable fibre spacing, *Composite Structures*, 14, (1990), pp 339–357
- [35] S Nakagiri, H. Takabatake and S Tani, Uncertain eigenvalue analysis of composite laminated plates by the stochastic finite element method, *Trans ASME J of Engineering for Industry*, 109, (1987), pp 9–12
- [36] S P Engelstad and J N Reddy, Probabilistic methods for the analysis of metal–matrix composites, *Composites Science and Technology*, 50, (1994), pp 91–107

- [37] S Adali, I Elishakoff, A Richter and VE Verijenko, Optimal design of symmetric angle-ply laminates for maximum buckling load with scatter in material properties, Proc of AIAA Conference, (1994), pp 1041-1045
- [38] J R Vinson and R L Sierakowski, *The behavior of structures composed of composite materials*, Martinus Nijhoff Publishers, Dordrecht, (1986)
- [39] S W Tsai and H T Hahn, *Introduction to composites*, Technomic, Lancaster, (1980)
- [40] J M Whitney, *Structural analysis of laminated anisotropic plates*, Technomic, Lancaster, (1987)
- [41] R M Jones, *Mechanics of composite materials*, McGraw-Hill, New York, (1975)

APPENDIX A

RESPONSE RELATIONS

The bending stiffness matrix terms D_{ij} are expressed in Chapter 3 in compact form as

$$D_{ij} = \frac{1}{3} \sum_{k=1}^{N_{lay}} (\bar{Q}_{ij})_k (h_k^3 - h_{k-1}^3) \quad (A.1)$$

This set of equations can be expressed in terms of the primary random variables as

$$D_{ij} = \frac{1}{3} \sum_{k=1}^{N_{lay}} \left\{ \sum_{q=1}^7 (C_{ijq})_k \left\{ \sum_{i=1}^6 \sum_{j=1}^6 a_{qij} \left\{ \sum_{n=0}^{\infty} f_{ij} \left\{ \prod_{l=1}^5 (b_l)^{[e_{ijl}(n)]} \right\} \right\} \right\} \right\} (h_k^3 - h_{k-1}^3) \quad i, j = 1, 2 \text{ and } 6 \quad (A.2)$$

where $b_1 = E_{11}$, $b_2 = E_{22}$, $b_3 = \mu_{12}$, $b_4 = G_{12}$ and $b_5 = G_{23}$, as defined in Chapter 3

Equation A.2 f_{ij} are constants, $e_{ijl}(n)$ the powers of b_l are functions of n — the counter index for the infinite series approximation of Q_{ij} , $(C_{ij})_k$ are functions of the fiber orientation θ_k for k^{th} layer of the laminate, a_{qij} are constants and h_k is the thickness of k^{th} layer. These parameters can be expressed as

$$C_{ijq}, \quad q = 1, 2, \dots, 7, \quad i = 1, 2 \text{ and } 6, \quad j = 1, 2 \text{ and } 6 \quad (A.3)$$

$$\begin{aligned}\mathcal{C}_{111} &= 1, \quad C_{112} = \cos(2\theta), \\ \mathcal{C}_{221} &= 1, \quad C_{222} = -\cos(2\theta),\end{aligned}$$

$$a_{qij}, \quad q = 1, 2, \dots, 7, \quad i = 1, 2 \text{ and } 6 \quad j = 1, 2 \text{ and } 6 \quad (\text{A } 4)$$

$$\begin{aligned}a_{111} &= \frac{3}{8}, \quad a_{122} = \frac{3}{8}, \\ a_{211} &= \frac{1}{2}, \quad a_{222} = -\frac{1}{2},\end{aligned}$$

$$f_{ij}, \quad i = 1, 2 \text{ and } 6 \quad j = 1, 2 \text{ and } 6 \quad (\text{A } 5)$$

$$\begin{aligned}f_{11} &= 1, \quad f_{12} = 1, \\ f_{21} &= 1, \quad f_{22} = 1,\end{aligned}$$

$$e_{ijl}, \quad l = 1, 2, \dots, 5, \quad i = 1, 2 \text{ and } 6 \quad j = 1, 2 \text{ and } 6 \quad (\text{A } 6)$$

$$\begin{aligned}e_{111} &= (1 - n), \quad e_{112} = 2n, \\ e_{221} &= -n, \quad e_{222} = (n + 1),\end{aligned}$$

Specific terms in D_{ij} matrix can be expressed as

$$\begin{aligned}D_{11} &= \frac{1}{3} \sum_{k=1}^{N_{lay}} \left\{ \sum_{q=1}^7 (C_{11q})_k \left\{ \sum_{i=1}^6 \sum_{j=1}^6 a_{q11} \left\{ \sum_{n=0}^{\infty} f_{11} \left\{ \prod_{l=1}^5 (b_l)^{[e_{11l}(n)]} \right\} \right\} \right\} \right\} (h_k^3 - h_{k-1}^3) \\ D_{12} &= \frac{1}{3} \sum_{k=1}^{N_{lay}} \left\{ \sum_{q=1}^7 (C_{12q})_k \left\{ \sum_{i=1}^6 \sum_{j=1}^6 a_{q12} \left\{ \sum_{n=0}^{\infty} f_{12} \left\{ \prod_{l=1}^5 (b_l)^{[e_{12l}(n)]} \right\} \right\} \right\} \right\} (h_k^3 - h_{k-1}^3) \\ D_{16} &= \frac{1}{3} \sum_{k=1}^{N_{lay}} \left\{ \sum_{q=1}^7 (C_{16q})_k \left\{ \sum_{i=1}^6 \sum_{j=1}^6 a_{q16} \left\{ \sum_{n=0}^{\infty} f_{16} \left\{ \prod_{l=1}^5 (b_l)^{[e_{16l}(n)]} \right\} \right\} \right\} \right\} (h_k^3 - h_{k-1}^3) \\ D_{22} &= \frac{1}{3} \sum_{k=1}^{N_{lay}} \left\{ \sum_{q=1}^7 (C_{22q})_k \left\{ \sum_{i=1}^6 \sum_{j=1}^6 a_{q22} \left\{ \sum_{n=0}^{\infty} f_{22} \left\{ \prod_{l=1}^5 (b_l)^{[e_{22l}(n)]} \right\} \right\} \right\} \right\} (h_k^3 - h_{k-1}^3) \\ D_{26} &= \frac{1}{3} \sum_{k=1}^{N_{lay}} \left\{ \sum_{q=1}^7 (C_{26q})_k \left\{ \sum_{i=1}^6 \sum_{j=1}^6 a_{q26} \left\{ \sum_{n=0}^{\infty} f_{26} \left\{ \prod_{l=1}^5 (b_l)^{[e_{26l}(n)]} \right\} \right\} \right\} \right\} (h_k^3 - h_{k-1}^3) \\ D_{66} &= \frac{1}{3} \sum_{k=1}^{N_{lay}} \left\{ \sum_{q=1}^7 (C_{66q})_k \left\{ \sum_{i=1}^6 \sum_{j=1}^6 a_{q66} \left\{ \sum_{n=0}^{\infty} f_{66} \left\{ \prod_{l=1}^5 (b_l)^{[e_{66l}(n)]} \right\} \right\} \right\} \right\} (h_k^3 - h_{k-1}^3) \end{aligned} \quad (\text{A } 7)$$

A 1 Static Deflection

A 1.1 Specially Orthotropic Case

For the simply supported case the mean deflection can be found by solving for the expectation of L_{mn} given by Equation 4.12

$$E[L_{mn}] = E[D_{11}]\lambda_m^4 + 2(E[D_{12}]\lambda_m^4 + 2E[D_{66}])\lambda_m^2\lambda_n^2 + E[D_{22}]\lambda_n^4 \quad (A.8)$$

Where $\lambda_m = \frac{m\pi x}{a}$ and $\lambda_n = \frac{n\pi y}{b}$

From Equation 4.11, knowing the transverse load coefficient terms q_{mn} , we can find out the statistical characteristics of a_{mn} and hence mean of deflection from Equation 4.8. To solve for the SD of deflection, the expectation of partial derivatives of L_{mn} are found using Equation 4.13

$$\frac{\partial E[L_{mn}]}{\partial b_i^R} = \frac{\partial E[D_{11}]}{\partial b_i^R}\lambda^4 + 2\left(\frac{\partial E[D_{12}]}{\partial b_i^R} + 2\frac{\partial E[D_{66}]}{\partial b_i^R}\right)\lambda_m^2\lambda_n^2 + \frac{\partial E[D_{22}]}{\partial b_i^R}\lambda_n^4 \quad (A.9)$$

From the expectation of derivatives defined in Equation A.9 and using Equations 3.15 and 3.31, we can find out variance and hence the SD of deflection. The expressions for D_{ij} , given by Equations A.7 can be substituted in Equations A.8 and A.9 to arrive at the relations that are to be solved for finding the response statistics for the plate simply supported along all edges.

For the clamped boundary condition, the final response relations that are to be solved are given by $M \times N$ algebraic equations given by Equation 4.20 as

$$\sum_{i=1}^M \sum_{j=1}^N \left\{ D_{11} \int_0^a \frac{d^2 X_i}{dx^2} \frac{d^2 X_m}{dx^2} dx \int_0^b Y_j Y_n dy \right.$$

$$\begin{aligned}
& +D_{12} \left[\int_0^a X_m \frac{d^2 X_i}{dx^2} dx \int_0^b Y_j \frac{d^2 Y_n}{dy^2} dy + \int_0^a X_i \frac{d^2 X_m}{dx^2} dx \int_0^b Y_n \frac{d^2 Y_j}{dy^2} dy \right] \\
& +D_{22} \int_0^a X_i X_m dx \int_0^b \frac{d^2 Y_j}{dy^2} \frac{d^2 Y_n}{dy^2} dy + 4D_{66} \int_0^a \frac{dX_i}{dx} \frac{dX_m}{dx} dx \int_0^b \frac{dY_j}{dy} \frac{dY_n}{dy} dy \Big\} a_{ij} \\
& = \int_0^b \int_0^a p(x, y) X_m Y_n dx dy \\
& m = 1, 2, \dots, M \text{ and } n = 1, 2, \dots, N
\end{aligned} \tag{A 10}$$

The expectation and expectation of derivatives of a_{ij} can be obtained from Equation A 10. Using these results mean and SD of deflection can be found out from equations 3.15, 3.31 and 4.18. Expressions to be solved can be found by substituting Equations A 7 in A 10.

A 1.2 Midplane Symmetric Case

Here the response relations are given by Equation 4.25

$$\begin{aligned}
& \sum_{i=1}^M \sum_{j=1}^N \left\{ D_{11} \int_0^a \frac{d^2 X_i}{dx^2} \frac{d^2 X_m}{dx^2} dx \int_0^b Y_j Y_n dy \right. \\
& +D_{12} \left[\int_0^a X_m \frac{d^2 X_i}{dx^2} dx \int_0^b Y_j \frac{d^2 Y_n}{dy^2} dy + \int_0^a X_i \frac{d^2 X_m}{dx^2} dx \int_0^b Y_n \frac{d^2 Y_j}{dy^2} dy \right] \\
& +D_{22} \int_0^a X_i X_m dx \int_0^b \frac{d^2 Y_j}{dy^2} \frac{d^2 Y_n}{dy^2} dy + 4D_{66} \int_0^a \frac{dX_i}{dx} \frac{dX_m}{dx} dx \int_0^b \frac{dY_j}{dy} \frac{dY_n}{dy} dy \\
& +2D_{16} \left[\int_0^a \frac{d^2 X_i}{dx^2} \frac{dX_m}{dx} dx \int_0^b Y_j \frac{dY_n}{dy} dy + \int_0^a \frac{dX_i}{dx} \frac{d^2 X_m}{dx^2} dx \int_0^b Y_n \frac{dY_j}{dy} dy \right] \\
& +2D_{26} \left[\int_0^a X_m \frac{dX_i}{dx} dx \int_0^b \frac{dY_j}{dy} \frac{d^2 Y_n}{dy^2} dy + \int_0^a X_i \frac{dX_m}{dx} dx \int_0^b \frac{d^2 Y_j}{dy^2} \frac{dY_n}{dy} dy \right] \Big\} a_{ij} \\
& = \int_0^b \int_0^a p(x, y) X_m Y_n dx dy \\
& m = 1, 2, \dots, M \text{ and } n = 1, 2, \dots, N
\end{aligned} \tag{A 11}$$

This is of the form of Equation 3.2. Here loading $p(x, y)$, D_{ij} and all other terms except a_{ij} are known. Thus Equation A 11 can be solved for the expectation of a_{ij} and

expectation of derivatives of a_{ij} , by using transformations of the form of Equations 3 10, 3 11 and 3 13 SD of a_{ij} and hence that of the deflection $w(x,y)$ can be found using the relation given by Equation 3 15 and 3 31 The expressions to be solved can be found by substituting Equations A 7 in the $M \times N$ linear simultaneous equations given by Equation A 11

A 2 Natural Frequencies

A 2 1 Specially Orthotropic Case

For this case the final response relations to be solved are given by Equation 5 10

Thus we have the following $M \times N$ homogeneous algebraic equations

$$\begin{aligned} \sum_{i=1}^M \sum_{j=1}^N \left\{ D_{11} \int_0^a \frac{d^2 X_i}{dx^2} \frac{d^2 X_m}{dx^2} dx \int_0^b Y_j Y_n dy \right. \\ + D_{12} \left[\int_0^a X_m \frac{d^2 X_i}{dx^2} dx \int_0^b Y_j \frac{d^2 Y_n}{dy^2} dy + \int_0^a X_i \frac{d^2 X_m}{dx^2} dx \int_0^b Y_n \frac{d^2 Y_j}{dy^2} dy \right] \\ + D_{22} \int_0^a X_i X_m dx \int_0^b \frac{d^2 Y_j}{dy^2} \frac{d^2 Y_n}{dy^2} dy + 4D_{66} \int_0^a \frac{dX_i}{dx} \frac{dX_m}{dx} dx \int_0^b \frac{dY_j}{dy} \frac{dY_n}{dy} dy \\ \left. - \rho \omega_{mn}^2 \int_0^a X_i X_m dx \int_0^b Y_j Y_n dy \right\} a_{ij} = 0 \\ m = 1, 2, \dots, M \text{ and } n = 1, 2, \dots, N \end{aligned} \quad (A 12)$$

For a non-trivial solution, the coefficients associated with a_{ij} must go to zero for all values of i and j The resulting eigenvalue problem can be solved for mean of ω_{mn}^2 and SD of ω_{mn}^2 by transformations of the form of Equations 3 10 and 3 11, along with Equations 3 15 and 3 31 The final exact relations can be found by substituting Equations A 7 in A 12 given above.

A 2.2 Midplane Symmetric Case

The final response relations for this case contains terms containing D_{16} and D_{26} in addition to those in Equation A 12

$$\begin{aligned}
 \sum_{i=1}^M \sum_{j=1}^N \left\{ D_{11} \int_0^a \frac{d^2 X_i}{dx^2} \frac{d^2 X_m}{dx^2} dx \int_0^b Y_j Y_n dy \right. \\
 + D_{12} \left[\int_0^a X_m \frac{d^2 X_i}{dx^2} dx \int_0^b Y_j \frac{d^2 Y_n}{dy^2} dy + \int_0^a X_i \frac{d^2 X_m}{dx^2} dx \int_0^b Y_n \frac{d^2 Y_j}{dy^2} dy \right] \\
 + D_{22} \int_0^a X_i X_m dx \int_0^b \frac{d^2 Y_j}{dy^2} \frac{d^2 Y_n}{dy^2} dy + 4D_{66} \int_0^a \frac{dX_i}{dx} \frac{dX_m}{dx} dx \int_0^b \frac{dY_j}{dy} \frac{dY_n}{dy} dy \\
 + 2D_{16} \left[\int_0^a \frac{d^2 X_i}{dx^2} \frac{dX_m}{dx} dx \int_0^b dY_j \frac{dY_n}{dy} dy + \int_0^a \frac{dX_i}{dx} \frac{d^2 X_m}{dx^2} dx \int_0^b Y_n \frac{dY_j}{dy} dy \right] \\
 + 2D_{26} \left[\int_0^a X_m \frac{dX_i}{dx} dx \int_0^b \frac{dY_j}{dy} \frac{d^2 Y_n}{dy^2} dy + \int_0^a X_i \frac{dX_m}{dx} dx \int_0^b \frac{d^2 Y_j}{dy^2} \frac{dY_n}{dy} dy \right] \\
 \left. - \rho \omega_{mn}^2 \int_0^a X_i X_m dx \int_0^b Y_j Y_n dy \right\} a_i = 0 \\
 m = 1, 2, \dots, M \text{ and } n = 1, 2, \dots, N
 \end{aligned} \tag{A 13}$$

An eigenvalue problem is obtained from Equation A 13 by applying the condition for non-trivial solution. This eigenvalue problem given by equating the coefficient term of a_i to zero can be solved for mean and SD of natural frequencies ω_{mn}^2 by employing transformations given by Equation 3.10 and 3.11, along with Equation 3.15 and 3.31. Here the final expressions to be solved can be found by substituting Equation A 7 in Equation A 13.

A 3 Critical Buckling Load

A 3.1 Specially Orthotropic Case

For the simply supported boundary condition case the final critical buckling load expression is given by Equation 6.11

$$N_{cr} = \frac{\pi^2}{m^2 a^2} [D_{11} m^4 + 2(D_{12} + 2D_{66})m^2 R^2 + D_{22} R^4] \quad (\text{A } 14)$$

Mean of N_{cr} can be found by finding the expectation of Equation A.14. SD of N_{cr} can be found using Equation 3.15 along with 3.31. The final expressions can be found by substituting Equations A.7 in the above

For the clamped boundary condition case the final equations to be solved are given by Equation 6.19

$$\begin{aligned} \sum_{i=1}^M \sum_{j=1}^N \left\{ D_{11} \int_0^a \frac{d^2 X_i}{dx^2} \frac{d^2 X_m}{dx^2} dx \int_0^b Y_j Y_n dy \right. \\ + D_{12} \left[\int_0^a X_m \frac{d^2 X_i}{dx^2} dx \int_0^b Y_j \frac{d^2 Y_n}{dy^2} dy + \int_0^a X_i \frac{d^2 X_m}{dx^2} dx \int_0^b Y_n \frac{d^2 Y_j}{dy^2} dy \right] \\ + D_{22} \int_0^a X_i X_m dx \int_0^b \frac{d^2 Y_j}{dy^2} \frac{d^2 Y_n}{dy^2} dy + 4D_{66} \int_0^a \frac{dX_i}{dx} \frac{dX_m}{dx} dx \int_0^b \frac{dY_j}{dy} \frac{dY_n}{dy} dy \\ \left. + N_i \int_0^a \frac{dX_i}{dx} \frac{dX_m}{dx} dx \int_0^b Y_j Y_n dy \right\} a_{ij} = 0 \\ m = 1, 2, \dots, M \text{ and } n = 1, 2, \dots, N \end{aligned} \quad (\text{A } 15)$$

For non-trivial solution of this equation the coefficient of a_{ij} must go to zero. This gives an eigenvalue problem, which can be transformed to a form similar to Equations 3.10 and 3.11 and solved for mean of critical buckling load N_{cr} . Now, using Equations 3.15 and 3.31 the SD of N_{cr} can be found out. The final expressions to be solved can be found by substituting Equations A.7 in the set of $M \times N$ equations given by Equation A.15.

A.3.2 Midplane Symmetric Case

Here the final equations to be solved are given by Equation 6.22:

$$\begin{aligned}
 \sum_{i=1}^M \sum_{j=1}^N \left\{ D_{11} \int_0^a \frac{d^2 X_i}{dx^2} \frac{d^2 X_m}{dx^2} dx \int_0^b Y_j Y_n dy \right. \\
 + D_{12} \left[\int_0^a X_m \frac{d^2 X_i}{dx^2} dx \int_0^b Y_j \frac{d^2 Y_n}{dy^2} dy + \int_0^a X_i \frac{d^2 X_m}{dx^2} dx \int_0^b Y_n \frac{d^2 Y_j}{dy^2} dy \right] \\
 + D_{22} \int_0^a X_i X_m dx \int_0^b \frac{d^2 Y_j}{dy^2} \frac{d^2 Y_n}{dy^2} dy + 4D_{66} \int_0^a \frac{dX_i}{dx} \frac{dX_m}{dx} dx \int_0^b \frac{dY_j}{dy} \frac{dY_n}{dy} dy \\
 + 2D_{16} \left[\int_0^a \frac{d^2 X_i}{dx^2} \frac{dX_m}{dx} dx \int_0^b Y_j \frac{dY_n}{dy} dy + \int_0^a \frac{dX_i}{dx} \frac{d^2 X_m}{dx^2} dx \int_0^b Y_n \frac{dY_j}{dy} dy \right] \\
 + 2D_{26} \left[\int_0^a X_m \frac{dX_i}{dx} dx \int_0^b \frac{dY_j}{dy} \frac{d^2 Y_n}{dy^2} dy + \int_0^a X_i \frac{dX_m}{dx} dx \int_0^b \frac{d^2 Y_j}{dy^2} \frac{dY_n}{dy} dy \right] \\
 \left. + N_1 \int_0^a \frac{dX_i}{dx} \frac{dX_m}{dx} dx \int_0^b Y_j Y_n dy \right\} a_{mn} = 0 \\
 m = 1, 2, \dots, M \quad \text{and} \quad n = 1, 2, \dots, N
 \end{aligned} \tag{A.16}$$

Here also the eigenvalue problem to be solved, for finding the critical buckling load N_{cr} is obtained by equating the coefficient term of a_{mn} in Equation A.16 to zero. The mean of N_{cr} is found by applying the transformations given by Equations 3.10 and 3.11 to this eigenvalue problem. The SD of N_{cr} is obtained by employing Equations 3.31 and 3.15. The exact final expressions to be solved for finding the statistics of the critical buckling load for this case can be found by substituting Equations A.7 in the set of $M \times N$ linear equations A.16.

APPENDIX B

GOVERNING EQUATIONS OF ANISOTROPIC PLATES

The governing equations as given in the beginning of Chapter 4, 5 and 6 are taken from reference [10]. A general derivation for these equations are presented here along with the physical explanation of the different terms. The *co-ordinate system* used is given by Figure 3.1. The displacements in x , y and z directions are denoted by u , v and w respectively. The main assumptions made in deriving the governing equations for u , v and w are,

1. The plate consists of an arbitrary number of orthotropic layers. The material axes of the individual layers need not coincide with the geometric axes of the plate.
2. The plate is thin.
3. Deformations of the plate u , v and w are small compared with the plate thickness.
4. Inplane strains are small compared to unity.

5. All nonlinear terms in the equations of motion except those involving products of stress and plate slopes are neglected.
6. Transverse shear strains are negligible.
7. Displacements u and v are linear functions of z co-ordinate.
8. Transverse normal strain is negligible.
9. Each ply obeys Hooke's law.
10. The plate is of constant thickness.
11. Rotatory inertia terms are negligible.
12. No body forces act on the system.
13. Transverse shear strains vanish on the z surfaces.

From these, the strains are given by:

$$\begin{aligned} \epsilon_x^0 &= \frac{\partial u^0}{\partial x} & \epsilon_y^0 &= \frac{\partial v^0}{\partial y} & \epsilon_{xy}^0 &= \frac{\partial u^0}{\partial y} + \frac{\partial v^0}{\partial x} \\ \chi_x &= -\frac{\partial^2 w}{\partial x^2} & \chi_y &= -\frac{\partial^2 w}{\partial y^2} & \chi_{xy} &= -2\frac{\partial^2 w}{\partial x \partial y} \end{aligned} \quad (\text{B.1})$$

Here u^0 and v^0 are the mid-plane tangential displacements and w is the transverse displacement.

The equations of motion for the k^{th} layer of laminate are given by:

$$\begin{aligned} \frac{\partial \sigma_x^k}{\partial x} + \frac{\partial \sigma_{xy}^k}{\partial y} + \frac{\partial \sigma_{xz}^k}{\partial z} &= \rho_0^k \frac{\partial^2 u}{\partial t^2} \\ \frac{\partial \sigma_{xy}^k}{\partial x} + \frac{\partial \sigma_y^k}{\partial y} + \frac{\partial \sigma_{yz}^k}{\partial z} &= \rho_0^k \frac{\partial^2 v}{\partial t^2} \end{aligned}$$

$$\begin{aligned} \frac{\partial}{\partial x} \left(\sigma_{xz}^k + \sigma_x^k \frac{\partial w}{\partial x} \sigma_{xy}^k \frac{\partial w}{\partial y} \right) + \frac{\partial}{\partial y} \left(\sigma_{yz}^k + \sigma_{xy}^k \frac{\partial w}{\partial x} \sigma_y^k \frac{\partial w}{\partial y} \right) \\ + \frac{\partial}{\partial z} \left(\sigma_z^k + \sigma_{xz}^k \frac{\partial w}{\partial x} \sigma_{yz}^k \frac{\partial w}{\partial y} \right) = \rho_0^k \frac{\partial^2 w}{\partial t^2} \end{aligned} \quad (\text{B.2})$$

Here ρ^k is the density of the individual layers Stress and moment resultants are defined as:

$$\begin{aligned} (N_x, N_y, N_{xy}) &= \int_{-\frac{h}{2}}^{\frac{h}{2}} (\sigma_x^k, \sigma_y^k, \sigma_{xy}^k) dz \\ (Q_x, Q_y) &= \int_{-\frac{h}{2}}^{\frac{h}{2}} (\sigma_{xz}^k, \sigma_{yz}^k) dz \\ (M_x, M_y, M_{xy}) &= \int_{-\frac{h}{2}}^{\frac{h}{2}} (\sigma_x^k, \sigma_y^k, \sigma_{xy}^k) z dz \end{aligned} \quad (\text{B.3})$$

From Equations B.2 and B.3 the following relations can be derived:

$$\frac{\partial N_x}{\partial x} + \frac{\partial N_{xy}}{\partial y} = \rho \frac{\partial^2 u^0}{\partial t^2} \quad (\text{B.4})$$

$$\frac{\partial N_{xy}}{\partial x} + \frac{\partial N_y}{\partial y} = \rho \frac{\partial^2 v^0}{\partial t^2} \quad (\text{B.5})$$

$$\frac{\partial^2 M_x}{\partial x^2} + 2 \frac{\partial^2 M_{xy}}{\partial x \partial y} + \frac{\partial^2 M_y}{\partial y^2} + N_x \frac{\partial^2 w}{\partial x^2} + 2 N_{xy} \frac{\partial^2 w}{\partial x \partial y} + N_y \frac{\partial^2 w}{\partial y^2} + q = \rho \frac{\partial^2 w}{\partial t^2} \quad (\text{B.6})$$

Equations B.4, B.5 and B.6 together form the equations of motion.

Now the constitutive relations for the plate are given by:

$$\begin{bmatrix} N_x \\ N_y \\ N_{xy} \\ M_x \\ M_y \\ M_{xy} \end{bmatrix} = \begin{bmatrix} A_{11} & A_{12} & A_{16} & B_{11} & B_{12} & B_{16} \\ A_{12} & A_{22} & A_{26} & B_{12} & B_{22} & B_{26} \\ A_{16} & A_{26} & A_{66} & B_{16} & B_{26} & B_{66} \\ B_{11} & B_{12} & B_{16} & D_{11} & D_{12} & D_{16} \\ B_{12} & B_{22} & B_{26} & D_{12} & D_{22} & D_{26} \\ B_{16} & B_{26} & B_{66} & D_{16} & D_{26} & D_{66} \end{bmatrix} \begin{bmatrix} \epsilon_x^0 \\ \epsilon_y^0 \\ \epsilon_{xy}^0 \\ \chi_x \\ \chi_y \\ \chi_{xy} \end{bmatrix} \quad (\text{B.7})$$

where the various stiffness matrix elements are given by:

$$(A_{ij}, B_{ij}, D_{ij}) = \int_{-\frac{h}{2}}^{\frac{h}{2}} Q_{ij}^{(k)}(1, z, z^2) dz \quad (\text{B.8})$$

From Equations B.4, B.5, B.6, strain-displacement and curvature-displacement relations given by Equations B.1 and constitutive relations given by Equations B.7, we can arrive at equations of motion in terms of displacements for the case when any transverse load $p(x, y)$ acting on the plate as:

$$\begin{aligned} & A_{11} \frac{\partial^2 u^0}{\partial x^2} + 2A_{16} \frac{\partial^2 u^0}{\partial x \partial y} + A_{66} \frac{\partial^2 u^0}{\partial y^2} + A_{16} \frac{\partial^2 v^0}{\partial x^2} \\ & + (A_{12} + A_{66}) \frac{\partial^2 v^0}{\partial x \partial y} + A_{26} \frac{\partial^2 v^0}{\partial y^2} - B_{11} \frac{\partial^3 w}{\partial x^3} \\ & - 3B_{16} \frac{\partial^3 w}{\partial x^2 \partial y} - (B_{12} + 2B_{66}) \frac{\partial^2 w}{\partial x \partial y^2} - B_{26} \frac{\partial^3 w}{\partial y^3} = 0 \end{aligned} \quad (\text{B.9})$$

$$\begin{aligned} & A_{16} \frac{\partial^2 u^0}{\partial x^2} + (A_{12} + A_{66}) \frac{\partial^2 u^0}{\partial x \partial y} + A_{26} \frac{\partial^2 u^0}{\partial y^2} + A_{66} \frac{\partial^2 v^0}{\partial x^2} \\ & + 3A_{26} \frac{\partial^2 v^0}{\partial x \partial y} + A_{22} \frac{\partial^2 v^0}{\partial y^2} - B_{16} \frac{\partial^3 w}{\partial x^3} - (B_{12} + 2B_{66}) \frac{\partial^3 w}{\partial x^2 \partial y} \\ & - 3B_{26} \frac{\partial^3 w}{\partial x \partial y^2} - B_{22} \frac{\partial^3 w}{\partial y^3} = 0 \end{aligned} \quad (\text{B.10})$$

$$\begin{aligned} & D_{11} \frac{\partial^4 w}{\partial x^4} + 4D_{16} \frac{\partial^4 w}{\partial x^3 \partial y} + 2(D_{12} + 2D_{66}) \frac{\partial^4 w}{\partial x^2 \partial y^2} + 4D_{26} \frac{\partial^4 w}{\partial x \partial y^3} \\ & + D_{22} \frac{\partial^4 w}{\partial y^4} - B_{11} \frac{\partial^3 u^0}{\partial x^3} - 3B_{16} \frac{\partial^3 u^0}{\partial x^2 \partial y} - (B_{12} + 2B_{66}) \frac{\partial^3 u^0}{\partial x \partial y^2} \\ & - B_{26} \frac{\partial^3 u^0}{\partial y^3} - B_{16} \frac{\partial^3 v^0}{\partial x^3} - (B_{12} + 2B_{66}) \frac{\partial^3 v^0}{\partial x^2 \partial y} \\ & - 3B_{26} \frac{\partial^3 v^0}{\partial x \partial y^2} - B_{22} \frac{\partial^3 v^0}{\partial y^3} = p(x, y) \end{aligned} \quad (\text{B.11})$$

It is observed that for a general laminate the governing equation in u , v and w are coupled. These equations simplify for specific configuration of the stacking of the lamina, wherein several terms dropout depending on the coefficient matrix of Equation B.7.

In the case of free vibration analysis the general governing equations are obtained in the form given below. Here the load coming on the plate due to free vibration is

taken into account by the terms containing effective density of the lamina ρ . These terms account for the force due to inplane and transverse acceleration.

$$\begin{aligned}
 & A_{11} \frac{\partial^2 u^0}{\partial x^2} + 2A_{16} \frac{\partial^2 u^0}{\partial x \partial y} + A_{66} \frac{\partial^2 u^0}{\partial y^2} + A_{16} \frac{\partial^2 v^0}{\partial x^2} \\
 & + (A_{12} + A_{66}) \frac{\partial^2 v^0}{\partial x \partial y} + A_{26} \frac{\partial^2 v^0}{\partial y^2} - B_{11} \frac{\partial^3 w}{\partial x^3} \\
 & - 3B_{16} \frac{\partial^3 w}{\partial x^2 \partial y} - (B_{12} + 2B_{66}) \frac{\partial^2 w}{\partial x \partial y^2} - B_{26} \frac{\partial^3 w}{\partial y^3} = \rho \frac{\partial^2 u^0}{\partial t^2}
 \end{aligned} \quad (B.12)$$

$$\begin{aligned}
 & A_{16} \frac{\partial^2 u^0}{\partial x^2} + (A_{12} + A_{66}) \frac{\partial^2 u^0}{\partial x \partial y} + A_{26} \frac{\partial^2 u^0}{\partial y^2} + A_{66} \frac{\partial^2 v^0}{\partial x^2} \\
 & + 3A_{26} \frac{\partial^2 v^0}{\partial x \partial y} + A_{22} \frac{\partial^2 v^0}{\partial y^2} - B_{16} \frac{\partial^3 w}{\partial x^3} - (B_{12} + 2B_{66}) \frac{\partial^3 w}{\partial x^2 \partial y} \\
 & - 3B_{26} \frac{\partial^3 w}{\partial x \partial y^2} - B_{22} \frac{\partial^3 w}{\partial y^3} = \rho \frac{\partial^2 v^0}{\partial t^2}
 \end{aligned} \quad (B.13)$$

$$\begin{aligned}
 & D_{11} \frac{\partial^4 w}{\partial x^4} + 4D_{16} \frac{\partial^4 w}{\partial x^3 \partial y} + 2(D_{12} + 2D_{66}) \frac{\partial^4 w}{\partial x^2 \partial y^2} + 4D_{26} \frac{\partial^4 w}{\partial x \partial y^3} \\
 & + D_{22} \frac{\partial^4 w}{\partial y^4} - B_{11} \frac{\partial^3 u^0}{\partial x^3} - 3B_{16} \frac{\partial^3 u^0}{\partial x^2 \partial y} - (B_{12} + 2B_{66}) \frac{\partial^3 u^0}{\partial x \partial y^2} \\
 & - B_{26} \frac{\partial^3 u^0}{\partial y^3} - B_{16} \frac{\partial^3 v^0}{\partial x^3} - (B_{12} + 2B_{66}) \frac{\partial^3 v^0}{\partial x^2 \partial y} \\
 & - 3B_{26} \frac{\partial^3 v^0}{\partial x \partial y^2} - B_{22} \frac{\partial^3 v^0}{\partial y^3} + \rho \frac{\partial^2 w}{\partial t^2} = 0
 \end{aligned} \quad (B.14)$$

Here also, depending on the actual laminate configuration and the terms present in the $[A]$, $[B]$, $[D]$ matrix of Equation B.7, several terms dropout. Generally the inplane stiffness is higher than the bending stiffness. Therefore if one is interested in the first few natural frequencies of the plate, the transverse oscillation frequencies are important as compared to inplane oscillations. Hence one can simplify the equations further by ignoring the inplane acceleration terms.

In the case of stability analysis the effect of inplane loads can be taken into consideration by using post buckling equilibrium displacement relations, along with

the constitutive relations given by Equations B.7. The effect due to the inplane loads is expressed in the form of an effective lateral load. Thus the governing equations are obtained as:

$$\begin{aligned}
 & A_{11} \frac{\partial^2 u^0}{\partial x^2} + 2A_{16} \frac{\partial^2 u^0}{\partial x \partial y} + A_{66} \frac{\partial^2 u^0}{\partial y^2} + A_{16} \frac{\partial^2 v^0}{\partial x^2} \\
 & + (A_{12} + A_{66}) \frac{\partial^2 v^0}{\partial x \partial y} + A_{26} \frac{\partial^2 v^0}{\partial y^2} - B_{11} \frac{\partial^3 w}{\partial x^3} \\
 & - 3B_{16} \frac{\partial^3 w}{\partial x^2 \partial y} - (B_{12} + 2B_{66}) \frac{\partial^2 w}{\partial x \partial y^2} - B_{26} \frac{\partial^3 w}{\partial y^3} = 0
 \end{aligned} \tag{B.15}$$

$$\begin{aligned}
 & A_{16} \frac{\partial^2 u^0}{\partial x^2} + (A_{12} + A_{66}) \frac{\partial^2 u^0}{\partial x \partial y} + A_{26} \frac{\partial^2 u^0}{\partial y^2} + A_{66} \frac{\partial^2 v^0}{\partial x^2} \\
 & + 3A_{26} \frac{\partial^2 v^0}{\partial x \partial y} + A_{22} \frac{\partial^2 v^0}{\partial y^2} - B_{16} \frac{\partial^3 w}{\partial x^3} - (B_{12} + 2B_{66}) \frac{\partial^3 w}{\partial x^2 \partial y} \\
 & - 3B_{26} \frac{\partial^3 w}{\partial x \partial y^2} - B_{22} \frac{\partial^3 w}{\partial y^3} = 0
 \end{aligned} \tag{B.16}$$

$$\begin{aligned}
 & D_{11} \frac{\partial^4 w}{\partial x^4} + 4D_{16} \frac{\partial^4 w}{\partial x^3 \partial y} + 2(D_{12} + 2D_{66}) \frac{\partial^4 w}{\partial x^2 \partial y^2} + 4D_{26} \frac{\partial^4 w}{\partial x \partial y^3} \\
 & + D_{22} \frac{\partial^4 w}{\partial y^4} - B_{11} \frac{\partial^3 u^0}{\partial x^3} - 3B_{16} \frac{\partial^3 u^0}{\partial x^2 \partial y} - (B_{12} + 2B_{66}) \frac{\partial^3 u^0}{\partial x \partial y^2} \\
 & - B_{26} \frac{\partial^3 u^0}{\partial y^3} - B_{16} \frac{\partial^3 v^0}{\partial x^3} - (B_{12} + 2B_{66}) \frac{\partial^3 v^0}{\partial x^2 \partial y} \\
 & - 3B_{26} \frac{\partial^3 v^0}{\partial x \partial y^2} - B_{22} \frac{\partial^3 v^0}{\partial y^3} = N_x \frac{\partial^2 w}{\partial x^2} + 2N_{xy} \frac{\partial^2 w}{\partial x \partial y} + N_y \frac{\partial^2 w}{\partial y^2}
 \end{aligned} \tag{B.17}$$

Modifications and simplification of the governing equations given above are often possible by taking into account the actual laminate configurations used.

APPENDIX C

ENERGY METHODS AND RAYLEIGH-RITZ TECHNIQUE

C.1 Energy Methods

Strain energy is stored in a structure, when it is subjected to deformations due to forces acting on it. The total strain energy stored in a body is given by the product of force and corresponding displacement vectors. When external forces act on a body, corresponding resistive forces are developed internally. If the system is conservative the internal resistive forces disappear and the body returns to its unstrained state, upon removal of the external forces. If we consider the law of conservation of energy, the sum total of the work done by the internal forces should be equal and opposite to the work done by the external loads. Thus for a system with an applied force of P_i undergoing a virtual displacement δr_i along the direction of the applied force, the resulting virtual work done δW_e is given by

$$\delta W_e = \sum P_i \delta r_i \quad (C.1)$$

Also if δV_e is the change in potential energy due to the virtual displacement we get

$$\delta V_e = -\delta W_e \quad (C.2)$$

Work is done by forces developed internally. If δU is the work done by internal forces, we have

$$\delta U = \delta W_e = 0 \quad (C.3)$$

Hence we can write

$$\delta(U + V_e) = 0 \quad (C.4)$$

If the total potential $\pi_p = U + V_e$, from the above we can write

$$\delta \pi_p = 0 \quad (C.5)$$

or

$$U + V_e = \pi_p = \text{constant} \quad (C.6)$$

If the above conditions are applied to total potential expression for a structural system, the governing differential equations and boundary conditions can be obtained.

C.2 Rayleigh Ritz Technique

Rayleigh Ritz technique makes use of the principle of minimum potential energy given by Equation (C.4). The principle states that of all the possible equilibrium states that satisfy boundary conditions of a system, that which makes the total potential minimum tend to make the system stable.

To solve for the response of structure an approximating function satisfying at least the geometric boundary conditions of the system, with unknown constants is assumed. This can be of the form

$$\sum_{n=1}^N C_n F_n \quad (C.7)$$

where C_n are unknown constants and F_n are functions that satisfy at least the geometric boundary conditions of the system. This approximating function is substituted into the energy condition specified by the principle of minimum potential energy given by the Equation C.1. The resulting total potential energy expression is minimized with respect to the constants C_n . The minimization process gives a set of simultaneous algebraic equations. This set of equations can be solved to obtain specific values of C_n corresponding to the solution of the system equations.

When exact solution of the differential equation of a system is difficult, Rayleigh-Ritz approach can be used, to find an approximate solution. The accuracy of the solution depends on the number of terms in the approximating function and the functions F_n chosen, to satisfy the boundary conditions.

Date Slip

date last stamped.

AE-1995-D 9/21 - 11/11

